ANALYSIS OF ADAPTIVE RESPONSE TO DNA DAMAGE CHECKPOINT INDUCED ARREST

YIO WEE KHENG

NATIONAL UNIVERSITY OF SINGAPORE

2009

ANALYSIS OF ADAPTIVE RESPONSE TO DNA DAMAGE CHECKPOINT INDUCED ARREST

YIO WEE KHENG

B.Eng.(Hons.), M.Sc., NUS

A THESIS SUBMITTED

FOR THE DEGREE OF DOCTOR OF PHILOSOPHY

Acknowledgements

Professor Uttam Surana, Dr Lim Hong Hwa, and Dr Dave Wee are the three persons that I can never thank enough for their guidance and assistance. Without their advice and selfless support, this thesis would never have become a reality. Prof Surana is my supervisor. He is truly an excellent scientist; a role model to learn from. Dr Lim is a friend and mentor; an efficient and proficient experimentalist. She taught me most of the molecular biology techniques. Dr Wee is a brilliant budding scientist. He has many marvelous ideas which are still in progress.

I would like to express my gratitude to Prof Baltazar Aguda, my ex-supervisor, who has taught me computational modeling of biology. Next, I would also like to thank the members of my Thesis Advisory Committee: Prof Mohan Balasubramanian (TLL) and Prof Wang Yue (IMCB) for their constructive comments.

Special thanks to the special people, the current and ex-members of US Lab (IMCB), who have helped me in one way or another. They are San Ling, Zhang Tao, Joan Cher, Jenn Hui, Hong Qing, David Goh, Karen Crasta and Jonathan Wong.

I would like to thank Dr Jayantha Gunraratne and Associate Professor Walter Blackstock (IMCB) for the collaboration on mass spectrometry, Prof James Haber (Brandeis Un\iversity) and Prof Rodney Rothstein (Columbia University) for providing valuable reagents.

I would also wish to thank the staff at the NUS Graduate School for Integrative Sciences and Engineering (NGS), A*STAR Graduate Academy (AGA) and Institute of Molecular and Cell Biology (IMCB), for their assistance.

Most importantly, I wish to thank my family for their support.

Preface

After completing my degrees in electrical engineering and bioinformatics, I initiated my PhD studies under the supervision of Professor Baltazar Aguda at the Bioinformatics Institute (A*STAR), Singapore. The research project was purely computational in nature and involved analysis of biological networks.

However, after 1.5 years into my PhD program, Professor Aguda decided to move to the USA due to unforeseen circumstances. To continue my PhD program, I joined Professor Uttam Surana's lab at the Institute of Molecular and Cell Biology (A*STAR, Singapore) and undertook the analysis of DNA damage response in budding yeast. The remaining 3 years of my graduate studies were spent first learning the genetic and molecular biological techniques and then analyzing cells' adaptation to DNA damage.

The format of this thesis reflects this change in the circumstances surrounding my PhD program. The thesis consists of two parts: experimental (Chapters 3, 4) and computational (Chapter 5). The first part (experimental) focuses on investigating the role of Cdc5 polo-like kinase in adaptation, whereas the second part (computational) attempts to unravel the mechanism of gene-expression response due to oscillatory transcription factors.

Table of Contents

Summary

Cells frequently incur genetic damage during their life times. To counter these, eukaryotic cells have evolved surveillance mechanisms, known as checkpoint controls, to detect such damages.

When activated, the checkpoint pathways transiently halt progression through the division cycle. This allows cells to repair the DNA damage by either homologous recombination (HR) or non-homologous end joining (NHEJ). Once the DNA damage is repaired, the cell cycle can resume. Such corrective measures are critical to the maintenance of genomic stability through successive cell divisions.

Cells defective in checkpoint controls accumulate chromosomal aberrations which may eventually lead to uncontrolled division or, in extreme cases, even cell death. Checkpoint pathways are frequently found to be defective in human tumors. However, in some instances when repair responses cannot be mounted, the cells escape the DNA damage imposed arrest and progress to mitosis with damaged DNA. This behavior, which is detrimental to chromosome stability, is known as 'adaptation'. This phenomenon was first observed in the budding yeast *Saccharomyces cerevisiae* (the organism used in this study) [1-3], subsequently, adaptation was also found to occur in Xenopus [4], and in human cells [5]. Although Polo kinase (Cdc5 in yeast) is known to be required for adaptation [3], its exact role remains to be elucidated.

In the first part of this study, we have investigated the role of Cdc5 polo kinase in the adaptive response. We have developed a new method to quantify adaptation in a cell population and have found that ectopic expression of Cdc5 accelerates the adaptation response. This is consistent with our observation that the level of Cdc5

increases as cells prepare to undergo adaptation. High level of Cdc5 activity also suppresses the adaptation defect in cells deficient in Sae2, Ptc2, Ptc3 or Ckb1. We have shown that the requirement of Cdc5 for adaptation is not because of its role in mitotic progression as is generally believed. Instead, Cdc5 activity is necessary for extinguishing the checkpoint and to turn off the checkpoint by inhibiting the recruitment of checkpoint response protein Ddc2 to an unrepaired double-strand-break (DSB). In addition, our model suggests that the prolonged period of G2/M arrest imposed before adaptation, could provide sufficient time for cells to accumulate enough Cdc5 activity needed to overcome the initial inhibition imposed by DNA damage-activated Rad53. Collectively, our results strongly suggest that Cdc5 polo kinase regulates upstream signaling events in the checkpoint pathway during the adaptive response.

In the second part, a mathematical approach was taken to analyze the gene expression response due to oscillatory transcription factors (TFs). Oscillatory TFs have been reported in many diverse biological processes such as the: circadian clock [6, 7], somite segmentation during development [8], DNA damage response [9-12], inflammation [13-15], cell cycle [16, 17] and yeast glucose metabolism [18] (see Table 1). The resultant oscillatory gene expression appears to have specific functions. For instance, different oscillating dynamics of NF-κB activates specific sets of genes [13], and p53 exhibits oscillatory profiles depending on the extent of DNA damage [9, 19, 20]. The effects elicited by oscillating TFs have been demonstrated, but are not well understood.

Our findings stem from the estimated trends of gene expression responses we have modeled. It appears that the various effects caused by oscillatory TFs are intrinsic to the system. As an example (as shown in Figure 24), we have demonstrated

a Hill kinetic system which involves oscillating gene expression and exhibits differential regulation of different target genes, suggesting that an oscillating TF could up-regulate a set of genes while others could be down-regulated or remain unchanged. These changes would not be possible for non-varying TFs without involving other entities. Therefore, oscillatory behaviour provides the TFs with additional degree of dynamics and.renders specificity to their responses. In the context of DNA damage in mammalian cells, an attractive possibility is that p53 may possess similar molecular properties that allow it to selectively up-regulate apoptotic genes upon severe DNA damage. Taken together, our analyses of the mathematical gene-expression models uncover a plausible mechanism to differentially regulate genes - an interesting intrinsic property hidden within the regulatory landscape relevant to gene expression.

List of Tables

List of Figures

List of Symbols

Ab	Antibody
bp	base pairs
CDK	Cyclin Dependent Kinase
DAPI	4', 6-diamidino-2-phenylindole
DDC	DNA Damage Checkpoint
DDR	DNA damage response
DIC	differential interference contrast
DNA	deoxyribonucleic acid
DSB	double-strand break
dsDNA	double-stranded DNA
DTT	Dithiothreitol
EDTA	ethylenediamine tetraacetic acid
g	Gram
Gal	Galactose
GFP	Green Fluorescent Protein
Glu	Glucose
h / hr	Hour
HA	Haemagglutinin
HR	Homologous Recombination
HRP	Horseradish peroxidase
IP	Immunoprecipitation
kb	Kilobases
kDA	kiloDalton
M	Molar
Met	Methionine
mg	Milligram
mins	Minutes
ml	Milliliter
mM	Millimolar
mRNA	messenger RNA
NHEJ	Non-homologous End Joining
nm	Nanometer
^{o}C	degree Celsius
OD	optical density
ODE	ordinary differential equations
PBS	Phosphate-buffered saline
PCR	Polymerase Chain Reaction
PEG	polyethylene glycol
PMSF	phenymethylsulfonylfluoride
raff	Raffinose
RNA	ribonucleic acid
RPA	replication protein A
SDS	sodium dodecyl sulphate
ss	single strand
ssDNA	single-stranded DNA
TE	Tris-EDTA buffer

TF	transcription factor
TRP	Tryptophan
ts	temperature sensitive
URA	Uracil
YEP	yeast extract peptone
µg	Microgram
µl	Microliter
A_M	oscillation amplitude of mRNA intracellular concentration
α_M	mRNA
$\alpha_П$	protein phase-shift
A_P	oscillation amplitude of protein intracellular concentration
A_P^*	normalized protein oscillation amplitude = AP / XP
A_{TF}	oscillation amplitude of TF intracellular concentration
d_M	mRNA self-degradation rate
d_P	protein self-degradation rate
j_M	TF dissociation constant from its gene promoter
k_M	rate of mRNA transcription
k_P	rate of protein translation
M	mRNA
P	intracellular concentration of protein
P_M	mRNA oscillation period
P_P	protein oscillation period
P_{TF}	TF oscillation period
θ_M	transcriptional time-delay
$\theta_П$	translational time-delay
X_M	mean level of mRNA intracellular concentration
X_P	mean level of protein intracellular concentration
X_{TF}	mean level of TF intracellular concentration

Chapter 1 Introduction

1.1 Part 1

Faithful chromosome duplication and maintenance are essential for the survival of all cells. Cell cycle checkpoints are surveillance mechanisms that participate in the coordinated execution of the cell cycle events and thus protect the genome integrity. One such mechanism, the DNA damage checkpoint, inhibits cell cycle progression in response to DNA damage and causes cells to arrest in G2/M until the offending lesions are repaired.

A failure to repair DNA damage prolongs the G2/M arrest. However, cells eventually escape the checkpoint arrest and progress through mitosis with damaged chromosomes [1-3]. This cellular behavior has been termed 'adaptation'. First identified in the budding yeast *Saccharomyces cerevisiae*, studies have shown that adaptation is a reproducible and non-random process [1-3, 21] (also verified in this work), and is under genetic control. As the DNA damage checkpoint pathway and its components are conserved in eukaryotes (see Table 1), it is not surprising that adaptation has been also been reported in *Xenopus* [4] and in human cells [5]. In a teleological sense, 'adaptation' appears to be an anomalous cellular behavior with a high possibility of further chromosome damage which may eventually threaten the fitness and/or survival of the cell. However, keeping with a general belief in the 'evolutionary dictum' that cellular processes are selected for an eventual advantage to the organism, it has been suggested that adaptation provides cells with an opportunity to attempt repair in the subsequent cycle.

Polo-like kinase has been implicated in checkpoint adaptation; but its function has not been elucidated. The first part of this study aims to address the role of polo kinase during the adaptive response. Since yeast cells are amenable to genetic manipulation, and cell cycle regulation is highly conserved between eukaryotes, we have used budding yeast as an experimental system for our studies. Before embarking on a discussion of DNA damage checkpoint control and events associated with it, it is useful to begin with a brief description of the general regulatory landscape of the cell cycle in which the DNA damage response pathways are embedded.

1.1.1 Cell cycle in brief

Every living organism, whether uni- or multicellular, depends on the division process for successful transmission of genetic information that is critical for survival. The cell division process comprises a series of highly regulated molecular events, collectively known as the "cell cycle". The cell cycle is divided into 4 major phases (G1, S, G2 and M) based on chromosomal events. DNA replication occurs in S-phase (Synthesis phase), whereas the duplicated chromosomes are equally partitioned in M-phase (Mitotic phase). G1 and G2 are two gap phases which prepare the cell for the subsequent phases.

Cdks (cyclin-dependent kinases) and their regulatory subunits, cyclins, are among the major drivers of progression through the cell cycle. In the budding yeast, Cdc28 (Cdk1) is the major Cdk that regulates various aspects of the division cycle [22]. It associates with different cyclins to catalyze various events in different phases of the cell cycle. Cdc28, when associated with G1 cyclins (Cln1, Cln2 and Cln3), helps cells undergo START, a stage in late G1 after which cells become irreversibly committed to one cycle of division [23]. This is also the time when the daughter cell

emerges as a small bud from the surface of the parental cell. In the budding yeast, the parental and progeny cells are referred to as mother and daughter respectively. The bud continues to grow throughout the division cycle to reach almost the same size as the mother cell by the end of the cycle, while the mother cell grows minimally. Traversing through START is also a prerequisite for the duplication of centrosomes, the microtubule organizing center (MTOC, also referred to as spindle pole bodies), that play a central role in the assembly of a mitotic spindle in late S phase [24]. Soon after traversing START, Cdc28-Clb5, Clb6 kinase complex promotes initiation of S phase during which DNA is replicated [25-28]. G2 phase is remarkably short in budding yeast. By some estimates, it occupies only 3 mins in a 90-120 mins long division cycle.

The onset of M phase (also referred to as simply ‘mitosis’) is catalyzed by a kinase complex formed by association of Cdc28 with the mitotic cyclins (Clb1, Clb2, Clb3, Clb4). Cdc28-Clb2 kinase contributes a major part of the total Cdc28 mitotic activity [29-31]. At the time of entry into mitosis, the inter-SPB bridge is broken and cells assemble a mitotic spindle. In addition, kinetochore-microtubules emanating from the SPBs establish connection to the chromosomes such that one kinetochore is connected to one SPB while the other is connected to the opposite SPB (bi-orientation). Unlike vertebrate cells, budding yeast cells undergo closed mitosis in which the onset of mitosis is not accompanied by breakdown of the nuclear envelope [32].

1.1.1.1 Chromosome segregation

The duplicated chromosomes or sister chromatids are partitioned equally during transition from metaphase to anaphase. Until the onset of anaphase, sister chromatids are held together by a protein complex known as cohesins. The cohesin complex in the budding yeast is composed of four subunits: Smc1, Smc3, Scc1 and Scc3 [33]. The cohesin subunits are assembled in a roughly 'ring-shaped' structure that encircle the sister chromatids along the entire length of the chromosomes. Segregation of sister chromatids into progeny cells requires dissolution of the cohesion that holds them together. The dissolution of cohesion is accomplished by proteolytic cleavage of cohesin subunit Scc1 by separase, a caspase-like protease encoded by *ESP1* gene [34, 35]. However, cohesin cleavage is controlled by an inhibitory protein called securin (encoded by *PDS1* gene) which is physically associated with the separase. Inhibition of separase by securin ensures that cohesins are not cleaved until the onset of anaphase. Anaphase is triggered by proteolytic destruction of securin by a multi-subunit ubiquitin ligase known as the anaphase-promoting complex (APC) [36, 37]. Once the chromosomes have established a bipolar attachment to the mitotic spindle, APC is activated by its association with Cdc20, an evolutionarily conserved protein [38, 39]. Proteolytic destruction of securin by APC^{Cdc20} sets the separase free, which in turn dissolves sister-chromatid cohesion and allows progressive separation of chromosomes into the mother and daughter compartments by the mitotic spindle. When cells incur 'injuries' to its chromosomes or the mitotic spindle the checkpoint controls disable the chromosome segregation-machinery until the damages are repaired (see below).

1.1.1.2 Mitotic Exit

In telophase, nuclei containing one set of chromosomes each are positioned closer to the cell cortex with a long spindle stretching between them. The final exit from M phase into the G1 phase of the subsequent cycle is the next major transition cells undertake. The most conspicuous event associated with the exit from M phase is the rapid proteolytic destruction of the mitotic cyclins [40-42], which dramatically reduces the mitotic kinase activity. This allows cells to enter G1, trigger the onset of cytokinesis and induce the expression of G1 specific transcripts [43, 44]. Cyclin proteolysis is regulated by a signal transduction pathway known as the mitotic exit network (MEN) involving a small GTPase Tem1, four Ser/Thr kinases namely Cdc15, Cdc5 polo kinase, Dbf2 and Dbf20, Cdc14 phosphatase and the APC [45, 46]. It has been shown that the APC can be activated by Cdc20 or its homologue Cdh1 (APC^{Cdc20} and APC^{Cdh1}, respectively) and that both complexes participate in the destruction of mitotic cyclins [45, 47, 48]. Both APC complexes collaborate to destroy Clb1 and Clb2 cyclins in a biphasic manner [45, 47, 48]. The first wave of cyclin destruction, mediated by APC^{Cdc20}, begins at the onset of anaphase and reduces the cyclin abundance to ~50% by the time cells reach telophase. This is necessary for the activation of APC^{Cdh1} which is inhibited via phosphorylation by mitotic kinase. Reduction in mitotic kinase activity by APC^{Cdc20} paves the way for the activation of APC^{Cdh1} by Cdc14 phosphatase which is released from the nucleolus under the influence of the MEN. Activated APC^{Cdh1} mediates further destruction of mitotic cyclins, thus allowing cells' timely exit from mitosis. Another auxiliary pathway called FEAR (Fourteen Early Anaphase Release) has been proposed to participate in efficient proteolysis of mitotic cyclins [49]. It involves a number of proteins including Cdc5 polo kinase, Slk19, Spo12 and Esp1; however, the exact functional relationship

amongst them is not clear. Unlike MEN, FEAR pathway is not essential for cyclin proteolysis [49, 50]. It has been suggested that while FEAR pathway initiates cyclin proteolysis, MEN maintains it until the mitotic kinase activity becomes sufficiently low to trigger the final exit from mitosis [49, 51]. Hence, proteolytic destruction plays a critical role in the progression of the division cycle.

1.1.1.3 Regulation of Cdk1 activity in budding yeast

Cdk1 (Cdc28) activity is regulated at multiple levels. Regulation of cyclin transcription may be considered as the first level of regulation. During a normal cell cycle, expression of Cln and Clb cyclins occurs in a sequential fashion so that Cdk1 is activated by the appropriate group of cyclins at the right stages of the cell division cycle. The mitotic kinase complex Cdc28/Clb is also regulated post-translationally. The association of Cdc28 and Clb1/2 is inherently unstable; it is stabilized by phosphorylation of a highly conserved Thr167 residue of Cdc28 by Cak (Cdk activating kinase) [52, 53]. Another important modification occurs close to the ATP binding domain at the evolutionarily conserved Tyr19 residue. While phosphorylation of Tyr19 by tyrosine kinase Swe1 (orthologue of fission yeast and human wee1) inactivates the Cdc28 kinase, dephosphorylation of this residue by Mih1 (homologous to fission yeast and human Cdc25) activates the kinase at the onset of mitosis. Unlike in the case of the fission yeast, *SWE1* and *MIH1* in the budding yeast are nonessential genes suggesting that other mechanisms regulating the timely activation of Cdc28 may be present. Tyr19 is also the target of regulation by both the replication checkpoint [54-56] and the DNA damage checkpoint [57]. Cdk inhibitors constitute an additional layer of regulation of the master kinase Cdc28. Sic1, an inhibitor of

Cdc28/Clb kinase, acts at two different stages of the cell cycle: in late G1 where it inhibits the S phase kinase Cdc28-Clb5/Clb6 and regulates the timing of S phase initiation and, in late telophase when it participates in the inactivation of mitotic kinase to aid the final exit from mitosis.

1.1.1.4 Cell cycle regulation by checkpoint pathways

To ensure proper functioning of the cell cycle, the cells employ checkpoints that monitor various cellular events [58]. Four major checkpoints are now known in the budding yeast: morphogenetic checkpoint, DNA replication checkpoint, DNA damage checkpoint (DDC) and spindle assembly checkpoint (SAC). The morphogenetic checkpoint monitors conditions that affect proper bud formation [59]. It responds to a defect in bud emergence and delays the initiation of nuclear division. The replication checkpoint is triggered if DNA synthesis is disrupted, while the DDC responds to any insult to the DNA such as modification of nitrogenous bases or breakage of the phosphodiester backbone (please note that this study will focus on the DDC response triggered by double strand breaks). Any perturbation in the mitotic spindle or a defect in the kinetochore-microtubule attachment, leading to a defect in bi-orientation, is monitored by the spindle assembly checkpoint. In this study, our interest is primarily focused on the DNA damage checkpoint.

1.1.2 DNA damage checkpoint (DDC)

As expected, the DNA damage checkpoint pathway and its components are well-conserved across eukaryotes (see Table 1). The checkpoint components can be broadly classified into three types: sensors, mediators/transducers and effectors [60].

In response to DSB(s) (Double Strand Breaks), the sensors trigger a signaling cascade mediated via transducers; this leads to effector-mediated cell cycle arrest (reviewed in [61]) and subsequent DNA repair, either via homologous recombination or non-homologous end joining (NHEJ). If the damage is repaired, cells proceed through the cell cycle via a recovery process. However, if the damage persists, cells escape from the checkpoint arrest after a prolonged period through a process known as "adaptation". Cdc5, a polo-like kinase, is reported to be essential for adaptation. The following sections summarize the information gleaned from the recent relevant literature.

Role	Sc	Sp	Dm	Vertebrates	Type
Sensor	Ddc1	Rad9		RAD9	PCNA-like
Sensor	Rad17	Rad1		RAD1	PCNA-like
Sensor	Mec3	Hus1		HUS1	PCNA-like
Sensor	Rad24	Rad17		RAD17	RFC1-like
DNA synthesis/sensor	RFC2-5	RFC3		RFC2-5	RFC component
DNA synthesis/sensor	RFA			RPA	ssDNA-binding
synthesis/sensor				BRCA1	BRCT-domain
Mediator				TOBP1	BRCT-domain
Mediator				MDC1	BRCT-domain
Mediator	Rad9	Crb2/Rhp9			BRCT-domain
Mediator	Dpb11	Cut5			BRCT-domain
Sensor/transducer	Mec1	Rad3	Mei-41	ATR	PI3K-like
Sensor/transducer	Ddc2	Rad26	Mus304	ATRIP	ATR-binding
Sensor/transducer	Tel1	Tel1	ATM	ATM	PI3K-like
Transducer	Chk1	Chk1	Grapes	Chk1	Kinase
Transducer	Rad53	Cds1	Chk2	Chk2	Kinase
Multiple	Mre11	Rad32	Mre11	MRE11	Nuclease
Multiple	Rad50	Rad50	Rad50	RAD50	
Multiple	Xrs2	nbs1	Nbs1	NBS1	
Effector			Dp53	p53	Transcription factor
Effector			String	Cdc25A-C	Phosphatase
Effector	Pds1	Cut2		Securin	APC-inhibitor
Effector	Cdc28	Cdc2	Cdk1	Cdk1	Kinase
Polo kinase	Cdc5	Plo1	Polo, Plk4/Sak	Plk1-4	

Table 1. DNA damage checkpoint proteins
DNA damage checkpoint proteins [62] found in *Saccharomyces cerevisiae* (Sc), *Schizosaccharomyces pombe* (Sp), *Drosophila melanogaster* (Dm) and vertebrates. Proteins can be classified into 3 groups: Sensors, Mediator/Transducer, and Effectors. The response pathway is well conserved, since most proteins have homologues / orthologues in other species with similar pathway structure.

1.1.2.1 DNA damage response

In both yeast and mammalian cells, MRX (Mre11–Rad50–Xrs2 in yeast, / Mre11–Rad50–NBS1 in mammalian) complex is among the first to be recruited to the site of DSB in the DNA, and binds directly to either blunt or minimally processed DNA ends (Figure 1) [63-65]. This is independent of DNA resection or Mec1 [63-65]. Subsequently, this complex recruits Tel1 kinase which phosphorylates histone H2A. The endonuclease MRX, Sae2, exonuclease Exo1 and helicase Sgs1 are involved in 5'-3' resection of the DNA ends [66, 67]. The efficency of resection is affected by the cell cycle phases [63]. As DNA is resected, MRX, Sae2 and Tel1 dissociate from the DSB site. However, MRX dissociation is inhibited in *sae2*Δ cells [68]. The newly formed single stranded DNA (ssDNA) with 3' overhang attracts RPA (Replication Protein A) heterotrimer consisting of Rfa1,Rfa2, Rfa3. Subsequently, the bound RPA is joined by the two key transducers: Mec1-Ddc2 heterodimer (ATR/ATRIP in mammals) and 9-1-1 clamp (Rad9/Rad1/Hus1 in mammals, Ddc1/Rad17/Mec3 in *S. cerevisiae*). The 9-1-1 complex is loaded onto the RPA coated ssDNA by Rad24–RFC clamp loader [69]. In the absence of RPA, 9-1-1 can be loaded onto DNA with either a 3'- or 5'-junction [70]. However, if the DNA is coated with RPA, loading of 9-1-1 complex onto the 3'-junction of the DNA is prevented. As for Mec1-Ddc2, its binding to RPA appears to be intrinsic in that the recruitment of Mec1-Ddc2 complex depends on a conserved checkpoint protein recruitment domain (CRD) in Ddc2 [71, 72]. Initial studies [73, 74] reported that 9-1-1 (Ddc1/Rad17/Mec3 in yeast) and Mec1-Ddc2 can bind to the damage sites independently. However later investigations showed that the formation of Ddc2 foci are inhibited in *mec3Δ* cells (in which 9-1-1 would be dysfunctional without one of its subunits). These cells arrested in G1 but not those in S/G2 phase [75]. Moreover, inefficient loading of 9-1-1 in *rad24Δ* cells

prevents Mec1 foci formation [76]. Nevertheless, either complex alone is not sufficient to activate the checkpoint [75-78]. An *in vitro* study [78] demonstrated that Ddc1 can bind to and activate Mec1-Ddc2, which would be necessary to initiate the activation of downstream checkpoint cascades.

In yeast, Mec1 is the primary checkpoint signaling molecule [79]. One of its key functions is to phosphorylate effector kinases, Rad53 (Chk2 in mammals) and Chk1, via the adaptor protein Rad9 [80]. Following this, phosphorylated Rad53 achieves full activation by trans-autophosphorylation. The activated kinases Rad53 and Chk1 are together responsible for a number of downstream responses. These include DNA damage-induced transcriptional regulation, increase in the dNTP pool for DNA repair and inhibition of the progression to mitosis [81].

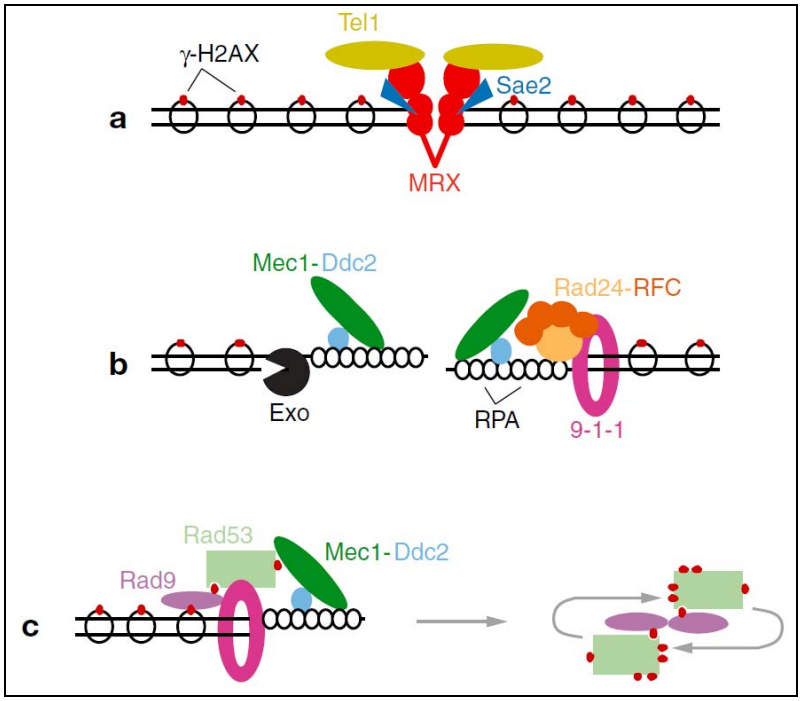

Figure 1. Proteins involved in DNA damage responses due to a DSB.
(a) MRX complex (Mre11, Rad50, and Xrs2; red) are the first checkpoint proteins to bind to the DSB ends. The MRX recruits Tel1 (dark yellow) which create a region of phosphorylated histone H2A (γ-H2AX, red spot on nucleosome). Sae2 (blue wedge) regulates the nuclease activity of the MRX complex.
(b) DNA resection at a DSB is carried out by MRX and Exo1 (black). Resected ssDNA with 3'-end ssDNA recruits RPA heterotrimer (white). The bound Rad24 (orange) with Rfc2-5 (dark orange) loads the 9-1-1 clamp (magenta). In addition, RPA-coated ssDNA attracts the Mec1-Ddc2 heterodimer (green and light blue), which activates the downstream cascade.
(c) Activation of the checkpoint cascade. Rad9 (purple) is recruited by the modified histones including γ-H2AX. Next, the Mec1-phosphorylated Rad9 recruits Rad53 (avocado) for phosphorylation (red dot) by Mec1, probably facilitated by the 9-1-1 clamp. Rad9 and phosphorylated Rad53 then dissociate and multimerize to allow further trans-autophosphorylation, and achieve full activation of Rad53. Chk1 is activated by Mec1 and Rad9 in a similar way.
Reprinted, with permission, from the *Annual Review of Genetics*, Volume 40 © 2006 by Annual Reviews <http://www.annualreviews.org> [61]

1.1.2.2 DNA checkpoint induced cell cycle arrest

In the budding yeast, activation of the DDC leads to a cell cycle arrest. Once DNA damage is detected, the checkpoint signal is transduced via the Mec1 kinase. Mec1 in turn activates two kinases, Rad53 and Chk1 that act in parallel pathways resulting in a cell cycle arrest. Pds1 or securin (the downstream target of Chk1) is an inhibitor of anaphase initiation. Its degradation is a prerequisite for mitotic progression. In a normal cell cycle, Pds1 binds to and inhibits the activity of the separase Esp1 during metaphase thus delaying chromosome segregation [82]. To initiate anaphase, active APC^{Cdc20} complex ubiquitylates Pds1 thereby promoting its degradation. Pds1 degradation releases the Esp1 separase which is now free to cleave cohesins [34]. Once the cohesins are cleaved. the spindle elongates and separation of the sister chromatids ensues.

In *S. cerevisiae*, DDC blocks the metaphase to anaphase transition and hence exit from mitosis [83]. Cells are arrested at metaphase through the action of Rad53 and Chk1 kinases. The activated Rad53 inhibits the Pds1-APC^{Cdc20} interaction while Chk1-dependent phosphorylation of Pds1 prevents Pds1 ubiquitylation and degradation by APC^{Cdc20} [84].

As mentioned earlier, in the budding yeast, two signal transduction cascades, namely the mitotic exit network (MEN) and FEAR control mitotic exit by regulating the localization of the phosphatase Cdc14. Members of the MEN pathway comprise the protein kinases Cdc5, Cdc15, and Dbf2; a GTPase, Tem1; a phosphatase, Cdc14; and Mob1 (a Dbf2 binding protein). Of these, Tem1 is crucial in regulating the MEN pathway. Prior to anaphase, the spindle pole body (SPB)-localized Tem1 remains inactive by virtue of its association with Bfa1-Bub2, a GAP complex. Upon migration

of one of the SPBs into the daughter cell, SPB-associated Tem1 comes into close proximity with its activator Lte1 which is localized to the bud cortex of the daughter cell, leading to the activation of the MEN pathway. At the same time, Cdc5 phosphorylates Bfa1, thus releasing Tem1 from its inhibition by Bfa1-Bub2. The FEAR pathway, on the other hand, consists of the Polo kinase Cdc5, the separase Esp1, the kinetochore-associated protein Slk19, and Spo12. While the MEN pathway secures the release of Cdc14 phosphatase in telophase, the FEAR network contributes to Cdc14 release from the nucleolus during early anaphase. The FEAR-dependent Cdc14 release promotes activation of the MEN pathway by dephosphorylating Cdc15.

However, during the DNA damage checkpoint arrest, Rad53-mediated phosphorylation of Bfa1 promotes its binding to Tem1 which results in the inhibition of Tem1 activity. Activated Chk1 kinase also inhibits the FEAR pathway-dependent Cdc14 release [85, 86].

1.1.3 DNA repair

The DNA repair systems aim to restore DNA to its native state by repairing the offending lesions. In eukaryotic cells, DSBs are repaired by two principal pathways: homologous recombination (HR) and non-homologous end-joining (NHEJ). DNA repair by homologous recombination results in a precise repair of DNA lesions and requires the presence of a homologous template (reviewed in [87]). The template can exist in the form of a homologous chromosome or a sister chromatid [87]., NHEJ-mediated repair, on the other hand, can occur in the absence of homologous sequences. Here, DNA-break ends are ligated, but the end products may contain insertions or deletions. Hence the DNA junctions can vary in their sequence composition. While

NHEJ appears to be the dominant mode of repair in mammalian cells, the predominant form of repair in yeast is HR [88-90]. This is especially so when the homologous template is available in G2 phase or when the yeast is in the diploid state. When HR is not a viable option, e.g. when haploid yeast cells are in the G1 phase, NHEJ appears to be the pathway of choice. The following sections describe in greater detail the molecular processes involved in HR and NHEJ.

1.1.3.1 Homologous recombination (HR)

Genetic analyses of the processes involved in DNA double-strand break repair, as well as mitotic and meiotic recombination in the budding yeast, have resulted in the identification of several genes known collectively as the *RAD52* epistasis group, including Rad50-57, 59, Mre11 and Xrs2 [91-93]. Amongst these, *RAD51* is the most prominent. It has structural homology to *E. coli* RecA and T4 UvsX proteins and is highly conserved among eukaryotes. Rad51 behaves like RecA in homologous DNA pairing and strand exchange.

In response to DNA damage and subsequent generation of ssDNA, the *RAD52* epistasis group mediates replacement of RPA with Rad51 [94]. Like RecA, Rad51 also forms a right-handed helical filament on ssDNA in which the DNA is held in an extended state. The Rad51-ssDNA nucleoprotein filament (also known as the presynaptic filament) contains a binding site for dsDNA and searches for an undamaged homologous sequence. The incoming duplex is integrated into the presynaptic filament and tested for homology. The duplex is held briefly within the secondary binding site of the filament, and if homology is not found, the duplex is released. This process of binding and release continues until homologous DNA is

found. The complementary strand in the duplex molecule is continuously taken up into the presynaptic filament to base pair with the initiating ssDNA, resulting in the extension of the initial DNA joint. This process is termed "DNA strand exchange" or "DNA branch migration". The extent of DNA branch migration is determined by the length of the presynaptic filament. The homologous DNA is used as a template to synthesize new DNA, and forms a D loop structure [95]. The DNA structures are processed by synthesis-dependent strand annealing (SDSA) or via a double Holliday junction. Once resolved, the remaining ssDNA gaps are filled-in and ligated by DNA polymerase and DNA ligase, respectively.

1.1.3.2 Non-homologous end joining (NHEJ)

DNA double-strand breaks (DSB) can be repaired via direct ligation of DSB ends through non-homologous end joining (NHEJ). DNA-dependent protein kinase (DNA-PK), comprising the DNA end binding Ku70/Ku80 heterodimer, the kinase catalytic subunit DNA-PKcs and the DNA ligase IV/XRCC4 complex (the yeast equivalents are Dnl4 and Lif1) are essential components of NHEJ. During NHEJ, DNA ends are brought together by end-bridging factors. Yku70/Yku80 (Ku70/Ku80 in mammals) heterodimers are the first components to recognize and to bind broken DNA ends [96]. In yeast, the Mre11/Rad50/Xrs2 complex associates with DNA-bound Yku70/Yku80 to form an end-bridging complex which holds the broken DNA ends together [97].

However, most DNA double-strand breaks have terminal structures which could not be directly ligated. Hence, the DNA break ends are processed by DNA polymerases and nucleases to generate ligatable termini. Studies in *S. cerevisiae* have indicated a role for the DNA polymerase Pol4 and the DNA structure-specific

endonuclease Rad27 in the processing of these DNA ends leading to end joining by Dnl4/Lif1 which had been recruited to the break-site [98-100]. Rad27 interacts with both Pol4 and Dnl4/Lif1 [101] and these proteins coordinately process and ligate DNA molecules with incompatible 5' ends. The Nej1 protein interacts with Lif1 and enhances the ligase activity of the Dnl4/Lif1 complex for efficient NHEJ [102].

1.1.4 Recovery and adaptation

When yeast cells are subject to a single DSB, the DNA damage checkpoint is activated, and the cells arrest at G2/M phase. Once the DNA damage is repaired, the DDC signal is turned off, and the cell resumes its cell cycle progression. This process is known as 'recovery'. Contrary to the conventional models, if the damage is not repaired, cells are not permanently arrested in G2. Instead, they arrest for a relative long period but eventually escape from the cell cycle arrest and enter M phase. This phenomenon was first observed in the budding yeast [1, 3], and subsequently also reported to occur in human cells [5].

1.1.4.1 Budding yeast

As mentioned earlier, after a prolonged period of arrest spanning 10-12 hrs, yeast cells begin to escape from the arrest and undergo rebudding [2] despite the presence of persistent DNA damage. This phenomenon is known as adaptation. The broken chromosome is inherited for many cell divisions until it is lost.. Adaptable yeast cells exhibit higher viability after exposure to DNA-damaging agents [103], but they are

also more prone to genomic instability such as translocations and break-induced replication.

Thus far, several adaptation defective mutants have been identified; they are *cdc5-ad, ckb1Δ, ckb2Δ, yku70Δ, rad51Δ, tid1Δ, sae2Δ, srs2Δ* and PP2C phosphatase (*ptc2Δ /ptc3Δ*) [3, 68, 104-107]. These mutants fail to adapt and show persistently phosphorylated checkpoint kinase Rad53 [21], underscoring the requirement for the turning-off of the checkpoint prior to adaptation. Consistent with this notion, Ddc2 foci (presence of these foci can be taken as an indication of checkpoint activation), but not Ddc1 foci, disappear during the course of adaptation [74].

Amongst these mutants, *cdc5-ad, yku70Δ*, and *tid1Δ* mutants exhibit a stronger phenotype yet they are normal as far as recovery is concerned [61, 106]. *cdc5-ad* cells contain a point mutation in Cdc5 resulting in the substitution of amino acid residue 251 from Lysine (L) to Tryptophan (W). It is deemed to be a "gain-of-function" mutation with a defective mitotic exit phenotype [108]. Forced inactivation of the checkpoint by shifting *mec1-td* (temperature sensitive degron) mutants to restrictive temperature can suppress *cdc5-ad* [21] adaptation defects. Intriguingly, cells with *rfa1-t11* (a mutation in RPA) are checkpoint defective, and are able to suppress both *yku70Δ* and *tid1Δ* mutant phenotypes, but not that of *cdc5-ad* [21]. On the other hand, Yku70 is known to bind to the DNA ends at the break site to inhibit resection, thus allowing NHEJ to occur. Deletion of *YKU70* leads to an increase in the extent of resection which probably leads to a stronger checkpoint signal, thus inhibiting adaptation [2].

While *cdc5-ad, yku70Δ,* and *tid1Δ* are defective only in adaptation, *ptc2Δ /ptc3Δ, sae2Δ* and *srs2Δ* mutants are unable to recover or adapt. Dephosphorylation of checkpoint proteins is clearly essential for adaptation and recovery. Studies have

shown that PP2C phosphatases, Ptc2 and Ptc3, can mediate the inactivation of Rad53 via dephosphorylation. [107]. The inactivation requires CKII (which includes the Ckb1 and Ckb2 subunits), since CKII phosphorylation of Ptc2 facilitates its interaction with FHA1 domain of Rad53, and subsequently the dephosphorylation of Rad53. In contrast, Sae2 regulates the most upstream of the DDC pathway. Lack of Sae2 in cells causes MRX to remain associated with DNA. This suggests that MRX constitutively triggers the checkpoint, thus preventing recovery [79]. Since Srs2 helicase could remove Rad51 from ssDNA, it is proposed that in *srs2Δ* cells, Rad51 remains associated with DNA and maintains the checkpoint activation through an unknown mechanism. Interestingly, the phenotypic response in adaptation and recovery is not restricted to *S cerevisiae*. The following section describes similar behavior reported in other eukaryotes.

1.1.4.2 Other eukaryotes

In *Xenopus*, egg extracts adapt after a prolonged interphase arrest due to aphidicolin-induced DNA replication checkpoint and enter mitosis with unreplicated DNA [4]. In the presence of aphidicolin, Claspin (checkpoint mediating protein) is phosphorylated. This phosphorylation creates a docking site for Plx1 (the Xenopus homologue of polo-like kinase) and hence ensinuates phosphorylation of Claspin by Plx1. Claspin phosphorylation leads to dissociation of Claspin from the chromatin. Due to a lack of Claspin-facilitated Chk1 phosphorylation by ATR [4], Chk1 is subsequently inactivated. A similar relationship between Plk1 (human homologue of polo-like kinase) and Chk1 was also demonstrated in human cells. During checkpoint recovery after HU or adriamycin-induced DNA damage, Plk1 mediates the phosphorylation of

Claspin, which facilitates its recognition by the β-TrCP-SCF ubiquitin ligase and subsequently ubiquitin-dependent degradation. As a result, Chk1 is inactivated [109-111]. In addition, it is reported that Plk1-mediated degradation of Wee1 is essential for recovery from a DNA damage-induced arrest but not for mitotic entry during a normal cell cycle [112]. Phosphorylation of Wee1 by Plk1 leads to Wee1 degradation, and also to less inhibition on Cdk1/cyclin B complex [112].

Adaptation to DNA damage checkpoint has also been reported recently in human cells [5]. Following ionizing radiation-induced damage, human osteosarcoma cells divided with unrepaired DNA breaks as indicated by the presence of γ-H2AX foci [5]. While excessive amounts of Chk1 or deficiency in Plk1 delays the exit from the G2 checkpoint arrest, suppression of Chk1 activity can accelerate the exit.

1.1.5 Polo-like kinase, Cdc5

Earlier studies have shown that polo-like kinase Cdc5 is essential for adaptation[3]. Therefore, it is of interest to review the current knowledge pertaining to Cdc5 and its functions, in order to set the context for our investigations into its role in adaptation in the subsequent chapters,

Polo-like kinases are evolutionarily conserved proteins which belong to a subfamily of Ser/Thr protein kinases. Each polo kinase contains a N-terminal kinase domain and at least one polo box domain (PBD) in the C-terminal non-catalytic region. There are four polo kinases in mammalian cells (Plk1, Plk2, Plk3, Plk4), three in *Xenopus laevis* and *Caenorhabditis elegans,* two in *Drosophila melanogaster*; but only one in other species like *Schizosaccharomyces pombe* and *Saccharomyces cerevisiae*(Plo1 and Cdc5 respectively) (reviewed in [113]).

In the budding yeast, Polo-like kinase Cdc5 is well known for its multiple roles in mitosis [114]. During mitosis, Cdc5 regulates transcription of mitotic genes through its phosphorylation of Ndd1, a subunit of the Mcm1-Fkh2-Ndd1 transcription factor [115]. In anaphase, an essential role of Cdc5 is to promote chromosome condensation by phosphorylating the subunits of condensin and hence stimulating the latter's DNA supercoiling activity [116]. In addition, phosphorylation by Cdc5 stimulates the cohesins' efficient cleavage and removal by separase [117]. Cdc5 has also been implicated strongly in APC/C regulation and in degradation of cyclin B during anaphase [118, 119]. As a member of the FEAR pathway, Cdc5 mediates the release of Cdc14 phosphatase in early anaphase through direct phosphorylation of the latter [120, 121]. Furthermore, to promote mitotic exit, Cdc5 phosphorylates Bfa1, the negative regulator of the MEN pathway [85]. During cytokinesis, Cdc5 controls Rho1 activation and contractile actin ring (CAR) assembly [122]. Interestingly, despite all these involvements during mitosis, *cdc5Δ* mutant cells can still transit through metaphase and anaphase, but are unable to exit mitosis eventually arresting with a large bud, a long spindle and a divided nucleus. This suggests that the regulation of mitotic exit may be the sole essential function of Cdc5 kinase in mitotic cycle of budding yeast.

Besides mitosis, Cdc5 is also implicated in DNA damage checkpoint and meiosis. During meiosis, it is required for resolution of Holliday junctions, exit from pachytene and chromosome segregation [123-125]. As a mediator of mitosis, Cdc5 is phosphorylated and thus inhibited by Rad53 when the DDC is activated [83, 126]. However, its role during adaptation remains largely unknown.

In this thesis, we explore the role of Cdc5 in the adaptive response to DNA damage. Chapter 2 details, both the experimental and computational methods employed during the course of these investigations. Experimental results from the study on adaptation are presented and discussed in Chapters 3 and 4.

1.2 Part II

Studies on DNA damage and cancer have reported that the extent of p53oscillation (a tumor suppressor) increased with DNA damage [9]. Further literature searches pertaining to transcription factors (TFs) revealed the existence of oscillating gene expression in a myriad of biological processes. In fact, the two widely studied transcription factors (TFs), NF-κB and p53 showed oscillating expression patterns. Different oscillatory profiles of NF-κB lead to the expression of different genes [13-15], and p53 oscillatory behavior is distinctly different in cancerous cells when compared to that in normal cells [19].

The causal relationship between oscillating TFs and different gene expression response is known but not well understood. In the second part of this study, we employed mathematical models (i) to represent gene expression triggered by an oscillating TF and (ii) to elucidate molecular properties that could influence this response. Although the analytical solutions to the general model will not be restricted by specific parameter values, we have used specific values to facilitate the analysis. As gene expression is the center piece of molecular biology, any insights gleaned from this analysis would certainly be helpful.

1.2.1 Gene Expression

The expression level of most genes is regulated by specific transcription factors (TFs) that bind to certain DNA sequence motifs found in the promoter and enhancer regions of genes. Through interactions with components of the transcription machinery, TFs promote access to DNA and facilitate the recruitment of RNA polymerase to the start site for the commencement of transcription [127]. The fact that more than 5% of our genes encode TFs and that many signal transduction pathways frequently end with the activation of TFs underscores the significance of TFs in cell physiology [127-129].

1.2.2 Oscillating Transcriptional Factors

A wide repertoire of diverse TFs has been observed to display oscillatory dynamics such that their intracellular levels vary periodically over time. In particular, TF oscillations occur during key biological processes such as day/night or circadian cycle, somite segmentation in embryogenesis, spermatogenesis, cell cycle and yeast glucose metabolism (summarized in Table 2). On the other hand, response to DNA damage (p53), serum (Stat3 and Smad1/5/8), or receptor ligands (NF-κB) could also induce TF oscillations (Table 4). Interestingly, oscillatory TFs of the latter are each involved in one or more auto-regulatory transcriptional feedback loops wherein their transcriptional activities are inhibited by the respective target gene products. Such feedback loops have been proposed as a mechanistic basis for TF oscillations [130].

At the molecular level, the dynamic occupancy of an oscillatory TF on its target gene promoters tracks its oscillation profile. For instance, both NF-κB and RNA Pol II recruited by it bind to the promoters of target genes (MIP-2, IκBα and IP-10) in close synchrony with NF-κB oscillation profiles [13, 131, 132]. The close

tracing between total and promoter-bound NF-κB is due to rapid turnover of promoter-bound NF-κB by proteasomal degradation, which is a general cellular mechanism to regulate transcription initiation in response to differing TF levels [127, 133-137]. That is, if a signal is prolonged, a newly activated TF will replace the degraded TF, whereas if the signal stops, the degraded TF is not replaced and transcription halts.

1.2.3 Genome widespread oscillating transcription

Depending on the biological processes, external stimuli and cell types, between tens to thousands of transcripts exhibit oscillatory dynamics (Column 4 of Table 2). The oscillatory TFs listed in Table 2 regulate between tens to hundreds of genes (Column 5 of Table 2). However, only a proportion of the oscillatory transcripts are under the TFs' direct control. The remaining transcripts are downstream targets of TF cascades in which the topmost TF is oscillatory. In a TF cascade, a TF induces gene expression of another TF, and so forth (for examples, see Column 5 of Table 2). Indeed, among the oscillatory transcripts, many of them encode TFs. TF cascades are also prevalent in yeast – 188 cascades comprising 3 to 10 levels have been reported [128].

Biological process	Oscillation period	Differential propagation of oscillatory dynamics	Oscillatory transcripts	TF cascades
Circadian	**~ 24hrs**	**28 out of 650 transcripts oscillate in both mouse SCN and liver[6].** **52 out of 933 transcripts oscillates in both mouse heart and liver[7].**	**9995 (14 mouse tissues)[140]** **650 (mouse SCN and liver)[6]** **523 (mouse liver)[7]** **410 (mouse heart)[7]** **134 – 158 (*Drosophila* head)[141, 142]** **85 (rat fibroblasts)[50] [143]** **453 (Arabidopsis)[51] [144]**	**Small subset of oscillatory transcripts are direct transcriptional targets of core circadian oscillator [6, 142].** **Many oscillatory transcripts have no known circadian transcription promoters [141].** **TFs among oscillatory transcripts [140, 142, 143, 145].**
Cell cycle	**1.5 – 2hrs (yeast)[16]** **hrs – days (mammals)[17]**	**Oscillatory E2F1 selectively propagates oscillations to target genes such as cyclin A2, cyclin B1, cyclin B2, cyclin E1 and Rad51 [146, 147]**	**407 – 747 (yeast) [148-150]** **731 (human fibroblasts)[151]** **874 (HeLa S3 cells)[146]**	**Cell cycle genetic networks analysis reveals prevalent TF cascades[128].** **Differential propagation and silencing of oscillations in a 4-level TF cascade[152]: 2 TFs → 12 TFs → 33 TFs → 30 TFs.** **G1 TFs → G2 TFs → M TFs → G1 TFs[148, 149, 153, 154].** **Examples:** **a. TF Sep1p forkhead → TF Ace2p → G1 phase genes** **b. TF Mob1/Df2 → TF Cdc14 → Sic1 & APC/Cdh1** **c. TF Cdk/Cln3 → TF Swi4/Swi6 → TF Cdk/Cin5,6 → Cdc45** **d. TF Cdk/Cln3 → Swi4/Swi6 → Cdk/Cln1,2**
Yeast metabolic cycle[18]	**40min[155]** **4 – 5hr[18]**		**3552[18]**	**60% of annotated TFs oscillate[18]. Examples:** **a. Cellular reduction: TF Cbf1 → TFs Met4, Met28, Met31, Met32 → oscillatory genes protein[155].** **b. Amino acid biosynthesis: TF Gcn4p → TF Met4 → oscillatory genes protein[155].**
Somite segmentation in embryogenesis [156-159]	**94 – 112min[156]**	**Not all components of a pathway oscillates[156]**	**At least 36 genes (estimated to be 50 – 100)[156]**	**TFs among oscillatory transcripts [156].**
Spermatogenesis[160]	**12hr[160]**	**Oscillatory CREB regulate target genes exhibiting CREs (cAMP response element) in their promoters [161-167].**		

Table 2. Summary of reported oscillatory gene expressions in key biological processes.

(Table 2 – continued on next page)

(Table 2 - continued from previous page)
Oscillation period (column 2) refers to the time interval between successive maxima or minima of the transcript's intracellular concentration. An oscillatory transcription factor (TF) does not necessarily induce oscillatory expression of its target gene transcripts (column 3). In a TF cascade (last column), TF at the upper level expresses TF at the immediate lower level, and so forth.

Species	E	Periods
Bacillus subtilis	**Periodic synthesis of OCT-ase, ACT-ase, DHQ-ase and histidase.**	**1h**
Pseudomonas aeruginosa	**Periodic synthesis of creatine dehydrogenase; Oscillation in amidase activity.**	**2h; 40min**
E. coli	**Periodic synthesis of beta-galactosidase; Periodic synthesis of pyruvate synthesizing enzymes.**	**50min; 1h**
Klebsiella aerogenes (bacteria)	**Long-period oscillation in respiration**	**4h**
Saccharomyces cerevisiae	**Periodic synthesis of glutamate dehydrogenase; Periodic synthesis of alpha-glucosidase.**	**6.5h; 1.5h**
Chinese hamster cells	**Periodic activity of lactate dehydrogenase, aldolase and G6P dehydrogenase.**	**3 – 4h**
Rat, in vivo	**Oscillation in haem biosynthesis**	**10h**
Sea-urchin embryo	**Cyclic protein synthesis**	**0.5 – 1h**

Table 3. Summary of reported oscillations in protein synthesis.
Oscillation period of protein synthesis ranges from 40min to 6.5hr [245]. These proteins could also be regulated by oscillatory TFs.

Oscillatory TF	TF oscillation period	Stimulus	Oscillatory transcripts	TF cascades
NF-κB	**100min[14]**	**TNF[13-15], VP16[14], LPS[15], RANK-L[15]**	**5970[168]**	**Targets 200 – 300 genes that including TFs [139, 169, 170]**
p53	**4 – 7hrs [9-12]**	**DNA damage**	**51[19, 171]**	**Targets more than 100 gene including TFs [171, 172]**
Stat3	**2hr[173]**	**Serum[173], IL-6[173]**	**Target cell proliferation and cell survival genes [174-177]**	
Smad 1/5/8	**2hr [173]**	**Serum[173], BM4[173]**		

Table 4. Summary of reported oscillatory gene expressions induced under specific stimuli.
See caption of Table 2 for definition of column description. Note that the oscillatory TFs listed in Column 1 are each involved in a negative-feedback loop wherein the TF quantity or transcriptional activity is inhibited by its target gene.

1.2.4 Various examples of oscillating transcription

The following sections aim to discuss the roles and significance of oscillating transcription.

1.2.4.1 NF-κB

NF-κB is a family of transcription factors regulating myriads of genes including those involved in cell division, apoptotic, stress response and inflammation [138, 139]. Upon stimulation, NF-κB protein oscillation is induced. In addition, studies have shown that the profile of oscillation depends on the type and length of stimuli [14]. For instance, continuous TNFα stimulation leads to sustained (damping slowly) NF-κB oscillations with a period of ~100 min for >20 hrs, whereas treatment with topoisomerase II inhibitor etoposide (VP16) showed damped oscillations with a lower amplitude [14].

Furthermore, different oscillatory profiles could lead to differential gene expression. Short stimulation of NF-κB activates genes such as IP-10 while RANTES induction required prolonged activation [13]. This highlights the significance of oscillation in signal transduction.

1.2.4.2 p53 response to DNA damage.

p53 is a well researched tumor suppressor which acts as a TF that targets 122 genes (Table 4). Activated DNA damage checkpoint leads to damped oscillations in the levels of p53 and its inhibitor, Mdm2 [9]. The oscillation period could range from 4 to

7 hrs, but the phenomenon could last for as long as three days. It appears that the number of peaks depends on the extent of DNA damage [9].

A recent study had proposed that p53 oscillation could facilitate apoptosis in cells [20]. Consistently, it was reported that the oscillatory response of p53 in fibroblast cells from Bloom's syndrome patients was markedly different from normal cells [19]. This implies a correlation between oscillation and phenotypic response.

1.2.4.3 Circadian

Circadian clock is a conserved biological oscillator tracking the day/night cycle of Earth. In mammals, the circadian rhythm is controlled by a master clock in suprachiasmatic nuclei (SCN) of the hypthalamus [178, 179]. 16 known genes comprises this control network in mammals [180], including two TFs. Interestingly, there are about 400 to ~10000 genes that displayed circadian oscillations found in mouse tissues [140], even though only a small subset of these genes are direct targets of the core oscillator.

Evidently, oscillations could propagate from the core control. However, not all of its targets would exhibit similar dynamics. A study showed that only 28 of the 644 oscillating circadian transcripts are common to both mouse SCN and liver cells [6]. Likewise, another study reported that out of 933 circadian transcripts, only 52 are common to both mouse heart and liver [7]. This suggests that the core clock can limit the propagation of its oscillatory dynamics to specific gene and cell types.

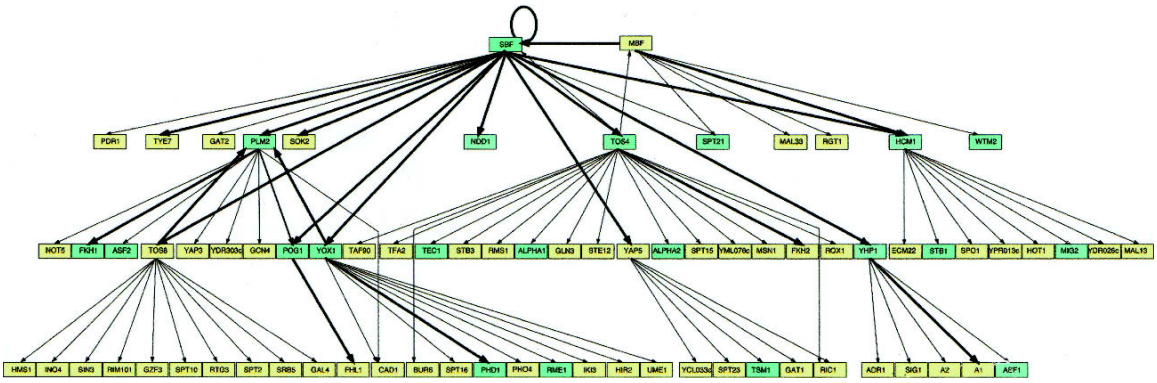

Figure 2. Transcription factor network of SBF and MBF
"The network illustrates the regulation of transcription factors and promoters of other transcription factor genes. Bold arrows indicate an interaction that has been verified by PCR assay [152]; green boxes correspond to genes that have a cell cycle periodicity of expression."
Figure and caption adapted from Horak et al 2002 [152].

1.2.4.4 Cell cycle

Genetic network analyses in yeast have revealed the presence of prevalent transcriptional cascades [128]. For instance, SBF (Swi4-Swi6 cell cycle box binding factor) and MBF (MluI binding factor) are two transcriptional regulators of G1/S that bind to promoters of 235 genes [181]; these include 12 TFs which control another 33 TFs. Through these TF cascades, SBF and MBF control expression of hundreds of genes. Although the expression profiles of SBF and MBF oscillate, expression of several of their downstream targets do not show cell cycle periodicity (Figure 2), implying some form of oscillation silencing [152]. Serial cascades of TFs were found to be responsible for CDK-independent periodic gene expression during cell cycle progression. Such a 'ring network' is also a positive feedback loop, resulting in an amplification of molecular signals. Naturally, a form of oscillation propagation control is in place.

Our computational work is presented in Chapter 5 with some supplementary results documented in the Appendices. In Chapter 5, we formulate the mathematical models (Section 5.2.1) and, the solutions derived from these models are presented in Section 5.2.2. In Section 5.2.3, we estimated the trends of the gene expression response and the summary is tabulated in Table 10. Section 5.2.4 documents the possible effects of oscillating TFs on differential gene expression and their implications are discussed in Section 5.3. Finally, in Chapter 6, we present our general conclusions and perspectives stemming from this part of the work.

THIS PAGE IS INTENTIONALLY LEFT BLANK

THIS PAGE IS INTENTIONALLY LEFT BLANK

Chapter 2 Materials and Methods

2.1 Yeast strains and culture conditions

All *Saccharomyces cerevisiae* strains are derivatives of JKM139 (non-repairable) or tGI354 (repairable) and listed in Table 5. (Please refer to Section 3.1 for an introduction to the strains JKM139 and tGI354.) A combination of standard molecular biology and molecular genetic techniques such as gene transplacement, gene disruption, PCR-based tagging of endogenous genes and tetrad dissection were used to construct plasmids and strains with various genotypes. PCR and Southern blot analysis were performed to confirm gene disruptions and transplacements. Deletion of various genes (*CKB1, SAE2, PTC3, ARG4*) that were replaced by a KANMX cassette were done by gene transplacement using PCR amplified deletion cassettes of the relevant strains from *Saccharomyces Genome Deletion Project* [182]. Strains with proteins tagged with yeCitrine or yeVenus were constructed using one-step tagging protocol as described in earlier studies [183, 184].

Yeast cells were grown in YEP medium (1.1% yeast extract, 2.2% peptone and 50mg/l adenine) supplemented with 2% raffinose/ 0.5% glucose, 2% glucose or 2% galactose/2% raffinose depending on the objectives of the experiments. Since deletion of *CDC5* is lethal, *cdc5Δ* cells were kept alive with a methionine-repressible *MET-CDC5* construct. *cdc5Δ MET-CDC5* cells were grown in methionine free synthetic media (0.67% yeast nitrogen base from Difco, amino acid drop out mix) with 2% raffinose/ 0.5% glucose, 2% glucose or 2% galactose/2% raffinose. Yeast cells were grown in a water bath at 24^{o}C with constant shaking for good aeration at 200rpm. Temperature sensitive mutants were cultured at the permissive temperature

of 24°C, but filtered and transferred to restrictive temperature at 30°C to impose telophase arrest. To induce HO endonuclease, 2% galactose was added to the glucose-free-medium, which is normally supplemented with 2% raffinose..

Strain	Genotype	Source
JKM139 / US4877	MATa *hoΔ hmlΔ::ADE1 hmrΔ::ADE1* ade1-110 leu2-3,112 lys5 trp1::hisG ura3-*52 ade3::GAL10::HO*	[2]
tGI354 / US5332	*hoΔ hmlΔ::ADE1 MATa-inc hmrΔ::ADE1* ade1 leu2-3,112 lys5 trp1::hisG ura3-52 *ade3::GAL::HO* arg5,6::HPH::MATa	[106]
US5338	*hoΔ hmlΔ::ADE1 MATa-inc hmrΔ::ADE1* ade1 leu2-3,112 lys5 trp1::hisG ura3-52 *ade3::GAL::HO* arg5,6::HPH::MATa *bar1Δ*	this study
US5339	MATa *hoΔ hmlΔ::ADE1 hmrΔ::ADE1* ade1-110 leu2-3,112 lys5 trp1::hisG ura3-*52 ade3::GAL10::HO bar1Δ*	this study
US5750	MATa *hoΔ hmlΔ::ADE1 hmrΔ::ADE1* ade1-110 leu2-3,112 lys5 trp1::hisG ura3-*52 ade3::GAL10::HO bar1Δ slk19Δ::LEU2 cdc15-2*	this study
US5776	*hoΔ hmlΔ::ADE1 MATa-inc hmrΔ::ADE1* ade1 leu2-3,112 lys5 trp1::hisG ura3-52 *ade3::GAL::HO* arg5,6::HPH::MATa *bar1Δ slk19Δ::LEU2 cdc15-2*	this study
US5828	MATa *hoΔ hmlΔ::ADE1 hmrΔ::ADE1* ade1-110 leu2-3,112 lys5 trp1::hisG ura3-*52 ade3::GAL10::HO bar1Δ slk19Δ::LEU2 cdc15-2 GAL-myc6-CDC5::TRP1*	this study
US5880	MATa *hoΔ hmlΔ::ADE1 hmrΔ::ADE1* ade1-110 leu2-3,112 lys5 trp1::hisG ura3-*52 ade3::GAL10::HO bar1Δ slk19Δ::LEU2 cdc15-2 RAD53-HA2::URA3*	this study
US5881	*hoΔ hmlΔ::ADE1 MATa-inc hmrΔ::ADE1* ade1 leu2-3,112 lys5 trp1::hisG ura3-52 *ade3::GAL::HO* arg5,6::HPH::MATa *bar1Δ slk19Δ::LEU2 cdc15-2 RAD53-HA2::URA3*	this study
US5866	MATa *bar1Δ hoΔ hmlΔ::ADE1 hmrΔ::ADE1* arg5,6Δ::HPH::*MATa-inc* ade1-100 leu2,3-112 lys5 trp::hisG *ade3::GAL::HO cdc15-2 slk19Δ::URA3 MET-CDC5-LEU2 cdc5Δ::TRP1*	this study
US5868	MATa *hoΔ hmlΔ::ADE1 hmrΔ::ADE1* ade1-110 leu2-3,112 lys5 trp1::hisG ura3-*52 ade3::GAL10::HO cdc5Δ::TRP1 MET3-CDC5-LEU2*	this study
US5885	MATa *hoΔ hmlΔ::ADE1 hmrΔ::ADE1* ade1-110 leu2-3,112 lys5 trp1::hisG ura3-*52 ade3::GAL10::HO bar1Δ slk19Δ::LEU2 cdc15-2 RAD53-HA2::URA3 ckb1Δ::KANMX*	this study
US5909	MATa *hoΔ hmlΔ::ADE1 hmrΔ::ADE1* ade1-110 leu2-3,112 lys5 trp1::hisG ura3-*52 ade3::GAL10::HO cdc5Δ::TRP1 MET3-CDC5-LEU2 RAD53-HA2::URA3*	this study
US5998	MATa *hoΔ hmlΔ::ADE1 hmrΔ::ADE1* ade1-110 leu2-3,112 lys5 trp1::hisG ura3-*52 ade3::GAL10::HO bar1Δ slk19Δ::LEU2 cdc15-2 RAD53-HA2::URA3 sae2Δ::KANMX*	this study
US5999	MATa *hoΔ hmlΔ::ADE1 hmrΔ::ADE1* ade1-110 leu2-3,112 lys5 trp1::hisG ura3-*52 ade3::GAL10::HO bar1Δ slk19Δ::LEU2 cdc15-2 GAL-myc6-CDC5::TRP1 RAD53-HA2::URA3*	this study
US6072	MATa *hoΔ hmlΔ::ADE1 hmrΔ::ADE1* ade1-110 leu2-3,112 lys5 trp1::hisG ura3-*52 ade3::GAL10::HO bar1Δ slk19Δ::LEU2 cdc15-2 RAD53-HA2::URA3 ckb1Δ::KANMX GAL-myc6-CDC5::TRP1*	this study

US6106	MATa *hoΔ hmlΔ::ADE1 hmrΔ::ADE1* ade1-110 leu2-3,112 lys5 trp1::hisG ura3-*52 ade3::GAL10::HO bar1Δ slk19Δ::LEU2 cdc15-2 RAD53-HA2::URA3 sae2Δ::KANMX GAL-myc6-CDC5::TRP1*	this study
US6215	MATa *hoΔ hmlΔ::ADE1 hmrΔ::ADE1* ade1-110 leu2-3,112 lys5 trp1::hisG ura3-*52 ade3::GAL10::HO bar1Δ slk19Δ::LEU2 cdc15-2 RAD53-HA2::URA3 ptc2Δ ptc3Δ::KANMX*	this study
US6266	MATa *hoΔ hmlΔ::ADE1 hmrΔ::ADE1* ade1-110 leu2-3,112 lys5 trp1::hisG ura3-*52 ade3::GAL10::HO bar1Δ slk19Δ::LEU2 cdc15-2 RADd53-HA2::URA3 ptc2Δ ptc3Δ::KANMX GAL-myc6-CDC5::URA3*	this study
US6267	MATa *hoΔ hmlΔ::ADE1 hmrΔ::ADE1* ade1-110 leu2-3,112 lys5 trp1::hisG ura3-*52 ade3::GAL10::HO bar1Δ slk19Δ::LEU2 cdc15-2 arg4Δ::KANMX*	this study
US6350	MATa *hoΔ hmlΔ::ADE1 hmrΔ::ADE1* ade1-110 leu2-3,112 lys5 trp1::hisG ura3-*52 ade3::GAL10::HO bar1Δ slk19Δ::LEU2 cdc15-2 DDC2-yeVenus::KANMX myc-CDC5::TRP1*	this study
US6380	MATa *hoΔ hmlΔ::ADE1 hmrΔ::ADE1* ade1-110 leu2-3,112 lys5 trp1::hisG ura3-*52 ade3::GAL10::HO cdc5Δ::TRP1 MET3-CDC5-LEU2 DDC2-yeCitrine::URA3*	this study
US6381	MATa *hoΔ hmlΔ::ADE1 hmrΔ::ADE1* ade1-110 leu2-3,112 lys5 trp1::hisG ura3-*52 ade3::GAL10::HO cdc5Δ::TRP1 MET3-CDC5-LEU2 DDC2-yeCitrine::URA3*	this study
US6382	MATa *hoΔ hmlΔ::ADE1 hmrΔ::ADE1* ade1-110 leu2-3,112 lys5 trp1::hisG ura3-*52 ade3::GAL10::HO bar1Δ slk19Δ::LEU2 cdc15-2 DDC2-yeCitrine::URA3*	this study
US6391	MATa *hoΔ hmlΔ::ADE1 hmrΔ::ADE1* ade1-110 leu2-3,112 lys5 trp1::hisG ura3-*52 ade3::GAL10::HO bar1Δ slk19Δ::LEU2 cdc15-2 arg4Δ::KANMX GAL-myc6-CDC5::TRP1*	this study
US6416	MATa *hoΔ hmlΔ::ADE1 hmrΔ::ADE1* ade1-110 leu2-3,112 lys5 trp1::hisG ura3-*52 ade3::GAL10::HO bar1Δ slk19Δ::LEU2 cdc15-2 DDC2-yeCitrine::KANMX GAL-myc6-CDC5::URA3*	this study
US6446	MATa *hoΔ hmlΔ::ADE1 hmrΔ::ADE1* ade1-110 leu2-3,112 lys5 trp1::hisG ura3-*52 ade3::GAL10::HO bar1Δ slk19Δ::LEU2 cdc15-2 DDC1-yeCitrine::KANMX*	this study
US6448	MATa *hoΔ hmlΔ::ADE1 hmrΔ::ADE1* ade1-110 leu2-3,112 lys5 trp1::hisG ura3-*52 ade3::GAL10::HO bar1Δ slk19Δ::LEU2 cdc15-2 DDC1-yeCitrine::KANMX GAL-myc6-CDC5::URA3*	this study

Table 5. Yeast strains used in this study.

2.2 Plasmids

For cloning purposes and plasmid DNA amplification, *E. coli* XL1 Blue cells (Stratagene) were used as bacterial hosts. The *E. coli* cells were cultured in either 2X TY liquid medium (1.6% bacto- tryptone, 1% bacto- yeast extract, 0.5% NaCl) or on 2X TY plates containing 2% bacto agar at 37°C. 100μg/ml Ampicillin (Sigma) were added to the medium or plates for selection of cells carrying recombinant plasmids.

Name	Description	Source
pUS149	pJGsst1-*bar1Δ:URA3*	US Lab
pUS1450	YIPlac204-*slk19Δ:LEU2*	US Lab
pUS1857	YIPlac211-5' truncated *Rad53-HA2*	US Lab
pUS2224	pUC19-*cdc15-2-GFP-URA3*	US Lab
pUS2536	pBluescript II *ptc2Δ::hisG-klURA3-hisG*	this study
pUS2451	YIPlac204-*GAL-cmyc6*-CDC5-TRP1	this study
pUS2433	YIPlac211-*GAL-cmyc6-CDC5 -URA3*	this study
pUS2583	pGEM-11Z(+) vector containing part of *MATa* locus.	this study
pUS2589	YIPlac204-5'UTR-cmyc6-*CDC5*(truncated)-*TRP1*	this study

Table 6. List of plasmids used in this study.

2.3 Yeast strains and culture conditions

To synchronize cells in G1 phase, cycling yeast cells were diluted to an absorbance of 0.5 at OD_{600}, and yeast pheromone α-factor was added at 1μg/ml (for *bar1Δ*) or 5μg/ml (for *BAR1*). After incubation for 2 hrs at 24°C, the cultures were filtered, washed and re-suspended in liquid medium.

For *cdc5Δ MET-CDC5* strains, cultures were grown and diluted in methionine free medium with 1μg/ml α-factor. After 1.5 hrs, methionine was added to final concentration of 20mM. Subsequently, after another 0.5 hr, cultures were filtered, washed and re-suspended into YEP medium supplemented with 20mM methionine and the desired carbon source.

2.4 Yeast transformation

Yeast cultures were grown overnight. Cells were collected and spun down at 3500 rpm for 2 minutes. Subsequently, the pellets were washed once with Li-TE buffer (0.1M lithium acetate, 10mM Tris-HCl pH 7.5, 1mM EDTA) and then resuspended in 2ml of Li-TE buffer. The cells were incubated on a roller at room temperature for 1 hr. For each transformation, 10µl of 1mg/ml salmon sperm DNA, linearized DNA of interest or plasmid DNA, 100µl of cells in Li-TE buffer and 140µl of 70% PEG 6000 were mixed and incubated at 24^{o}C for 3 hrs. This was followed by a heat shock (30mins) at 43^{o}C. Finally, cells were spun down, resuspended in 80µl sterile H_20 and spread onto the appropriate selective plates.

2.5 Yeast DNA extraction

Yeast cells were pelleted, washed with ddH_20 and resuspended in 0.2 ml of spheroplasting mix containing 80% SCE (1M Sorbitol, 0.1 M sodium citrate, 0.06 M EDTA, pH 7.0), 10% lyticase and 10% β-mercaptoethanol. The mixture was incubated at 37^{o}C with occasional shaking for 1 hr or more when required (cells were checked under microscope for complete digestion of cell). Upon complete lysis, 0.2ml SDS solution (2% SDS, 0.1M Tris-HCl, 0.05M EDTA) was added to the mixture and the mixture was heated at 65^{o}C for 5mins. 0.2ml 5M KOAc was added and the mixture incubated on ice for 20mins. The mixture was centrifuged at 13000rpm for 5mins. The supernatant was transferred to a fresh tube containing 0.2ml 5M NH_4OAc and 1ml isopropanol and the DNA precipitated in dry ice for 5mins. The DNA pellets were collected by low speed centrifugation for 5mins, washed once in 70% ethanol, and dissolved in 50µl TE or ddH_20.

2.6 Southern blot analysis

Chromosomal DNA was digested at 37^{o}C (> 12 hrs) in a total volume of 100µl. The restriction enzyme digest was set up as follows: 10µl DNA, 10µl 10X restriction buffer, 1µl EcoR1, 1µl 10mg/ml RNAse and 78µl sterile water. The digested DNA was precipitated by addition of 10µl 3M sodium acetate (pH 5.2), 1µl 0.5M EDTA (pH 8) and 200µl cold ethanol in dry ice for a minimum of 10mins. The samples were centrifuged at 13000rpm for 10mins. The supernatant was discarded and the pellets rinsed in 80% ethanol. The DNA pellet was dried and dissolved in 15µl 1X gel loading buffer (6X gel loading buffer: 0.25% bromophenol blue, 0.25% xylene cyanol FF, 15% Ficoll [Type 400; Pharmacia] in water). The DNA samples were loaded onto 1% agarose gels in 1X TBE (Tris-borate/ EDTA; 0.09M Tris-borate, 0.002M EDTA) running buffer. A few µl of ethidium bromide (10mg/ml) was added to the gel to stain the DNA fragments. The DNA fragments were imaged using a UVIdoc gel documentation system (Uvitec, Cambridge). Subsequently, the gel was denatured with 0.5N NaOH, 1.5M NaCl for 1 hr and neutralized with 1M TrisHCl (pH 7.4), 1.5M NaCl for 1 hr. Next, the gel was transferred to nylon membrane (Amersham Hybond N, GE Healthcare) according to Sambrook et al 1989 [185]. After the transfer, the membrane was prehybridized for a minimum of 1 hr (without radioactive probe) and hybridized overnight at 65^{o}C with radioactive α-^{32}P dATP labeled probe (prepared using random priming kit from Roche Boehringer Mannheim and radioactive label from NEN). The hybridization mix contained 0.46 volumes sterile water, 0.0046 volumes 10mg/ml denatured salmon sperm DNA and 0.56 volumes of Scp/ Sarc/ DS mix. To make Scp/ Sarc/ DS mix, 20 g Dextran sulphate was dissolved in 60 ml of 20 X Scp (2M NaCl, 0.6M Na2HPO4, 0.02M EDTA, final pH 6.2), topped up to 101 ml with sterile water before addition of 7 ml of 30% SLS (sodium lauroyl sarcosine). The

mix was filtered. After hybridization, the blots were washed in 2 X SSC/ 0.1% SDS (2 X 15mins at 65^{o}C) and then in 0.1 X SSC/ 0.1% SDS (2 X 15 mins at 55^{o}C). The blot was then exposed to film at -70^{o}C for appropriate amount of time before the films were developed. Probe A was generated using PCR with oligos: OUS 1761 (Probe_AF: Sequence 5' -ATG TCC TGA CTT CTT TTG ACG AGG-3') and OUS 1762 (Probe_AR: Sequence 5'-CCG CAT GGG CAG TTT ACC T-3') [186].

2.7 Southern blot analysis with single-stranded probe

2.5g agarose was melted in 250ml of 50mM NaCl, 1mM NaCl to make a 1% agarose gel. The gel was submerged in 50mM NaOH, 1mM EDTA (pH 8) and allowed to equilibrate for 30mins or more. Chromosomal DNA was digested at 37^{o}C (> 12 hrs) in a total volume of 100µl. The restriction enzyme digest was set up as follows: 10µl DNA, 10µl 10X restriction buffer, 1µl Ssp1, 1µl 10mg/ml RNAse and 78µl sterile water. The digested DNA was precipitated by addition of 10µl 3M sodium acetate (pH 5.2), 1 µl 0.5M EDTA (pH 8) and 200µl cold ethanol in dry ice for a minimum of 10 mins. The samples were centrifuged at 13000 rpm for 10mins. The supernatant was discarded and the pellets rinsed in 80% ethanol. The DNA pellet was dried and dissolved in 15µl 1X alkaline gel loading buffer (6X alkaline gel loading buffer: 300mN NaOH, 6mM EDTA, 18% Ficoll, 0.15% bromocresol green, 0.25% xylene cyanol FF). The DNA samples were loaded onto 1% alkaline agarose gels and run at 30V (4^{o}C, 15 hrs) in freshly made alkaline electrophoresis buffer (50mN NaOH, 1 mM EDTA pH 8). After the DNA had been loaded and after the dye had migrated out of the loading slot, glass plates were put onto the gel to prevent the dye from diffusing out of the agarose.

The gel was stained with ethidium bromide (0.5μg/ml) in 1X TAE (0.04M Tris-acetate, 0.001M EDTA pH 8) electrophoresis buffer (two washes of 2 hrs each). The gel was soaked in 0.25N HCl for 6 – 7mins, rinsed with water and immersed in denaturing solution (0.5N NaOH, 1.5M NaCl) for 30 mins with gentle agitation. The gel was rinsed briefly with water before being transferred onto nylon membrane (Amersham Hybond N, GE Healthcare).

The blots were hybridized as described above but at 50^{o}C and with α-^{32}P rCTP labeled probe (α-^{32}P rCTP at 10 μCi/μl from NEN) prepared with Promega's Riboprobe in vitro Transcription System kit and purified using ProbeQuant G50 microcolumns (Amersham, GE Healthcare). After hybridization, the blots were washed in 2 X SSC/ 0.1% SDS (2 X 15mins at room temperature) and then in 0.1 X SSC/ 0.1% SDS (2 X 15mins at 50^{o}C). The blot was then exposed to film at -70^{o}C for appropriate amount of time before the films were developed.

2.8 Real-Time PCR (RT-PCR)

Yeast DNAs were extracted as described in Section 2.5. To minimize interference from DNA secondary structure, the chromosomal DNAs were digested using StyI (10µl 10X NEB buffer, 2µl StyI enzyme, 1µl RNase and 77µl H_20). StyI is used as its recognition site is commonly found in the yeast genome sequences. Thus, the restriction enzyme would cleave the chromosomes into shorter fragments, thereby reducing the tendency to form DNA secondary structure. Next, the digested samples were normalized to 10ng/µl. RT-PCR reactions containing 10µl 2x SYBR Green (Bio-Rad), 1µl DNA (20ng/µl), 0.5µl forward primers (100µM), 0.5µl reverse primers (100µM) and 8µl H_20 were prepared. The sequences of primers used are as follows:

HOsite:	(ous2059) 5'-CGGGTTTTTCTTTTAGTTTCAGCTTTCCGC-3' and (ous2060) 5'-ACCTCCGTCACGACCACACTCT-3';
Arg5,6:	(ous2481) 5'-GCGCAACAGCAAAGTGGCGG-3'and (ous2582) 5'-TCATCGCCGCCGGTGAAGGT-3'

The RT-PCR cycle program is as follows:

RT-PCR cycling:	Step 1: 95.0 °C for 03:00. Step 2: 95.0 °C for 00:10. Step 3: 57.0 °C for 00:30. Step 4: 72.0 °C for 00:40. Data collection Step 5: 72.0 °C for 10:00.	Repeat step 2-4 for 40x
Melting curve data collection:	Step 6: 95.0 °C for 01:00. Step 7: 55.0 °C for 01:00 Step 8: 55.0 °C-95.0 °C for 00:10. Increase set point temperature after cycle 2 by 0.5 °C Step 9: 15.0 °C forever.	

.

Data were analyzed by IQ5 optical system software version 2 (Bio-Rad). To ensure accuracy, each sample was run in triplicates and procedure repeated 3 times. The results were then combined and analyzed.

2.9 Protein extraction using TCA

Frozen yeast samples were thawed, washed once and resuspended in ddH20. Next, the samples are normalized to absorbance of 2.0 at OD600 (1 ml final volume). To each normalized sample, 150µl YEX lysis buffer (1.85 M NaOH, 7.5% β-mercaptoethanol) was added. After 10 mins' incubation on ice, 150µl 50% TCA was added and the mixture again incubated on ice for 10mins. The protein pellets were collected by centrifugation at 4^{o}C for 10mins at 13000rpm and resuspended in 50µl of 1X gel loading buffer and 10µl 1M Tris-HCl (pH 8.0). The samples were boiled for 5mins, and 8µl were loaded onto SDS-PAGE gels for Western blot analysis.

2.10 Western blot analysis

Protein samples were resolved by sodium dodecyl sulphate polyacrylamide gel electrophoresis (SDS-PAGE) using 10% acrylamide:bis-acrylamide (29:1) gels. For analysis of Rad53, 12% acrylamide:bis-acrylamide (79:1) gels were used.

S/N	Antibodies	Source
1	Rabbit polyclonal anti-cmyc	Santa Cruz Biotechnology, Inc
2	Rabbit polyclonal anti-HA	Sigma-Aldrich
3	Mouse monoclonal anti-cmyc	Santa Cruz Biotechnology, Inc
4	Mouse monoclonal anti-HA	Santa Cruz Biotechnology, Inc
5	Rabbit polyclonal anti-G6PDH	Roche Diagnostics
6	Goat polyclonal anti-Rad53	Santa Cruz Biotechnology, Inc
7	Rat monoclonal anti-Tubulin YOL1/34	Serotec

Table 7. List of antibodies used in this study

2.11 Protein extraction using acid washed glass beads

For immunoprecipitation, protein was extracted using acid washed glass beads. Cells were spun down and washed once with Stop Mix buffer (0.9%NaCl, 1mM NaN3, 10mM EDTA, and 50mM NaF). Cell pellets were immediately frozen by liquid nitrogen, and stored in -20^{o}C for later use. Cell pellets were later thawed on ice. 0.2 ml of ice cold lysis buffer with protease inhibitors (1% Triton X-100, 1% sodium deoxycholate, 0.1% SDS, 50mM Tris- HCl pH 7.2, 1mM PMSF, 20µg/ml leupeptin, 40µg/ml aprotinin, 0.1mM Na-orthovanadate, 15mM p-nitrophenylphosphate) and 150-200µl of acid-washed glass beads (Biospec) were added. The cells were lysed by vigorous vortexing at 4^{o}C (IKA-Vibrax shaker). After centrifugation at 4^{o}C for 15 mins at 13000 rpm, the supernatant was transferred to a fresh Eppendorf tube, quick frozen in liquid nitrogen and stored at -80^{o}C for later use. Protein concentration was determined by using the Bradford Protein Assay (Bio-Rad) according to manufacturer's instructions.

2.12 Co-immunoprecipitation

Collected samples were lysed using the glass bead method as described above; the lysis buffer was modified: NP40 buffer (20mM Tris HCl pH 8, 150mM NaCl, 10% glycerol (Fresh), 1% Nonidet P-40 or NP-40, 2mM EDTA, 1mM DTT) supplemented with protease inhibitors (1mM PMSF, 20µg/ml leupeptin, 40µg/ml aprotinin, 0.1mM Na-orthovanadate, 15mM p-nitrophenylphosphate). Next, 1mg of cell lysate was transferred to an Eppendoff tube containing 40µl of antibody-conjugated beads (Santa Cruz). The final volume was adjusted to 1ml with lysis buffer containing protease inhibitors so that the cell lysate can interact with the antibody-conjugated beads completely. This was followed by 3-4 hrs of incubation in a roller at 4^{o}C. The beads

were then washed 4-6 times with lysis buffer. After removing all the remaining supernatant, 5µl of 5× gel loading buffer was added to the beads. The samples were heat inactivated by boiling for 5mins and loaded for SDS- PAGE electrophoresis and subsequent Western blot analysis.

2.13 Sample preparation for SILAC mass spectrometry

Samples for mass spectrometry were prepared as described in [187, 188]. To prepare samples for SILAC [189], the yeast strains must be defective in endogenous lysine or arginine production, thus facilitating the incorporation of exogenous amino acids. Therefore, *ARG4* and *LYS1* were deleted. Control yeast strain, US6267 (control) was grown overnight in liquid labeling medium (6.7% Yeast nitrogen base, 30mg/L [$^{13}C_6/^{15}N_4$] L-arginine and 30mg/L [$^{13}C_6/^{15}N_2$] L-lysine, Cambridge Isotope Laboratories, and other normal amino acid mix), while the other strain, US6391, was grown in non-labeling medium (6.7% Yeast nitrogen base supplemented with complete normal amino acid mix including 30mg/L arginine and 30mg/L lysine). Both cultures were supplemented with the desired carbon source. Samples were collected and frozen in liquid nitrogen immediately. The samples were thawed on ice, and the proteins were extracted using the glass bead method (refer to Section 1.1). 5 mg of crude extracts (both labeled and unlabelled) were subjected to immunoprecitation as described in Section 2.12, except that 50 µl of beads were used. The beads from labeled and unlabelled samples were mixed just before the washing steps. Prior to boiling, the beads were resuspended in sample buffer (NuPAGE LDS Sample Buffer, Invitrogen). Finally, the protein samples were sent to our collaborator

(Dr Gunraratne from Walter Blackstock' Lab) for subsequent 1D gel electrophoresis, in-gel trypsin digestion and mass spectrometric analysis.

2.14 Immunofluorescent staining (IF)

Yeast samples were immediately fixed with 3.7% formaldehyde, collected by centrifugation and, resuspended in 1ml KPF buffer (0.1M KH_2PO_4 pH6.4, 3.7% formaldehyde) and left at room temperature for 1-2 hrs. The cells were washed 3 times with 0.1 M KH_2PO_4 pH 6.4, and once in 1ml sorb/phos/cit buffer (1.2 M sorbitol, 0.1M K2HPO4 pH5.9, 0.7% citric acid). To digest the cell wall, cells were resuspended in 0.2ml sorb/phos/cit buffer, 20µl glusulase and 5µl 10mg/ml lyticase, and incubated at 37^{o}C for 15-90 mins. The digested cells were washed once with sorb/phos/cit buffer and re-suspended in 20µl of the same buffer. 5µl of cell suspension was applied to one well of a 30 -well slide previously coated with 0.1% polylysine (Sigma). The slide was immersed first in methanol at -20^{o}C for 6 mins, and then acetone at -20^{o}C for 30 secs. Next, the slide was air-dried and the samples incubated with primary antibody overnight at 4 ^{o}C. Samples were washed 3 times with PBS-BSA (1% BSA, 0.04M K_2HPO_4, 0.01M-KH_2PO_4, 0.15M-NaCl, 0.1% NaN_3) and incubated with secondary antibodies for 2 hrs at 30 ^{o}C. The samples were washed 4 times as before, Finally, mounting medium Vectashield (Vector Laboratories) containing DAPI (4',6 diamidino-2-phenylindole) was added to each well. Coverslips were added to protect the samples and the coverslips sealed in place with nail polish. For visualization of tubulin, rat monoclonal anti-tubulin YOL1/34 was the primary antibody (Serotec) and Alexa Fluor 594 goat anti- rat IgG (Invitrogen, Molecular Probes) the secondary antibody.

2.15 Microscopy

To visualize signals from the YFP variant fusion proteins, cells collected at various time points were frozen immediately in dry ice without fixation and stored until further use. Cells were later thawed and mounted on slides with Vectashield containing DAPI (Molecular Probes). The images were captured using a Zeiss AxioImager upright motorized microscope with Plan Apochromat 100X objective equipped with EXFO 120W metal halide illuminator and attached to a Photometrics CoolSNAP HQ2 high sensitivity monochrome camera driven by the Metamorph software (Universal Imaging Corporation) or Zeiss Axiovert 200M Microscope connected to a Photometrics COOLSNAP HQ digital camera driven by Metamorph software.

2.16 Flow cytometry analysis (FACS)

Yeast samples were resuspended in 1ml 70% ethanol and incubated at room temperature for 1 hr or overnight at 4^{o}C. After fixation, the samples were washed with 0.2M Tris-HCl pH7.5, 20mM EDTA, and resuspended in 100µl 0.2M Tris-HCl pH7.5, 20mM EDTA, 0.1% RNase A (1mg/ml), before incubating at 37^{o}C for 4 hrs. The samples were washed 1X in PBS and incubated in 0.1ml PI solution (50mg/ml propidium iodide in PBS) at 4^{o}C overnight. The samples were diluted by addition of 900µl PBS and samples were sonicated for 5 secs. The DNA content was determined using the FACScan flow cytometer (Becton Dickinson Immunocytometry Systems, USA). The data was analyzed using WinMDI program.

2.17 Effects of TF oscillations on gene expression

To obtain trends of target gene products mean level (X_M and X_P), oscillation amplitude (A_M and A_P) and phase-shift (α_M and α_P) as a function of each kinetic parameter in each model, first and second partial derivatives with respect to each parameter were derived. The directional trend and properties of possible stationary points were inferred from the signs of the first and second partial derivatives respectively. On the other hand, by equating the first and second partial derivatives to zero, possible stationary points and points of inflexion were identified and the conditions for their existence determined.

2.18 Numerical simulations

To obtain time-series trajectories of species' concentrations in the model, the ODEs were integrated using a modified Rosenbrock formula of order 2 that is implemented in the MATLAB (The MathWorks, Natick, MA) platform (version 6.5, Release 13). Source codes are displayed in the Appendices.

THIS PAGE IS INTENTIONALLY LEFT BLANK

THIS PAGE IS INTENTIONALLY LEFT BLANK

Chapter 3 Adaptation in cells with Telophase trap

3.1 Background

Double strand beaks (DSB) are amongst the most detrimental DNA lesions which can pose a grave threat to a cell's viability [190, 191]. The cell's response to such damages and the subsequent repair of these lesions involve a close coordination between cell cycle machinery and the repair pathways. In the budding yeast, a DSB activates the DNA damage checkpoint which leads to a G2/M arrest; thus allowing the cell sufficient time to repair the damage. In yeast, DSBs are repaired predominantly by the homologous recombination repair pathway (HR) or, less frequently, by non-homologous end joining (NHEJ) [88-90]. In the event that cells are unable to repair the damage, the cells continue to arrest in G2/M for a longer period but they finally escape the DNA damage imposed cell cycle arrest and enter mitosis with damaged chromosomes (a process termed "adaptation"). Subsequent segregation of these damaged chromosomes subjects cells to further chromosomal aberrations.

To understand the mechanism behind the adaptation phenomenon, we have adopted an experimental system [2] in which cells transiently express the HO endonuclease. The cells suffer one DSB at a defined chromosomal site and consequently arrest in G2/M. HO (homothallic) endonuclease is normally expressed by yeast cells during mating type switching. To initiate mating type switching, the HO endonuclease recognizes a specific site in the *MAT* locus and introduces a double strand break [192, 193]. The *MAT* locus, located on chromosome III, contains an active genetic-information-cassette (*MATa* and *MATα*) and two silent cassettes, *HMLα* (on the left) and *HMRa* (on the right). The DSB close to the active *MATa* (or α)

cassette initiates a gene conversion event during which the silent cassette of the opposite mating type is used as a donor template to 'convert' the active *MAT* cassette to the opposite mating type. Although the end-purpose of the gene-conversion event is to switch the mating type information, it can be considered as an event that utilizes homologous regions to repair the DSB. We use this innate cell-behavior to construct two basic strains (Figure 3) from which we derive many other strains for our study: (i) the 'repairable' (RP) contains a mutated *MATa* cassette (denoted as *MATa-inc*) on chromosome III (Chr III) but lacks both silent cassettes (*HMLα* and *HMRa*) [106]. In addition, it contains a copy of the *MATa* cassette on chromosome V (Chr V). While the *MATa-inc* cassette is resistant to HO endonuclease, it can be used as a homologous template to repair a DSB in the *MATa* copy. This strain also expresses HO endonuclease from the galactose-inducible *GAL10* promoter, hence HO induction can be controlled. (ii) The 'adaptable' or 'non-repairable' strain (AD) is almost identical to the 'repairable strain'; the differences being that the *MATa* cassette (Chr III) is not mutated and that it lacks a copy of *MATa* on Chromosome V. When a DSB is introduced at the active *MATa* cassette (Chr III), this strain is unable to repair the DSB using homologous recombination. Consequently, these cells will arrest in G2/M for an extended period and undergo adaptation i.e. enter mitosis with the DSB in chromosome III.

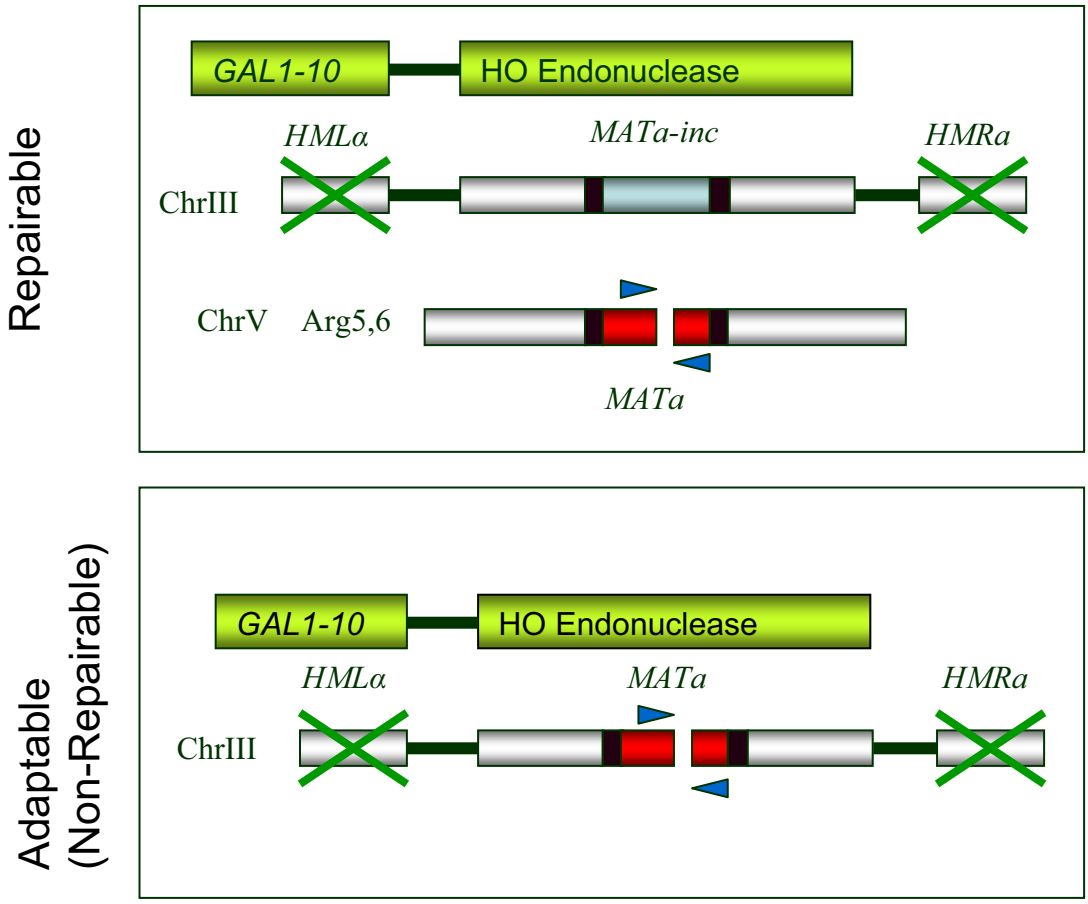

Figure 3. Schematics of the Repairable (RP) and Adaptation (AD) strains.
The experimental systems used in this study each contains a galactose-inducible HO endonuclease, and lacks both silent cassettes (*HMLα* and *HMRa*). In addition, the repairable (RP) strain contains a mutated *MATa-inc* cassette (at the endogenous site, ChrIII) which is non-cleavable by HO, and a copy of cleavable form of *MATa* cassette inserted at chromosome V (ChrV). Thus, if HO is expressed and generated a cut at ChrV, the RP strain is able to repair the DSB via homologous recombination (HR) using the template at ChrIII. On the other hand, the adaptable (AD) strain contains the normal *MATa* cassette at ChrIII which could be recognized and cut by HO. However, lacking a homologous template, the strain is unable to repair via HR. In addition, if the HO is persistently induced and cut at ChrIII, repair by non-homologous end joining through simple ligation will be prevented. Arrows ("▶" , "◀") refer to annealing sites of RT-PCR primers.

What approach should one take to quantitatively ascertain the adaptive response in a cell population? In previous studies, the adaptive response has been monitored by the emergence of new buds and dephosphorylation of Rad53. However, in order to construct a new bud, a cell undergoing adaptation has to escape the G2/M arrest, traverse mitosis, complete mitotic exit, enter G1, and undergo START. These transitions require several components which may not be involved in checkpoint adaptation per se. Adaptation, therefore, has been monitored in terms of an event distant from G2/M. Moreover, the escape from G2/M arrest is not synchronous i.e. cells undergo bud emergence at different times and do not halt cell cycle progression after the bud has emerged. Thus, bud emergence as a marker for adaptation tends to underestimate the degree of adaptation in a cell population. The fact that the G2/M checkpoint causes DNA-damaged cells to arrest prior to chromosome segregation suggests (in a teleological sense) that the primary aim of this surveillance mechanism is to prevent segregation of damaged chromosomes. Indeed, in yeast, the DNA damage checkpoint inhibits chromosome segregation by preventing cohesin cleavage [194-196]. We reasoned that the 'proportion of cells undergoing chromosome segregation' (completion of anaphase) may serve as an apt parameter for monitoring adaptation. Hence, to prevent adapted cells from exiting mitosis, we introduced *cdc15-2* and *slk19Δ* mutation into both repairable and adaptable strains. Efficient exit from mitosis requires two pathways, namely, MEN (mitotic exit network) and FEAR (fourteen early anaphase release) [49, 197]. While Cdc15 is an essential component of MEN, Slk19 is an effector of FEAR pathway [49]. Cells deficient in both Cdc15 and Slk19 functions are, therefore, unable to exit mitosis and arrest in telophase with a large bud, segregated chromosomes and a long spindle at 30ºC. Having responded to a DSB, both repairable and adaptable cells carrying *cdc15* and *slk19* mutations will be

expected to undergo chromosome segregation and accumulate in telophase. The proportion of these cells in a given population can thus be easily quantified.

Since we are utilizing a different approach for quantifying cells' behavior, we first characterized the recovery (in repairable strain) and adaptive responses (in non-repairable strain) in these modified genetic backgrounds. In this chapter, we describe the results of this study.

3.2 Results

3.2.1 The telophase trap using combined deficiencies of Cdc15 and Slk19

For our experiments, it is imperative that cells escaping from G2/M arrest in telophase and do not exit mitosis. Mitotic exit requires proteolytic destruction of mitotic cyclins (Clb1 and Clb2 in budding yeast) catalyzed by a signaling pathway known as the mitotic exit network (MEN). Cdc15 kinase is an essential component of MEN. A mutant carrying temperature-sensitive allele of *CDC15*, namely *cdc15-2*, is unable to exit mitosis and arrests in telophase at 37°C. Therefore, *cdc15-2* mutation can serve as a telophase trap. However, we have noticed that cells' ability for adaptation is compromised at 37°C (data not shown). In our laboratory, an earlier attempt to identify mutations in genes, which would render MEN pathway completely inactive in combination with *cdc15-2* allele at semi-permissive temperature (30°C), had yielded Slk19 (*Hong Hwa Lim, personal communication*). Subsequently, Slk19 was shown to be a component of the FEAR network [49], an auxiliary pathway required for efficient exit from mitosis, though not essential for it. Further characterization showed that *cdc15-2 slk19Δ* double mutant cells are unable to exit mitosis at 30°C and uniformly arrest in telophase with divided nuclei and long spindles, presumably due to inactivation of both the MEN and FEAR pathways. We found that the ability of non-repairable (hence adaptable) cells to undergo adaptation at 30°C is comparable to that at 24°C (data not shown). Therefore, we used the combined deficiencies of Cdc15 and Slk19 at 30°C as a 'telophase-trap' in our experiments.

3.2.2 Recovery and adaptation in cells with telophase trap

As briefly mentioned above, the RP strain carries *GAL10* promoter-driven *HO* endonuclease gene, *hmlαΔ-MATa-inc-hmraΔ* on chromosome III, *MATa* on chromosome V and *cdc15-2 slk19Δ* mutations to allow cells to be trapped in telophase at 30ºC. *MATa-inc* on Chromosome III is mutated in this strain; hence it is resistant to HO-induced cleavage. Thus, a DSB is introduced only at the *MATa* cassette on chromosome V upon HO induction. The AD strain carries the same markers; it does not however contain an extra *MATa* copy and therefore cannot repair the DSB in *MATa* cassette by HR.

To study the kinetics of cell cycle progression in response to a DSB in RP (US5881) and AD (US5880) strains, cells were synchronized in G1 by α-factor treatment in YEP+raff and then released at 30ºC into YEP+raff+gal to induce HO expression (hence introducing a DSB). HO was expressed throughout this experiment. Samples were withdrawn at different time points and processed for immunofluorescence staining, Western blotting and real-time PCR (RT-PCR). By the 4^{th} hr after release, RP cells had accumulated at G2/M with a large bud, short spindle and an undivided nucleus due to activation of the DNA damage checkpoint (Figure 4). Unlike the AD strain, Rad53 hyper-phosphorylation is not detected after the release, probably due to efficient HR repair (but other studies have reported transient Rad53 phosphorylation which disappears very rapidly [106]). RP cells begin to undergo anaphase at 4^{th} hr with ~80% cells reaching telophase by 14 hrs, as indicated by the presence of divided nuclei and a long spindle. Progression into mitosis is accompanied by the disappearance of the hyper-phosphorylated forms of Rad53 suggesting that the checkpoint is extinguished as cells initiate anaphase. AD cells also arrest at G2/M with a large bud, a short spindle and an undivided nucleus. As

expected, Rad53 is hyper-phosphorylated indicating that checkpoint is activated in response to DSB. However, these cells remain arrested in G2/M for ~8 hrs after which they begin to divide their nuclei at 10 hrs (about 10% cells in telophase as opposed to 50% cells in RP strain at the same time point) (Figure 4C). The proportion of AD cells in telophase reaches almost 80% at 14 hrs.

To ascertain if the DSB is still present in cells that have progressed to telophase, we used both Southern blot analysis and real-time polymerase chain reaction (RT-PCR). In the case of Southern blot analysis, a specific probe corresponding to the region containing the HO cleavage site was used to follow the fate of the DSB. As shown in Figure 5, HO-induced DSB in RP strain is indicated by the progressive disappearance of the 3kb fragment and concomitant appearance of two smaller (2.1 kb and 0.9 kb) fragments. Reappearance of the larger size fragment in RP cells, coincidental with increasing proportion of telophase cells suggests that the DSB is repaired. Disappearance of the 6.5 kb fragment and appearance of smaller-size fragments are also observed in AD cells after induction of HO. However, the 6.5 kb fragment never reappears even after a high proportion of cells have reached telophase (Figure 4C). This suggests that AD cells escape G2/M arrest and traverse to telophase without repairing the HO-induced double strand break. RT-PCR analysis (Figure 5C) using primers specific to HO-susceptible region further confirmed that while RP cells repair the DNA legion, DSB is still present in AD cells even though ~80% cells have reached telophase (Figure 4C).

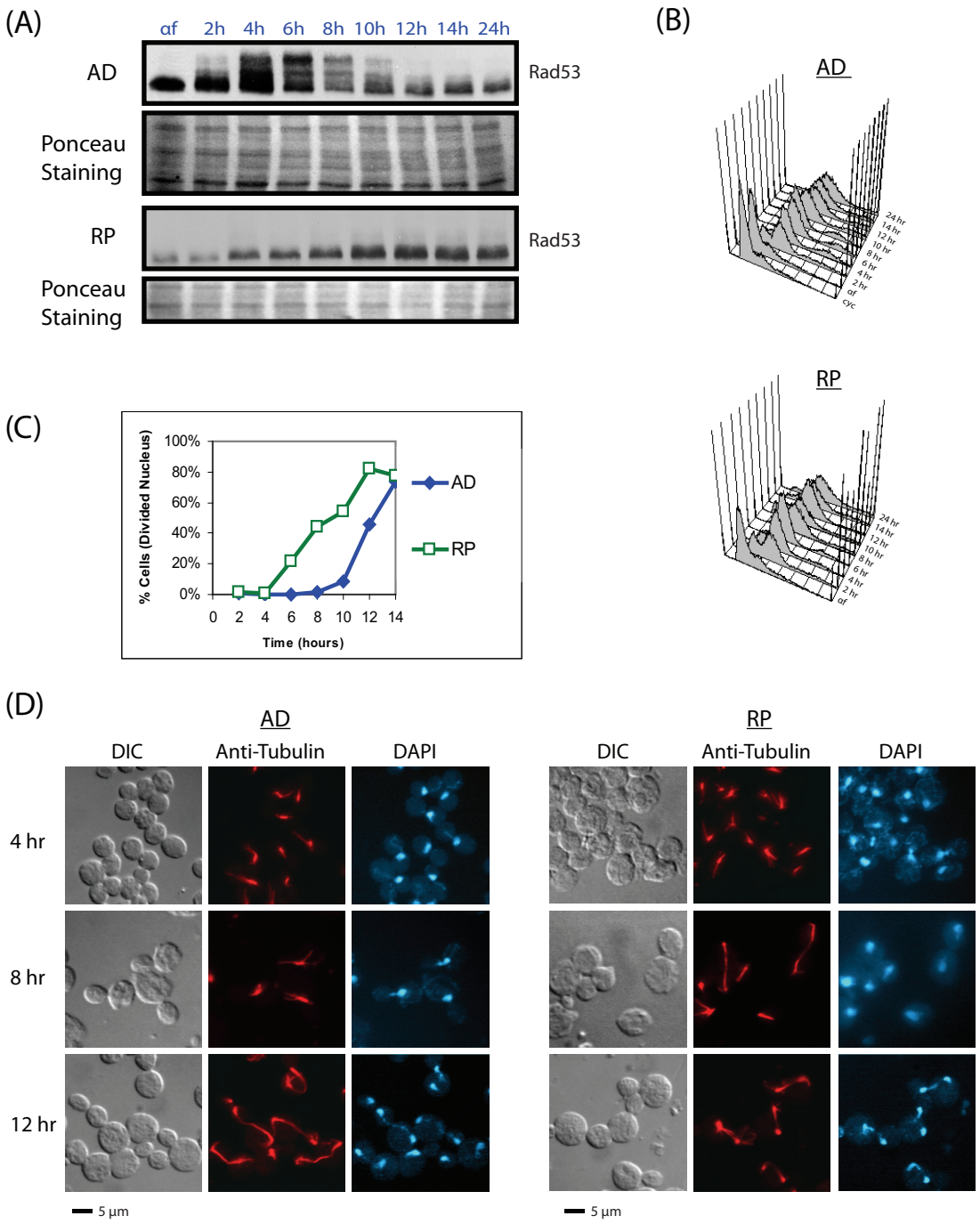

Figure 4. Adaptation and recovery in cells with telophase trap.
AD (US5880) and RP (US5881) cells were synchronized at G1 with α-factor in YEP+raff medium, and released into cell cycle in YEP+raff/gal medium at 30^{o}C. Samples were collected every 2 hrs for 14 hrs. **(A)** Western blot analysis and **(B)** FACS profiles are shown. **(C)** The plot shows percentage of cells with divided nucleus at the indicated times. **(D)** The state of the spindle and nuclear division were monitored using anti-tubulin antibodies (Red) and DAPI (Blue).

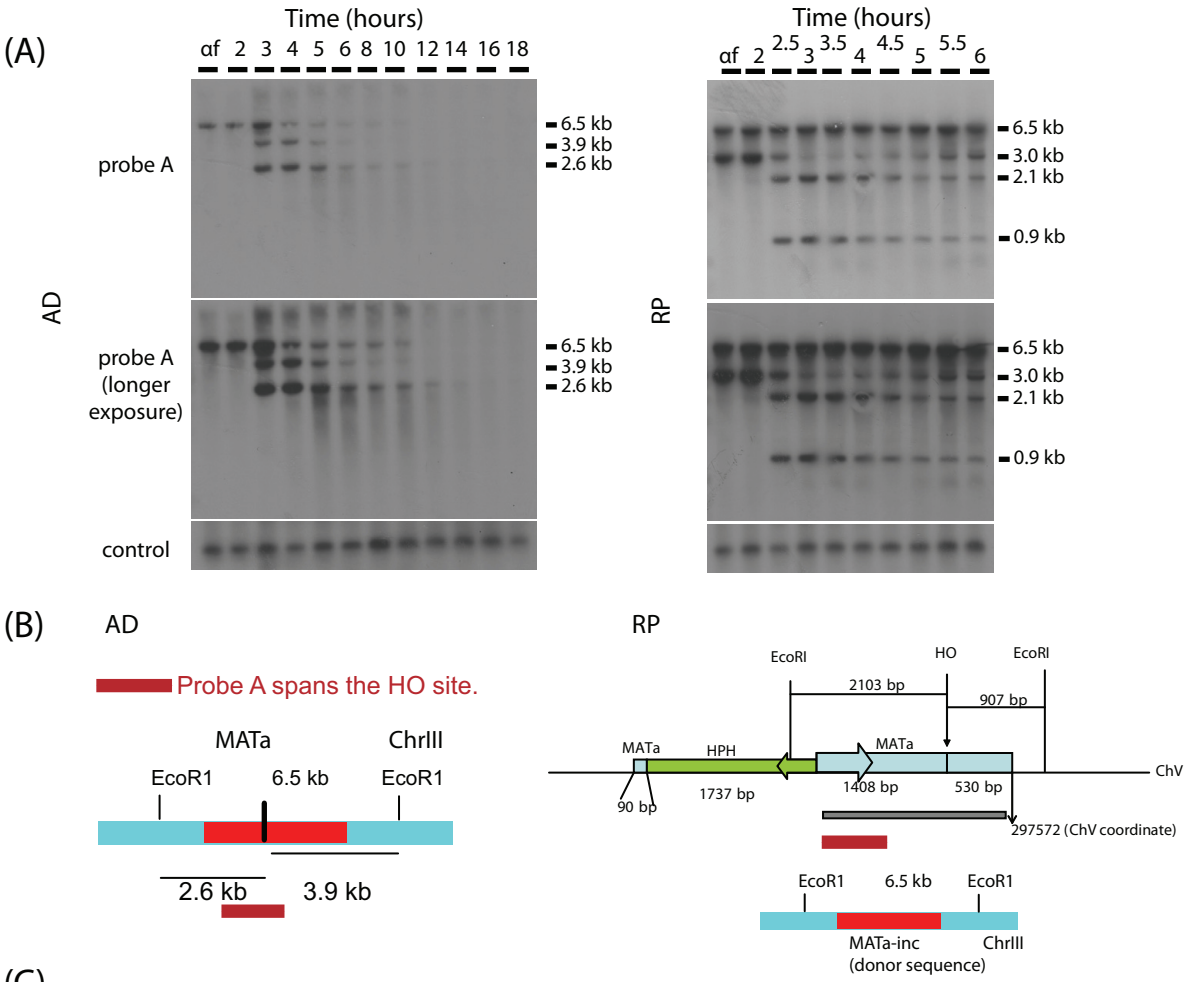

Figure 5. Southern blot and RT-PCR analysis in AD and RP cells.
DNA from AD (US5880) and RP (US5881) cells were subjected to Southern Blot and RT-PCR analysis.
(A) Southern blot hybridization of DNA samples obtained from AD and RP strains. Probe A, spanning the HO site, is used as the probe. The sizes of the DNA fragments are indicated on the right of the blot.
(B) Schematics of EcoRI sites at the *MATa* locus in RP and AD strains. For AD strain, a 6.5kb band indicates an intact HO site. If the HO site cleaved, 3.9kb and 2.6kb bands are released. For RP strain, in addition to the 3 kb band spanning the HO site, a 6.5kb is detected due to presence of *MATa-inc* sequences. If HO site is cleaved, the 3 kb band yields 2.1 kb and 0.9 kb fragments.
(C) Real-time PCR results. Chromosomal DNAs are digested with EcoRI, and subjected to Real-Time PCR reactions. A 166bp PCR fragment spanning the HOsite is amplified. Plots show the normalized fold change at the indicated times for the respective strains (AD and RP).

3.2.3 Dramatic loss of viability in AD cells

Since AD cells escape G2/M arrest and progress through mitosis without repairing the DNA lesion, they would be expected to lose viability as more chromosome aberrations are introduced during segregation. Hence we compared the loss of viability in RP (US5338) and AD (US5339) strains as they overcome G2/M arrest to progress through mitosis. The strains used in this study do not contain the telophase trap so as to allow colony formation. The RP and AD strains were synchronized in G1 by α-factor treatment in YEP+raff medium and then were allowed to resume cell cycle progression in YEP+raff+gal medium to induce HO expression. Cell samples were withdrawn after 2 hrs, plated on YEP+raff+gal plates and incubated for 72 hrs to allow colony formation. While >70% of RP cells formed colonies, ~0.1% of AD cells were able to so (Figure 6A), suggesting that AD (non-repairable) cells undergo a dramatic loss of viability.

It was somewhat surprising that a few AD cells do eventually form colonies. Therefore, we examined the state of the HO-susceptible region by analyzing the DNA of 14 colonies obtained from both RP and AD strains (these strains were used in the experiment described in the preceding paragraph). The DNA was isolated and sequenced over the HO-cleavable region. As expected, the DSB in the HO-susceptible region had been repaired in all fourteen clones and the sequence was identical to the 'homologous region' (on chromosome III, see Figure 5) used during HR repair. On the other hand, in the surviving AD colonies, the sequence in this region of all fourteen clones showed mutations or small deletions (Figure 6B). Because of these changes, this region is no longer susceptible to HO endonuclease. These results suggest that AD cells (which are unable to undergo repair by HR) lose their viability

dramatically when they escape G2/M arrest without repairing the DSB. The very small percentage of cells which are able to survive are those that have managed to undertake error-prone repair and thus, have introduced mutations in this region.

(A)

	(i) AD	AD	(ii) RP
Cells Plated	50,000	100,000	500
Avg Survival	36	78	366
% Percentage	0.072%	0.078%	73.2%
Normalized%	0.098%	0.107%	85%

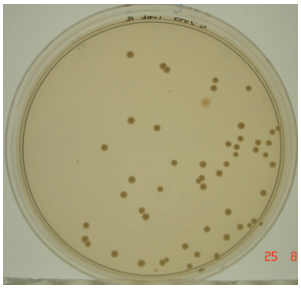

(i) AD
Plated: 50k
Colonies: ~36

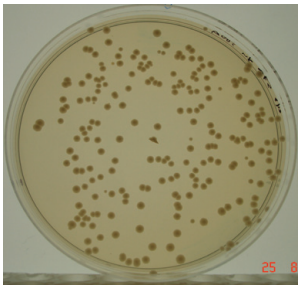

(ii) RP
Plated: 500
Colonies: ~366

(B)

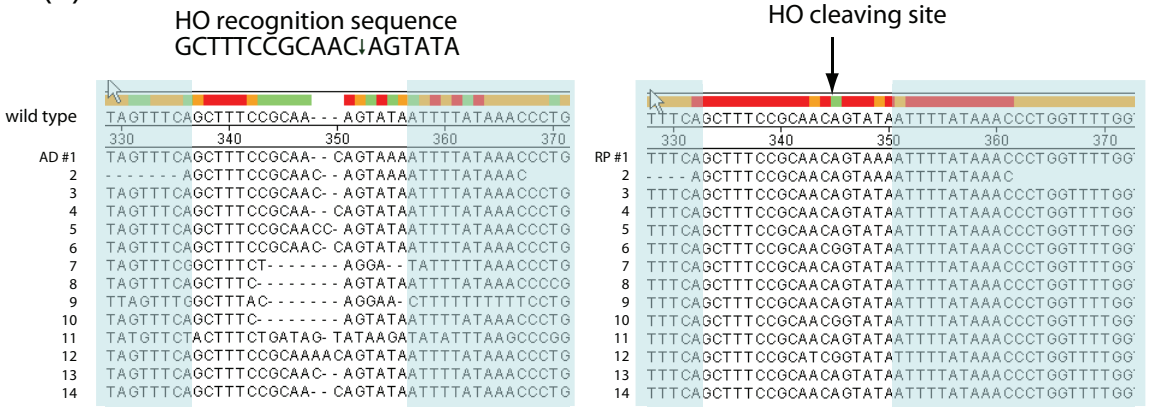

AD + YEP raffinose/galactose

RP + YEP raffinose/galactose

Figure 6. Viability of repairable (RP) and adaptable (AD) strains.
G1 arrested cells from AD (US5339) and RP (US5338) strains were filtered and released into YEP+raff+gal medium at 24^{O}C. After 4 hrs, triplicates of 50,000 and 100,000 of AD cells, and 500 RP cells (quantified using a haemocytometer) were spread onto YEP+raff+gal plates. Subsequently, after 3 days of incubation at 24^{O}C, colonies were counted. Next, DNA of the colonies (14 each from AD and RP) were extracted and sequenced. **(A)** shows the number of colonies formed by RP and AD strains, while **(B)** shows the sequences obtained.

3.2.4 Polo-like kinase Cdc5 is necessary for adaptation

Toczyski et al [3] had conducted a genetic screen in an attempt to identify genes required for adaptive response in budding yeast. The strategy was to isolate mutants that fail to adapt and remain arrested in G2/M. This screen identified *cdc5-ad*, a mutation in Cdc5 which abolished the adaptive response, suggesting a role for Cdc5 in the process of adaptation. However, it is not clear what role Cdc5 plays in adaptation. Cdc5 is an essential gene in budding yeast. Though not required for entry into or progression through mitosis, it is a critical effector of the mitotic exit network and plays an essential role in the final exit from mitosis [85, 198]. It is also involved in efficient cohesin cleavage during anaphase but this requirement is not absolute [117]. Thus, cells deficient in Cdc5 progress through the cell cycle fairly normally but arrest in telophase due to their failure to degrade mitotic cyclins.

cdc5-ad allele is specifically defective in adaptation in that it retains its normal kinase activity and mitotic functions. To rule out any atypical allele-specific effects, we wished to characterize the adaptive response in cells completely deficient in Cdc5 function. For this purpose, we deleted the *CDC5* gene in a non-repairable strain, kept it alive by a copy of *CDC5* driven by a methionine-repressible promoter (US5909). These cells are non-viable on methionine containing medium due to Cdc5 deficiency. Since Cdc5 deficiency also acts as a telophase trap, *cdc15-2/slk19Δ* was not introduced in these cells. *AD* (with *cdc15-2/slk19Δ* trap) and *AD cdc5Δ* cells were synchronized in G1 by α factor treatment in –met+raff medium and then released into YEP+raff+gal medium at 30ºC. As expected, AD cells begin to arrive at telophase after 10 hrs as indicated by the presence of a divided nucleus and a long mitotic spindle (>60% at 14^{th}hr) as shown in Figure 7. Consistent with this, hyper-

phosphorylated forms of Rad53 begin to disappear starting from 10 hrs, indicating the turning-off of the checkpoint (Figure 7A). *AD cdc5Δ* cells, on the other hand, remain arrested with a short spindle and an undivided nucleus (Figure 7C). In addition, Rad53 remains hyper-phosphorylated in these cells throughout the experiment, implying the existence of an active checkpoint in the absence of Cdc5 and the inability of cells to undergo adaptation.

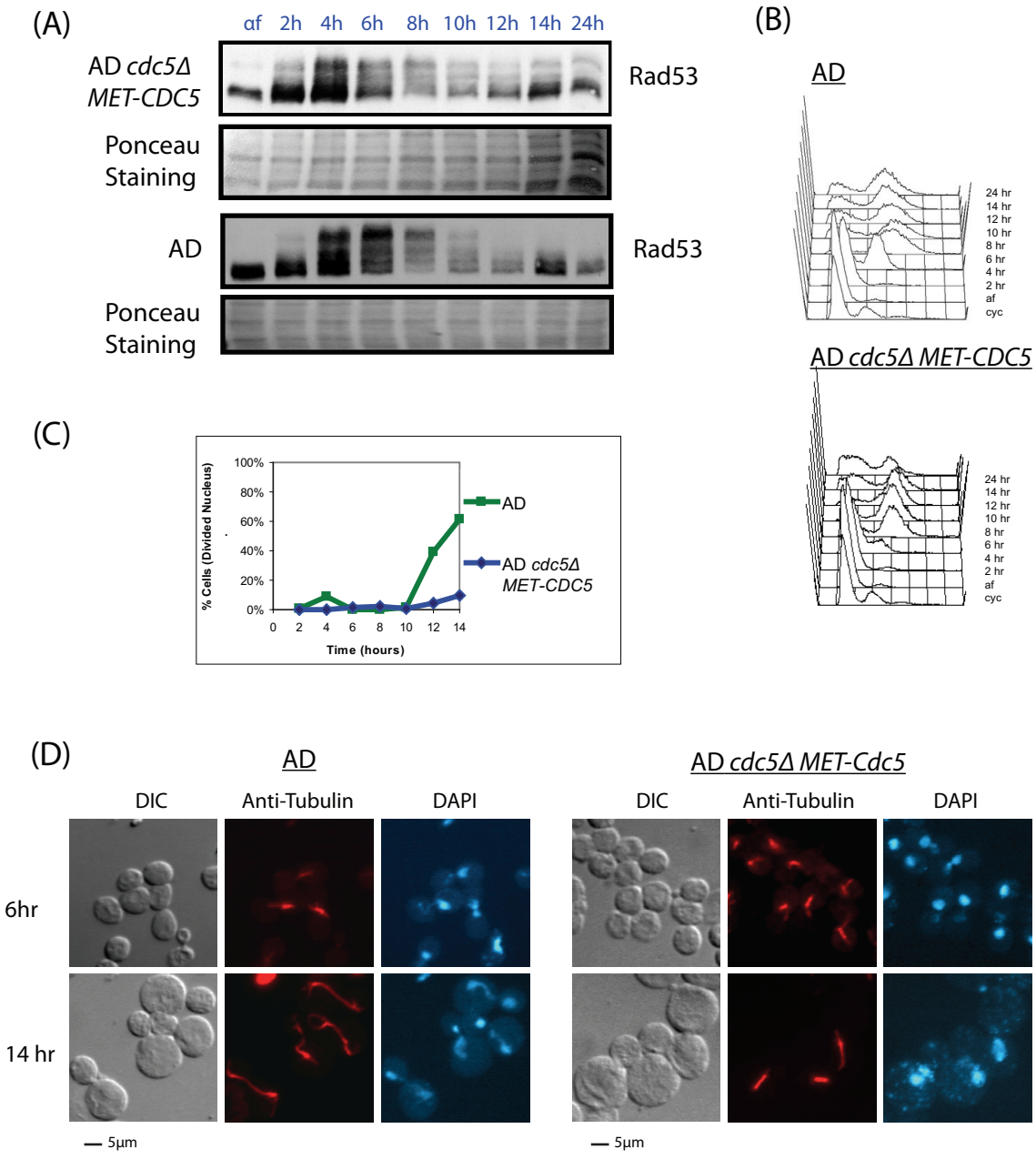

Figure 7. Polo-like kinase CDC5 is essential for adaptation.
AD cells (US5880) were synchronized at G1 with α-factor in YEP+raff medium, and released into cell cycle in YEP+raff/gal medium at 30^{O}C; whereas AD *cdc5Δ MET-CDC5* cells (US5909) were synchronized in methionine-free medium with raffinose, added with 20mM methionine 30mins before being released into YEP+raff+gal+20mM methionine medium at 30^{O}C. Results from **(A)** Western blots and **(B)** FACS analysis are presented. **(C)** The plot shows the percentage of cells with divided nucleus at the indicated times. **(D)** The state of the spindle and nuclear division were monitored using anti-tubulin anti-bodies (Red) and DAPI (Blue).

3.2.5 Cdc5 polo kinase does not affect recovery in RP cells

DNA damage checkpoint appears to be extinguished in both RP and AD strains (Figure 3) as they undergo recovery or adaptation, respectively, at least as estimated from the disappearance of hyper-phosphorylated Rad53. This implies that turning off of the checkpoint is a prerequisite for both recovery (damage repaired) and adaptation (no repair). In the preceding section, we have seen that in the absence of Cdc5, AD cells are unable to extinguish the checkpoint and fail to undergo adaptation (Figure 7), raising the possibility that Cdc5 is required for extinguishing the checkpoint. Therefore, we asked if Cdc5 is also required to turn off the checkpoint during the recovery process in RP cells.

RP cells carrying *cdc5Δ MET-CDC5* (with *cdc15-2/slk19Δ trap*) (US5866) were synchronized in G1 with α-factor treatment in –met+raff medium and then released into YEP+raff+gal medium to induce HO and repress the expression of Cdc5. Cells were monitored for Rad53 phosphorylation and their ability to reach telophase. Interestingly, unlike the AD strain, Rad53 hyper-phosphorylation is not detected after the release (but other studies reported transient Rad53 phosphorylation which disappears very rapidly [106]) and cells accumulate in telophase with divided nuclei and a long mitotic spindle (Figure 8). This is rather surprising since RP cells would be expected to activate the damage checkpoint, arrest in G2/M and repair the single DSB. However, if Cdc5 is required for extinguishing the checkpoint, RP cells will be expected to remain arrested in G2/M, despite having repaired the DSB. One possible explanation is that the repair process via HR itself causes the checkpoint to be turned off when single-stranded DNA regions (that are critical for activating the checkpoint) disappear as repair process proceeds. Such a scenario, thus, ascribes the checkpoint-extinction function to the repair process itself and precludes the requirement for Cdc5.

The ability of RP cells to reach telophase in the absence of Cdc5 also suggests that progression through mitosis (metaphase to anaphase transition) after cells escape from G2/M arrest (in the checkpoint context) does not require Cdc5 activity.

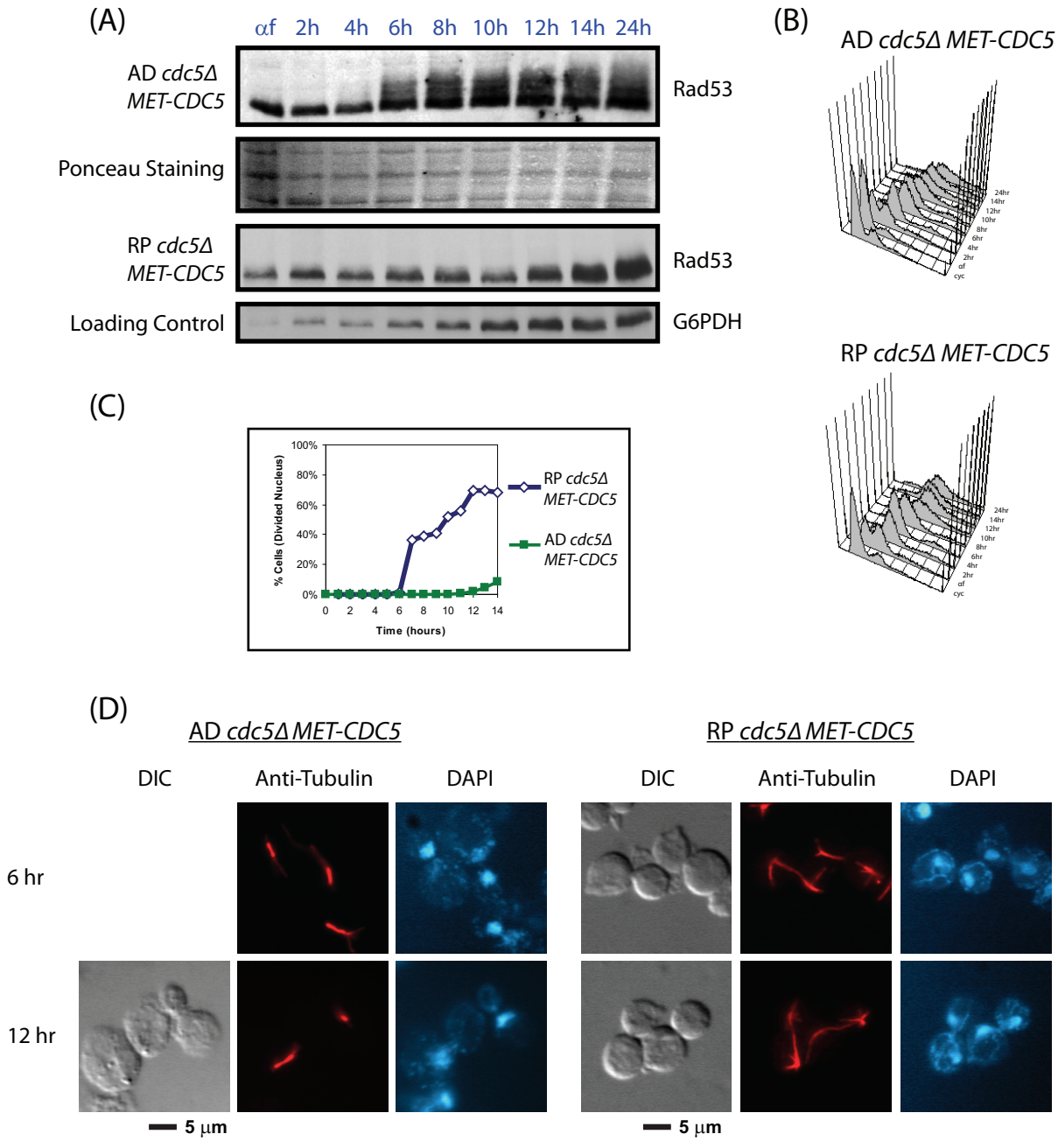

Figure 8. Recovery is unaffected in Cdc5 deficient cells.
AD *cdc5Δ MET-CDC5* (US5868) and RP *cdc5Δ MET-CDC5* (US5866) cells were synchronized at G1 with α-factor in methionine-free medium with raffinose. 20mM methionine was added 30mins before cells were released into YEP + raff/gal + 20mM methionine medium at 30^{O}C. Results for **(A)** Western blot analyses and **(B)** FACS profiles are shown. **(C)** The graph shows the percentage of cells exhibiting nuclear division over time. **(D)** The state of the spindle and nuclear division are shown using anti-tubulin (Red) staining and DAPI (Blue).

3.3 Discussion

We have used the terms 'recovery' and 'adaptation' in the sense employed by Hartwell and colleagues to describe cells' escape from DNA damage-induced G2/M arrest [3]. However, we wish to sound a note of caution particularly with regard to usage of the term 'adaptation'. The term 'adaptation' is very frequently used within the evolutionary context, where it is considered as an outcome of natural selection leaving the survivors better 'fitted' to their environment, hence better 'adapted'. In the context of DNA damage, the use of the term 'adaptation' may, therefore, seem inappropriate. However, in the present scenario, 'adaptation' is meant as a process which allows cells to become 'desensitized' to the checkpoint-induced arrest (this is not necessarily accompanied with improved fitness) and to resume cell cycle progression. Desensitization has long been known in chemotactic and hormonal responses where a system is geared to respond to a change in concentration rather than the absolute concentration itself [199, 200]. However, it should be noted that checkpoint controls are designed to respond to absolute amount of damage, not the change in the extent of DNA damage.

In this study, we have explored adaptation in a somewhat restricted sense in that we monitor, in most experiments, the cells' ability to overcome the G2/M arrest and progress to metaphase and anaphase/telophase but not beyond. We reasoned this to be a better indicator (as opposed to budding) of adaptation because the DNA damage checkpoint's central function is to prevent metaphase to anaphase transition and thus segregation of damaged chromosomes. Indeed, using this parameter to 'quantitate' the adaptive response in a cell population can be difficult if cells overcome G2/M arrest in an asynchronous manner. However, this problem was

resolved by making use of the synthetic lethal interaction between *cdc15-2* and *slk19Δ* mutations at 30ºC which causes cells to arrest uniformly in telophase and can act as an efficient telophase trap.

At a primary level, adaptation (desensitization) can be considered akin to slippages inherent to control systems such that the checkpoint regulation tends to dissipate after a prolonged arrest in G2/M. The fact that adaptive response in budding is almost completely abolished by a mutation in polo-like kinase Cdc5 (*cdc5-ad*) strongly suggests that it is a regulated process [3]. However, what role Cdc5 may play in adaptation pertaining to DNA damage is not known. *cdc5-ad* allele appears to be specifically defective in the adaptive response since this allele is not defective in its other cell cycle functions. To eliminate any allele specific effects, we have tested adaptation and recovery in cells completely deficient in Cdc5 function. We indeed find that in *cdc5Δ* cells, the adaptive response is largely abolished (Figure 7). The fact that Rad53 remains hyper-phosphorylated (Figure 7A) in these cells implies that turning-off of the checkpoint signaling is a pre-requisite for adaptation. However, RP cells carrying *CDC5* deletion recover efficiently and accumulate in telophase (Figure 8), suggesting that the absence of Cdc5 function does not affect the recovery process. This is rather surprising because during both 'adaptation' and 'recovery', the checkpoint is apparently extinguished (as monitored by dephosphorylation of Rad53) so that cells can initiate mitosis and proceed to telophase. Our results, thus, argue that while Cdc5 is required for checkpoint turn-off during adaptation, the mechanism for extinguishing the checkpoint during 'recovery' may be different and does not require Cdc5 function. We note that, unlike in AD strain, hyper-phosphorylation of Rad53 after HO induction (Figure 4) is barely detectable in RP cells before they proceed to telophase, as if the checkpoint is activated only very transiently. In previous studies

[106], Rad53 phosphorylation has been detected in RP cells, but only transiently. How do RP cells extinguish the checkpoint independently of Cdc5?

One possibility is that the repair response itself switches-off the checkpoint control. The single-stranded DNA generated by the repair machinery (MRX complex-mediated resection of 5'end at the DSB), which is a prerequisite for the activation of DNA damage checkpoint, progressively disappears and is restored to double-stranded DNA as repair-reactions take root. This will eventually dislodge the upstream checkpoint effectors such as Mec1-Ddc2 complex which is recruited to the RPA-bound single-stranded DNA to initiate the activation of checkpoint. Hence, the progression of repair processes and 'turning-off of the checkpoint' can be visualized as coupled events. This notion is consistent with the behavior of AD cells; without the capacity to repair the DSB by HR, they maintain the DNA-damage checkpoint in the activated state for prolonged periods of time and require a different mechanism (Cdc5-dependent) to extinguish it during adaptation.

Cdc5 polo kinase-independent 'recovery' in budding also strongly suggests that initiation of mitosis or progression to telophase is not dependent on Cdc5. This is different from 'recovery' in mammalian cells. It has been known that initiation of mitosis in mammalian cells is regulated by redundant pathways. It has been shown that while Plk1 (polo like kinase 1) is not essential for mitotic entry in undamaged U2OS cells, the onset of mitosis in U2OS cells recovering from DNA damage becomes acutely dependent on Plk1 [112]. The Plk1 requirement appears to be because of its role in the degradation of the mitotic inhibitor Wee1 since inactivation of Wee1 abrogates the requirement of Plk1 for 'recovery' in DNA-damaged cells. This also suggests that the control circuitry regulating the onset of mitosis is possibly reset upon DNA damage in mammalian cells. Adaptation has also been studied in

U2OS cells exposed to ionizing radiation. The DNA damaged cells showed Chk1-dependent arrest in G2, followed by Chk1 dephosphorylation and cells' entry into mitosis [5]. The persistence of DNA damage in these cells was indicated by the presence of γ-H2AX foci. Interestingly, Plk1 is also implicated since depletion of Plk1 or overexpression of Chk1 delays the adaptation process. Chk2 is also phosphorylated (at Thr168 within SQ/TQ cluster) by ATM upon DNA damage [201]. Like Rad53 in *S. cerevisiae*, Chk2 Thr168 is dephosphorylated by PP2C type of phosphatase, namely Wip1 [202] in mammals. Wip1 also dephosphorylates Chk1 on Ser345 and Ser317 (phosphorylated by ATM) and is proposed to play an important role in the reversal of the DNA damage response [203]. Although Plk1 has been implicated in adaptation to replication checkpoint in both human cells [109-111] and *Xenopus* egg extracts [4], and in the 'adaptation' to DNA damage in mammalian cells [5], the role of Plk1 in the adaptation process is not clear.

How does Cdc5 polo kinase extinguish the DNA damage checkpoint control during adaptive response in the budding yeast? This is the theme we explore in Chapter 4.

Chapter 4 Polo-like kinase Cdc5 and Adaptation

4.1 Background

As described in the preceding sections, 'adaptation' is a desensitization process during which *S. cerevisiae* cells, if unable to repair a double strand break, escape from the checkpoint imposed G2/M arrest. During 'recovery', cells also escape G2/M arrest but they do so after having repaired the DNA lesion. At one level, 'adaptation' and 'recovery' both can be broadly considered as involving two common steps: (i) turning-off of the checkpoint control and (ii) reactivation of the mitotic machinery. In Chapter 3, we have seen that during recovery, Cdc5 kinase is required neither for switching off the checkpoint nor for the onset of mitosis or for chromosome segregation. However, it is also clear that Cdc5 function is required for 'adaptation' (Figure 7). This could be either because cells defective in HR repair are unable to extinguish the checkpoint control in the absence of Cdc5 or they are unable to progress through mitosis without Cdc5 function. In budding yeast, Cdc5 is essential for mitotic exit. Moreover, the undamaged, Cdc5-deficient cells can traverse through mitosis and reach telophase quite efficiently (unlike mammalian cells where polo kinase Plk1 is required for the onset of mitosis). Therefore, it is likely that AD cells are unable to undergo 'adaptation' in the absence of Cdc5 because they fail to switch off the checkpoint and not because they are unable to initiate mitosis. What role does Cdc5 polo kinase play in extinguishing the DNA damage checkpoint?

Polo-like kinase (Plx1 in Xenopus) has been implicated in the adaptive response in aphidicolin treated Xenopus egg extracts [4]. Aphidicolin blocks DNA replication and causes activation of the replication checkpoint (ATR-Chk1 axis)

which arrests egg extracts in interphase. Claspin, the checkpoint mediator protein, is necessary for this arrest because it mediates ATR-dependent activation of Chk1. It has been shown that during checkpoint response, Claspin itself gets phosphorylated on Thr906 (T906) which creates a Plx1 binding site [4]. Recruitment of Plx1 to this site leads to further phosphorylation of Claspin at Ser934 (S934). After a prolonged arrest in aphidicolin, these extracts undergo adaptation and initiate mitosis. This is accompanied by dissociation of Claspin from chromatin and inactivation of Chk1. Substitution of T906 or S394 by alanine abolishes the adaptive response. This suggests that turning-off of the replication checkpoint response is accomplished through Plx1-dependent phosphorylation of Claspin.

Adaptation to DNA damage has been studied in human osteosarcoma cells (U2OS) [5]. When exposed to ionizing radiation, U2OS cells arrest in G2 in a Chk1 dependent manner. However, after a prolonged arrest, they escape and enter mitosis. Depletion of Plk1 or overexpression of Chk1 can delay this process. In addition, the entry into mitosis is accompanied by Chk1 dephosphorylation. Chk1 may also be inactivated by proteolytic degradation in transformed human cells [205]. It has been proposed that ATR-mediated phosphorylation of Chk1 not only activates it but also primes it for proteolytic destruction [205]. Hence, switching off of the checkpoint response is also a prerequisite for adaptive response in human cells. However, what role does polo-like kinase play in extinguishing the DNA damage checkpoint response in human cells is not known. PP2A like phosphatases (PP4 and PP6) have been implicated in reversing Chk1 phosphorylation on Ser317 and Ser345 [203]. Chk2 is also activated by ATM/ATR mediated Thr168 phosphorylation in response to treatment with cisplatin or ionizing radiation [201]. Wip1 phosphatase has been shown to promote dephosphorylation of Thr168, thus antagonizing Chk2 activation

by ATM/ATR and this may be important in reversing the DNA damage response [202].

Chk1 phosphorylation also plays a prominent role in imposing a G2 delay in DNA damage in fission yeast *Schizosaccharomyces pombe*. Activated Chk1 targets both Wee1 and Cdc25 to indirectly promote phosphorylation of Cdc2 (Cdk1) on the evolutionarily conserved tyrosine 15 (Tyr15) residue [206]. Dephosphorylation of Chk1 by PP1 phosphatase Dis2 allows DNA damaged cells to escape from G2 arrest since *dis2Δ* mutant remains arrested for a prolonged period upon DNA damage [207]. This correlates with the presence of persistent phosphorylation of Chk1 [206]. The theme of effector kinase inactivation extinguishing the DNA damage checkpoint also continues in the case of the budding yeast. Rad53 (yeast Chk2) is phosphorylated in response to DNA damage [208, 209]. During adaptive response, dephosphorylation of Rad53 correlates strongly with cells' escape from G2/M arrest, suggesting that Rad53 dephosphorylation is promoted by PP2C phosphatases Ptc2 and Ptc3 [107]. Another PP2A-like phosphatase, Pph3, also dephosphorylates activated Rad53 in cells subjected to MMS treatment [210]. However, switching off of replication checkpoint after hydroxyurea treatment appears to require a different set of phosphatases since Rad53 remains hyper-phosphorylated in *pph3Δ ptc2Δ ptc3Δ* triple mutant upon removal of hydroxyurea [211]. Thus, dephosphorylation of the checkpoint effector kinase is one of the main cellular strategies for dampening the checkpoint signaling allowing recovery or adaptation.

A loss of function of a number of other proteins such as Ku complex subunits Yku70 and Yku80, RecA like protein Rad51, the Srs2 helicase and Sae2 impair the adaptive response in budding yeast [2, 68, 105, 106]. Deficiency of single stranded binding protein subunit Rfa1 and MRX complex subunit Mre11, on the other hand,

are conducive to adaptation. These proteins are known to be involved in the processing of DSB ends. Their presence or absence is, therefore, likely to promote or dampen checkpoint signaling and to eventually impinge on cells' adaptive response. Casein Kinase II subunits Ckb1 and Ckb2 are also implicated in adaptation in that *ckb1Δ* and *ckb2Δ* mutants fail to undergo adaptation upon DNA damage. The exact mechanism of their involvement remains unclear.

The foregoing discussion suggests that extinction of checkpoint signaling required for adaptation can be eliminated by interfering with the regulatory hierarchy at different points. It can be accomplished either by dephosphorylation of Rad53 or can occur somewhat upstream at the level of DNA processing of the DSB ends. But at what stage Cdc5 polo kinase acts in the adaptive response pathway remains unclear. We explore this issue in the following sections.

4.2 Results

4.2.1 Overexpression of Cdc5 accelerates adaptation

We have seen in Chapter 3 that Cdc5 is essential for adaptation to DNA damage and for turning off of the checkpoint response. Without resorting to any preconceived assumptions of its role in adaptation, we asked if Cdc5 is a rate limiting factor in the adaptive response. Generally, the variation in the concentration or activity of a rate limiting factor determines the overall rate of the process. In the present context, an effector may be essential for adaptive response but, if not rate limiting, it may not be able to alter the kinetics of adaptation when its activity is spiked. Therefore, we tested if the kinetics of adaptation changes with altered physiological concentrations of Cdc5. AD cells (containing telophase trap) with (US5999) or without (US5880) one copy of

GAL-CDC5 integrated at its native locus were synchronized in G1 with α-factor treatment in YEP+raff medium and then released into raffinose medium at 30ºC. After 2 hrs, galactose was added to induce HO and Cdc5 expression. Since overexpression of Cdc5 dampens to some extent, cells' capacity to bud, Cdc5 was induced 2 hrs after the release when most cells in the culture had budded.

AD cells without *GAL-CDC5* (US5880) remained arrested in G2/M with short spindles and undivided nuclei until 10 hrs with only ~10.2% of cells escaping the arrest as evidenced by the presence of divided nucleus (nuclei are stained with DAPI). The proportion of cells overcoming the G2/M arrest reached 68.1% by 14^{th} hr (Figure 9C). This is consistent with the Rad53 hyper-phosphorylation at 6^{th} hr and its gradual disappearance by 12^{th} hr. 15% of Cdc5-overexpressing AD cells (US5999) escaped G2/M by 8^{th} hr, with ~69% cells reaching telophase by 10^{th} hr (Figure 9C). The extent of Rad53 hyper-phosphorylation was much less compared to AD cells without Cdc5 overexpression. Instead, there was a slight but distinct gel mobility shift starting from 6^{th} to 14^{th} hr. The extent of shift was between Rad53 profile of undamaged cells at G1 arrest, and Rad53 hyper-phosphorylation in AD cells at 4^{th} to 6^{th} hr. These results suggest that higher activity of Cdc5 causes adaptive response to initiate earlier in DNA damaged cells. It appears to do so by inactivating the checkpoint response. Acceleration of adaptation by overexpression of Cdc5 also implies that Cdc5 is perhaps a rate limiting factor in the adaptive response.

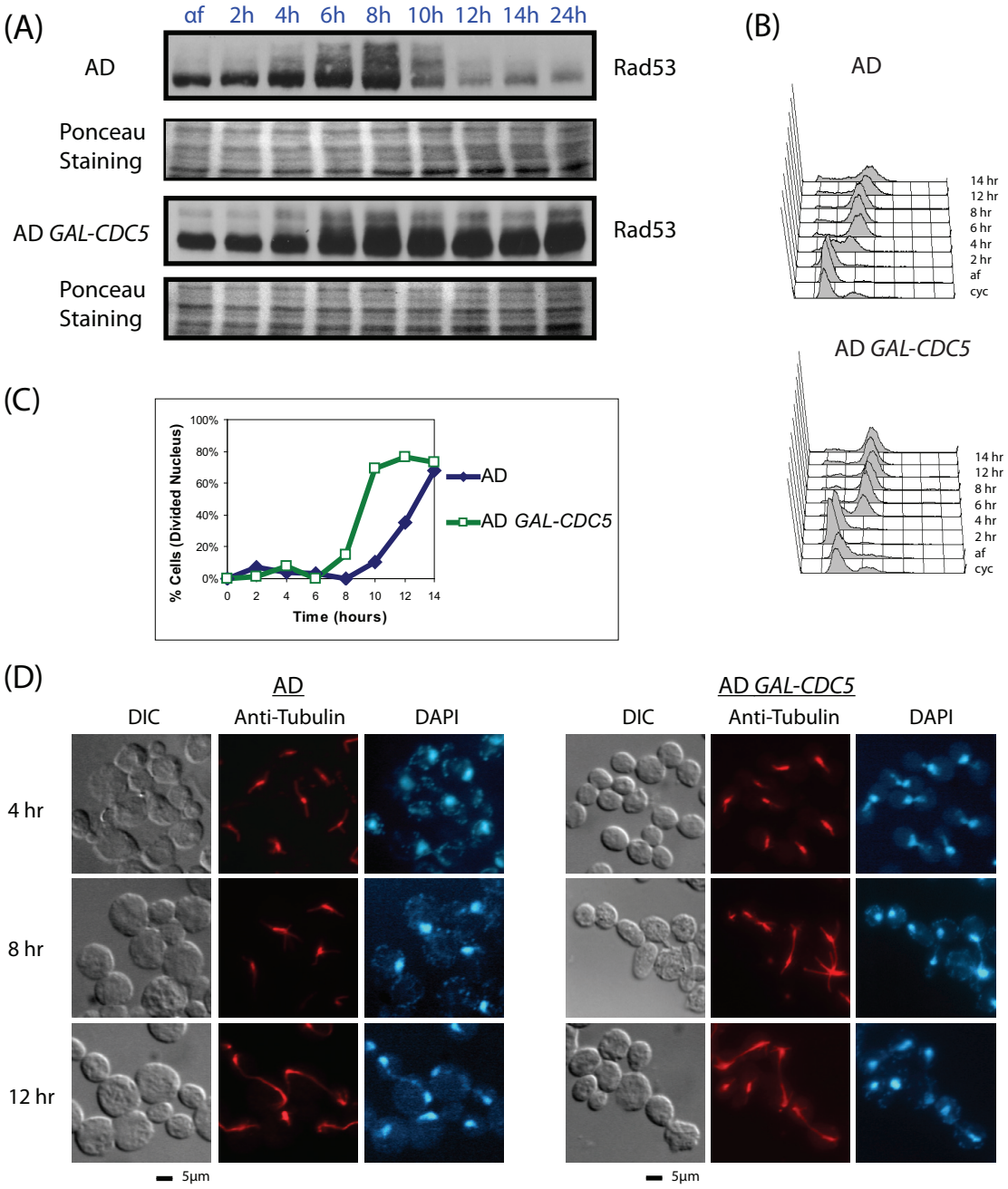

Figure 9. Overexpression of Cdc5 accelerates adaptation in normal cells.
AD (US5880) and AD *GAL-CDC5* (US5999) cells were synchronized at G1 with α-factor in YEP+raff medium, and released into the cell cycle in YEP+raff medium at 30°C with galactose added 2 hrs later. Samples were collected every 2 hrs for 14 hrs. **(A)** Western blots analyses and **(B)** FACS profiles are shown **(C)** The graph shows the percentage of cells exhibiting nuclear division over time. **(D)** The state of the spindle and nuclear division are shown using anti-tubulin (Red) staining and DAPI (Blue).

4.2.2 Overexpression of Cdc5 rescues other adaptation defective mutants

As mentioned earlier, cells lacking the function of a number of genes other than *CDC5* (such as *SAE2*, *PTC2/PTC3*, *CKB1*, *CKB2*, *YKU70* and *YKU80*) are known to be defective in mounting an adaptive response. Sae2 promotes the dissociation of MRX complex from DNA [68], whereas Ptc2 and Ptc3 are phosphatases belonging to PP2C family of phosphatases and are known to be responsible for dephosphorylation of Rad53 during adaptation [107]. Depletion of Ckb1 and Ckb2, subunits of Casein Kinase II (CKII), does not allow cells to adapt [3]. Yku70 and Yku80 are subunits of Ku-complex required for non-homologous end-joining (NHEJ). Since Cdc5 seems to be a rate-determining step in adaptive response, we asked if ectopic expression of Cdc5 kinase can overcome the adaptation defect in cells lacking these factors.

4.2.2.1 Sae2

In cells depleted of Sae2, MRX complex persists at the DSB site and leads to constitutive activation of the checkpoint. As a result, *sae2Δ* cells fail to adapt or undergo recovery [68]. If Cdc5 influences DNA damage response by affecting steps downstream of MRX complex, then overexpression of Cdc5 would cause *sae2Δ* cells to adapt. To test this, *sae2Δ, AD* cells (US6106) with or without (US5998) *GAL-CDC5* cells were synchronized in G1 with α-factor treatment and released into YEP+raff medium at 30ºC. After 2 hrs, galactose was added to induce both HO endonuclease and Cdc5. In *sae2Δ* cells without Cdc5 overexpression, Rad53 hyper-phosphorylation was seen from 4th hr onwards, and persisted even at 24th hr (Figure 10A). Immunofluorescence staining indicated that only 14.4% of these cells had adapted and arrested in telophase with long spindles and divided nuclei (Figure 10C).

Ectopic expression of Cdc5, however, allowed 34.9% of *sae2Δ* cells to escape G2/M arrest and reach telophase by 8th hr. This proportion increased to 56.7% by 14th hr (Figure 10C). Consistent with these observations, Rad53 was not hyper-phosphorylated. These results suggest that Cdc5 overexpression suppresses adaptation defect in *sae2Δ* cells.

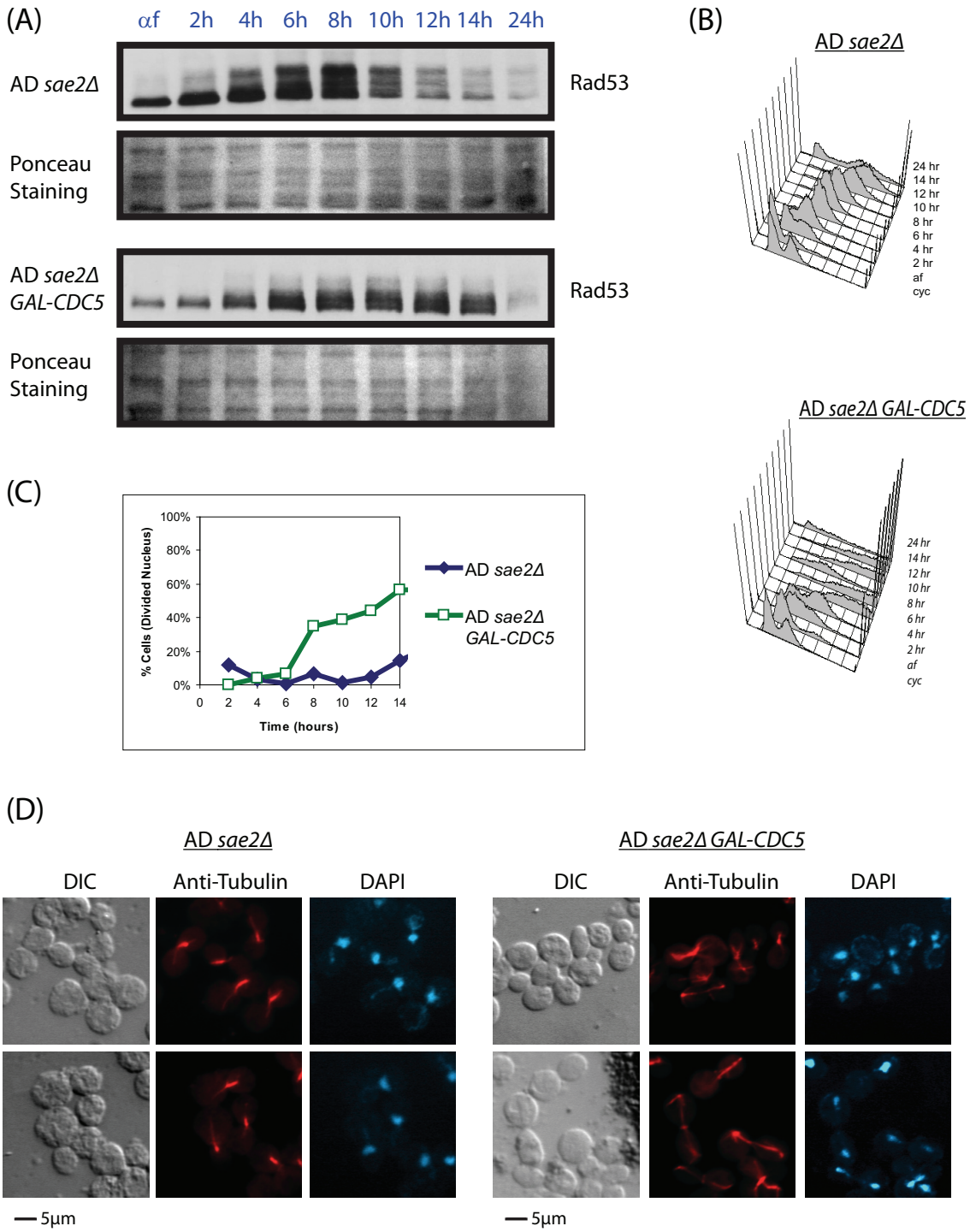

Figure 10. Overexpression of Cdc5 rescues adaptation defects in *sae2Δ* cells.
AD *sae2Δ* (US5998) and AD *sae2Δ GAL-CDC5* (US6106) cells were synchronized in G1 with α-factor in YEP+raff medium and released in YEP+raff medium at 30^{O}C with galactose added 2 hrs later. Results from various analyses are shown: **(A)** Western blot analysis, **(B)** FACS analysis, **(C)** percentage of cells with divided nucleus and **(D)** state of spindle using anti-tubulin (Red) antibody and state of nucleus using DAPI (Blue).

4.2.2.2 Ptc2/Ptc3

Cdc28 (Cdk1) is the main CDK that drives cell cycle progression in budding yeast. Its activity is regulated not only by its association with cyclins but also by phosphorylation events. Among these, phosphorylation of Thr169 residue, necessary for stabilization of Cdc28-cyclin interaction, is performed by Cdk-activating kinase (Cak1) [52, 212]. PP2C family kinase Ptc2 and Ptc3 were identified as phosphatases that reverse the phosphorylation of Thr169 [213]. Subsequently, Ptc2 and Ptc3 were implicated in switching-off the DNA damage response during adaptation by dephosphorylating Rad53 [107]. Consistent with this notion, *ptc2 ptc3* double mutant cells are defective in the adaptive response [107].

To test, if ectopic expression of Cdc5 suppresses adaptation defect of *ptc2Δ ptc3Δ* double mutant, a single copy of *GAL10* promoter-driven *CDC5* was integrated at the *URA3* locus. AD *ptc2Δ ptc3Δ* cells with or without *GAL-CDC5* (US6266, US6215) were synchronized in G1 and released into YEP+raff medium at 30ºC. After 2 hrs, galactose was added to induced HO endonuclease and Cdc5 expression. Most AD *ptc2Δ ptc3Δ* cells remained arrested in G2/M with only ~5.4% with divided nucleus at 8th hr (Figure 11C). In addition, distinct Rad53 hyper-phosphorylation was seen from 6th hr until 24th hr in these cells. However, Cdc5 overexpression induced ~51% of AD *ptc2Δ ptc3Δ* cells to progress to telophase at 10th hr (Figure 11C) with ~80.5% cells at 14th hr. Consistent with this, a concomitant absence of Rad53 hyper-phosphorylation was also seen. These observations suggest that Cdc5 is capable of deactivating checkpoint response in the absence of Ptc2 and Ptc3 phosphatases.

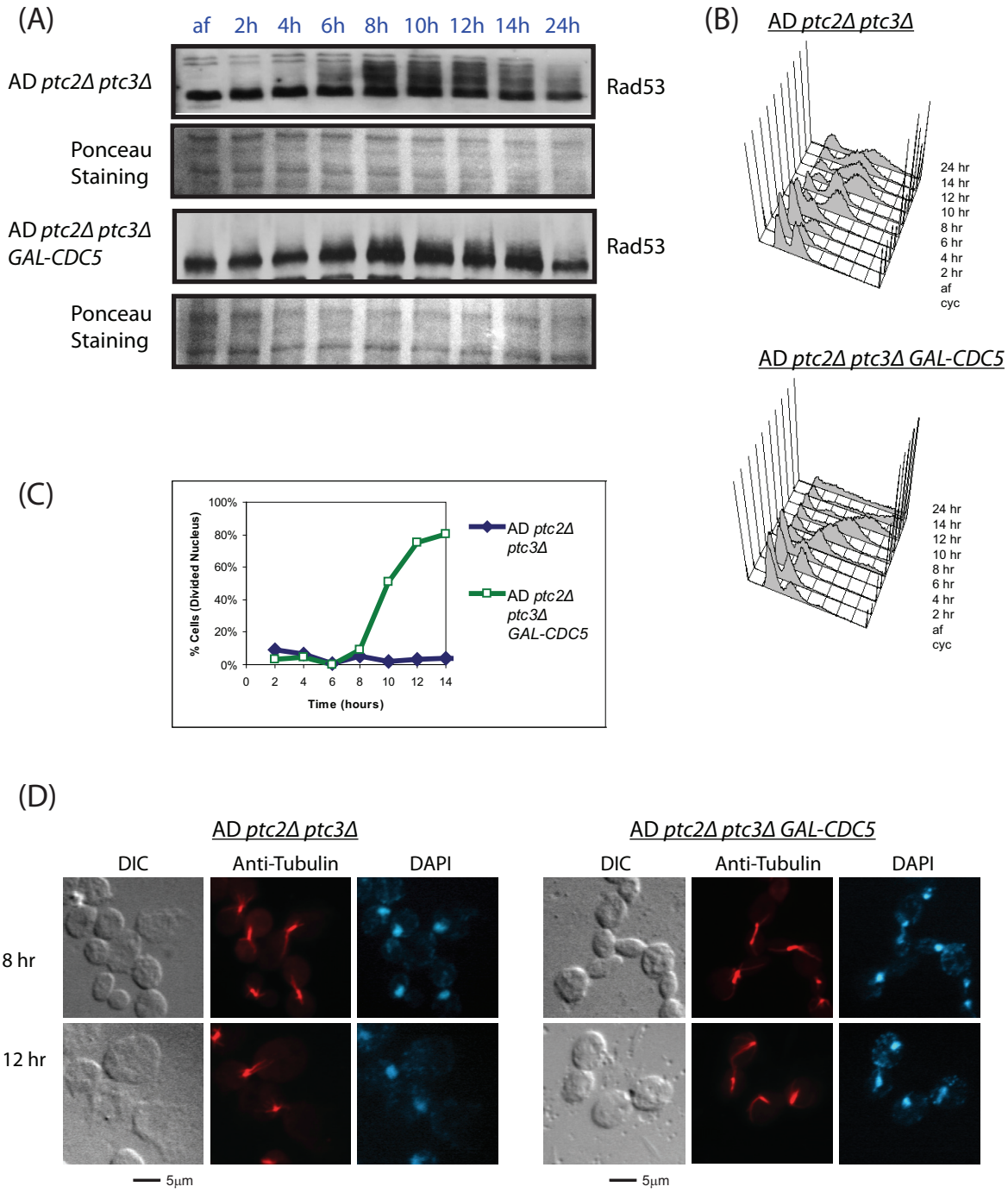

Figure 11. Overexpression of Cdc5 suppresses adaptation defects in *ptc2Δ ptc3Δ* cells. AD *ptc2Δ ptc3Δ* (US6215) and AD *ptc2Δ ptc3Δ GAL-CDC5* (US6266) cells were synchronized at G1 with α-factor in YEP+raff medium, and released cell cycle in YEP+raff medium at 30°C with galactose added 2 hrs later. Results for **(A)** Western blot analyses and **(B)** FACS profiles are shown. **(C)** The graph shows the percentage of cells exhibiting nuclear division over time. **(D)** The state of the spindle and nuclear division were monitored using anti-tubulin antibodies (Red) and DAPI (Blue).

4.2.2.3 Ckb1

Mutants lacking casein kinase 2 (CKII) subunits *ckb1Δ* or *ckb2Δ*, are also known to be defective in adaptation [3]. It has been suggested that CKII kinase is needed for Ptc2/Ptc3 and Rad53 interaction [107]. However, *ckb1Δ* mutants displayed more severe defects in adaptation compared to *ptc2Δ ptc3Δ* cells, suggesting that CKII may additionally regulate adaptive response in a Ptc2-independent manner [214]. To determine if ectopic expression of Cdc5 can alleviate the adaptation defects of *ckb1Δ* cells, AD *ckb1Δ* cells with and without *GAL-CDC5* (US6072, US5885) were synchronized in G1 as before and then allowed to resume cell cycle progression in YEP+raff medium at 30ºC. After 2 hrs, galactose was added to induce both HO endonuclease and Cdc5, and cells were monitored for their capacity to undergo nuclear division. As expected, almost all AD *ckb1Δ* cells arrested in G2/M throughout the duration of the experiment (Figure 12B & C). However, AD *ckb1Δ* cells over-expressing Cdc5 were able to escape G2/M arrest and traverse to telophase, starting from 27% at 8^{th} hr to 53.8% at 14^{th} hr (Figure 12C). Consistent with this, hyper-phosphorylation of Rad53 was absent in AD *ckb1Δ GAL-CDC5* cells. These results imply that Cdc5 is able to deactivate the checkpoint control without active CKII.

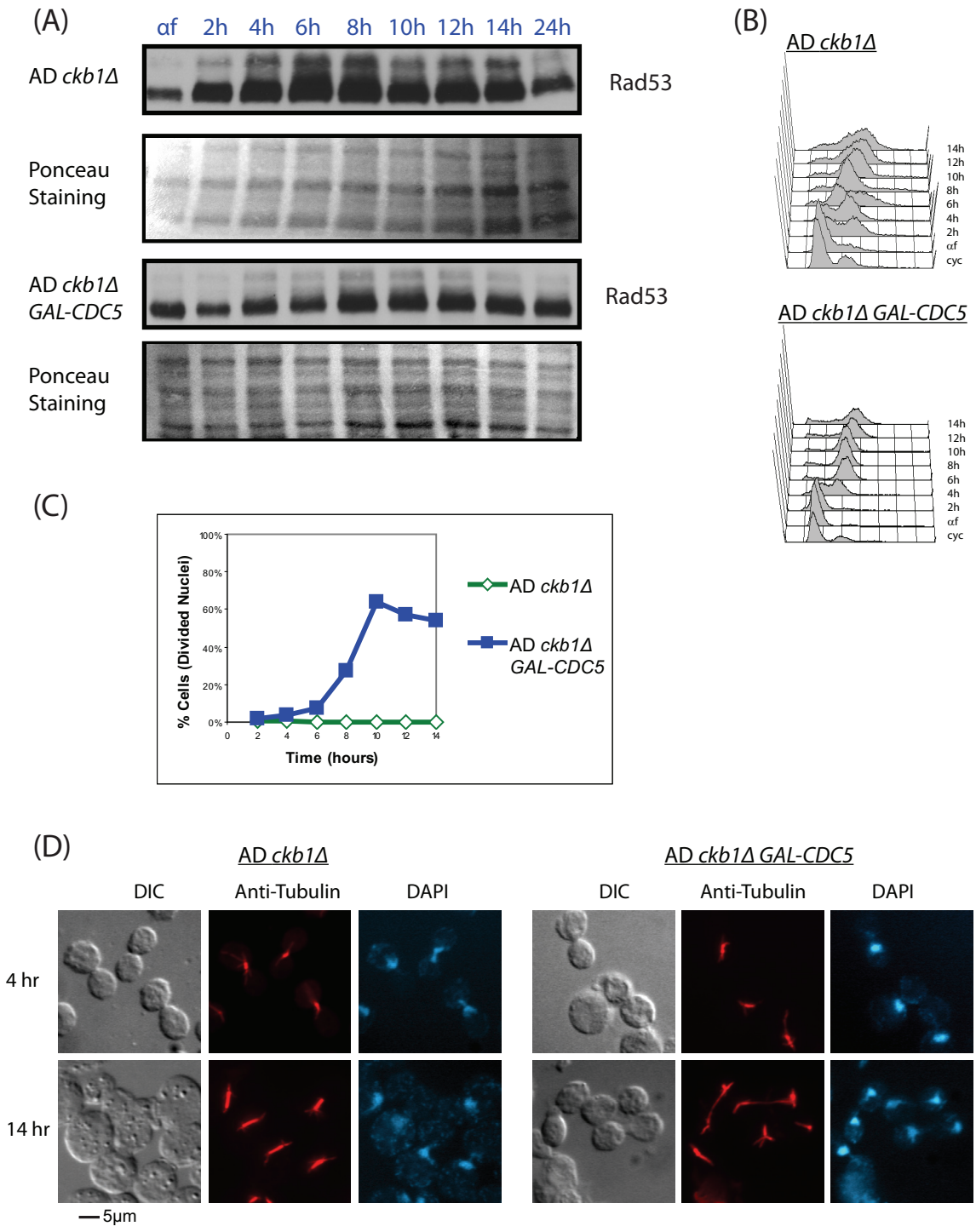

Figure 12. Overexpression of Cdc5 rescues adaptation defects of *ckb1Δ* cells.
AD *ckb1Δ* (US5885) and AD *ckb1Δ GAL-CDC5* (US6072) cells were synchronized at G1 with α-factor in YEP+raff medium, and released cell cycle in YEP+raff medium at 30^{O}C with galactose added 2 hrs later. Results for **(A)** Western blot analyses and **(B)** FACS profiles are shown. **(C)** The graph shows the percentage of cells exhibiting nuclear division over time. **(D)** The state of the spindle and nuclear division were visualized using anti-tubulin (Red) staining and DAPI (Blue).

4.2.3 Resection of DNA at DSB is not affected by ectopic expression of Cdc5

The experiments described in the preceding section suggest that ectopic expression of Cdc5 can extinguish the checkpoint independently of Ptc2, Ptc3 phosphatases or CKII. It is also clear that Rad53 is very transiently (or barely) hyper-phosphorylated in cells overexpressing Cdc5. One interpretation of these findings is that Cdc5 is capable of turning off the DNA damage checkpoint upstream of Rad53, perhaps the events associated at the very onset of DNA damage checkpoint. One of the early events after cells have experienced a DSB is the recruitment of MRX complex at the site of the lesion. The MRX complex and Exo1 are responsible for the resection of 5' end generating a stretch of 3'-ended single-strand DNA (ssDNA) which is subsequently coated by single stranded DNA-binding protein RPA (a heterotrimer composed of Rfa1, 2, 3). RPA bound ssDNA also recruits Mec1-Ddc2 heterodimer which in turn activates the checkpoint control cascade. It is possible that Cdc5 overexpression interferes with the DNA resection thereby preventing robust activation of the checkpoint.

To test this possibility, AD cells with or without *GAL-CDC5* (US5828, US5880) were synchronized in G1 and allowed to resume cell cycle progression in YEP+raff medium. After 2 hrs, galactose was added to induce HO and Cdc5 expression. DNAs, isolated from samples collected at various time points, were subjected to alkaline-gel electrophoresis. Southern blot analysis was performed using an appropriate strand-specific probe to detect the progression of DNA resection over time (refer to Section 2.7 for more details). As shown in Figure 13, no dramatic difference in the extent of ssDNA region is observed in cells with or without Cdc5

overexpression. This indicates that Cdc5 activity does not interfere with DNA resection step associated with DSB processing.

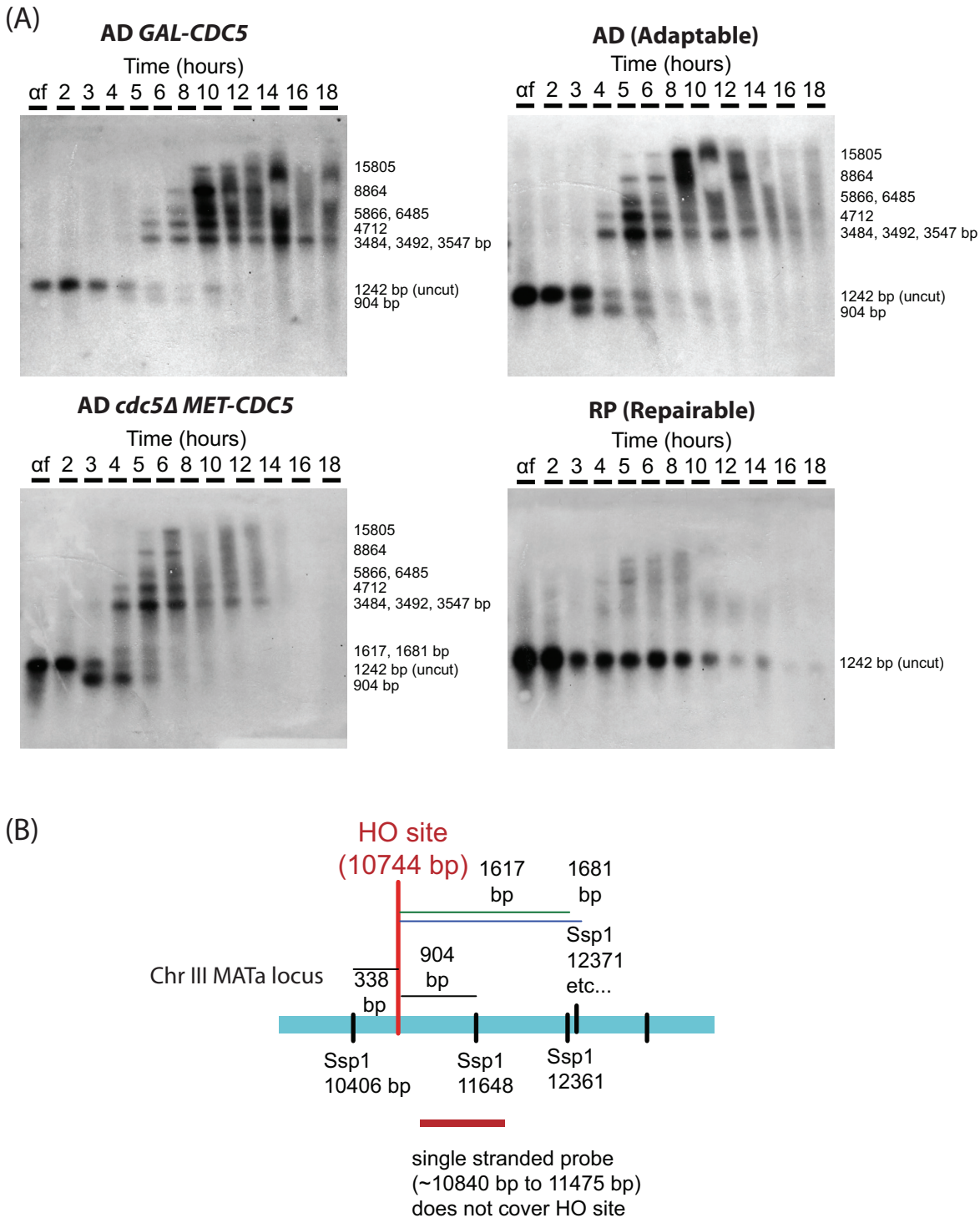

Figure 13. DNA resection is unaffected in *GAL-CDC5* or *cdc5Δ* strains.
G1 synchronized cells {RP (US5881), AD (US5880), AD *cdc5Δ MET-CDC5* (US5909) and AD *GAL-CDC5* (US5828)} were released into YEP+raff medium with galactose added 2 hrs later. Thereafter, samples were collected every 2 hrs for 18 hrs.
(A) Ssp1-digested genomic DNAs, collected from the indicated times, were separated on alkaline agarose gels and probed using a radioactive single-strand riboprobe specific for *MAT* locus. For more details, please refer to Chapter 2 Materials and Methods. **(B)** Schematic of *MATa* locus with SspI recognition sites.

4.2.4 High level of Cdc5 inhibits Ddc2 foci formation

Recruitment of Mec1 kinase is considered to be the most upstream event in the activation of the DNA damage checkpoint pathway. Ddc2 is a Mec1-partner protein (analogous to ATRIP for ATR) and accumulates near the site of DNA damage together as a complex. Both Ddc2 deficient and *mec1* mutant cells are found to be defective in DNA damage checkpoint activation. In the case of the latter, *mec1* mutant cells fail to phosphorylate Rad9, Rad53 and Chk1 [77, 215]. Since Mec1 kinase activity is intact in Ddc2 deficient cells, this implies that Ddc2's role in DNA damage response is to recruit Mec1 to the damaged DNA without which checkpoint signaling cannot be initiated. In the context of adaptation, it is possible that overexpression of Cdc5 in some way inhibits the recruitment of Ddc2 and Mec1 to the DNA or weakens the interaction between these proteins thereby preventing full activation of the checkpoint.

To test if ectopic expression of Cdc5 affects formation of Ddc2 foci, AD cells with or without *GAL-CDC5*, but all containing endogenous *DDC2* tagged with yeCitrine, were synchronized in G1 by α-factor treatment and then released into YEP+raff medium at 30°C. After 2 hrs, galactose was added to induce expression of HO and Cdc5. In AD cells with (US6416) and without (US6382) *GAL-CDC5* Ddc2-yeCitrine foci were clearly visible in ~38% cells within 3 hrs after HO induction. In AD cells, the percentage of cells with visible foci continued to increase and to peak at ~76% by 5th hr (Figure 14A). In cells overexpressing Cdc5, 32.6% to 40.2% of cells displayed Ddc2-yeCitrine foci from 2.5 to 3.5 hrs. However, at the 4th hr, the proportion of cells with Ddc2-yeCitrine foci suddenly dropped to 18% and hovered at 14.4%-22.2% for the next 2 hrs (Figure 14A). In addition, the intensity of the foci had also visibly decreased (Figure 14B), and long spindles started to appear (Figure

14C/D). Conversely, we found that Ddc2-yeCitrine foci persisted in cells depleted of Cdc5 (US6381) (Figure 15). These results imply that ectopic expression of Cdc5 inhibits efficient recruitment of Ddc2 and, by inference, of Mec1 to the site of DNA damage.

(A)

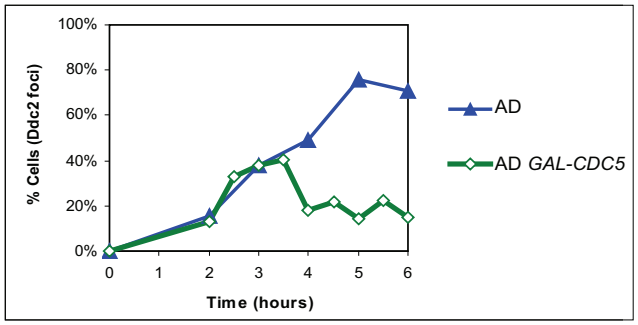

(B)

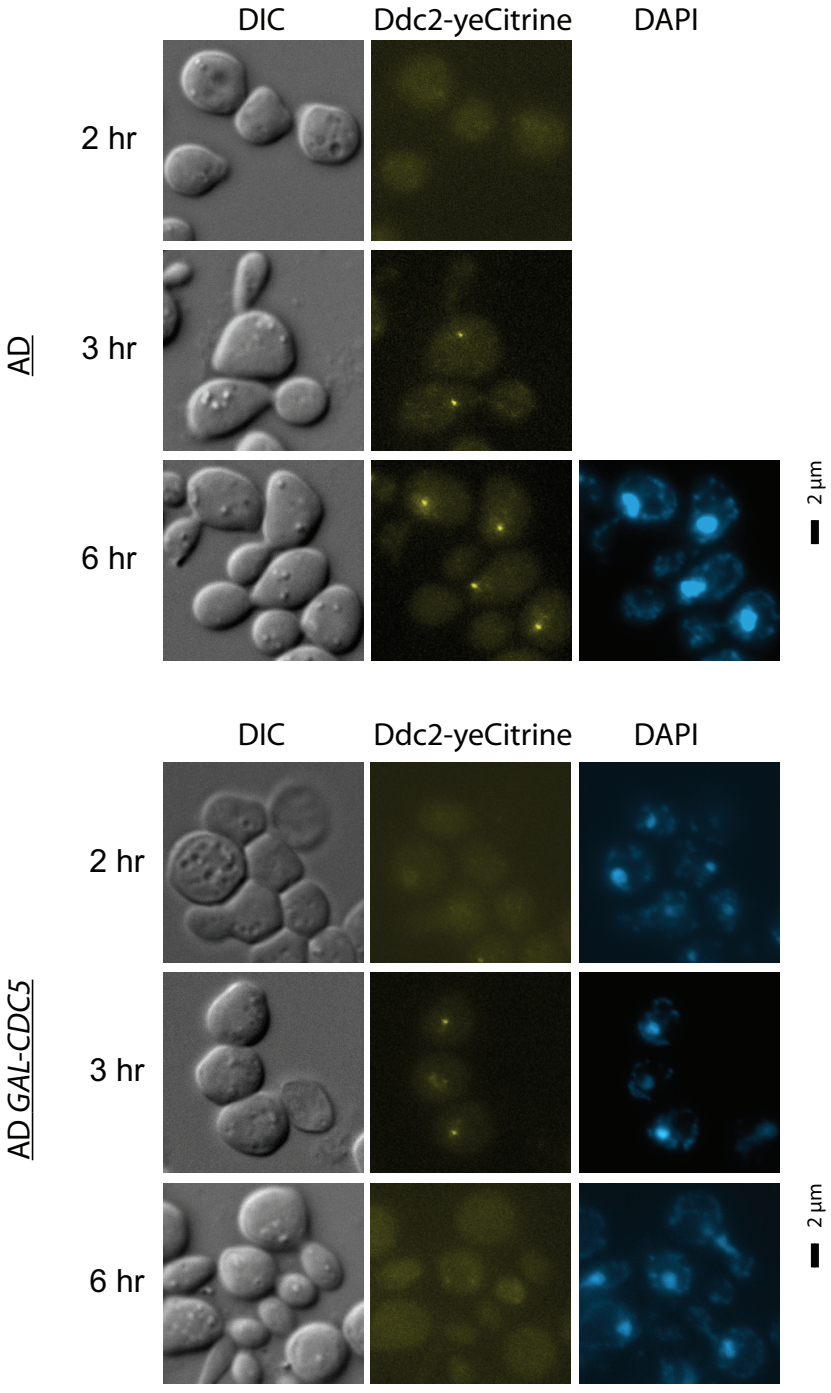

(Figure 14 - continued on next page)

(C)

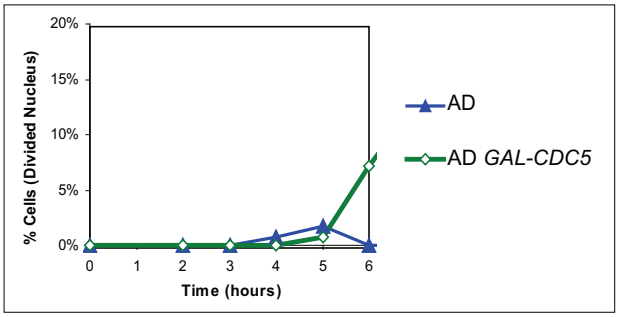

(D)

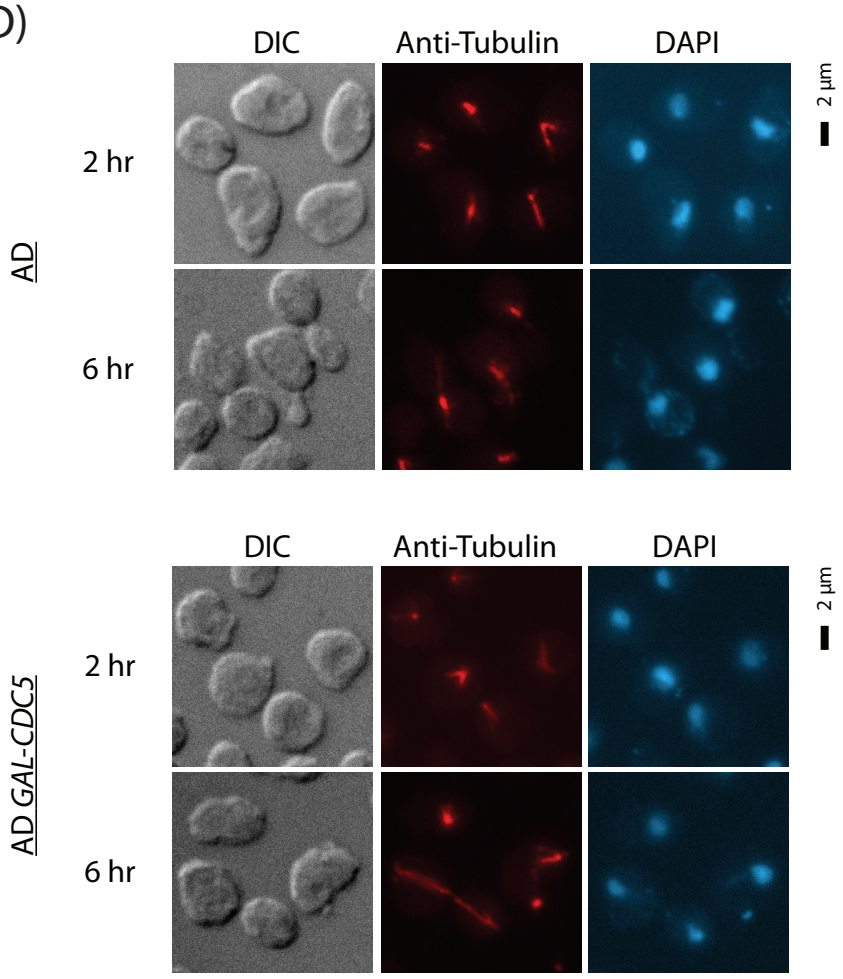

Figure 14. Overexpression of Cdc5 inhibits formation of Ddc2 foci.
AD *DDC2-yeCitrine* (US6382) and AD *GAL-CDC5 DDC2-yeCitrine* (US6416) cells were synchronized at G1 with α-factor in YEP+raff medium, and released in YEP+raff medium at 30°C with galactose added 2 hrs later. Samples were collected every hr. **(A)** Graph depicting percentage of Ddc2-yeCitrine tagged cells (▲: AD, ◇: AD *GAL-CDC5*) showing distinct Ddc2 foci. **(B)** Photomicrographs of AD and AD *GAL-CDC5* cells with Ddc2 foci and nucleus stained with DAPI (Blue). **(C)** Graph depicting percentage of cells with divided nucleus over time. **(D)** Photomicrographs of AD and AD *GAL-CDC5* cells with the mitotic spindle stained with anti-tubulin (Red) antibody and nucleus stained with DAPI (Blue).

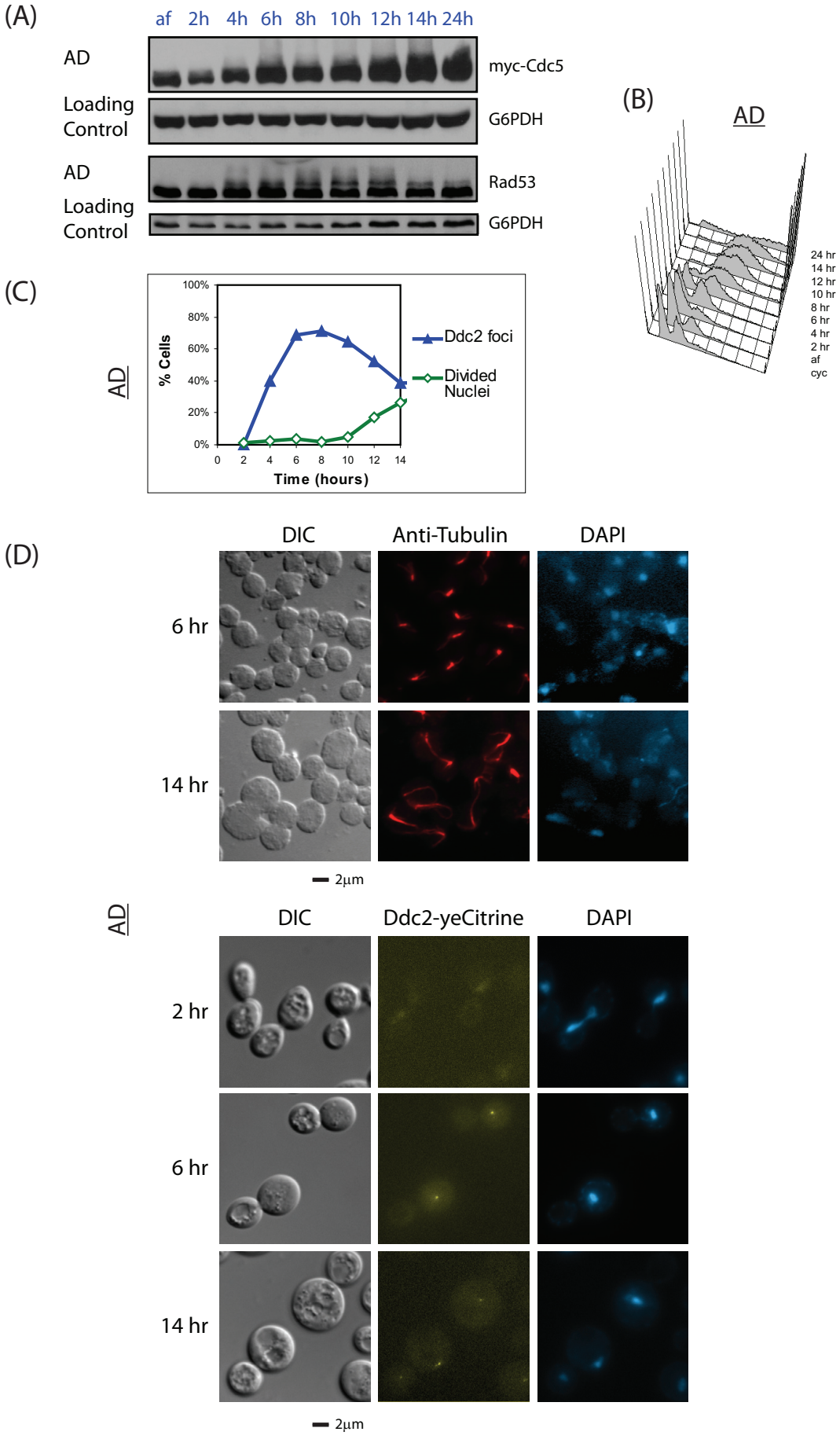

(Figure 15 - continued on next page)

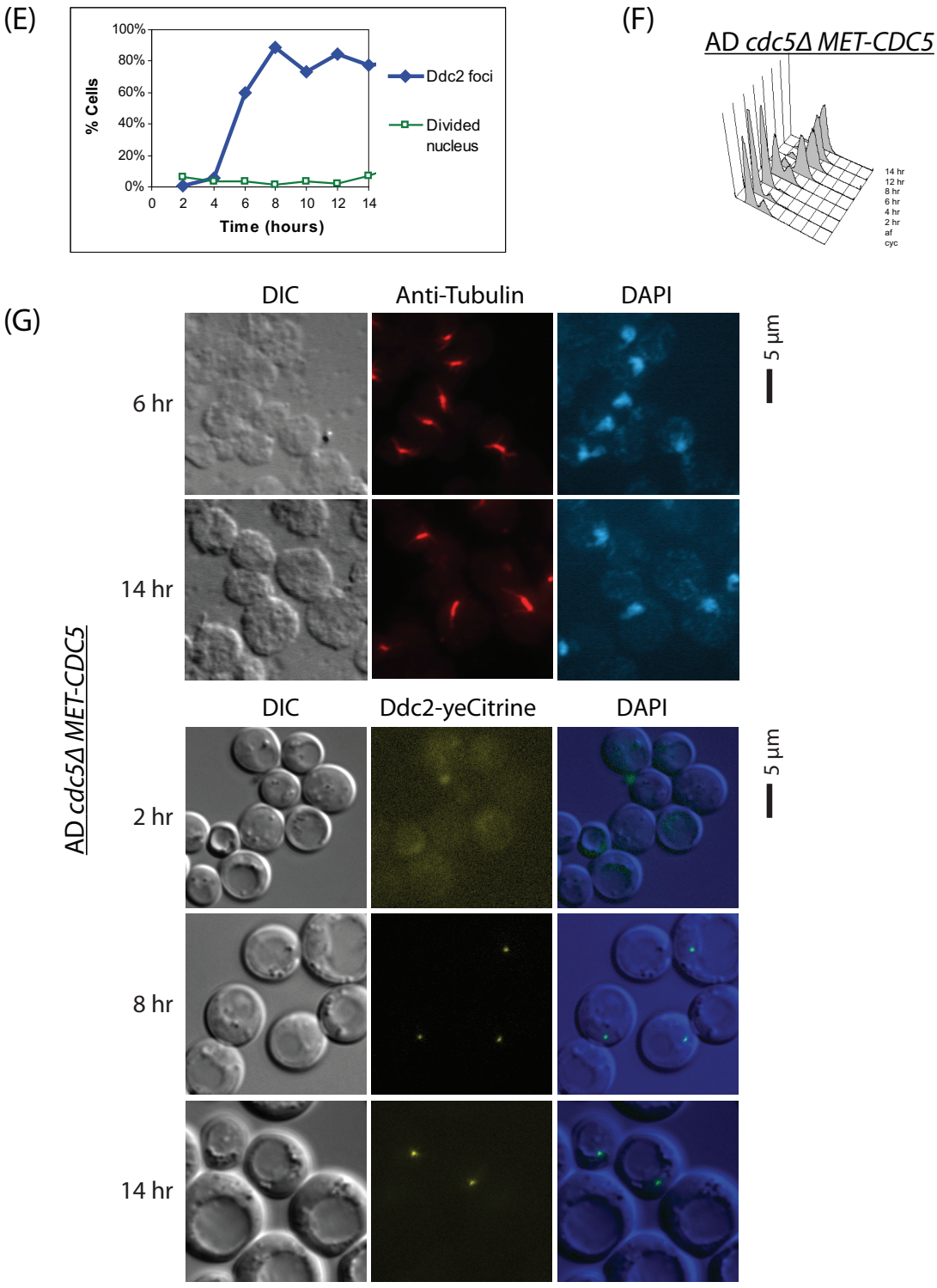

Figure 15. Ddc2 foci formation in adaptable and *cdc5Δ* strains.
AD (US6350) and AD *cdc5Δ MET-CDC5* (US6381) with *DDC2-yeCitrine* cells were synchronized at G1 with α-factor in YEP+raff medium, and released cell cycle in YEP+raff/gal medium at 30°C. **(A)** Western blot analyses and **(B)** FACS profile for AD cells. **(C)** The graph shows the percentage of cells exhibiting nuclear division and Ddc2 foci over the course of the experiment in AD cells. **(D)** The state of the spindle and nuclear division are shown using anti-tubulin (Red) staining and DAPI (Blue) in AD cells. For AD *cdc5Δ MET-CDC5* cells **(E)** The graph shows the percentage of cells exhibiting nuclear division and Ddc2 foci over the course of the experiment. **(F)** FACS profile **(G)** The state of the spindle and nuclear division are shown using anti-tubulin (Red) staining and DAPI (Blue).

4.2.5 Cdc5 inhibits formation of Ddc2 foci assembled at the site of DNA damage

It is clear from the results described in the previous section that Cdc5 prevents assembly of Ddc2 foci. To take the analysis further, we asked if Cdc5 polo kinase is capable of removing Ddc2 foci that have already been assembled at the site of DNA damage. To test this, we expressed Cdc5 only after Ddc2-yeCitrine foci have already been assembled on the DNA. AD cells (US6380) carrying *cdc5Δ* and *MET-CDC5* were arrested in G1 by α-factor treatment in YEP+raff medium containing 20mM methionine to deplete Cdc5. These cells were allowed to resume cell cycle at 24^{o}C in synthetic medium containing galactose (to induce HO expression) and methionine. Since cells take much longer to bud in synthetic medium, it took 10 hrs for >80% cells to arrest in G2/M with distinct Ddc2 foci. Cells were then washed and divided into two halves. One half was resuspended into synthetic medium containing methionine to continue repression of *MET-CDC5*, and the other half in medium without methionine for Cdc5 expression.

In the absence of Cdc5, the percentage of cells with Ddc2-yeCitrine foci remained high throughout the experiment (84.7% to 98.1%). For the first 6 hrs in the synthetic medium, the Ddc2-yeCitrine foci could also be seen in ~90% of Cdc5-expressing cells. However, the percentage of these cells dropped to 68.2% at 18 hrs to 37.4% at 22 hrs (Figure 16A). The decrease in Ddc2 foci was consistent with cells' progression into mitosis as indicated by presence of long spindles and divided nuclei (Figure 16D). At 18 hrs, long anaphase spindles began to appear in 5.4% of the Cdc5-expressing cells. These observations imply that Cdc5 polo kinase is able to dislodge the Ddc2 foci assembled at the site of DNA damage.

(A)

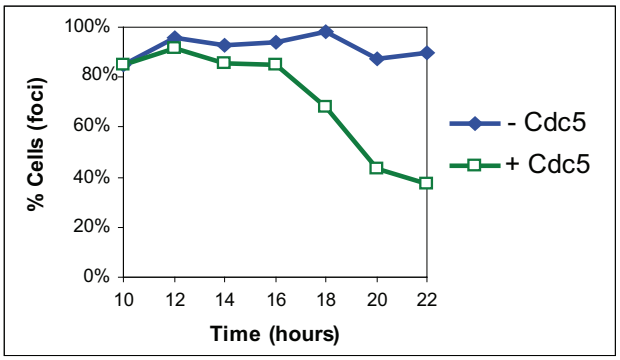

(B)

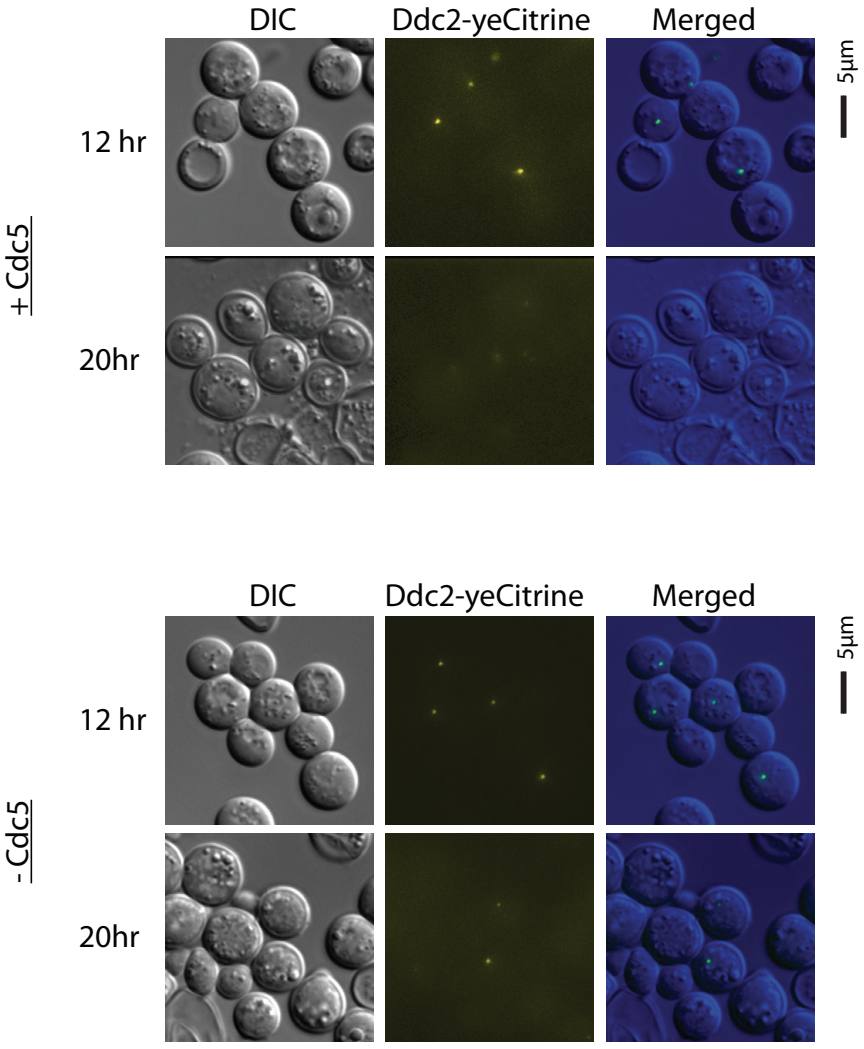

(Figure 16 - continued on next page)

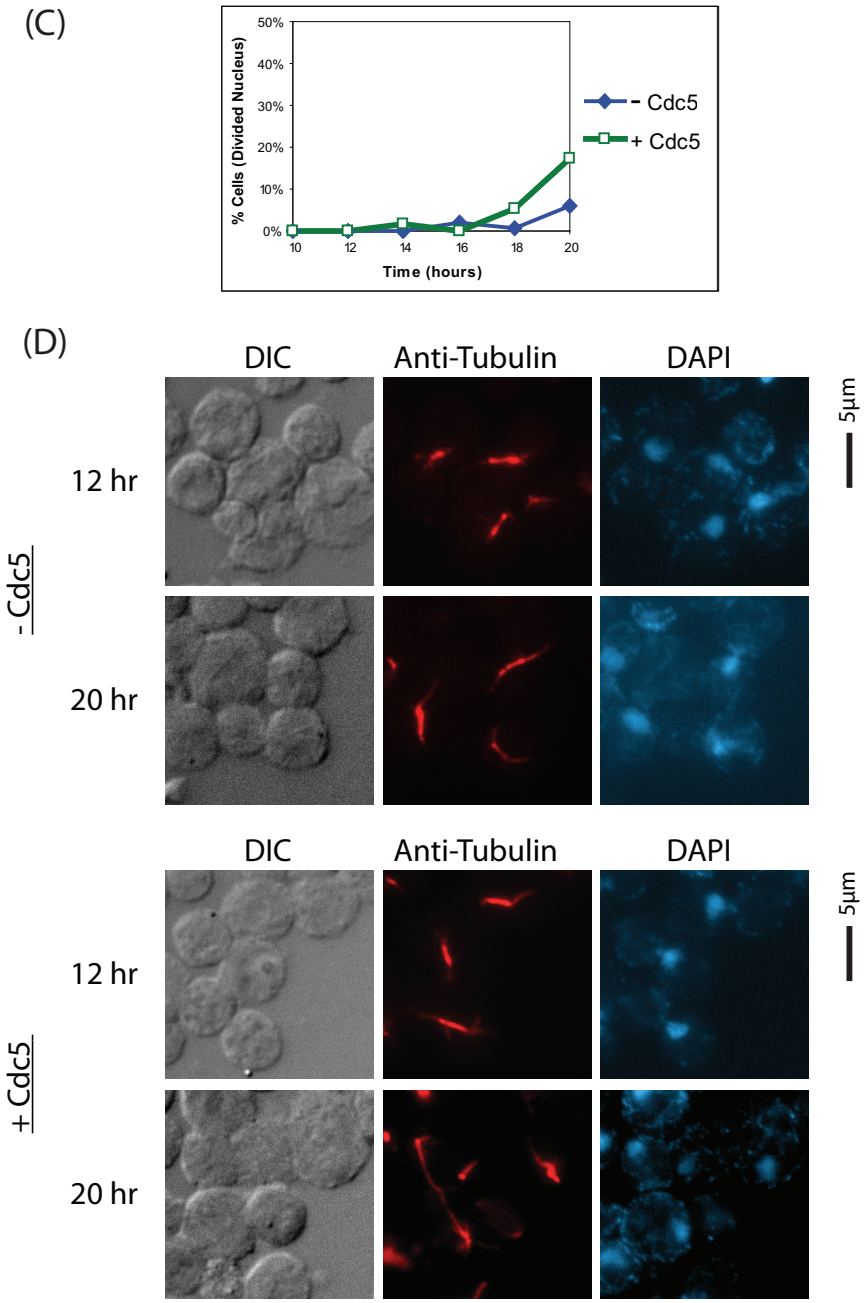

Figure 16. Cdc5 can dislodge Ddc2 foci.
AD *cdc5Δ MET-CDC5* (US6380) cells were synchronized at G1 with α-factor in methionine-free medium containing raffinose. 20mM methionine was added 30mins before releasing into +met medium (synthetic complete medium + raff/gal + 20mM methionine) at 24^{O}C. After 10 hrs, the cell culture was divided into two halves. The cultre were filtered and washed and the cells resuspended in -met (methionine-free medium with raff/gal for **+ CDC5** sample) and +met (synthetic complete medium + 20mM methionine + raff/gal for **- CDC5** sample) medium. Thereafter, samples were collected every 2 hrs for 12 hrs.
(A) Graph (♦: **- CDC5**, □: **+ CDC5)** depicting percentage of Ddc2-yeCitrine tagged cells showing distinct Ddc2 foci. **(B)** Photomicrographs of cells with Ddc2 foci and nucleus stained with DAPI (Blue). **(C)** Graph depicting percentage of cells with divided nucleus over time. **(D)** Photomicrographs of cells with spindle stained with anti-tubulin (Red) antibody and nucleus stained with DAPI (Blue).
Note: "**+ CDC5**" refers cells with active Cdc5; and "**- CDC5**" refers to cells depleted of Cdc5. Both were derived from the same strain (US6380).

4.2.6 Cdc5 polo kinase and the checkpoint clamp

In response to DNA damage, the checkpoint clamp complex (also known as 9-1-1 complex, consisting of Ddc1-Rad17-Mec3 in *S. cerevisiae*, Rad9-Rad1-Hus1 in mammals) and Mec1-Ddc2 heterodimer (ATR/ATRIP in mammals) are recruited to RPA-coated ssDNA. Earlier studies in *S. cerevisiae* have shown that the two complexes are recruited independently [73, 74]. However, more recent reports suggest that 9-1-1 may also participate in recruiting Mec1-Ddc2 to double strand breaks [75, 76]. Nevertheless, both complexes seem to be necessary for checkpoint activation [77], as activation of Mec1 may require 9-1-1 [78].

In the preceding section, we have discovered that overexpression of *CDC5* prevents the formation of Ddc2 foci. Therefore, we wish to ask if Cdc5 dampened the checkpoint signaling by interfering with the recruitment of 9-1-1 complex to DNA, and hence causing the delocalization of Ddc2. We monitored the 9-1-1 complex by tagging the endogenous *DDC1* with yeCitrine; allowing us to visualize foci formation at the DSB. Therefore, AD cells expressing Ddc1-yeCitrine and with (US6448) or without (US6446) integrated *GAL-CDC5* were synchronized in G1 and then released into raffinose medium at 30ºC. Galactose was added to induce HO and Cdc5 expression after 2 hrs. Samples were collected and imaged every hour. The data revealed no significant difference in Ddc1 accumulation between cells with or without *GAL-CDC5* (Figure 17); ~85% of Cdc5-overexpressing AD cells and ~73% of AD cells exhibited distinct Ddc1 foci by the 6th hr. These results show that the inactivation of checkpoint and delocalization of Ddc2 is not causally connected to 9-1-1 clamp. It suggests that either Mec1-Ddc2 or the upstream complex, RPA, is the target of Cdc5.

Nevertheless, it is also possible that Cdc5 may mediate indirectly or through multiple targets.

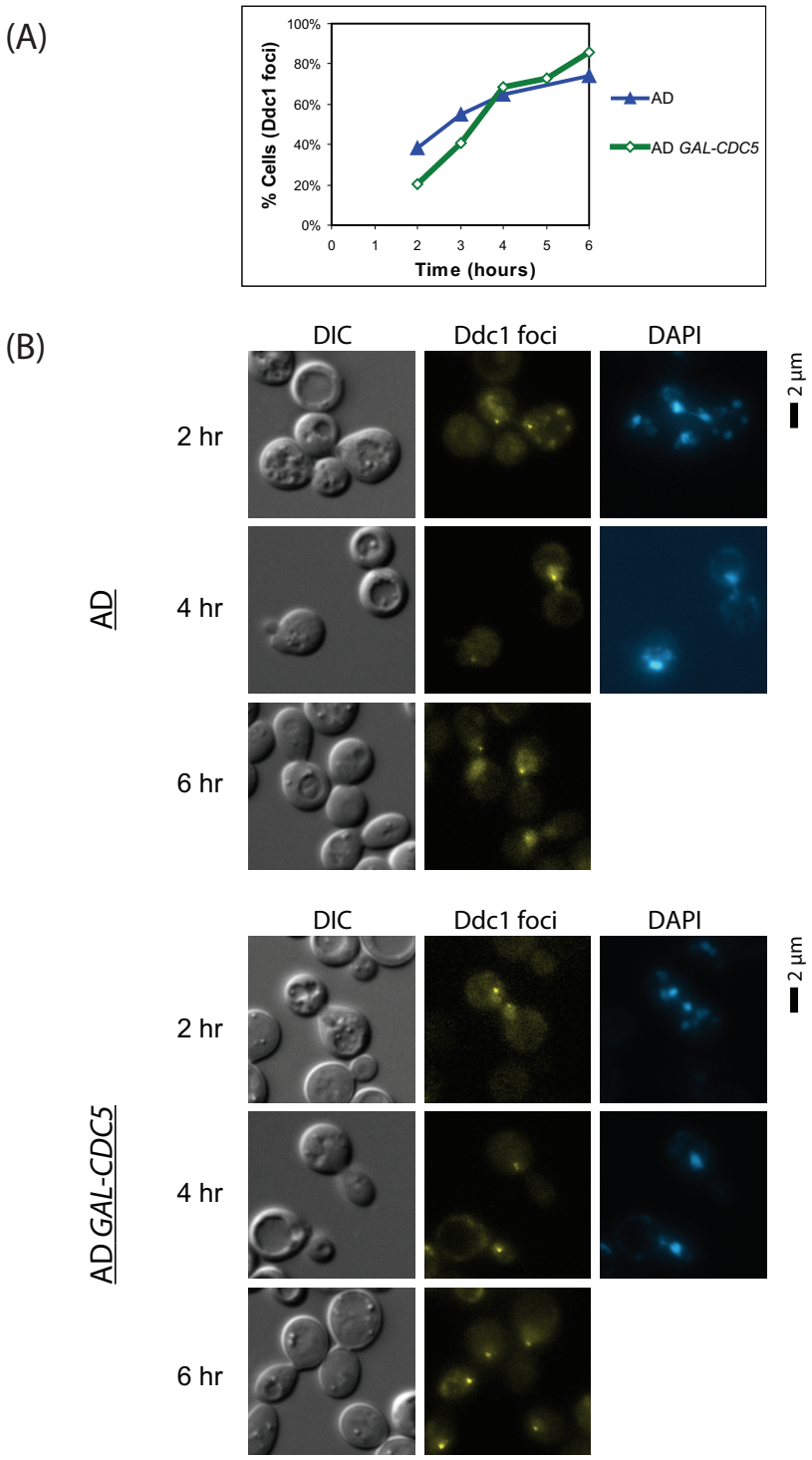

Figure 17. Overexpression of Cdc5 does not affect the localization of Ddc1.
AD *DDC1-yeCitrine* (US6446) and AD *GAL-CDC5 DDC1-yeCitrine* (US6448) cells were synchronized in G1 with α-factor in YEP+raff medium, and released in YEP+raff medium at 30°C with galactose added 2 hrs later. Samples were collected every hr.
(A) Plot of percentage of Ddc2-yeCitrine tagged cells (▲: AD, ◇: AD *GAL-CDC5*) showing distinct Ddc1 foci at indicated times.
(B) Photomicrographs of cells with Ddc1 foci and nucleus stained with DAPI (Blue).

4.2.7 A search for Cdc5 substrate(s) in adaptive response pathway

As described above,, we have observed that ectopic expression of Cdc5 polo kinase is capable of inactivating the checkpoint signaling. Our results suggest that Cdc5 may do so by specifically destabilizing the formation of Ddc2 foci, but not Ddc1 (checkpoint clamp component) foci. However, it is possible that Cdc5 exerts its influence through other aspects of checkpoint signaling.

During adaptation, Cdc5 may interact and form a (transient) complex with its substrates. In order to screen for candidate substrates of Cdc5, we employed a strategy that combines the labeling of cells with stable amino acid isotopes (SILAC) [189], co-immunoprecipitation of Cdc5 together with its substrates during adaptation, and identification of these substrates through quantitative mass spectrometry [187]. SILAC is a metabolic labeling method that utilizes a cell's machinery to incorporate exogenous heavy isotopes of amino acid residues into expressed proteins. This labeling strategy facilitates subsequent mass spectrometric analysis to differentiate between peptide signals from labeled or unlabeled source.

To prepare cells for SILAC mass spectrometry, AD cells with or without *GAL-cmyc$_6$-CDC5* (US6391 and US6267) were grown overnight in labeled or unlabeled liquid medium, respectively (refer to Section 2.13 for more details), supplemented with raffinose. The next day, cells were diluted and synchronized in G1 as described previously and then released into their respective medium at 30ºC. Two hrs later, galactose was added to induce HO and Cdc5. Cells were collected after 6 hrs for the preparation of cell extracts. Immunoprecipitates obtained using anti-cmyc antibodies were subsequently subjected to mass spectrometric analysis as described in Section 2.13.

In total, 1115 proteins were identified. Of these, 962 were detected in both samples. The remaining 153 proteins or ~13% were found only in control samples and this was probably due to the different physiological states of the samples, therefore, these were discarded.. Proteins involved in metabolic pathways, ribosomal biogenesis, heat shock response and other "house keeping" proteins were also removed from consideration. Since Cdc5 affects the recruitment of Ddc2 to the break site, it is more probable that Cdc5 mediates through a substrate that is involved in the DNA damage checkpoint response, and upstream of Ddc2 recruitment. Therefore, a total of 20 proteins (out of ~80 candidate targets) relevant in the checkpoint context and based on their (possible) involvement in DNA damage response or interaction with Cdc5, was selected (Table 8). The most interesting candidate protein amongst them is the RPA complex, since all 3 subunits of RPA (Rfa1, Rfa2 and Rfa3) were identified with relatively high confidence (Table 9). The RPA complex is known to affect Ddc2 recruitment. The mean sequence coverage (mean of the three RPA subunits) from 32 peptides is ~36%, and the mean ratio is ~0.291 (a value smaller than 1 is better). Note that the normalized ratios are comparisons of protein ratio versus the medium ratio of all proteins. This method of normalization is often used in the analysis of whole proteome or transcriptome. It assumes that the majority of the proteins or transcripts are for housekeeping, and thus do not vary significantly. Since this is a mass spectrometry of Cdc5 immunoprecipates, the normalized ratio is not an insightful comparison. Subsequent scrutiny of Rfa1 protein sequence revealed a consensus Cdc5 phosphorylation site (D/E-X-S/T-Φ-D, where Φ denotes a hydrophobic reside [216]) at Thr346 and 3 polo-box binding domains (S-[pS/pT]-P/X, where 'p' denotes the phosphorylated form and proline at +1 position confers a slight advantage but is not necessary [217]) (refer to Table 9). Although RPA is not a candidate substrate with

the lowest ratio, it is the only one with a direct role in the recruitment of Ddc2 [73, 74]. These results raises the possibility that RPA could be targeted for phosphorylation by Cdc5 during adaptation. However, this scenario should be treated with caution since RPA does not uniquely stand out amongst the 20 candidates. Therefore, this possibilty must be corroborated with alternative assays.

S/N	Protein Descriptions	Unique Peptides (seq)	Sequence Coverage [%]	Ratio H/L	Ratio H/L Normalized	Log2 summed intensity
1.	Bmh1	3	61.8	0.20805	0.71313	24.0827
2.	Cdc14	1	2.4	0.20842	0.60846	18.82724
3.	Cdc28	2	8.1	0.61409	1.8504	20.75515
4.	Cka1	9	24.2	0.2816	0.90328	22.6826
5.	Ckb1	3	12.6	0.27099	1.0335	22.39375
6.	Glc7	9	33	0.26859	0.90673	23.2717
7.	H2A1	3	34.8	0.27462	0.83291	26.53022
8.	Pin4	9	17.5	0.20951	0.60685	23.78706
9.	Pph21	3	24.9	0.18887	0.66713	23.54887
10.	Pph22	3	22.8	0.29726	0.94269	22.87819
11.	Rad27	2	3.7	0.43609	1.3764	18.6826
12.	Rad6	1	9.8	0.18121	0.42045	21.00854
13.	Rfa1	24	46.7	0.29201	0.84808	25.87514
14.	Rfa2	5	22	0.28427	0.92853	23.59412
15.	Rfa3	3	41.8	0.29674	0.69292	22.84963
16.	Rfc5p	2	6.8	0.56268	1.9703	18.81694
17.	Smc1	4	3.1	0.53097	0.91059	21.08596
18.	Smc3	3	2.5	0.45512	0.65193	19.52816
19.	Tpd3	9	15.6	0.2738	0.89258	23.58646
20.	Yku80	1	1	0.01992	0.05068	24.79521

Table 8. Cdc5 candidate substrates.
Column 3 indicates the number of peptides identified corresponding to the protein in column 2. Column 4 is the percentage sequence coverage of the protein based on peptides identified in column 3. Column 5 is the ratio (H/L) of quantity of protein found in samples with heavy (H) or light (L) isotopes. Since the control sample was labeled with heavy, the ratio refers to the amount of protein found in the control sample divided by those found in *GAL-CDC5* samples. Therefore, a lower ratio indicates a higher confidence in the proteins bound by Cdc5. Column 6 displays the ratio normalized with the median. Column 7 shows $\log_2$ of the signal intensity.

	Position in protein	Sequence in protein	Consensus motif
1	2 - 4	SSV	S[pS/pT]X
2	117 - 119	STF	S[pS/pT]X
3	344 - 349	DITIVD	[E/D]X[pS/pT][I/L/V/M]X[E/D]
4	395 - 397	SST	S[pS/pT]X

Table 9. Possible Cdc5 phosphorylation and binding sites in Rfa1.
Column 4 contains the consensus motifs: S[pS/pT]P/X for polo box binding domain [217], and [E/D]X[pS/pT][I/L/V/M]X[E/D] for Cdc5 phosphorylation site [216].

4.3 Discussion

It has been shown previously that Cdc5 is involved in the adaptive response in the budding yeast [3]. This conclusion was primarily gleaned from the behavior of the *cdc5-ad* allele in that *cdc5-ad* cells are largely defective in adaptation in response to DNA damage. Since *cdc5-ad* protein is normal with respect to other mitotic functions, it has been suggested that *cdc5-ad* may be a gain-of-function allele [108]. For some reason, *cdc5-ad* does not exhibit a strong phenotype in our experimental regimes (data not shown); therefore we have used *cdc5Δ* in our investigations described in Chapter 3. Our results clearly show that *cdc5Δ* cells are completely defective in adaptation, implying that Cdc5 function is essential for adaptive response. In Chapter 4, we have taken a reverse approach to show that ectopic expression of Cdc5 accelerates adaptation. AD cells with high Cdc5 activity escape from the arrest and traverse to telophase in 8-10 hrs as compared to 'normal' AD cells (not over-expressing Cdc5) that take 12-14 hrs (Figure 9C). RT-PCR analysis (Figure 5) confirms that cells reaching telophase still contain unrepaired DSB, implying that Cdc5 overexpression does not cause escape from G2/M by increasing cells' capacity to repair DSB, but by accelerating the adaptive response. We are aware that the experiments involving overexpression may, in some instances, lead to artefacts that are not valid at physiological concentrations of the relevant protein. However, our results show that ectopic expression of Cdc5 inhibits Ddc2 foci formation (Figure 14) but not the formation of Ddc1 foci (Figure 17). This specificity and our other observations give us a reasonable degree of confidence in our results.

Cdc5 serves multiple functions in mitosis such as spindle assembly [218, 219], efficient cleavage of cohesin [117] and mitotic exit [85]. In mammalian cells,

recovery (after repair) from DNA damage checkpoint induced arrest has been shown to require polo-like kinase Plk1 [109-112]. Therefore, Cdc5's contribution to adaptation via its mitotic function is a distinct possibility. Since cells undergoing recovery or adaptation need to traverse through mitosis we investigated this possibility by examining the recovery process in yeast. We find that RP (repairable) cells undergo recovery by inactivating the checkpoint, cleave cohesins, divide their nuclei and elongate their spindle in the absence of Cdc5 (Figure 8). These results strongly suggest that in the context of DNA damage, cells' progression through mitosis during recovery does not require Cdc5 function. It is reasonable to expect, therefore, that mitotic progression during adaptation is also not dependent on Cdc5. Thus, we chose to look more closely at Cdc5's role in the inactivation of the checkpoint signaling.

Ectopic expression of Cdc5 is able to suppress the adaptation defect of *sae2Δ*, *ptc2Δ ptc3Δ* and *ckb1Δ* mutants. Of these, Sae2 is required for disassociation of MRX complex from DNA damage sites [68]. Without Sae2, MRX complex remained bound to the damage site with persistent checkpoint activation. As a result, *sae2Δ* cells are unable to adapt or recover. Ptc2/Ptc3 phosphatases, on the other hand, are required for an event further downstream i.e. inactivation of Rad53 by dephosphorylation [107]. As inactivation of Rad53 by Ptc2/Ptc3 phosphatase is thought to involve CKII activity, it is not surprising that *ckb1Δ* is also defective in the adaptive response. The fact that Cdc5 overexpression corrects the adaptation defect of these mutants leads to the argument that Cdc5 is acting downstream of these effectors. However, our observation that Rad53 hyper-phosphorylation is seen very transiently in cells over-expressing Cdc5 suggests that cells may not be able to mount a robust checkpoint

response in the presence of high Cdc5 activity. How, then, does Cdc5 dampen cells' capacity to activate the DNA damage checkpoint?

MRX complex and Exo1-mediated DNA resection of the 5'end is one of the initial events to happen in response to a double strand break and it is necessary for checkpoint activation. As we have seen, Cdc5 overexpression does not adversely affect 5' end resection significantly (Figure 13), implying that Cdc5 does not participate in the adaptive response by influencing resection. It is known that loading of the checkpoint clamp (Rad17-Mec3-Ddc1 complex) and binding of Mec1-Ddc2 complex to RPA-coated DNA are the most upstream events initiating the checkpoint signaling [75-78]. When expression of Cdc5 was induced concurrently with generation of a DSB, formation of Ddc2 foci was prevented. Conversely, in the absence of Cdc5, Ddc2 foci persisted (Figure 15), Rad53 remained hyper-phosphorylated and cells were unable to undergo adaptation (Figure 7). These observations suggest that Cdc5 impedes recruitment of 'Ddc2-Mec1' complex to the DNA lesion. As a result, checkpoint signaling is not executed robustly and cells fail to arrest in G2/M.

What is the mechanism by which Cdc5 impede recruitment of Ddc2-Mec1 complex? Since Cdc5-overexpression causes delocalization of Ddc2 during DNA damage, it is tempting to suggest that phosphorylation of Ddc2 by Cdc5 reduces its affinity for the RPA-coated ssDNA. It is also possible that Cdc5 does not inhibit Ddc2 'activity' directly, but does so via a yet-to-be-identified factor X. However, such inhibitory schemes must take into account two additional observations: (i) adaptive response normally takes 10 hrs to initiate when Cdc5 is not over-expressed (ii) Cdc5 is inhibited by activated Rad53 during DNA damage response. Three 'bare-bone' systems (Figure 18) containing functionally interacting effectors can be imagined

which, given sufficient time, can switch from one steady state (G2/M arrest) to another (adaptation).

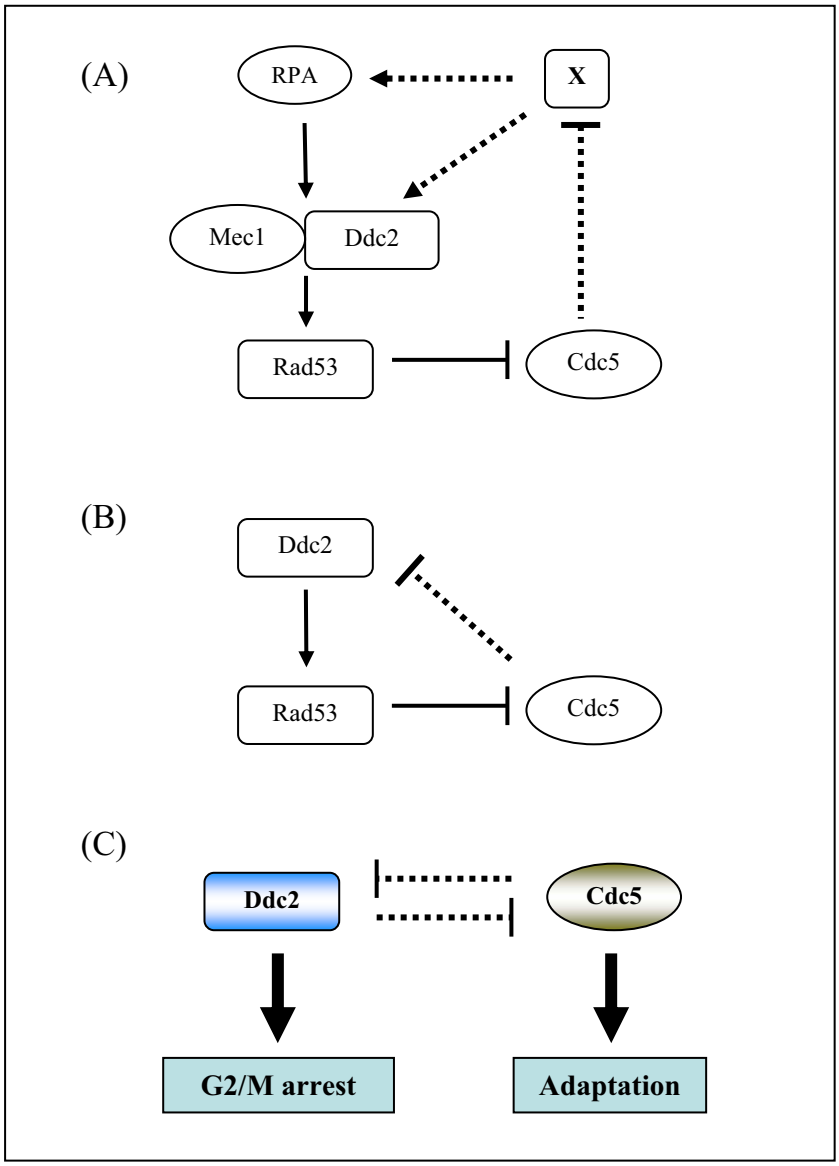

Figure 18. Qualitative behaviors of networks are similar.
Protein interaction networks of (A), (B) and (C) display similar qualitative behaviors, since (A) and (B) could be summarized to form the mutual inactivation network of Ddc2 and Cdc5 as shown in (C). (A) Cdc5 may inactivate the checkpoint through an unknown protein "X" or (B) directly inactivate Ddc2. The self amplifying double-negative feedback loop of Cdc5 (B: Cdc5⊣Ddc2→Rad53⊣Cdc5; C: Cdc5⊣Ddc2⊣Cdc5) could serve as a molecular clock to trigger adaptation after failed attempts to repair DNA damage during the prolonged cell cycle arrest. Dotted lines refer to indirect or unknown interactions; hammer heads "⊣" refer to inhibition and arrow heads "→" refer to activation.

During DNA damage (initial state), checkpoint signaling is initiated via recruitment of Ddc2-Mec1 complex to the site of DNA damage leading to Rad53 activation. Activated Rad53 in turn inhibits the activity of Cdc5 [83, 126]. As our results show, Cdc5 continues to accumulate while cells are arrested in G2/M (Figure 15A). Once the level of Cdc5 surpasses a critical threshold (present in a mutual inactivation network, see Figure 18), the system progressively switches into reverse gear such that Cdc5 begins to dampen the affinity of Ddc2-Mec1 complex for the RPA coated ssDNA. By deactivating the checkpoint protein Ddc2, more Cdc5 would be freed to participate in the deactivation, eventually setting up a self-amplifying positive feedback loop. Therefore, the prolonged period of G2/M arrest before adaptation could very well be the time needed for Cdc5 to reach and exceed the threshold level. Such a system can serve as a molecular clock which leads to adaptation in the absence of HR repair. These schemes also accommodate the requirement of CKII for adaptive response. CKII is a ubiquitous and constitutively active Ser/Thr protein kinase which can serve as a priming kinase for polo kinase, as Cdc5 binding sites have to be phosphorylated [217, 220]. According to the 'priming model', polo kinase substrate is first phosphorylated by CKII, thus creating a polo-box binding domain. These sites in turn help to recruit polo kinase to the substrate for further phosphorylation. It is possible that Ddc2 is a substrate for both CKII and Cdc5.

The schemes described above center around the functional relationship between Ddc2 and Cdc5. However, Ddc2 was not detected in Cdc5 immunoprecipitates in our mass spectrometric analysis. Instead, RPA subunits Rfa1, Rfa2 and Rfa3 were detected (Table 8). Moreover, sequence analysis revealed a possible Cdc5 phosphorylation site (Table 9) in Rfa1. Although more experimental validation is needed, based on current data, it is possible that the switching-off of the

checkpoint by Cdc5 is mediated via trimeric RPA complex such that phosphorylation of RPA subunits by progressively accumulating Cdc5 reduces its affinity to ssDNA. This, in turn, will prevent recruitment of Ddc2-Mec1 complex (Figure 14). Our observation that ectopic expression of Cdc5 prevents Ddc2 foci formation but not Ddc1 foci would then suggest that while clamp loading is not affected by Cdc5, Ddc2 recruitment is. This is consistent with the previous reports that the clamp-loading does not require extensive DNA resection [221] i.e. extensive RPA-coated ssDNA. This model also explains why checkpoint remains permanently inactivated in the subsequent generation of adapted cells even though they inherit a double strand break.

In conclusion, our results are most consistent with a scheme (Figure 19) in which progressive accumulation of Cdc5 polo kinase during G2/M arrest allows phosphorylation of RPA complex, thereby disrupting its interaction with Mec1-Ddc2 heterodimer. This eventually results in the inactivation of the checkpoint signaling and AD cell's escape from G2/M arrest.

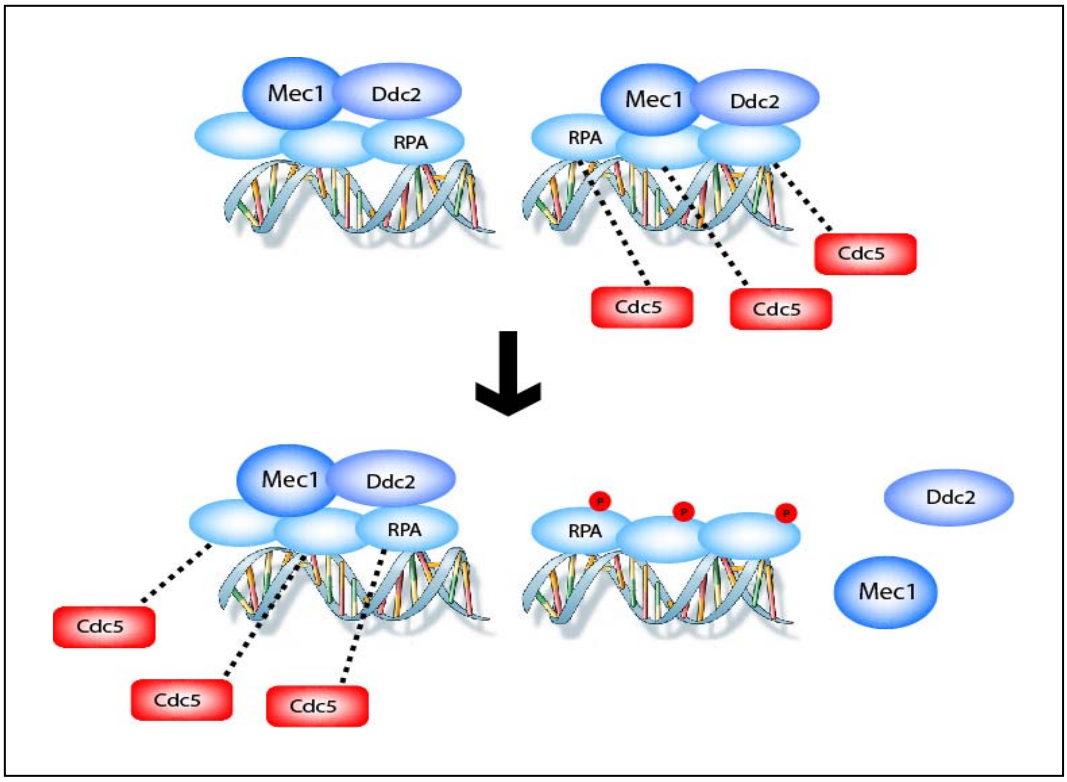

Figure 19. A proposed scheme for Cdc5-mediated inactivation of the DNA damage checkpoint.

During active DNA Damage checkpoint, Cdc5 is inhibited by Rad53. However, as the former continues to accumulate during G2/M arrest, once the critical threshold is exceeded, the mutual inactivation interaction (as shown in Figure 18) of Cdc5 and Rad53 further amplifies the activity of Cdc5. The active Cdc5 is able to trigger the dissociation of Ddc2 from RPA, probably via direct phosphorylation of RPA on RPA-Ddc2 interaction sites. As a result, heterodimer Mec1-Ddc2 could no longer activate the downstream checkpoint cascades.

Chapter 5 Regulation of Gene Expression by Oscillatory Transcription Factors

5.1 Background

Oscillatory gene expression is quite widespread in cells of various types. Reported observations indicate this oscillatory behavior is not random but highly regulated. This suggests that oscillatory transcriptions are essential for normal functioning of a cell. This is notion is reinforced by the data from animal models and *in vitro* studies where oscillatory gene expression dynamics are either altered or eliminated.. Circadian oscillations are required for functional electrical responses to light in the mouse retina [222] and somite segmentation oscillations are required for proper differentiation of neuronal cells [8]. Distinct differences exist between the p53 oscillation profiles of normal and cancer-prone Bloom's syndrome patients [19]. Cells manifesting p53 oscillations may possess a lowered death threshold upon DNA damage [20]. Differential expression of target genes has also been reported for different NF-κB oscillation profiles [13, 15]. The transcription factor (TF) oscillations allow the cell to discern and respond appropriately to diverse stimuli. Genome-wide oscillations of transcription in yeast and in metabolic cycles have also been suggested to facilitate temporal compartmentalization and coordination of biological processes [223-225].

A prerequisite to understanding mechanisms underlying oscillatory transcription-induced biological responses is to elucidate how oscillatory TFs induces oscillatory dynamics to specific gene expressions and its ensuing effects. Prior studies have focused on investigating mechanisms that induce TF oscillations and not their

effects on gene expressions. Due to the diversity of oscillatory TFs, it is desirable to determine in general terms their molecular properties and their target genes that shape the response to TF oscillations.

In this chapter, general and analytically tractable gene expression models are constructed, solved and analyzed. Such mathematical models would avert the need to make inference from numerical simulations which requires the usage of specific model parameter values, and would facilitate the analyses of plausible responses to TF oscillations.

5.2 Results

5.2.1 Formulation of gene expression models

A kinetic model is a mathematical representation of biological processes involving the concentrations of various biochemical components as functions of time. ODEs (ordinary differential equations) are commonly used in modeling of various forms of dynamical systems, mostly due to the availability of several mathematical theories that facilitate subsequent analytical and numerical solutions [226].

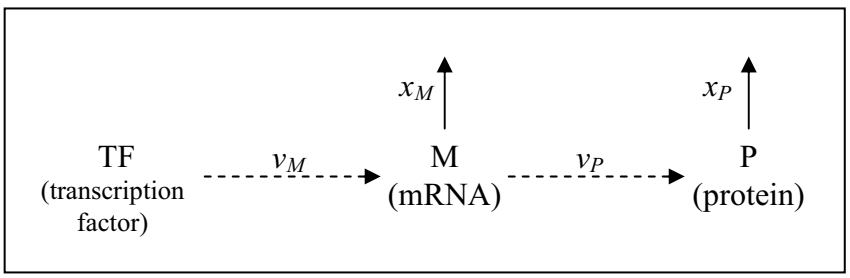

Figure 20. Schematics of gene expression process.
The gene expression process consists of transcription (v_M), translation (v_P) and self-degradation (x_M, x_P) processes.

In general, gene expression consists mainly of 3 species (transcription factor, mRNA and protein) and 4 processes: transcription (v_M), translation (v_P), degradation of mRNA (x_M) and protein (x_P), as shown in Figure 20. To formulate a kinetic model, an equation is assigned to each species to account for changes in its concentration with time in the form of an ODE.

$$\frac{dS}{dt} = \textit{Rate of formation} - \textit{Rate of removal or degradation} \qquad \text{Eqn(1)}$$

The left-hand side (LHS) denotes rate of change of the concentration of a species "*S*", which equals to its rate of formation minus its rate of removal on the right-hand side (RHS). The equations for the mRNA (*M*) and protein (*P*) in the model are listed in Equation 2.

$$\frac{dM}{dt} = v_M - x_M$$
$$\frac{dP}{dt} = v_P - x_P \qquad \text{Eqn(2)}$$

The TF oscillation profile is approximated by a sinusoidal function, which is often a good physical approximation [227, 228]. Therefore,

$$TF(t) = X_{TF} + A_{TF} \sin \frac{2\pi}{P_{TF}} t \qquad \text{Eqn(3)}$$

where X_{TF} is mean level of TF intracellular concentration

A_{TF} is oscillation amplitude of TF intracellular concentration ($< X_{TF}$)

P_{TF} is TF oscillation period

$TF(t)$ is the TF intracellular concentration with respect to time, and $TF(t \le 0) = 0$.

To model transcription (v_M), two expressions generally encapsulate the kinetics of gene expression regulation by a TF. In the first, the rate of transcript production follows mass action kinetics - an empirical law stating that transcriptional rates are proportional to TF intracellular concentration, denoted as Model M

henceforth. Therefore, the expression is given by $v_M = k_M[TF(t-\theta)]^n$, where k_M is the rate constant of transcription, n is the stoichiometry, θ is the time delay for transcription.

The second model includes the binding co-operativity of a TF to its gene promoters, which is commonly captured by the Hill function [229-231], denoted as Model H henceforth. The Hill function is expressed as $\frac{k_M[TF(t-\theta)]^n}{j_M^n + [TF(t-\theta)]^n}$, where k_M and j_M are parameters that denote the maximal rate of production and the dissociation constant respectively, n is the Hill coefficient, and θ is the time delay for product transcripts X that is dependent on concentration of transcription factors TF. Studies have suggested that the concentration of gene transcripts normally follows that of a sigmoidal curve (S shape) as represented by a Hill function [232-234].

In both models, self degradation reactions (x_M and x_P) are assumed to have first-order kinetics as expressed by $x_M = d_M S$, where d_M is the rate constant of degradation and S represents the species undergoing the reaction. The ODEs describing the kinetics of target gene transcription in Models M and H are given in Eqn(4) and (5) respectively.

Model M: $$\frac{dM}{dt} = k_M[TF(t-\theta_M)]^n - d_M M \qquad \text{Eqn(4)}$$

where M is intracellular concentration of mRNA

k_M is rate constant of mRNA transcription

θ_M is transcriptional time-delay

n is TF stoichiometry

d_M is mRNA self-degradation rate

Model H: $$\frac{dM}{dt} = \frac{k_M [TF(t-\theta_M)]^n}{j_M^n + [TF(t-\theta_M)]^n} - d_M M \qquad \text{Eqn(5)}$$

where M, k_M, θ_M, d_M are as defined in Equation 1

j_M is TF dissociation constant from its gene promoter

n is TF binding co-operativity to its gene promoter (binding co-operativity is negative if $n < 1$ and is positive if $n > 1$; $n = 1$ indicates no binding co-operativity.)

Finally, the ODE describing the kinetics of protein production for both models is given in Eqn(6).

$$\frac{dP}{dt} = k_P M(t-\theta_P) - d_P P \qquad \text{Eqn(6)}$$

where P is intracellular concentration of protein

k_P is rate of protein translation

θ_P is translational time-delay

d_P is protein self-degradation rate

5.2.2 Solutions of gene expression models

5.2.2.1 Solving model M

$$\frac{dM}{dt} = k_M\left[TF\left(t-\theta_M\right)\right]^n - d_M M \qquad \text{Eqn(4)}$$

$$\frac{dP}{dt} = k_P M\left(t-\theta_P\right) - d_P P \qquad \text{Eqn(6)}$$

Integrating Equation (4) with respect to *t* (details are given in Appendices) yields

$$M(t) \;= k_M e^{-d_M t}\int\left[TF\left(t-\theta_M\right)\right]^n e^{d_M t}dt + C_1 e^{-d_M t}$$

substituting Equation (3) yields

$$M(t) = k_M e^{-d_M t}\int\left[X_{TF} + A_{TF}\sin\frac{2\pi}{P_{TF}}\left(t-\theta_M\right)\right]^n e^{d_M t}dt + C_1 e^{-d_M t} \qquad \text{Eqn(7)}$$

Since Equation (7) is intractable,

$$\text{Approximate}\left[X_{TF} + A_{TF}\sin\frac{2\pi}{P_{TF}}\left(t-\theta_M\right)\right]^n \approx \overline{X_{TF}} + \overline{A_{TF}}\sin\frac{2\pi}{P_{TF}}\left(t-\theta_M\right), \qquad \text{Eqn(8)}$$

$$\text{when } \overline{X_{TF}} = \frac{\left(X_{TF}+A_{TF}\right)^n + \left(X_{TF}-A_{TF}\right)^n}{2}, \quad \overline{A_{TF}} = \frac{\left(X_{TF}+A_{TF}\right)^n - \left(X_{TF}-A_{TF}\right)^n}{2}.$$

Therefore, substituting Equation(8) into Equation (7) yields

$$\begin{aligned} &M(t) \\ &\approx k_M e^{-d_M t}\int\left[\overline{X_{TF}} + \overline{A_{TF}}\sin\frac{2\pi}{P_{TF}}\left(t-\theta_M\right)\right]e^{d_M t}dt + C_1 e^{-d_M t} \qquad \text{Eqn(9)} \\ &= \frac{k_M\overline{X_{TF}}}{d_M} + \frac{k_M\overline{A_{TF}}}{\sqrt{d_M^2 + \left(\frac{2\pi}{P_{TF}}\right)^2}}\sin\frac{2\pi}{P_{TF}}\left(t-\theta_M - \frac{P_{TF}}{2\pi}\arctan\frac{2\pi}{P_{TF}}\frac{1}{d_M}\right) + \left(C_1 + C_2 k_M\right)e^{-d_M t} \end{aligned}$$

Put Equation (7) into Equation (6) and integrate with respect to *t* yields

$$
\begin{aligned}
&P(t)\\
&=k_P e^{-d_P t}\int\left[M(t-\theta_P)\right]e^{d_P t}dt+C_3 e^{-d_P t}\\
&\approx k_P e^{-d_P t}\int_0\left[\begin{array}{l}\dfrac{k_M\overline{X_{TF}}}{d_M}e^{d_P t}+\dfrac{k_M\overline{A_{TF}}}{\sqrt{d_M^2+\left(\dfrac{2\pi}{P_{TF}}\right)^2}}e^{d_P t}\sin\dfrac{2\pi}{P_{TF}}\left(t-\theta_M-\theta_P-\dfrac{P_{TF}}{2\pi}\arctan\dfrac{2\pi}{P_{TF}}\dfrac{1}{d_M}\right)\\ +\left(C_1+C_2k_M\right)e^{-d_M(t-\theta_P)}e^{d_P t}\end{array}\right]dt+C_3e^{-d_P t}\\
&=\frac{k_Pk_M\overline{X_{TF}}}{d_Pd_M}+\frac{k_Pk_M\overline{A_{TF}}}{\sqrt{d_P^2+\left(\dfrac{2\pi}{P_{TF}}\right)^2}\sqrt{d_M^2+\left(\dfrac{2\pi}{P_{TF}}\right)^2}}\sin\frac{2\pi}{P_{TF}}\left(t-\theta_M-\theta_P-\frac{P_{TF}}{2\pi}\arctan\frac{2\pi}{P_{TF}}\frac{1}{d_M}-\frac{P_{TF}}{2\pi}\arctan\frac{2\pi}{P_{TF}}\frac{1}{d_P}\right)\\
&\quad+\frac{k_P\left(C_1+C_2k_M\right)}{d_P-d_M}e^{-d_M(t-\theta_P)}+\left(C_3+C_4k_P\right)e^{-d_P t}
\end{aligned}
\qquad \text{Eqn(10)}
$$

As $t\to\infty$,

$$
\begin{aligned}
M(t)&\to X_M+A_M\sin\frac{2\pi}{P_{TF}}\left(t-\alpha_M\right)\\
P(t)&\to X_P+A_P\sin\frac{2\pi}{P_{TF}}\left(t-\alpha_P\right)
\end{aligned}
\qquad \text{Eqn(11)}
$$

where

$$
X_M=\frac{k_M\overline{X_{TF}}}{d_M},\quad A_M=\frac{k_M\overline{A_{TF}}}{\sqrt{d_M^2+\left(\dfrac{2\pi}{P_{TF}}\right)^2}},\quad \alpha_M=\theta_M+\frac{P_{TF}}{2\pi}\arctan\frac{2\pi}{P_{TF}}\frac{1}{d_M}
$$

$$
X_P=\frac{k_P}{d_P}X_M,\quad A_P=\frac{k_P}{\sqrt{d_P^2+\left(\dfrac{2\pi}{P_{TF}}\right)^2}}A_M,\quad \alpha_P=\alpha_M+\theta_P+\frac{P_{TF}}{2\pi}\arctan\frac{2\pi}{P_{TF}}\frac{1}{d_P}
$$

Note: analytical solution is exact for *n = 1*.

5.2.2.2 Solving model H

$$\frac{dM}{dt} = \frac{k_M\left[TF\left(t-\theta_M\right)\right]^n}{j_M^n + \left[TF\left(t-\theta_M\right)\right]^n} - d_M M \qquad \text{Eqn(5)}$$

$$\frac{dP}{dt} = k_P M\left(t-\theta_P\right) - d_P P \qquad \text{Eqn(6)}$$

Integrating Equation (5) with respect to t and substituting Equation (3) yields

$$\begin{aligned} M(t) &= \frac{k_M}{d_M} - k_M j_M^n e^{-d_M t}\int \frac{e^{d_M t}}{j_M^n + \left[TF\left(t-\theta_M\right)\right]^n} dt + C_1 e^{-d_M t} \\ &= \frac{k_M}{d_M} - k_M j_M^n e^{-d_M t}\int \frac{e^{d_M t}}{j_M^n + \left[X_{TF} + A_{TF}\sin\frac{2\pi}{P_{TF}}\left(t-\theta_M\right)\right]^n} dt + C_1 e^{-d_M t} \end{aligned} \qquad \text{Eqn(12)}$$

Since Equation (12) is intractable,

$$\text{Approximate } \frac{1}{j_M^n + \left[X_{TF} + A_{TF}\sin\frac{2\pi}{P_{TF}}\left(t-\theta_M\right)\right]^n} \approx \overline{X_{TF}} + \overline{A_{TF}}\sin\left[\frac{2\pi}{P_{TF}}\left(t-\theta_M\right)+\pi\right],$$

$$\text{where } \begin{aligned} \overline{X_{TF}} &= \frac{2j_M^n + \left(X_{TF}+A_{TF}\right)^n + \left(X_{TF}-A_{TF}\right)^n}{2\left[j_M^n + \left(X_{TF}-A_{TF}\right)^n\right]\left[j_M^n + \left(X_{TF}+A_{TF}\right)^n\right]} \\ \overline{A_{TF}} &= \frac{\left(X_{TF}+A_{TF}\right)^n - \left(X_{TF}-A_{TF}\right)^n}{2\left[j_M^n + \left(X_{TF}-A_{TF}\right)^n\right]\left[j_M^n + \left(X_{TF}+A_{TF}\right)^n\right]} \end{aligned} \qquad \text{Eqn(13)}$$

Therefore,

$$\begin{aligned} & M(t) \\ &\approx \frac{k_M}{d_M} - k_M j_M^n e^{-d_M t}\int\left\{\overline{X_{TF}} + \overline{A_{TF}}\sin\left[\frac{2\pi}{P_{TF}}\left(t-\theta_M\right)+\pi\right]\right\} e^{d_M t} dt + C_1 e^{-d_M t} \\ &= \frac{k_M\left(1 - j_M^n\overline{X_{TF}}\right)}{d_M} + \frac{k_M j_M^n \overline{A_{TF}}}{\sqrt{d_M^2 + \left(\frac{2\pi}{P_{TF}}\right)^2}}\sin\frac{2\pi}{P_{TF}}\left(t - \theta_M - \frac{P_{TF}}{2\pi}\arctan\frac{2\pi}{P_{TF}}\frac{1}{d_M}\right) + \left(C_1 - C_2 k_M j_M^n\right)e^{-d_M t} \end{aligned}$$

Eqn(14)

Put Equation (12) into Equation (6) and integrate with respect to t yields

$$
\begin{aligned}
&P(t)\\
&=k_P e^{-d_P t}\int\left[M(t-\theta_P)\right]e^{d_P t}dt+C_3 e^{-d_P t}\\
&\approx k_P e^{-d_P t}\int\left[\begin{array}{l}\dfrac{k_M\left(1-j_M^n\overline{X_{TF}}\right)}{d_M}e^{d_P t}+\dfrac{k_M j_M^n\overline{A_{TF}}}{\sqrt{d_M^2+\left(\dfrac{2\pi}{P_{TF}}\right)^2}}e^{d_P t}\sin\dfrac{2\pi}{P_{TF}}\left(t-\theta_M-\theta_P-\dfrac{P_{TF}}{2\pi}\arctan\dfrac{2\pi}{P_{TF}}\dfrac{1}{d_M}\right)\\ +\left(C_1-C_2k_Mj_M^n\right)e^{-d_M(t-\theta_P)}e^{d_P t}\end{array}\right]dt+C_3e^{-d_P t}\\
&=\frac{k_Pk_M\left(1-j_M^n\overline{X_{TF}}\right)}{d_Pd_M}+\frac{k_Pk_Mj_M^n\overline{A_{TF}}}{\sqrt{d_P^2+\left(\dfrac{2\pi}{P_{TF}}\right)^2}\sqrt{d_M^2+\left(\dfrac{2\pi}{P_{TF}}\right)^2}}\sin\frac{2\pi}{P_{TF}}\left(t-\theta_M-\theta_P-\frac{P_{TF}}{2\pi}\arctan\frac{2\pi}{P_{TF}}\frac{1}{d_M}-\frac{P_{TF}}{2\pi}\arctan\frac{2\pi}{P_{TF}}\frac{1}{d_P}\right)\\
&\quad+\frac{k_P\left(C_1-C_2k_Mj_M^n\right)}{d_P-d_M}e^{-d_M(t-\theta_P)}+\left(C_3+C_4k_P\right)e^{-d_P t}
\end{aligned}
$$

As $t\to\infty$,

$$
\begin{aligned}
M(t)&\to X_M+A_M\sin\frac{2\pi}{P_{TF}}(t-\alpha_M)\\
P(t)&\to X_P+A_P\sin\frac{2\pi}{P_{TF}}(t-\alpha_P)
\end{aligned}
\qquad \text{Eqn(15)}
$$

where

$$
X_M=\frac{k_M\left(1-j_M^n\overline{X_{TF}}\right)}{d_M},\quad A_M=\frac{k_Mj_M^n\overline{A_{TF}}}{\sqrt{d_M^2+\left(\dfrac{2\pi}{P_{TF}}\right)^2}},\quad \alpha_M=\theta_M+\frac{P_{TF}}{2\pi}\arctan\frac{2\pi}{P_{TF}}\frac{1}{d_M}
$$

$$
X_P=\frac{k_P}{d_P}X_M,\quad A_P=\frac{k_P}{\sqrt{d_P^2+\left(\dfrac{2\pi}{P_{TF}}\right)^2}}A_M,\quad \alpha_P=\alpha_M+\theta_P+\frac{P_{TF}}{2\pi}\arctan\frac{2\pi}{P_{TF}}\frac{1}{d_P}
$$

As Equations 4 and 5 are analytically intractable, the functions, $\left[TF(t-\theta_M)\right]^n$ and $\dfrac{e^{d_Mt}}{j_M^n+\left[TF(t-\theta_M)\right]^n}$ (from Equations 4 and 5 respectively) are approximated as a sinusoidal wave with a mean level ignoring other higher terms, as given in Equations 8 and 13 respectively. Thereafter, the resultant equations are solved using integration by parts, giving rise to Equations 11 and 15. For elegance, we encapsulate the mean and amplitude of $M(t)$ into X_M / A_M, and $P(t)$ into X_P / A_P respectively.

5.2.3 Estimation of trends

In the last section, the approximated analytical solutions for *M* and *P* are obtained. For convenience, they are expressed here as:

$$M = X_M + A_M \sin\frac{2\pi}{P_M}(t-\alpha_M)$$
$$P = X_P + A_P \sin\frac{2\pi}{P_P}(t-\alpha_P) \qquad \text{Eqn(14)}$$

where X_M / X_P is mean level of mRNA/protein intracellular concentration

A_M / A_P is oscillation amplitude of mRNA/protein intracellular concentration

P_M / P_P is mRNA/protein oscillation period

α_M / α_P is mRNA/protein phase-shift

and each term in the equations is given below:

$$X_M = \frac{k_M}{2d_M}\left[(X_{TF}+A_{TF})^n + (X_{TF}-A_{TF})^n\right]$$

For Model M:
$$A_M = \frac{k_M}{2\sqrt{d_M^2+\left(\frac{2\pi}{P_{TF}}\right)^2}}\left[(X_{TF}+A_{TF})^n - (X_{TF}-A_{TF})^n\right] \qquad \text{Eqn(15)}$$

$$X_M = \frac{k_M}{d_M}\left\{1-\frac{j_M^n}{2}\left[\frac{1}{j_M^n+(X_{TF}-A_{TF})^n}+\frac{1}{j_M^n+(X_{TF}+A_{TF})^n}\right]\right\}$$

For Model H:
$$A_M = \frac{k_M j_M^n}{2\sqrt{d_M^2+\left(\frac{2\pi}{P_{TF}}\right)^2}}\left[\frac{1}{j_M^n+(X_{TF}-A_{TF})^n}-\frac{1}{j_M^n+(X_{TF}+A_{TF})^n}\right]$$

Eqn(16)

Common to both models:

$$X_P = \frac{k_P}{d_P}X_M, \quad A_P = \frac{k_P}{\sqrt{d_P^2+\left(\frac{2\pi}{P_{TF}}\right)^2}}A_M$$

$$P_M = P_P = P_{TF}$$

$$\alpha_M = \theta_M + \frac{P_{TF}}{2\pi}\arctan\frac{2\pi}{P_{TF}}\frac{1}{d_M}, \quad \alpha_P = \alpha_M + \theta_P + \frac{P_{TF}}{2\pi}\arctan\frac{2\pi}{P_{TF}}\frac{1}{d_P}$$

Eqn(17)

To elucidate the effects of TF oscillations, it is of interest to determine gene expression response resulting from various biologically plausible parameters, including the mean level of target gene products (X_M and X_P), oscillation amplitude (A_M and A_P) and phase-shift (α_M and α_P). Using standard differentiation, analytical solutions to each concerned parameter are obtained. Based on the equations, dynamic trends of gene expression are estimated (see Materials and Methods). Given those trends, we can determine if there is an association of the target protein mean level (X_P) or oscillating amplitude (A_P) with regards to the parameter. For instance, the trend of X_P vs. X_{TF} indicates that X_P generally increases with X_{TF}, thus a positive "+" association is assigned. Finally, the directionality of each trend is computed and tabulated in Table 10, wherein "*" denotes either non-monotonic or non-intuitive trends that will be explained in more detail in the next section (for more comprehensive and detailed trends, see Appendices).

In order to ascertain the accuracy of the solutions, Model H is simulated in MATLAB (see Materials and Methods). For the simulation, a total of 12,960 combinations of parameter values are selected based on biologically plausible range. Subsequently, results from the approximated solutions and simulations are analyzed and compared in Figure 21. As expected, the relative percentage error increases as non-linearity intensifies [for instance, compare the curves of $n = 1$ (red) vs. $n = 8$ (gray)]. Nevertheless, more than 80% of the 12,960 values have less than 10% relative error (black curves). Most importantly, all the qualitative trends predicted by the approximated analytical solutions (Table 10) agree with computer-simulated trends. This validates the accuracy of the approximated analytical solutions of the models.

	Directionality of trends	
	X_P	A_P
TF oscillation parameters		
X_{TF} **(TF mean level)**	+	*
A_{TF} **(TF amplitude)**	*	+
P_{TF} **(TF period)**		+
Kinetic parameters		
j_M **(TF dissociation constant – Model H)**	–	*
n **(TF co-operativity / stoichiometry)**	*	*
k_M / k_P **(transcription / translation rate)**	+	+
d_M / d_P **(mRNA / protein self-degradation rate)**	–	–

Table 10. Directionality of target protein trends as a function of Models M and H parameters

The directionality of target protein mean level (X_P) and oscillation amplitude (A_P) as the magnitude of each parameter in column 1 is increased are tabulated; "+" indicates that the trend is positively associated with the parameter, i.e., the target protein trend increases as the parameter value is increased. "–" indicates negative association whereas "*" means that the trend is either non-monotonic or non-intuitive (see main text for details). Shaded in black denotes 'no association'.

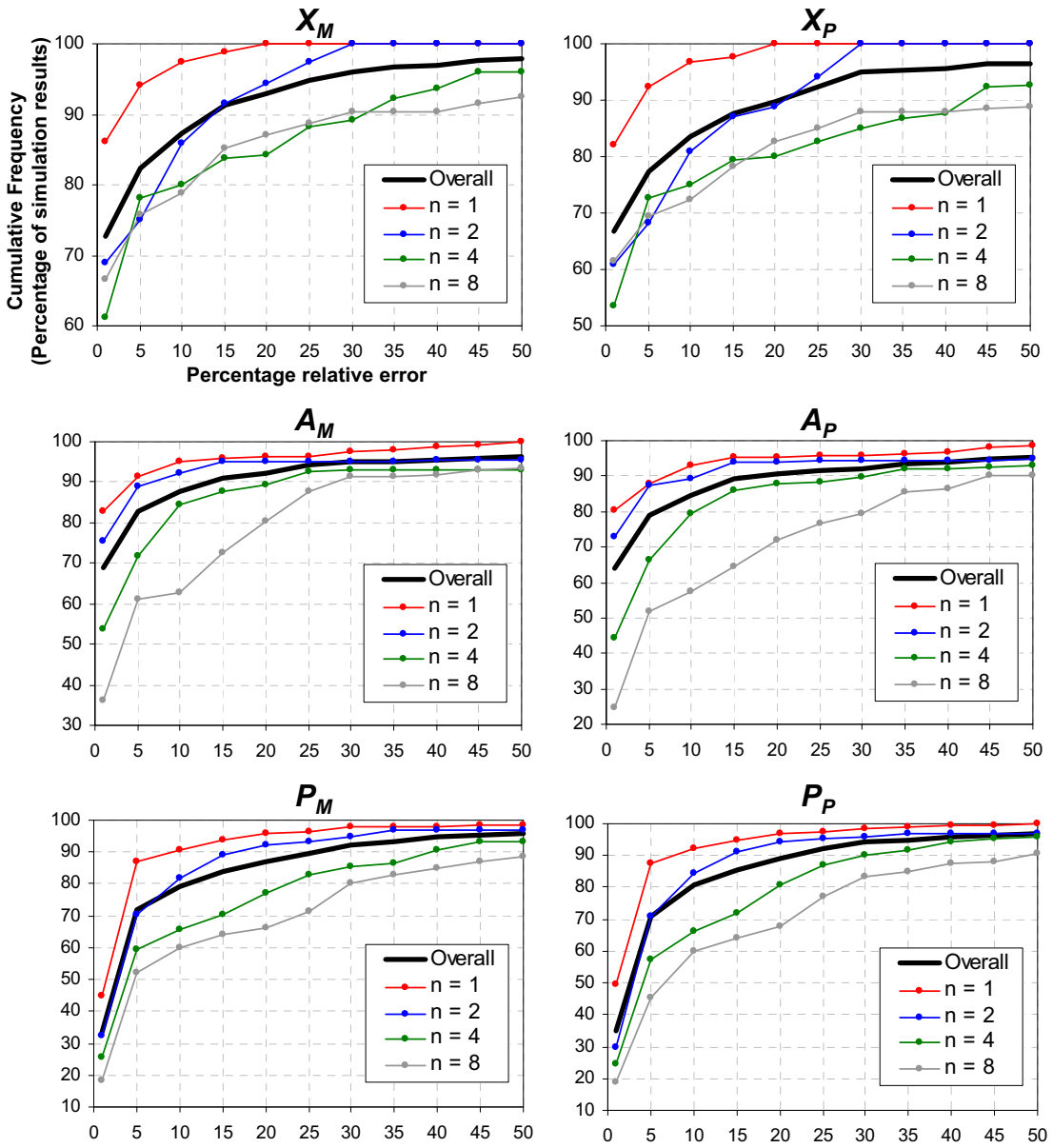

Figure 21. Quantitative comparisons between approximated analytical solutions and simulation results

Numerical values of target gene transcript and protein mean level (X_M and X_P), oscillation amplitude (A_M and A_P) and period (P_M and P_P) obtained from the approximated analytical solutions (Equation 14) and computer simulations are compared for Model H. The absolute difference between the two values is expressed as a percentage error relative to the simulated value, represented at the horizontal axis of the plots. In each plot, the vertical axis indicates the percentage of the total number of approximated analytical solutions with difference less than the percentage relative error on the horizontal axis. A total of 12,960 approximated analytical solutions, based on 12,960 unique sets of parameter values, are compared with computer simulations. These sets of parameter values are generated by permutations among different biologically plausible parameter values spanning over a wide range.

The specific parameter values used in the permutations to generate 12,960 unique sets of parameter values are as follows:

1. TF oscillation parameters
    a. X_{TF} = [0.0001, 0.001, 0.01, 0.1, 1, 10] μM
    b. A^*_{TF} = [0.1, 0.5, 0.9]
    c. P_{TF} = [2*60, 12*60, 24*60] min
2. Parameters
    a. j_M = [0.01, 0.05, 0.1, 0.5, 1, 5, 10] μM
    b. n = [1, 2, 4, 8]
    c. k_M = [0.001, 0.005, 0.01, 0.05, 0.1, 0.5, 1] $\mu M min^{-1}$
    d. k_P = [0.001, 0.01, 0.1, 1] min^{-1}
    e. d_M and d_P = [0.001, 0.005, 0.01, 0.05, 0.1, 0.5, 1] min^{-1}

5.2.4 Oscillatory vs. non-oscillatory TF induction of gene expression

Figure 22 depicts the trends of target protein mean level (X_P) as a function of A_{TF} and n under an oscillatory TF and a non-oscillatory TF. The consequences of TF oscillations on gene expression can thus be discerned by comparing the trends induced by an oscillatory (black) and a non-oscillatory (gray) TF.

The trends of X_P as a function of TF oscillation amplitude (A_{TF}) for both models are interesting and non-intuitive (Figure 22A). In Model M, while an oscillatory monomeric TF does not have any effect on X_P, an oscillatory polymeric TF ($n > 1$) always induce higher level of protein expression than its non-oscillatory counterpart. In contrast, in Model H, when there is no TF binding co-operativity to the gene promoter ($n=1$), an oscillatory TF always induced less protein than a non-oscillatory TF. However, for positive binding co-operativity ($n > 1$), complex trends are obtained. For instance, at $n=2$, an oscillatory TF always induces more protein than a non-oscillatory TF when either TF mean level (X_{TF}) or TF binding affinity to gene promoter is low (i.e. high j_M), or vice versa when either X_{TF} is high or j_M is low. Between these two boundaries, the TF oscillation amplitude dictates the trend – at small A_{TF}, an oscillatory TF induces less protein than a non-oscillatory TF. However, as A_{TF} is increased, the trend is reversed. In principle, a cell could exploit the above complex trends generated by an oscillatory TF to induce differential gene expressions that could not be achieved by a non-oscillatory TF.

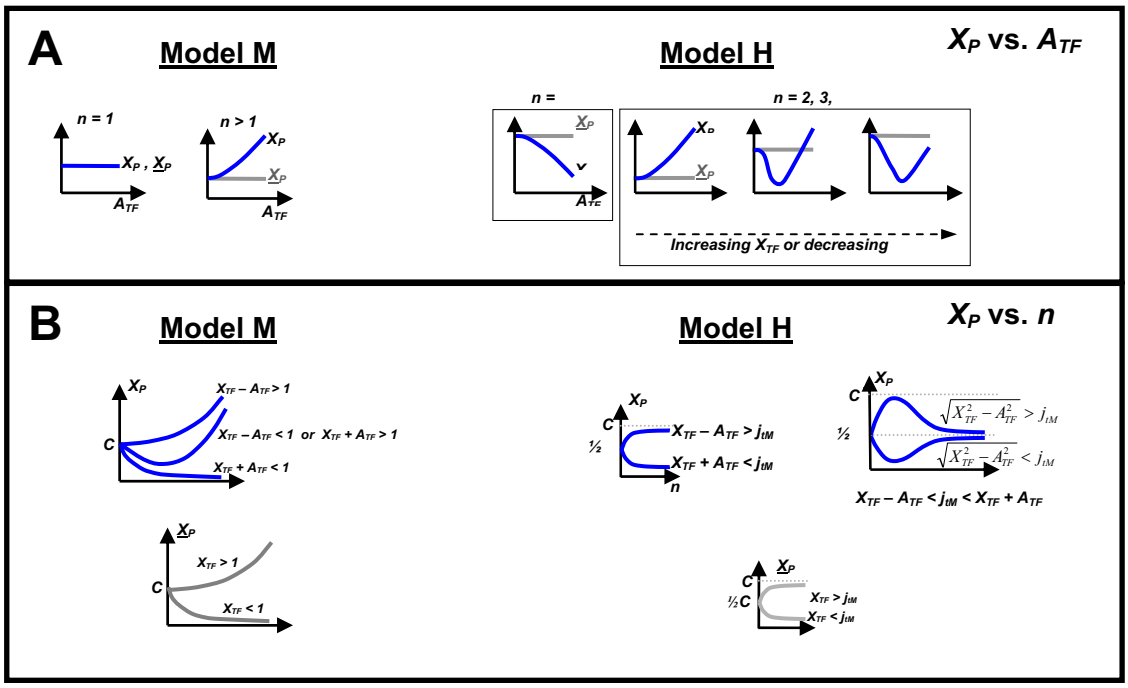

Figure 22. Comparison of gene expression induced by an oscillatory and a non-oscillatory TF.
Trends of X_P (protein mean level) as a function of **(A)** A_{TF} (TF oscillation amplitude) and **(B)** n (M: TF stoichiometry; H: TF binding affinity to gene promoter) of Models M and H are depicted. Trends generated by a non-oscillatory TF are shown as gray (if applicable). both the oscillatory and non-oscillatory TFs have equal mean level, i.e., X_{TF}. C is given as $k_M k_P / (d_M d_P)$.

Given that n is a key parameter conferring complexity of the trends above, the trends of X_P as a function of n are no less non-intuitive (Figure 22B). Two general trends are observed as n is increased under oscillatory and non-oscillatory TF for both models: X_P increases if X_{TF} is relatively high but decreases if X_{TF} is relatively low. However, if X_{TF} is intermediate, oscillatory TF produces additional X_P trends as n is increased. Specifically, a parabolic trend is observed for Model M whereas four trends are possible for Model H (Figure 22B).

Remarkably, the expression fold-difference between a protein induced by an oscillatory TF and its non-oscillatory counterpart is significant. As an illustration, two arbitrary sets of biologically plausible kinetic parameters are chosen for Model H computer simulation. Using the first set, an oscillatory TF always expressed more protein than the non-oscillatory TF (for $n > 2$) while the reverse is observed using the second set. As shown in Figure 23A, the fold difference gets even more considerable as n is increased for both sets (for Model M simulation results, see Figure 23B).

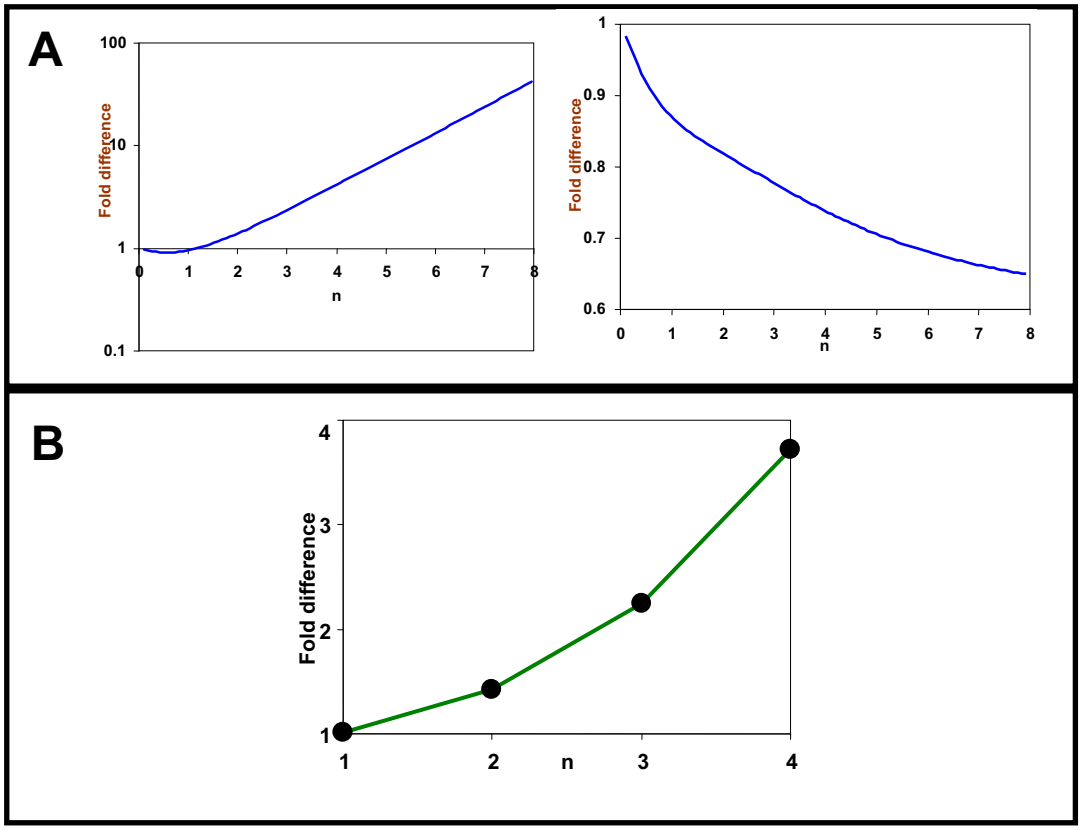

Figure 23. Fold difference between proteins expressed by an oscillatory to a non-oscillatory TF.

(A) For Model H, fold difference between proteins expressed by an oscillatory to a non-oscillatory TF at different TF binding co-operativity, n are obtained from computer simulations. Parameter values used to generate the representative plot on the left are: $X_{TF} = 0.015$ μM, $A^*_{TF} = 0.9$, $P_{TF} = 2$ hrs, $k_M = 0.01$ μM/min, $j_M = 0.05$ μM, $k_P = 0.01$ min^{-1} and $d_M = d_P = 0.01$ min^{-1}. Parameter values used to generate the representative plot on the right are identical to the left plot except $X_{TF} = 0.65$ μM and $j_M = 0.5$ μM.

(B) For Model M simulations, fold difference at different TF stoichiometry are obtained. Parameter values used to generate the plot are: $X_{TF} = 0.0001$ μM, $A^*_{TF} = 0.9$, $P_{TF} = 2$ hrs, $k_M = 0.01$ μM/min, $k_P = 0.01$ min^{-1} and $d_M = d_P = 0.01$ min^{-1}.

Specifically for gene whose expression dynamics resemble Hill kinetics (Model H), TF oscillations offer a mechanism for differential expression of target genes. As an illustration, consider three genes G1, G2 and G3 regulated by an oscillatory TF with positive binding co-operativity say $n = 4$. For simplicity, the model parameter values of each gene are identical except TF dissociation constant from gene promoter (j_M). Values of j_M are chosen so that the trend of X_P (protein mean level) vs. A_{TF} (TF oscillation amplitude) is distinct for each gene, as shown in Figure 24 (see inset). For each gene, the amount of proteins expressed by a non-oscillatory (gray) and oscillatory (black) TF are compared (Figure 24A). In the presence of TF oscillations, G1 is down-regulated by 30%, G2 is unaffected and G3 is up-regulated by 2.5 folds, relative to their respective level induced by a non-oscillatory TF. On the other hand, TF mean level could also influence the X_P vs. A_{TF} trend. Indeed, other patterns of differential gene expressions are observed by altering the TF mean level, as depicted in Figure 24B and Figure 24C. In contrast, in the absence of TF oscillations, none of the differential regulation of gene expression can be achieved. However, if the transcription kinetics follows Model M, differential gene expression by oscillatory TF is not possible since an oscillatory polymeric TF always induces more proteins than its non-oscillatory counterpart.

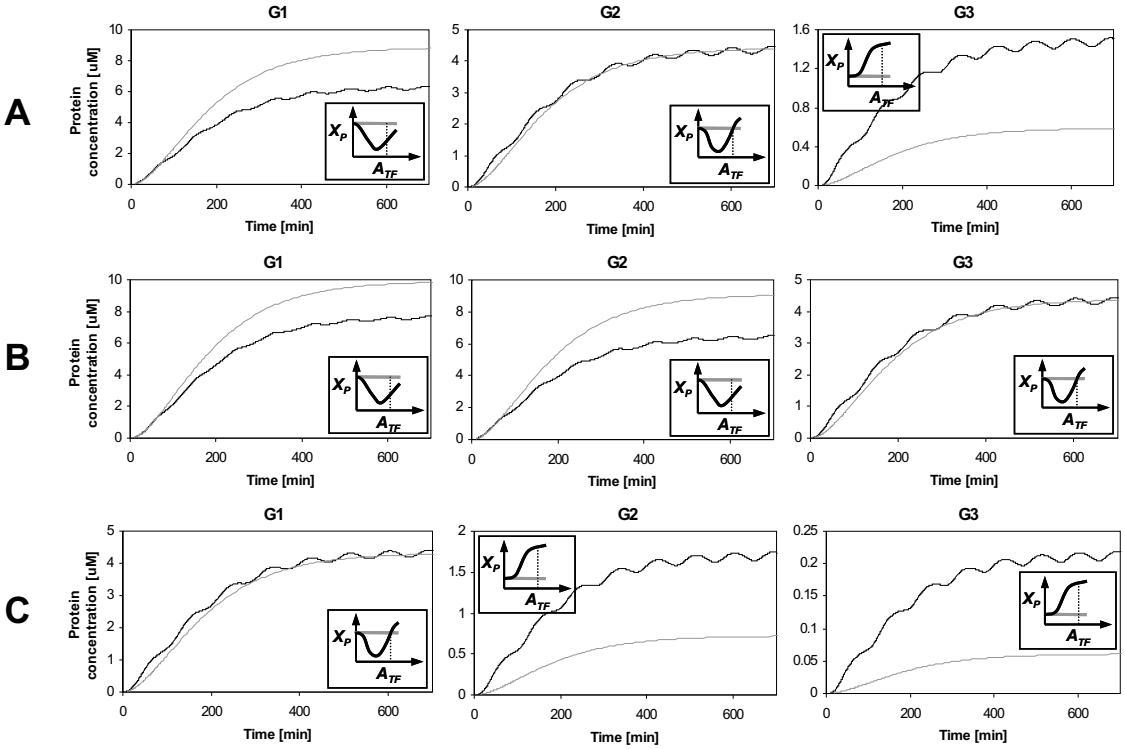

Figure 24. Differential gene expression.
Time-courses of the protein levels of three representative target genes (G1, G2 and G3) induced by a non-oscillatory (gray) and oscillatory (black) TF via computer simulations of Model H. G1, G2 and G3 differ by their TF dissociation constants (j_M) whose values are 0.3, 0.53 and 1 μM, respectively. **(A)** X_{TF} = 0.5 μM **(B)** X_{TF} = 0.94 μM **(C)** X_{TF} = 0.28 μM. The remaining parameter values are set to be: A_{TF}^{*} = 0.9, P_{TF} = 90 min, n = *4*, k_M = 0.1 μM/min, k_P = 0.01 min^{-1} and $d_M = d_P$ = 0.01 min^{-1}. Inset: trend of X_P vs. A_{TF} of each target gene; trends generated from a non-oscillatory and oscillatory TF are depicted in gray and black, respectively; the broken vertical line indicates the point at which the time-courses are based.

5.3 Discussion

Oscillating transcription factors (TFs) are observed in myriad biological processes, including circadian cycle, cell cycle and yeast glucose metabolism etc (see Table 1). Notably, insights obtained from studies on NF-κB and p53 showed different oscillating dynamics leading to differential gene expression [13], and distinct p53 profiles correlating with specific phenotypic response [19]. However, the underlying mechanism is.not well understood

In this chapter, we have formulated two mathematical models which could generally represent the response of gene expression with oscillating TFs. To explore the effects of oscillating TFs, we decided to include transcription, translation and degradation processes only. Other forms of regulation such as repressor and DNA enhancers are not considered as we wish to explore the effects emanating from a basic gene expression process. Moreover, it may dilute the significance of each individual molecular property in later analysis.

We decided to solve the model analytically since the solutions could provide more insights than simulations alone. Furthermore, this approach averts the need to employ specific model parameter values, but yet can reveal all plausible responses. In addition, it facilitates a subsequent study (which is still in progress) designed to investigate the propagation of oscillation amplitudes in (prevalent) TF cascades, which would require consideration of time-associated factors such as TF periodicity and transcriptional/translational time-delays etc. The choice of using ODEs is attractive since it facilitates derivation of analytical solutions, which would be challenging, if not, impossible for stochastic approaches.

In general, the rate of transcription follows either mass action kinetics (model M) or Hill type function (model H). The mass action kinetics is an empirical 'law' generally followed by a chemical species in a biochemical reaction. On the other hand, studies have shown that gene transcription could follow a sigmoidal curve function [232-234], especially when the system exhibits binding co-operativity. For instance, TFs are often composed of multiple subunits. A single subunit usually can activate transcription, while full activation requires all subunits. In addition, a sinusoidal wave is used to represent the shape of oscillating TFs to facilitate subsequent manipulation which is a common approach [227, 228]. In order to derive tractable solutions, the transcriptional response is approximated to be a sinusoidal wave. Numerical simulations are conducted to show that the error between our approximation and simulation is marginal (Figure 21). We reasoned that the difference would be insignificant especially when the primary interest is to determine the qualitative response. By analyzing the solutions with differentiation, the trends of gene expression response are estimated due to changes from individual system parameters, and tabulated a summary of their associations (Table 10).

The estimated trends yield interesting yet non-intuitive results. For a polymeric TF ($n > 1$) that follows mass action kinetics (model M), for the same mean concentration of TF molecules (X_{TF}), oscillating TFs tend to express more proteins than non-oscillating counterparts. On the other hand, for TFs with Hill type kinetics (model H) and positive co-operativity ($n > 1$), the amount of proteins expressed by oscillating TFs could differ from non-varying TFs. Furthermore, such TFs displayed non-monotonic trends dependent on its oscillating amplitude and dissociation constant. These features could be exploited to differentially regulate specific genes. As shown in Figure 24A, suppose a system with non-varying TFs could express three genes,

namely G1, G2 and G3. By oscillating, G1 is down-regulated, G3 is up-regulated while expression of G2 is unchanged.

What could be the reason underlying the effect of oscillatory TF on its target gene expression? Recall that for TFs with positive cooperativity, the transcription rate function (used for converting TF concentration to transcription rate) is a sigmoidal (S shape) curve which can be approximately divided into three regions of operation: for low TF concentration, the transcription rate increases gradually; for medium TF concentration, the transcription rate gradient is steep; for high TF concentration, the gradient is gradual as it approaches saturation. Suppose that the mean level of a TF is between low and medium concentration. If the TF is non-oscillating, based on the transcription rate function, the mean TF concentration would be converted to a constant transcription rate. However, if the TF is oscillating, the crest cycles will be operating in the steep gradient region, and the trough cycles will be in the gradual gradient region. Since in the steep gradient region, the TF concentration will be converted to a higher transcription rate relative to the gradual gradient region, the nett effect will be a higher mean TF transcription rate than the non-oscillating TF. Therefore, oscillatory TFs would express a higher mean protein levels. On the other hand, if the mean concentration of an oscillating TF is between medium and high, the crest cycles will be in the gradual region, and the trough cycles in the steep region. As a result, the nett mean TF transcription rate will be lower than that of a constant TF. Binding affinity ($1/j_M$) affects the concentration of TF to be bound at a gene promoter. Therefore, different genes (with different binding affinity to its promoter) would respond differently when TFs oscillates (see inset in Figure 24A).

Possible consequences of TF oscillations on regulation of cellular processes can be envisaged using p53 as an example. Because p53 target genes impinge on

various key biological functions (such as cell cycle arrest, DNA damage repair and apoptosis see Table 4), it is beneficial or even obligatory to selectively up-regulate genes involved in specific functions in response to prevailing cellular condition. Assuming that there is no feedback mechanism in a TF system, say p53, without oscillations, however, augmenting the levels of the TF would lead to non-selective up-regulation of all target genes. In particular, p53 has a larger dissociation constant for binding promoters associated with apoptotic genes than with cell cycle arrest genes [235]; this means that p53 induces less apoptotic transcripts compared to cell cycle arrest transcripts. In the same manner as illustrated in Figure 24A, by exhibiting oscillations, p53 could selectively up-regulate apoptotic genes (analogous to G3) but not other genes (analogous to G1 and G2) upon irreparable DNA damage, and thereby tip the cell towards death [20]. The TF dissociation constant of G3 promoter is largest among G1, G2 and G3.

Taken together, these analyses and results revealed an interesting ability of an oscillatory gene expression process to elicit differential gene expression. This ability appears to be intrinsic to the process, but mostly restricted to Hill type TFs with appropriate molecular properties. Since molecular properties such as reaction rates do not vary, thus by oscillating, the TFs alone could selectively up-regulate or down-regulate different genes. If not by oscillation, differential gene expression probably requires additional form of regulation involving other entities, e.g. residue specific phosphorylation of TFs requires certain kinases, or other forms of transcriptional control such as chromatin modification or transcriptional repression etc. We speculate that this feature might be exploited in the p53 system since the normal level of p53 is constant. Upon DNA damage, it starts to oscillate and concurrently, respond by either inducing pro-apoptotic or DNA repair genes. Nevertheless, this study suggests that

switching between constant and oscillating levels could provide TFs another layer of specificity over its target genes.

Given that multiple target genes, which impinge on myriad cellular processes, are common among the reported oscillatory TFs reported (Table 2/4), oscillatory TF mediated differential gene expression could be a general mechanism to specifically regulate cellular processes.

Chapter 6 Perspective and future directions

6.1 Role of Cdc5 in Adaptation

Detection of DNA damage, checkpoint activation, onset of repair processes, turning-off of checkpoint signaling after the offending lesion has been repaired and recovery from cell cycle arrest are all parts of the greater cellular scheme that maintain the integrity of the genetic heritage of a cell during cell division. Checkpoint-induced cell cycle arrest is an important part of this system which would provide cells sufficient time for the repair machinery to complete its task before chromosome-segregation apparatus gets activated. In the event that repair machinery fails to repair the damage, cells maintain G2/M arrest for a prolonged period but not indefinitely; eventually they switch to "get on with life" mode and progress through mitosis with the unrepaired DNA lesion. This diversion is called adaptation. First described in budding yeast [1-3], adaptation has also been shown to occur in *Xenopus* [4] and human cells [5] in response to replication stress and DNA damage, respectively.

At one level, both recovery (mitosis after repair) and adaptation (mitosis without repair) can be considered as processes that bring cells from a 'high alert state' (damage-checkpoint-repair) to the 'ground state' so that cell cycle progression can resume. Both recovery and adaptation require switching-off of the checkpoint control so that inhibition on mitotic progression can be lifted; however the outcomes of the two processes are very different. While cells undergoing recovery have repaired the DNA damage and undergo subsequent divisions with a very high survival rate, cells undergoing adaptation progress through mitosis with unrepaired DNA lesions and

have a very low rate of survival. How checkpoint signaling is turned off during recovery and adaptation has been under investigation for a few years now.

In the case of recovery, the answer may lie in the manner in which DNA damage checkpoint is activated. Generation of single stranded DNA by resection of 5'end of a double strand break via action of MRX complex and ExoI is necessary for the activation of the checkpoint. The ssDNA thus created is bound by RPA and helps in the recruitment of Ddc2-Mec1 complex. This is followed by the recruitment of Rad9 and phosphorylation of Chk1 and Rad53. It is easy to envision that with the completion of the repair process, ssDNA would disappear and consequently, the upstream checkpoint signaling would progressively cease. The effectors, already in the active state, can be inactivated by corresponding inhibitors to bring the entire system to the ground state and to relieve the inhibition on mitosis. One example of such reversal is the inactivation of active-Rad53 by Ptc2/Ptc3-mediated dephosphorylation [107]. Thus, repair-driven turning-off of the upstream checkpoint-signaling may not require additional regulation.

Extinguishing checkpoint control during adaptation poses a different problem. Since the DNA lesion is constantly present in cells that are unable to repair it, the conditions for checkpoint activation, are, in principle, always present for sustained signaling. In such a scenario, cells have to either become 'desensitized/resistant' to the checkpoint signaling or use an alternative way of extinguishing the checkpoint control. In this study, we have attempted to investigate the mechanism by which cells switch-off checkpoint signaling during adaptation. A number of genes have been reported previously to be necessary for adaptive response in budding yeast, namely, *YKU70, YKU80, PTC2, PTC3, SAE2, TID1, CKB1, CKB2* and *CDC5* polo kinase. Of these *Sae2, Tid1, Ptc2* and *Ptc3* are required for both recovery and adaptation [107].

Some of the previous studies used dephosphorylation of Rad53 as an indicator of cessation of checkpoint control [2] and found that the Ptc2/Ptc3 phosphatases mediate adaptation by inactivating Rad53 via dephosphorylation [107]. In the present study, we have specifically focused on the role of Cdc5.

The use of the telophase trap provided us with a means to quantify the adaptive response as well as to study the temporal dynamics of the adaptive response. Since *cdc5-ad* mutation does not show a strong defect in the adaptive response in our experimental set up (data not shown), we have resorted to using *cdc5Δ* cells. This allowed us to uncover that Cdc5 function is not required for recovery but is essential for adaptive response. That *CDC5*-deficient RP cells proceed to dephosphorylate Rad53 during recovery, suggested that requirement of Cdc5 in adaptive response is not, directly or indirectly, for Rad53 dephosphorylation. Our finding that ectopic expression of Cdc5 accelerates adaptive process provided us an opportunity to scan for 'sub-events' that correspondingly accelerated due to Cdc5 overexpression. The following observations were important in linking Cdc5 to Ddc2 foci formation: (i) overexpression of Cdc5 accelerated both adaptation and disappearance of Ddc2 foci (ii) Ddc2 foci persisted throughout the course of the experiment in the absence of Cdc5 (no adaptation) (iii) overexpression of Cdc5 can diminish the number of already-formed Ddc2 foci. The fact that ectopic expression of Cdc5 does not perturb Ddc1 (checkpoint clamp component) foci, suggests that the effect on Ddc2 foci is specific and most likely not a spurious effect of Cdc5 overexpression. It has been shown previously [74] that Ddc2 foci, but not Ddc1, disappear during normal adaptive response. However, their accelerated disappearance due to Cdc5 over-activity implies that this effect is functionally (directly or indirectly) associated with Cdc5 activity.

We also find that ectopic expression of Cdc5 is able to suppress the adaptation defect of *sae2Δ*, *ptc2Δ ptc3Δ*, and *ckb1Δ* mutants. We have argued in Chapter 4 that this suppression suggests Cdc5 to be the rate determining factor in the adaptive response. However, it has been reported that overexpression of Ptc2 can suppress the adaptation defect of *cdc5-ad* mutant [107]. Even though in this report [107], cells' capacity to rebud was taken as the criterion for suppression, unlike our study where transition through anaphase was the main criterion, our own conclusion about Cdc5 being a rate limiting factor should be taken with caution. Nevertheless, taken together with our other observations, Cdc5 appears to be acting upstream of other facilitators of adaptive response.

How does Cdc5 polo kinase interfere with Ddc2 foci formation or recruitment of Ddc2-Mec1complex to the DNA damage site? One possibility is that Ddc2 is a direct substrate of Cdc5 and this phosphorylation of Ddc2 either reduces its affinity for Mec1 or binding to RPA-coated ssDNA. However, examination of Ddc2 amino acid sequence did not reveal any Cdc5 phosphorylation site, tentatively suggesting that Ddc2 may not be a direct substrate of Cdc5 polo kinase. Our mass-spectrometric analysis indicated RPA subunits Rfa1, Rfa2 and Rfa3 as proteins present in the Cdc5 immunoprecipitates. Of these, Rfa1 does indeed contain a consensus Cdc5 phosphorylation site. It is therefore possible that Cdc5 phosphorylates RPA and compromises its affinity to bind the ssDNA. This, in turn, can affect the recruitment of Ddc2-Mec1 complex to the site of DNA damage, thereby dampening the checkpoint signaling.

It is known that Rad53, activated in response to DNA damage, inhibits the activity of Cdc5 polo kinase ([83, 126] and our unpublished observations). Since Cdc5 is an essential component of the mitotic exit network (MEN), this observation is

interpreted as checkpoint control's attempt to prevent mitotic exit. In the present context, we suggest that Cdc5 plays an important role in turning off the checkpoint signaling during adaptive response. This notion demands that Rad53 inhibition of Cdc5 progressively erodes during G2/M arrest to allow sufficient accumulation of Cdc5 protein to initiate adaptation. It is possible that progressive erosion of Rad53-imposed inhibition over time releases sufficient amount of Cdc5 to initiate a positive-feedback loop such that increasing activity of Cdc5 causes increasing dampening of the checkpoint control and, eventually, an escape from G2/M arrest. What, then, causes the progressive erosion of Rad53-imposed Cdc5 inhibition during prolonged G2/M arrest? This could be accomplished by either a slow degradation of active Rad53 or a slow but continuous action of Ptc2, Ptc3 phosphatases during the extended G2/M arrest. Further investigations are clearly required to resolve this issue.

The role of Ptc2, Ptc3 and CKII in adaptive response can be explained in terms of their involvement in Rad53 inactivation. As mentioned above, Ptc2 and Ptc3 are known to dephosphorylate the active Rad53. CKII phosphorylates Ptc2 and increases its interaction with Rad53 [107]. Similarly, the adaptation defect of *sae2Δ* can be explained in terms of sustained presence of MRX complex at the unrepaired DSB, which results in sustained checkpoint signaling. However, what possible roles Yku70 and Yku80 might play in adaptation is not clear at the moment. Double strand breaks in budding yeast are predominantly repaired by HR repair system [88-90]. By some estimates 70% of the DSB repairs are carried out by HR while ~30% are repaired by nonhomologous end joining (NHEJ) pathway. The involvement of Ku complex subunits may not occur through DSB repair during prolonged arrest because adapted cells go through mitosis with unrepaired DNA lesion. It has been suggested that the adaptation defect in *yku70Δ* cells is due to increased 5'-3' resection of the

unrepaired DSB since Mre11 deficiency suppresses the adaptation defect of *yku70Δ* mutant. However, an understanding of the exact role of Ku complex in adaptive response will require further work.

What advantage could the adaptive response possibly provide to a unicellular organism like budding yeast? As discussed earlier, it might offer cells an opportunity to repair DNA damage in the subsequent cell cycle, thereby increasing their chances of survival. However, this is at the risk of genomic instability which may also affect subsequent generations. It can also be argued that some of the DNA lesions may be repaired by error prone repair system which will alter the genetic information but may also help to increase the genetic diversity in small measures. In mammalian cells, entry into mitosis with unrepaired DNA lesions during adaptive response may enhance the chances of defective cells to undergo apoptosis thereby reducing the number of defective cells in a tissue.

Future Directions

Much remains to be done in order to achieve a full understanding of the mechanism underlying the adaptive response. Our mass spectrometric analysis together with other results suggests that Cdc5 polo kinase's participation in adaptation may occur through trimeric RPA complex. In order to test this hypothesis, it is imperative to investigate the following:

(i) Can any of the RPA subunits serve as a substrate for Cdc5 in vitro?

(ii) Is phosphorylation status of RPA subunits altered during adaptive response?

(iii) Is ectopic expression of Cdc5 accompanied by increased phosphorylation of RPA subunits?

(iv) Identification of the Cdc5 phosphorylation sites in RPA subunits.

(v) Does Cdc5 phosphorylated RPA subunits exhibit low affinity for ssDNA?

(vi) Do mutations in Cdc5 phosphorylation sites in RPA subunits lead to predicted behavior?

The double-negative feedback loop leading to increased activity of Cdc5 is an essential feature of the scheme we have proposed for amplification of the Cdc5-imposed suppression of the checkpoint signaling. Therefore it will be important to test if there is progressive erosion of Rad53 activity and concomitant increase in Cdc5 activity during the prolonged G2/M arrest. It will serve well to explore if the progressive erosion of Rad53 activity is due to specific factors or due to the innate fluctuation built into the checkpoint control network. During DNA damage, checkpoint activation is accompanied by post-translational modification of proteins not directly downstream of Mec1-Ddc2 such as modifications of histones or proteins involved in resection reactions. It might be productive to investigate the status of these proteins during adaptive response and their importance in determining the dynamics of adaptation.

6.2 Oscillating Transcription Factors

Studies have revealed diverse biological processes with oscillating TFs: in circadian clock for normal physiological functions [222], in somite segmentation during developmental stage [8], in p53 tumor suppression [20], as p53 displayed different oscillation profiles in tissues from normal and cancer patients [19] and for proper metabolism and coordination of biological processes as reported in yeast [223-225]. Together, these studies indicate that oscillating gene expressions are regulated biological processes.

Prior studies have reported that NF-κB display distinct oscillatory dynamics upon stimulation by different ligands, such as TNF or LPS (see Table 4). Similarly, p53 displayed oscillatory expression after DNA damage induction. As a consequence of NF-κB and p53 oscillations, different genes are expressed [13, 20, 171]. It is suggested that these oscillations are caused by feedback loops in the system [20, 130, 236-238]. However, the mechanism underlying the causal relationship of oscillatory TFs and differential gene-expression response is not well understood.

Most transcript productions follow the mass action or Hill kinetics; therefore results from our models should encompass behaviors from most TFs. In both models, the analyses showed non-intuitive results. Surprisingly, protein production from oscillatory TFs could differ from non-varying TFs, even if the mean number of TF molecules over a certain period is the same. Especially in model M, oscillatory TFs often exhibit higher efficiency in protein productions. On the other hand, model H displayed more non-monotonic response trends. These trends are dependent mainly on: (i) binding co-operativity (n), (ii) dissociation constant (j_M) and (iii) oscillation amplitude (A_{TF}). Whether a TF demonstrates positive binding co-operativity or not is mostly intrinsic depending on the system; for example, number of subunits in a TF or binding sites on promoters. While dissociation constant, which indicates binding affinity inversely, of a TF to its promoters could vary, e.g. by phosphorylation of TFs, these post-translational modifications often requires other entities, for instance phosphorylation of p53 (Ser46) requires p53DINP1 (p53-dependent damage-inducible nuclear protein 1) as a co-factor [239, 240] so as to express an apoptotic gene p53AIP1 (p53-regulated apoptosis-inducing protein-1). Thus, by oscillating, i.e. varying its A_{TF}, TFs alone could have different effects on its target genes, subjected to other properties (i) and (ii). This is another layer of dynamic and specific control for

TFs that can alter the gene expression response due to input changes. Together, the analyses presented here reveal interesting features that may be inherent in the dynamics of gene-expression process.

Future Directions

A mathematical model is an abstract representation of the biological system. It is often built according to the questions at hand, and is often not intended to be an *in silico* cell. Hence, assumptions are mostly made to facilitate the analysis. The following paragraphs aim to extend the study, making it more applicable to a wider range of TFs.

The basic gene expression process that is modeled here could represent most protein production. To be applicable to more TFs, the analyses and results should be extended to include other forms of gene regulation, including gene repressors, and co-activators etc. It would be interesting to understand how the additional layer of regulation shapes the response-trends or whether the addition of co-activators/-co-repressors can render the trend of TF response in model M non-monotonic. In this study, the input TF signal is represented by a sinusoidal function. It would be insightful to examine the trends of response due to different form of TF signals, such as damped or sustained oscillations, and sharp pulses. However, it should be noted that addition of more details often results in an increased complexity for the system, rendering analytical solutions intractable. Nevertheless, it is a possible extension for this work.

We have employed kinetic differential equations for this investigation. It is a deterministic approach which assumes a large quantity of each reactant in the process,

thus they can be modeled as continuous entities. On the other hand, when modeling biochemical entities, discrete or random fluctuations that might affect reaction-response can be accounted for [241]. These effects may become significant as the levels of reactants in a system become smaller. To be applicable to TFs with low abundunce, the gene expression model should be subjected to stochastic analysis. Since the model is manageable, the process can be simulated using the Gillespie algorithm [242]. Therefore, it would be interesting to determine if similar behaviors and trends could be predicted in the stochastic simulation.

Although the analyses revealed a possible mechanism for differential gene expression, as exhibited by NF-κB or p53, it is not known whether a biological cell can utilize such a mechanism. Therefore, an experimental validation is essential. One possible approach is to construct a synthetic oscillating TF, such as those reported previously [243, 244], and compare the quantities of gene products with those from non-varying TF. The alternative method is to make use of endogenous TFs such as NF-κB or p53, and measure the expression of its downstream target gene before and after oscillation. Such experiments would definitely help us gain better understanding of molecular regulation underlying cellular behaviour.

Bibliography

Bibliography

1. Sandell L L, Zakian V A. (1993) Loss of a yeast telomere: arrest, recovery, and chromosome loss. Cell 75:729-39.

2. Lee S E, Moore J K, Holmes A, Umezu K, Kolodner R D, Haber J E. (1998) Saccharomyces Ku70, mre11/rad50 and RPA proteins regulate adaptation to G2/M arrest after DNA damage. Cell 94:399-409.

3. Toczyski D P, Galgoczy D J, Hartwell L H. (1997) CDC5 and CKII control adaptation to the yeast DNA damage checkpoint. Cell 90:1097-106.

4. Yoo H Y, Kumagai A, Shevchenko A, Dunphy W G. (2004) Adaptation of a DNA replication checkpoint response depends upon inactivation of Claspin by the Polo-like kinase. Cell 117:575-88.

5. Syljuasen R G, Jensen S, Bartek J, Lukas J. (2006) Adaptation to the ionizing radiation-induced G2 checkpoint occurs in human cells and depends on checkpoint kinase 1 and Polo-like kinase 1 kinases. Cancer Res 66:10253-7.

6. Panda S, Antoch M P, Miller B H, Su A I, Schook A B, Straume M, Schultz P G, Kay S A, Takahashi J S, Hogenesch J B. (2002) Coordinated transcription of key pathways in the mouse by the circadian clock. Cell 109:307-20.

7. Storch K F, Lipan O, Leykin I, Viswanathan N, Davis F C, Wong W H, Weitz C J. (2002) Extensive and divergent circadian gene expression in liver and heart. Nature 417:78-83.

8. Kageyama R, Ishibashi M, Takebayashi K, Tomita K. (1997) bHLH transcription factors and mammalian neuronal differentiation. Int J Biochem Cell Biol 29:1389-99.

9. Lahav G, Rosenfeld N, Sigal A, Geva-Zatorsky N, Levine A J, Elowitz M B, Alon U. (2004) Dynamics of the p53-Mdm2 feedback loop in individual cells. Nat Genet 36:147-50.

10. Geva-Zatorsky N, Rosenfeld N, Itzkovitz S, Milo R, Sigal A, Dekel E, Yarnitzky T, Liron Y, Polak P, Lahav G, Alon U. (2006) Oscillations and variability in the p53 system. Mol Syst Biol 2:2006 0033.

11. Ramalingam S, Honkanen P, Young L, Shimura T, Austin J, Steeg P S, Nishizuka S. (2007) Quantitative assessment of the p53-Mdm2 feedback loop using protein lysate microarrays. Cancer Res 67:6247-52.

12. Hamstra D A, Bhojani M S, Griffin L B, Laxman B, Ross B D, Rehemtulla A. (2006) Real-time evaluation of p53 oscillatory behavior in vivo using bioluminescent imaging. Cancer Res 66:7482-9.

13. Hoffmann A, Levchenko A, Scott M L, Baltimore D. (2002) The IkappaB-NF-kappaB signaling module: temporal control and selective gene activation. Science 298:1241-5.

14. Nelson D E, Ihekwaba A E, Elliott M, Johnson J R, Gibney C A, Foreman B E, Nelson G, See V, Horton C A, Spiller D G, Edwards S W, McDowell H P, Unitt J F, Sullivan E, Grimley R, Benson N, Broomhead D, Kell D B, White M R. (2004) Oscillations in NF-kappaB signaling control the dynamics of gene expression. Science 306:704-8.

15. Werner S L, Barken D, Hoffmann A. (2005) Stimulus specificity of gene expression programs determined by temporal control of IKK activity. Science 309:1857-61.

16. Forsburg S L, Nurse P. (1991) Cell cycle regulation in the yeasts Saccharomyces cerevisiae and Schizosaccharomyces pombe. Annu Rev Cell Biol 7:227-56.

17. Norbury C, Nurse P. (1992) Animal cell cycles and their control. Annu Rev Biochem 61:441-70.

18. Tu B P, Kudlicki A, Rowicka M, McKnight S L. (2005) Logic of the yeast metabolic cycle: temporal compartmentalization of cellular processes. Science 310:1152-8.

19. Collister M, Lane D P, Kuehl B L. (1998) Differential expression of p53, p21waf1/cip1 and hdm2 dependent on DNA damage in Bloom's syndrome fibroblasts. Carcinogenesis 19:2115-20.

20. Wee K B, Surana U, Aguda B D. (2009) Oscillations of the p53-Akt network: implications on cell survival and death. PLoS One 4:e4407.

21. Pellicioli A, Lee S E, Lucca C, Foiani M, Haber J E. (2001) Regulation of Saccharomyces Rad53 checkpoint kinase during adaptation from DNA damage-induced G2/M arrest. Mol Cell 7:293-300.

22. Hartwell L H. (1974) Saccharomyces cerevisiae cell cycle. Bacteriol Rev 38:164-98.

23. Hartwell L H, Unger M W. (1977) Unequal division in Saccharomyces cerevisiae and its implications for the control of cell division. J Cell Biol 75:422-35.

24. Winey M. (1999) Cell cycle: driving the centrosome cycle. Curr Biol 9:R449-52.

25. Basco R D, Segal M D, Reed S I. (1995) Negative regulation of G1 and G2 by S-phase cyclins of Saccharomyces cerevisiae. Mol Cell Biol 15:5030-42.

26. Kuhne C, Linder P. (1993) A new pair of B-type cyclins from Saccharomyces cerevisiae that function early in the cell cycle. EMBO J 12:3437-47.

27. Schwob E, Nasmyth K. (1993) CLB5 and CLB6, a new pair of B cyclins involved in DNA replication in Saccharomyces cerevisiae. Genes Dev 7:1160-75.

28. Epstein C B, Cross F R. (1992) CLB5: a novel B cyclin from budding yeast with a role in S phase. Genes Dev 6:1695-706.

29. Richardson H, Lew D J, Henze M, Sugimoto K, Reed S I. (1992) Cyclin-B homologs in Saccharomyces cerevisiae function in S phase and in G2. Genes Dev 6:2021-34.

30. Fitch I, Dahmann C, Surana U, Amon A, Nasmyth K, Goetsch L, Byers B, Futcher B. (1992) Characterization of four B-type cyclin genes of the budding yeast Saccharomyces cerevisiae. Mol Biol Cell 3:805-18.

31. Surana U, Robitsch H, Price C, Schuster T, Fitch I, Futcher A B, Nasmyth K. (1991) The role of CDC28 and cyclins during mitosis in the budding yeast S. cerevisiae. Cell 65:145-61.

32. Byers B, *Cytology of the yeast life cycle.*, in *Molecular Biology of the Yeast Saccharomyces: Life Cycle and Inheritance*, J.N. Strathern, E.W. Jones, and J.R. Broach, Editors. 1981, Cold Spring Harbor Laboratory: Cold Spring Harbor, NY. p. 59-96.

33. Nasmyth K, Haering C H. (2005) The structure and function of SMC and kleisin complexes. Annu Rev Biochem 74:595-648.

34. Uhlmann F, Wernic D, Poupart M A, Koonin E V, Nasmyth K. (2000) Cleavage of cohesin by the CD clan protease separin triggers anaphase in yeast. Cell 103:375-86.

35. Uhlmann F, Lottspeich F, Nasmyth K. (1999) Sister-chromatid separation at anaphase onset is promoted by cleavage of the cohesin subunit Scc1. Nature 400:37-42.

36. Morgan D O. (1999) Regulation of the APC and the exit from mitosis. Nat Cell Biol 1:E47-53.

37. Shirayama M, Toth A, Galova M, Nasmyth K. (1999) APC(Cdc20) promotes exit from mitosis by destroying the anaphase inhibitor Pds1 and cyclin Clb5. Nature 402:203-7.

38. Fang G, Yu H, Kirschner M W. (1998) Direct binding of CDC20 protein family members activates the anaphase-promoting complex in mitosis and G1. Mol Cell 2:163-71.

39. Visintin R, Prinz S, Amon A. (1997) CDC20 and CDH1: a family of substrate-specific activators of APC-dependent proteolysis. Science 278:460-3.

40. Hoyt M A. (1997) Eliminating all obstacles: regulated proteolysis in the eukaryotic cell cycle. Cell 91:149-51.

41. King R W, Deshaies R J, Peters J M, Kirschner M W. (1996) How proteolysis drives the cell cycle. Science 274:1652-9.

42. Murray A. (1995) Cyclin ubiquitination: the destructive end of mitosis. Cell 81:149-52.

43. Surana U, Amon A, Dowzer C, McGrew J, Byers B, Nasmyth K. (1993) Destruction of the CDC28/CLB mitotic kinase is not required for the metaphase to anaphase transition in budding yeast. EMBO J 12:1969-78.

44. Murray A W, Solomon M J, Kirschner M W. (1989) The role of cyclin synthesis and degradation in the control of maturation promoting factor activity. Nature 339:280-6.

45. Wasch R, Cross F R. (2002) APC-dependent proteolysis of the mitotic cyclin Clb2 is essential for mitotic exit. Nature 418:556-62.

46. Jaspersen S L, Charles J F, Tinker-Kulberg R L, Morgan D O. (1998) A late mitotic regulatory network controlling cyclin destruction in Saccharomyces cerevisiae. Mol Biol Cell 9:2803-17.

47. Yeong F M, Lim H H, Padmashree C G, Surana U. (2000) Exit from mitosis in budding yeast: biphasic inactivation of the Cdc28-Clb2 mitotic kinase and the role of Cdc20. Mol Cell 5:501-11.

48. Baumer M, Braus G H, Irniger S. (2000) Two different modes of cyclin clb2 proteolysis during mitosis in Saccharomyces cerevisiae. FEBS Lett 468:142-8.

49. Stegmeier F, Visintin R, Amon A. (2002) Separase, polo kinase, the kinetochore protein Slk19, and Spo12 function in a network that controls Cdc14 localization during early anaphase. Cell 108:207-20.

50. Jensen S, Geymonat M, Johnston L H. (2002) Mitotic exit: delaying the end without FEAR. Curr Biol 12:R221-3.

51. Pereira G, Manson C, Grindlay J, Schiebel E. (2002) Regulation of the Bfa1p-Bub2p complex at spindle pole bodies by the cell cycle phosphatase Cdc14p. J Cell Biol 157:367-79.

52. Kaldis P, Sutton A, Solomon M J. (1996) The Cdk-activating kinase (CAK) from budding yeast. Cell 86:553-64.

53. Gould K L, Moreno S, Owen D J, Sazer S, Nurse P. (1991) Phosphorylation at Thr167 is required for Schizosaccharomyces pombe p34cdc2 function. EMBO J 10:3297-309.

54. Sorger P K, Murray A W. (1992) S-phase feedback control in budding yeast independent of tyrosine phosphorylation of p34cdc28. Nature 355:365-8.

55. Krishnan V, Nirantar S, Crasta K, Cheng A Y, Surana U. (2004) DNA replication checkpoint prevents precocious chromosome segregation by regulating spindle behavior. Mol Cell 16:687-700.

56. Rhind N, Russell P. (1998) Tyrosine phosphorylation of cdc2 is required for the replication checkpoint in Schizosaccharomyces pombe. Mol Cell Biol 18:3782-7.

57. Amon A, Surana U, Muroff I, Nasmyth K. (1992) Regulation of p34CDC28 tyrosine phosphorylation is not required for entry into mitosis in S. cerevisiae. Nature 355:368-71.

58. Hartwell L H, Weinert T A. (1989) Checkpoints: controls that ensure the order of cell cycle events. Science 246:629-34.

59. Lew D J, Reed S I. (1995) A cell cycle checkpoint monitors cell morphogenesis in budding yeast. J Cell Biol 129:739-49.

60. Zhou B B, Elledge S J. (2000) The DNA damage response: putting checkpoints in perspective. Nature 408:433-9.

61. Harrison J C, Haber J E. (2006) Surviving the breakup: the DNA damage checkpoint. Annu Rev Genet 40:209-35.

62. Su T T. (2006) Cellular responses to DNA damage: one signal, multiple choices. Annu Rev Genet 40:187-208.

63. Ira G, Pellicioli A, Balijja A, Wang X, Fiorani S, Carotenuto W, Liberi G, Bressan D, Wan L, Hollingsworth N M, Haber J E, Foiani M. (2004) DNA end resection, homologous recombination and DNA damage checkpoint activation require CDK1. Nature 431:1011-7.

64. Lisby M, Barlow J H, Burgess R C, Rothstein R. (2004) Choreography of the DNA damage response: spatiotemporal relationships among checkpoint and repair proteins. Cell 118:699-713.

65. Shroff R, Arbel-Eden A, Pilch D, Ira G, Bonner W M, Petrini J H, Haber J E, Lichten M. (2004) Distribution and dynamics of chromatin modification induced by a defined DNA double-strand break. Curr Biol 14:1703-11.

66. Mimitou E P, Symington L S. (2008) Sae2, Exo1 and Sgs1 collaborate in DNA double-strand break processing. Nature 455:770-4.

67. Zhu Z, Chung W H, Shim E Y, Lee S E, Ira G. (2008) Sgs1 helicase and two nucleases Dna2 and Exo1 resect DNA double-strand break ends. Cell 134:981-94.

68. Clerici M, Mantiero D, Lucchini G, Longhese M P. (2006) The Saccharomyces cerevisiae Sae2 protein negatively regulates DNA damage checkpoint signalling. EMBO Rep 7:212-8.

69. Majka J, Burgers P M. (2003) Yeast Rad17/Mec3/Ddc1: a sliding clamp for the DNA damage checkpoint. Proc Natl Acad Sci U S A 100:2249-54.

70. Majka J, Burgers P M. (2005) Function of Rad17/Mec3/Ddc1 and its partial complexes in the DNA damage checkpoint. DNA Repair (Amst) 4:1189-94.

71. Ball H L, Ehrhardt M R, Mordes D A, Glick G G, Chazin W J, Cortez D. (2007) Function of a conserved checkpoint recruitment domain in ATRIP proteins. Mol Cell Biol 27:3367-77.

72. Nakada D, Hirano Y, Tanaka Y, Sugimoto K. (2005) Role of the C terminus of Mec1 checkpoint kinase in its localization to sites of DNA damage. Mol Biol Cell 16:5227-35.

73. Kondo T, Wakayama T, Naiki T, Matsumoto K, Sugimoto K. (2001) Recruitment of Mec1 and Ddc1 checkpoint proteins to double-strand breaks through distinct mechanisms. Science 294:867-70.

74. Melo J A, Cohen J, Toczyski D P. (2001) Two checkpoint complexes are independently recruited to sites of DNA damage in vivo. Genes Dev 15:2809-21.

75. Barlow J H, Lisby M, Rothstein R. (2008) Differential regulation of the cellular response to DNA double-strand breaks in G1. Mol Cell 30:73-85.

76. Dubrana K, van Attikum H, Hediger F, Gasser S M. (2007) The processing of double-strand breaks and binding of single-strand-binding proteins RPA and Rad51 modulate the formation of ATR-kinase foci in yeast. J Cell Sci 120:4209-20.

77. Bonilla C Y, Melo J A, Toczyski D P. (2008) Colocalization of sensors is sufficient to activate the DNA damage checkpoint in the absence of damage. Mol Cell 30:267-76.

78. Majka J, Niedziela-Majka A, Burgers P M. (2006) The checkpoint clamp activates Mec1 kinase during initiation of the DNA damage checkpoint. Mol Cell 24:891-901.

79. Clerici M, Baldo V, Mantiero D, Lottersberger F, Lucchini G, Longhese M P. (2004) A Tel1/MRX-dependent checkpoint inhibits the metaphase-to-anaphase transition after UV irradiation in the absence of Mec1. Mol Cell Biol 24:10126-44.

80. Vialard J E, Gilbert C S, Green C M, Lowndes N F. (1998) The budding yeast Rad9 checkpoint protein is subjected to Mec1/Tel1-dependent hyperphosphorylation and interacts with Rad53 after DNA damage. EMBO J 17:5679-88.

81. Fu Y, Pastushok L, Xiao W. (2008) DNA damage-induced gene expression in Saccharomyces cerevisiae. FEMS Microbiol Rev 32:908-26.

82. Hirano T. (2000) Chromosome cohesion, condensation, and separation. Annu Rev Biochem 69:115-44.

83. Sanchez Y, Bachant J, Wang H, Hu F, Liu D, Tetzlaff M, Elledge S J. (1999) Control of the DNA damage checkpoint by chk1 and rad53 protein kinases through distinct mechanisms. Science 286:1166-71.

84. Agarwal R, Tang Z, Yu H, Cohen-Fix O. (2003) Two distinct pathways for inhibiting pds1 ubiquitination in response to DNA damage. J Biol Chem 278:45027-33.

85. Hu F, Wang Y, Liu D, Li Y, Qin J, Elledge S J. (2001) Regulation of the Bub2/Bfa1 GAP complex by Cdc5 and cell cycle checkpoints. Cell 107:655-65.

86. Liang F, Wang Y. (2007) DNA damage checkpoints inhibit mitotic exit by two different mechanisms. Mol Cell Biol 27:5067-78.

87. Aylon Y, Kupiec M. (2004) DSB repair: the yeast paradigm. DNA Repair (Amst) 3:797-815.

88. Shrivastav M, De Haro L P, Nickoloff J A. (2008) Regulation of DNA double-strand break repair pathway choice. Cell Res 18:134-47.

89. Clikeman J A, Khalsa G J, Barton S L, Nickoloff J A. (2001) Homologous recombinational repair of double-strand breaks in yeast is enhanced by MAT heterozygosity through yKU-dependent and -independent mechanisms. Genetics 157:579-89.

90. Lee S E, Paques F, Sylvan J, Haber J E. (1999) Role of yeast SIR genes and mating type in directing DNA double-strand breaks to homologous and non-homologous repair paths. Curr Biol 9:767-70.

91. Bai Y, Symington L S. (1996) A Rad52 homolog is required for RAD51-independent mitotic recombination in Saccharomyces cerevisiae. Genes Dev 10:2025-37.

92. Ajimura M, Leem S H, Ogawa H. (1993) Identification of new genes required for meiotic recombination in Saccharomyces cerevisiae. Genetics 133:51-66.

93. Ivanov E L, Korolev V G, Fabre F. (1992) XRS2, a DNA repair gene of Saccharomyces cerevisiae, is needed for meiotic recombination. Genetics 132:651-64.

94. Sung P, Krejci L, Van Komen S, Sehorn M G. (2003) Rad51 recombinase and recombination mediators. J Biol Chem 278:42729-32.

95. Aylon Y, Kupiec M. (2004) New insights into the mechanism of homologous recombination in yeast. Mutat Res 566:231-48.

96. Martin S G, Laroche T, Suka N, Grunstein M, Gasser S M. (1999) Relocalization of telomeric Ku and SIR proteins in response to DNA strand breaks in yeast. Cell 97:621-33.

97. Chen L, Trujillo K, Ramos W, Sung P, Tomkinson A E. (2001) Promotion of Dnl4-catalyzed DNA end-joining by the Rad50/Mre11/Xrs2 and Hdf1/Hdf2 complexes. Mol Cell 8:1105-15.

98. Wilson T E, Grawunder U, Lieber M R. (1997) Yeast DNA ligase IV mediates non-homologous DNA end joining. Nature 388:495-8.

99. Herrmann G, Lindahl T, Schar P. (1998) Saccharomyces cerevisiae LIF1: a function involved in DNA double-strand break repair related to mammalian XRCC4. EMBO J 17:4188-98.

100. Teo S H, Jackson S P. (2000) Lif1p targets the DNA ligase Lig4p to sites of DNA double-strand breaks. Curr Biol 10:165-8.

101. Tseng H M, Tomkinson A E. (2004) Processing and joining of DNA ends coordinated by interactions among Dnl4/Lif1, Pol4, and FEN-1. J Biol Chem 279:47580-8.

102. Frank-Vaillant M, Marcand S. (2001) NHEJ regulation by mating type is exercised through a novel protein, Lif2p, essential to the ligase IV pathway. Genes Dev 15:3005-12.

103. Galgoczy D J, Toczyski D P. (2001) Checkpoint adaptation precedes spontaneous and damage-induced genomic instability in yeast. Mol Cell Biol 21:1710-8.

104. Lee S E, Pellicioli A, Malkova A, Foiani M, Haber J E. (2001) The Saccharomyces recombination protein Tid1p is required for adaptation from G2/M arrest induced by a double-strand break. Curr Biol 11:1053-7.

105. Lee S E, Pellicioli A, Vaze M B, Sugawara N, Malkova A, Foiani M, Haber J E. (2003) Yeast Rad52 and Rad51 recombination proteins define a second pathway of DNA damage assessment in response to a single double-strand break. Mol Cell Biol 23:8913-23.

106. Vaze M B, Pellicioli A, Lee S E, Ira G, Liberi G, Arbel-Eden A, Foiani M, Haber J E. (2002) Recovery from checkpoint-mediated arrest after repair of a double-strand break requires Srs2 helicase. Mol Cell 10:373-85.

107. Leroy C, Lee S E, Vaze M B, Ochsenbien F, Guerois R, Haber J E, Marsolier-Kergoat M C. (2003) PP2C phosphatases Ptc2 and Ptc3 are required for DNA checkpoint inactivation after a double-strand break. Mol Cell 11:827-35.

108. Dotiwala F, Haase J, Arbel-Eden A, Bloom K, Haber J E. (2007) The yeast DNA damage checkpoint proteins control a cytoplasmic response to DNA damage. Proc Natl Acad Sci U S A 104:11358-63.

109. Mamely I, van Vugt M A, Smits V A, Semple J I, Lemmens B, Perrakis A, Medema R H, Freire R. (2006) Polo-like kinase-1 controls proteasome-dependent degradation of Claspin during checkpoint recovery. Curr Biol 16:1950-5.

110. Peschiaroli A, Dorrello N V, Guardavaccaro D, Venere M, Halazonetis T, Sherman N E, Pagano M. (2006) SCFbetaTrCP-mediated degradation of Claspin regulates recovery from the DNA replication checkpoint response. Mol Cell 23:319-29.

111. Mailand N, Bekker-Jensen S, Bartek J, Lukas J. (2006) Destruction of Claspin by SCFbetaTrCP restrains Chk1 activation and facilitates recovery from genotoxic stress. Mol Cell 23:307-18.

112. van Vugt M A, Bras A, Medema R H. (2004) Polo-like kinase-1 controls recovery from a G2 DNA damage-induced arrest in mammalian cells. Mol Cell 15:799-811.

113. Barr F A, Sillje H H, Nigg E A. (2004) Polo-like kinases and the orchestration of cell division. Nat Rev Mol Cell Biol 5:429-40.

114. Lee K S, Park J E, Asano S, Park C J. (2005) Yeast polo-like kinases: functionally conserved multitask mitotic regulators. Oncogene 24:217-29.

115. Darieva Z, Bulmer R, Pic-Taylor A, Doris K S, Geymonat M, Sedgwick S G, Morgan B A, Sharrocks A D. (2006) Polo kinase controls cell-cycle-dependent transcription by targeting a coactivator protein. Nature 444:494-8.

116. St-Pierre J, Douziech M, Bazile F, Pascariu M, Bonneil E, Sauve V, Ratsima H, D'Amours D. (2009) Polo kinase regulates mitotic chromosome condensation by hyperactivation of condensin DNA supercoiling activity. Mol Cell 34:416-26.

117. Alexandru G, Uhlmann F, Mechtler K, Poupart M A, Nasmyth K. (2001) Phosphorylation of the cohesin subunit Scc1 by Polo/Cdc5 kinase regulates sister chromatid separation in yeast. Cell 105:459-72.

118. Charles J F, Jaspersen S L, Tinker-Kulberg R L, Hwang L, Szidon A, Morgan D O. (1998) The Polo-related kinase Cdc5 activates and is destroyed by the mitotic cyclin destruction machinery in S. cerevisiae. Curr Biol 8:497-507.

119. Shirayama M, Zachariae W, Ciosk R, Nasmyth K. (1998) The Polo-like kinase Cdc5p and the WD-repeat protein Cdc20p/fizzy are regulators and substrates of the anaphase promoting complex in Saccharomyces cerevisiae. EMBO J 17:1336-49.

120. Visintin R, Stegmeier F, Amon A. (2003) The role of the polo kinase Cdc5 in controlling Cdc14 localization. Mol Biol Cell 14:4486-98.

121. Rahal R, Amon A. (2008) The Polo-like kinase Cdc5 interacts with FEAR network components and Cdc14. Cell Cycle 7:3262-72.

122. Yoshida S, Kono K, Lowery D M, Bartolini S, Yaffe M B, Ohya Y, Pellman D. (2006) Polo-like kinase Cdc5 controls the local activation of Rho1 to promote cytokinesis. Science 313:108-11.

123. Clyne R K, Katis V L, Jessop L, Benjamin K R, Herskowitz I, Lichten M, Nasmyth K. (2003) Polo-like kinase Cdc5 promotes chiasmata formation and cosegregation of sister centromeres at meiosis I. Nat Cell Biol 5:480-5.

124. Lee B H, Amon A. (2003) Role of Polo-like kinase CDC5 in programming meiosis I chromosome segregation. Science 300:482-6.

125. Sourirajan A, Lichten M. (2008) Polo-like kinase Cdc5 drives exit from pachytene during budding yeast meiosis. Genes Dev 22:2627-32.

126. Cheng L, Hunke L, Hardy C F. (1998) Cell cycle regulation of the Saccharomyces cerevisiae polo-like kinase cdc5p. Mol Cell Biol 18:7360-70.

127. Orphanides G, Reinberg D. (2002) A unified theory of gene expression. Cell 108:439-51.

128. Lee T I, Rinaldi N J, Robert F, Odom D T, Bar-Joseph Z, Gerber G K, Hannett N M, Harbison C T, Thompson C M, Simon I, Zeitlinger J, Jennings E G, Murray H L, Gordon D B, Ren B, Wyrick J J, Tagne J B, Volkert T L, Fraenkel E, Gifford D K, Young R A. (2002) Transcriptional regulatory networks in Saccharomyces cerevisiae. Science 298:799-804.

129. Tupler R, Perini G, Green M R. (2001) Expressing the human genome. Nature 409:832-3.

130. Novak B, Tyson J J. (2008) Design principles of biochemical oscillators. Nat Rev Mol Cell Biol 9:981-91.

131. Sun L, Yang G, Zaidi M, Iqbal J. (2008) TNF-induced oscillations in combinatorial transcription factor binding. Biochem Biophys Res Commun 371:912-6.

132. Bosisio D, Marazzi I, Agresti A, Shimizu N, Bianchi M E, Natoli G. (2006) A hyper-dynamic equilibrium between promoter-bound and nucleoplasmic dimers controls NF-kappaB-dependent gene activity. EMBO J 25:798-810.

133. Metivier R, Penot G, Hubner M R, Reid G, Brand H, Kos M, Gannon F. (2003) Estrogen receptor-alpha directs ordered, cyclical, and combinatorial recruitment of cofactors on a natural target promoter. Cell 115:751-63.

134. Reid G, Hubner M R, Metivier R, Brand H, Denger S, Manu D, Beaudouin J, Ellenberg J, Gannon F. (2003) Cyclic, proteasome-mediated turnover of unliganded and liganded ERalpha on responsive promoters is an integral feature of estrogen signaling. Mol Cell 11:695-707.

135. McNally J G, Muller W G, Walker D, Wolford R, Hager G L. (2000) The glucocorticoid receptor: rapid exchange with regulatory sites in living cells. Science 287:1262-5.

136. Stavreva D A, Muller W G, Hager G L, Smith C L, McNally J G. (2004) Rapid glucocorticoid receptor exchange at a promoter is coupled to transcription and regulated by chaperones and proteasomes. Mol Cell Biol 24:2682-97.

137. Nagaich A K, Walker D A, Wolford R, Hager G L. (2004) Rapid periodic binding and displacement of the glucocorticoid receptor during chromatin remodeling. Mol Cell 14:163-74.

138. Ghosh S, May M J, Kopp E B. (1998) NF-kappa B and Rel proteins: evolutionarily conserved mediators of immune responses. Annu Rev Immunol 16:225-60.

139. Pahl H L. (1999) Activators and target genes of Rel/NF-kappaB transcription factors. Oncogene 18:6853-66.

140. Yan J, Wang H, Liu Y, Shao C. (2008) Analysis of gene regulatory networks in the mammalian circadian rhythm. PLoS Comput Biol 4:e1000193.

141. Claridge-Chang A, Wijnen H, Naef F, Boothroyd C, Rajewsky N, Young M W. (2001) Circadian regulation of gene expression systems in the Drosophila head. Neuron 32:657-71.

142. McDonald M J, Rosbash M. (2001) Microarray analysis and organization of circadian gene expression in Drosophila. Cell 107:567-78.

143. Grundschober C, Delaunay F, Puhlhofer A, Triqueneaux G, Laudet V, Bartfai T, Nef P. (2001) Circadian regulation of diverse gene products revealed by mRNA expression profiling of synchronized fibroblasts. J Biol Chem 276:46751-8.

144. Harmer S L, Hogenesch J B, Straume M, Chang H S, Han B, Zhu T, Wang X, Kreps J A, Kay S A. (2000) Orchestrated transcription of key pathways in Arabidopsis by the circadian clock. Science 290:2110-3.

145. Duffield G E, Best J D, Meurers B H, Bittner A, Loros J J, Dunlap J C. (2002) Circadian programs of transcriptional activation, signaling, and protein turnover revealed by microarray analysis of mammalian cells. Curr Biol 12:551-7.

146. Whitfield M L, Sherlock G, Saldanha A J, Murray J I, Ball C A, Alexander K E, Matese J C, Perou C M, Hurt M M, Brown P O, Botstein D. (2002) Identification of genes periodically expressed in the human cell cycle and their expression in tumors. Mol Biol Cell 13:1977-2000.

147. Ishida S, Huang E, Zuzan H, Spang R, Leone G, West M, Nevins J R. (2001) Role for E2F in control of both DNA replication and mitotic functions as revealed from DNA microarray analysis. Mol Cell Biol 21:4684-99.

148. Rustici G, Mata J, Kivinen K, Lio P, Penkett C J, Burns G, Hayles J, Brazma A, Nurse P, Bahler J. (2004) Periodic gene expression program of the fission yeast cell cycle. Nat Genet 36:809-17.

149. Oliva A, Rosebrock A, Ferrezuelo F, Pyne S, Chen H, Skiena S, Futcher B, Leatherwood J. (2005) The cell cycle-regulated genes of Schizosaccharomyces pombe. PLoS Biol 3:e225.

150. Peng X, Karuturi R K, Miller L D, Lin K, Jia Y, Kondu P, Wang L, Wong L S, Liu E T, Balasubramanian M K, Liu J. (2005) Identification of cell cycle-regulated genes in fission yeast. Mol Biol Cell 16:1026-42.

151. Cho R J, Huang M, Campbell M J, Dong H, Steinmetz L, Sapinoso L, Hampton G, Elledge S J, Davis R W, Lockhart D J. (2001) Transcriptional regulation and function during the human cell cycle. Nat Genet 27:48-54.

152. Horak C E, Luscombe N M, Qian J, Bertone P, Piccirrillo S, Gerstein M, Snyder M. (2002) Complex transcriptional circuitry at the G1/S transition in Saccharomyces cerevisiae. Genes Dev 16:3017-33.

153. Simon I, Barnett J, Hannett N, Harbison C T, Rinaldi N J, Volkert T L, Wyrick J J, Zeitlinger J, Gifford D K, Jaakkola T S, Young R A. (2001) Serial regulation of transcriptional regulators in the yeast cell cycle. Cell 106:697-708.

154. Breeden L L. (2003) Periodic transcription: a cycle within a cycle. Curr Biol 13:R31-8.

155. Murray D B, Beckmann M, Kitano H. (2007) Regulation of yeast oscillatory dynamics. Proc Natl Acad Sci U S A 104:2241-6.

156. Dequeant M L, Glynn E, Gaudenz K, Wahl M, Chen J, Mushegian A, Pourquie O. (2006) A complex oscillating network of signaling genes underlies the mouse segmentation clock. Science 314:1595-8.

157. Pourquie O. (2003) The segmentation clock: converting embryonic time into spatial pattern. Science 301:328-30.

158. Bessho Y, Kageyama R. (2003) Oscillations, clocks and segmentation. Curr Opin Genet Dev 13:379-84.

159. Aulehla A, Herrmann B G. (2004) Segmentation in vertebrates: clock and gradient finally joined. Genes Dev 18:2060-7.

160. Waeber G, Meyer T E, LeSieur M, Hermann H L, Gerard N, Habener J F. (1991) Developmental stage-specific expression of cyclic adenosine 3',5'-monophosphate response element-binding protein CREB during spermatogenesis involves alternative exon splicing. Mol Endocrinol 5:1418-30.

161. Hall S H, Joseph D R, French F S, Conti M. (1988) Follicle-stimulating hormone induces transient expression of the protooncogene c-fos in primary Sertoli cell cultures. Mol Endocrinol 2:55-61.

162. Smith E P, Hall S H, Monaco L, French F S, Wilson E M, Conti M. (1989) A rat Sertoli cell factor similar to basic fibroblast growth factor increases c-fos messenger ribonucleic acid in cultured Sertoli cells. Mol Endocrinol 3:954-61.

163. Yoshikawa K, Aizawa T. (1988) Expression of the enkephalin precursor gene in rat Sertoli cells. Regulation by follicle-stimulating hormone. FEBS Lett 237:183-6.

164. Najmabadi H, Rosenberg L A, Yuan Q X, Bhatia N, Albiston A L, Burger H, Bhasin S. (1993) Transcriptional and posttranscriptional regulation of inhibin

alpha-subunit gene expression in rat Sertoli cells by 8-bromo-3',5'-cyclic-adenosine monophosphate. Mol Endocrinol 7:469-76.

165. Najmabadi H, Rosenberg L A, Yuan Q X, Reyaz G, Bhasin S. (1993) Transcriptional regulation of inhibin beta B messenger ribonucleic acid levels in TM.4 or primary rat Sertoli cells by 8-bromo-cyclic adenosine monophosphate. Mol Endocrinol 7:561-9.

166. Vihko K K, Penttila T L, Parvinen M, Belin D. (1989) Regulation of urokinase- and tissue-type plasminogen activator gene expression in the rat seminiferous epithelium. Mol Endocrinol 3:52-9.

167. Landmark B F, Fauske B, Eskild W, Skalhegg B, Lohmann S M, Hansson V, Jahnsen T, Beebe S J. (1991) Identification, characterization, and hormonal regulation of 3', 5'-cyclic adenosine monophosphate-dependent protein kinases in rat Sertoli cells. Endocrinology 129:2345-54.

168. Sun L, Yang G, Zaidi M, Iqbal J. (2008) TNF-induced gene expression oscillates in time. Biochem Biophys Res Commun 371:900-5.

169. Martone R, Euskirchen G, Bertone P, Hartman S, Royce T E, Luscombe N M, Rinn J L, Nelson F K, Miller P, Gerstein M, Weissman S, Snyder M. (2003) Distribution of NF-kappaB-binding sites across human chromosome 22. Proc Natl Acad Sci U S A 100:12247-52.

170. Natoli G, Saccani S, Bosisio D, Marazzi I. (2005) Interactions of NF-kappaB with chromatin: the art of being at the right place at the right time. Nat Immunol 6:439-45.

171. Mirza A, Wu Q, Wang L, McClanahan T, Bishop W R, Gheyas F, Ding W, Hutchins B, Hockenberry T, Kirschmeier P, Greene J R, Liu S. (2003) Global transcriptional program of p53 target genes during the process of apoptosis and cell cycle progression. Oncogene 22:3645-54.

172. Riley T, Sontag E, Chen P, Levine A. (2008) Transcriptional control of human p53-regulated genes. Nat Rev Mol Cell Biol 9:402-12.

173. Yoshiura S, Ohtsuka T, Takenaka Y, Nagahara H, Yoshikawa K, Kageyama R. (2007) Ultradian oscillations of Stat, Smad, and Hes1 expression in response to serum. Proc Natl Acad Sci U S A 104:11292-7.

174. Levy D E, Darnell J E, Jr. (2002) Stats: transcriptional control and biological impact. Nat Rev Mol Cell Biol 3:651-62.

175. Yu H, Jove R. (2004) The STATs of cancer--new molecular targets come of age. Nat Rev Cancer 4:97-105.

176. Massague J, Wotton D. (2000) Transcriptional control by the TGF-beta/Smad signaling system. EMBO J 19:1745-54.

177. ten Dijke P, Miyazono K, Heldin C H. (2000) Signaling inputs converge on nuclear effectors in TGF-beta signaling. Trends Biochem Sci 25:64-70.

178. King D P, Takahashi J S. (2000) Molecular genetics of circadian rhythms in mammals. Annu Rev Neurosci 23:713-42.

179. Lowrey P L, Takahashi J S. (2004) Mammalian circadian biology: elucidating genome-wide levels of temporal organization. Annu Rev Genomics Hum Genet 5:407-41.

180. Borgs L, Beukelaers P, Vandenbosch R, Belachew S, Nguyen L, Malgrange B. (2009) Cell "circadian" cycle: new role for mammalian core clock genes. Cell Cycle 8:832-7.

181. Iyer V R, Horak C E, Scafe C S, Botstein D, Snyder M, Brown P O. (2001) Genomic binding sites of the yeast cell-cycle transcription factors SBF and MBF. Nature 409:533-8.

182. Winzeler E A, Shoemaker D D, Astromoff A, Liang H, Anderson K, Andre B, Bangham R, Benito R, Boeke J D, Bussey H, Chu A M, Connelly C, Davis K, Dietrich F, Dow S W, El Bakkoury M, Foury F, Friend S H, Gentalen E, Giaever G, Hegemann J H, Jones T, Laub M, Liao H, Liebundguth N, Lockhart D J, Lucau-Danila A, Lussier M, M'Rabet N, Menard P, Mittmann M, Pai C, Rebischung C, Revuelta J L, Riles L, Roberts C J, Ross-MacDonald P, Scherens B, Snyder M, Sookhai-Mahadeo S, Storms R K, Veronneau S, Voet M, Volckaert G, Ward T R, Wysocki R, Yen G S, Yu K, Zimmermann K, Philippsen P, Johnston M, Davis R W. (1999) Functional characterization of the S. cerevisiae genome by gene deletion and parallel analysis. Science 285:901-6.

183. Janke C, Magiera M M, Rathfelder N, Taxis C, Reber S, Maekawa H, Moreno-Borchart A, Doenges G, Schwob E, Schiebel E, Knop M. (2004) A versatile toolbox for PCR-based tagging of yeast genes: new fluorescent proteins, more markers and promoter substitution cassettes. Yeast 21:947-62.

184. Sheff M A, Thorn K S. (2004) Optimized cassettes for fluorescent protein tagging in Saccharomyces cerevisiae. Yeast 21:661-70.

185. Sambrook J, Fritsch E F, Maniatis T, *Molecular Cloning: A Laboratory Manual*. 1989: Cold Spring Harbor Laboratory Press.

186. Keogh M C, Kim J A, Downey M, Fillingham J, Chowdhury D, Harrison J C, Onishi M, Datta N, Galicia S, Emili A, Lieberman J, Shen X, Buratowski S, Haber J E, Durocher D, Greenblatt J F, Krogan N J. (2006) A phosphatase complex that dephosphorylates gammaH2AX regulates DNA damage checkpoint recovery. Nature 439:497-501.

187. de Godoy L M, Olsen J V, Cox J, Nielsen M L, Hubner N C, Frohlich F, Walther T C, Mann M. (2008) Comprehensive mass-spectrometry-based proteome quantification of haploid versus diploid yeast. Nature 455:1251-4.

188. Gruhler S, Kratchmarova I. (2008) Stable isotope labeling by amino acids in cell culture (SILAC). Methods Mol Biol 424:101-11.

189. Ong S E, Blagoev B, Kratchmarova I, Kristensen D B, Steen H, Pandey A, Mann M. (2002) Stable isotope labeling by amino acids in cell culture, SILAC, as a simple and accurate approach to expression proteomics. Mol Cell Proteomics 1:376-86.

190. Khanna K K, Jackson S P. (2001) DNA double-strand breaks: signaling, repair and the cancer connection. Nat Genet 27:247-54.

191. van Gent D C, Hoeijmakers J H, Kanaar R. (2001) Chromosomal stability and the DNA double-stranded break connection. Nat Rev Genet 2:196-206.

192. Moore J K, Haber J E. (1996) Cell cycle and genetic requirements of two pathways of nonhomologous end-joining repair of double-strand breaks in Saccharomyces cerevisiae. Mol Cell Biol 16:2164-73.

193. Haber J E. (1998) Mating-type gene switching in Saccharomyces cerevisiae. Annu Rev Genet 32:561-99.

194. Gardner R, Putnam C W, Weinert T. (1999) RAD53, DUN1 and PDS1 define two parallel G2/M checkpoint pathways in budding yeast. EMBO J 18:3173-85.

195. Wang H, Liu D, Wang Y, Qin J, Elledge S J. (2001) Pds1 phosphorylation in response to DNA damage is essential for its DNA damage checkpoint function. Genes Dev 15:1361-72.

196. Yamamoto A, Guacci V, Koshland D. (1996) Pds1p, an inhibitor of anaphase in budding yeast, plays a critical role in the APC and checkpoint pathway(s). J Cell Biol 133:99-110.

197. Jaspersen S L, Morgan D O. (2000) Cdc14 activates cdc15 to promote mitotic exit in budding yeast. Curr Biol 10:615-8.

198. Park C J, Song S, Lee P R, Shou W, Deshaies R J, Lee K S. (2003) Loss of CDC5 function in Saccharomyces cerevisiae leads to defects in Swe1p regulation and Bfa1p/Bub2p-independent cytokinesis. Genetics 163:21-33.

199. Drastichova Z, Bourova L, Lisy V, Hejnova L, Rudajev V, Stohr J, Durchankova D, Ostasov P, Teisinger J, Soukup T, Novotny J, Svoboda P. (2008) Subcellular redistribution of trimeric G-proteins--potential mechanism of desensitization of hormone response: internalization, solubilization, down-regulation. Physiol Res 57 Suppl 3:S1-10.

200. DeFea K A. (2007) Stop that cell! Beta-arrestin-dependent chemotaxis: a tale of localized actin assembly and receptor desensitization. Annu Rev Physiol 69:535-60.

201. Matsuoka S, Rotman G, Ogawa A, Shiloh Y, Tamai K, Elledge S J. (2000) Ataxia telangiectasia-mutated phosphorylates Chk2 in vivo and in vitro. Proc Natl Acad Sci U S A 97:10389-94.

202. Oliva-Trastoy M, Berthonaud V, Chevalier A, Ducrot C, Marsolier-Kergoat M C, Mann C, Leteurtre F. (2007) The Wip1 phosphatase (PPM1D) antagonizes activation of the Chk2 tumour suppressor kinase. Oncogene 26:1449-58.

203. Lu X, Nannenga B, Donehower L A. (2005) PPM1D dephosphorylates Chk1 and p53 and abrogates cell cycle checkpoints. Genes Dev 19:1162-74.

204. Syljuasen R G. (2007) Checkpoint adaptation in human cells. Oncogene 26:5833-9.

205. Zhang Y W, Otterness D M, Chiang G G, Xie W, Liu Y C, Mercurio F, Abraham R T. (2005) Genotoxic stress targets human Chk1 for degradation by the ubiquitin-proteasome pathway. Mol Cell 19:607-18.

206. Raleigh J M, O'Connell M J. (2000) The G(2) DNA damage checkpoint targets both Wee1 and Cdc25. J Cell Sci 113 (Pt 10):1727-36.

207. den Elzen N R, O'Connell M J. (2004) Recovery from DNA damage checkpoint arrest by PP1-mediated inhibition of Chk1. EMBO J 23:908-18.

208. Sanchez Y, Desany B A, Jones W J, Liu Q, Wang B, Elledge S J. (1996) Regulation of RAD53 by the ATM-like kinases MEC1 and TEL1 in yeast cell cycle checkpoint pathways. Science 271:357-60.

209. Sun Z, Fay D S, Marini F, Foiani M, Stern D F. (1996) Spk1/Rad53 is regulated by Mec1-dependent protein phosphorylation in DNA replication and damage checkpoint pathways. Genes Dev 10:395-406.

210. O'Neill B M, Szyjka S J, Lis E T, Bailey A O, Yates J R, 3rd, Aparicio O M, Romesberg F E. (2007) Pph3-Psy2 is a phosphatase complex required for Rad53 dephosphorylation and replication fork restart during recovery from DNA damage. Proc Natl Acad Sci U S A 104:9290-5.

211. Travesa A, Duch A, Quintana D G. (2008) Distinct phosphatases mediate the deactivation of the DNA damage checkpoint kinase Rad53. J Biol Chem 283:17123-30.

212. Thuret J Y, Valay J G, Faye G, Mann C. (1996) Civ1 (CAK in vivo), a novel Cdk-activating kinase. Cell 86:565-76.

213. Cheng A, Ross K E, Kaldis P, Solomon M J. (1999) Dephosphorylation of cyclin-dependent kinases by type 2C protein phosphatases. Genes Dev 13:2946-57.

214. Guillemain G, Ma E, Mauger S, Miron S, Thai R, Guerois R, Ochsenbein F, Marsolier-Kergoat M C. (2007) Mechanisms of checkpoint kinase Rad53 inactivation after a double-strand break in Saccharomyces cerevisiae. Mol Cell Biol 27:3378-89.

215. Paciotti V, Clerici M, Lucchini G, Longhese M P. (2000) The checkpoint protein Ddc2, functionally related to S. pombe Rad26, interacts with Mec1 and

is regulated by Mec1-dependent phosphorylation in budding yeast. Genes Dev 14:2046-59.

216. Nakajima H, Toyoshima-Morimoto F, Taniguchi E, Nishida E. (2003) Identification of a consensus motif for Plk (Polo-like kinase) phosphorylation reveals Myt1 as a Plk1 substrate. J Biol Chem 278:25277-80.

217. Elia A E, Rellos P, Haire L F, Chao J W, Ivins F J, Hoepker K, Mohammad D, Cantley L C, Smerdon S J, Yaffe M B. (2003) The molecular basis for phosphodependent substrate targeting and regulation of Plks by the Polo-box domain. Cell 115:83-95.

218. Crasta K, Lim H H, Giddings T H, Jr., Winey M, Surana U. (2008) Inactivation of Cdh1 by synergistic action of Cdk1 and polo kinase is necessary for proper assembly of the mitotic spindle. Nat Cell Biol 10:665-75.

219. Park C J, Park J E, Karpova T S, Soung N K, Yu L R, Song S, Lee K H, Xia X, Kang E, Dabanoglu I, Oh D Y, Zhang J Y, Kang Y H, Wincovitch S, Huffaker T C, Veenstra T D, McNally J G, Lee K S. (2008) Requirement for the budding yeast polo kinase Cdc5 in proper microtubule growth and dynamics. Eukaryot Cell 7:444-53.

220. Elia A E, Cantley L C, Yaffe M B. (2003) Proteomic screen finds pSer/pThr-binding domain localizing Plk1 to mitotic substrates. Science 299:1228-31.

221. Nakada D, Hirano Y, Sugimoto K. (2004) Requirement of the Mre11 complex and exonuclease 1 for activation of the Mec1 signaling pathway. Mol Cell Biol 24:10016-25.

222. Storch K F, Paz C, Signorovitch J, Raviola E, Pawlyk B, Li T, Weitz C J. (2007) Intrinsic circadian clock of the mammalian retina: importance for retinal processing of visual information. Cell 130:730-41.

223. Reinke H, Gatfield D. (2006) Genome-wide oscillation of transcription in yeast. Trends Biochem Sci 31:189-91.

224. Lloyd D, Murray D B. (2005) Ultradian metronome: timekeeper for orchestration of cellular coherence. Trends Biochem Sci 30:373-7.

225. Tu B P, McKnight S L. (2006) Metabolic cycles as an underlying basis of biological oscillations. Nat Rev Mol Cell Biol 7:696-701.

226. Murray J D, *Mathematical Biology I*. 2004: Springer.

227. Stryer L, *Biochemistry*. 1988, New York: W. H. Freeman and Co.

228. Gray P, Scott S K, *Chemical Oscillations and Instabilities*. 1990, Oxford: Clarendon Press.

229. von Dassow G, Meir E, Munro E M, Odell G M. (2000) The segment polarity network is a robust developmental module. Nature 406:188-92.

230. Aldridge B B, Burke J M, Lauffenburger D A, Sorger P K. (2006) Physicochemical modelling of cell signalling pathways. Nat Cell Biol 8:1195-203.

231. Huang C Y, Ferrell J E, Jr. (1996) Ultrasensitivity in the mitogen-activated protein kinase cascade. Proc Natl Acad Sci U S A 93:10078-83.

232. Quach M, Brunel N, d'Alche-Buc F. (2007) Estimating parameters and hidden variables in non-linear state-space models based on ODEs for biological networks inference. Bioinformatics 23:3209-16.

233. de Jong H. (2002) Modeling and simulation of genetic regulatory systems: a literature review. J Comput Biol 9:67-103.

234. Rossi F M, Kringstein A M, Spicher A, Guicherit O M, Blau H M. (2000) Transcriptional control: rheostat converted to on/off switch. Mol Cell 6:723-8.

235. Vousden K H, Lu X. (2002) Live or let die: the cell's response to p53. Nat Rev Cancer 2:594-604.

236. Cheong R, Hoffmann A, Levchenko A. (2008) Understanding NF-kappaB signaling via mathematical modeling. Mol Syst Biol 4:192.

237. Monk N A. (2003) Oscillatory expression of Hes1, p53, and NF-kappaB driven by transcriptional time delays. Curr Biol 13:1409-13.

238. Lev Bar-Or R, Maya R, Segel L A, Alon U, Levine A J, Oren M. (2000) Generation of oscillations by the p53-Mdm2 feedback loop: a theoretical and experimental study. Proc Natl Acad Sci U S A 97:11250-5.

239. Okamura S, Arakawa H, Tanaka T, Nakanishi H, Ng C C, Taya Y, Monden M, Nakamura Y. (2001) p53DINP1, a p53-inducible gene, regulates p53-dependent apoptosis. Mol Cell 8:85-94.

240. Oda K, Arakawa H, Tanaka T, Matsuda K, Tanikawa C, Mori T, Nishimori H, Tamai K, Tokino T, Nakamura Y, Taya Y. (2000) p53AIP1, a potential mediator of p53-dependent apoptosis, and its regulation by Ser-46-phosphorylated p53. Cell 102:849-62.

241. McAdams H H, Arkin A. (1999) It's a noisy business! Genetic regulation at the nanomolar scale. Trends Genet 15:65-9.

242. Gillespie D T. (1977) Exact stochastic simulation of coupled chemical reactions. The Journal of Physical Chemistry 81:2340-2361.

243. Stricker J, Cookson S, Bennett M R, Mather W H, Tsimring L S, Hasty J. (2008) A fast, robust and tunable synthetic gene oscillator. Nature 456:516-9.

244. Fung E, Wong W W, Suen J K, Bulter T, Lee S G, Liao J C. (2005) A synthetic gene-metabolic oscillator. Nature 435:118-22.

245. Rapp PE. (1979) An atlas of cellular oscillators. J Exp Biol 81:281-306.

Appendices

Appendices

7.1 Estimation of Trends

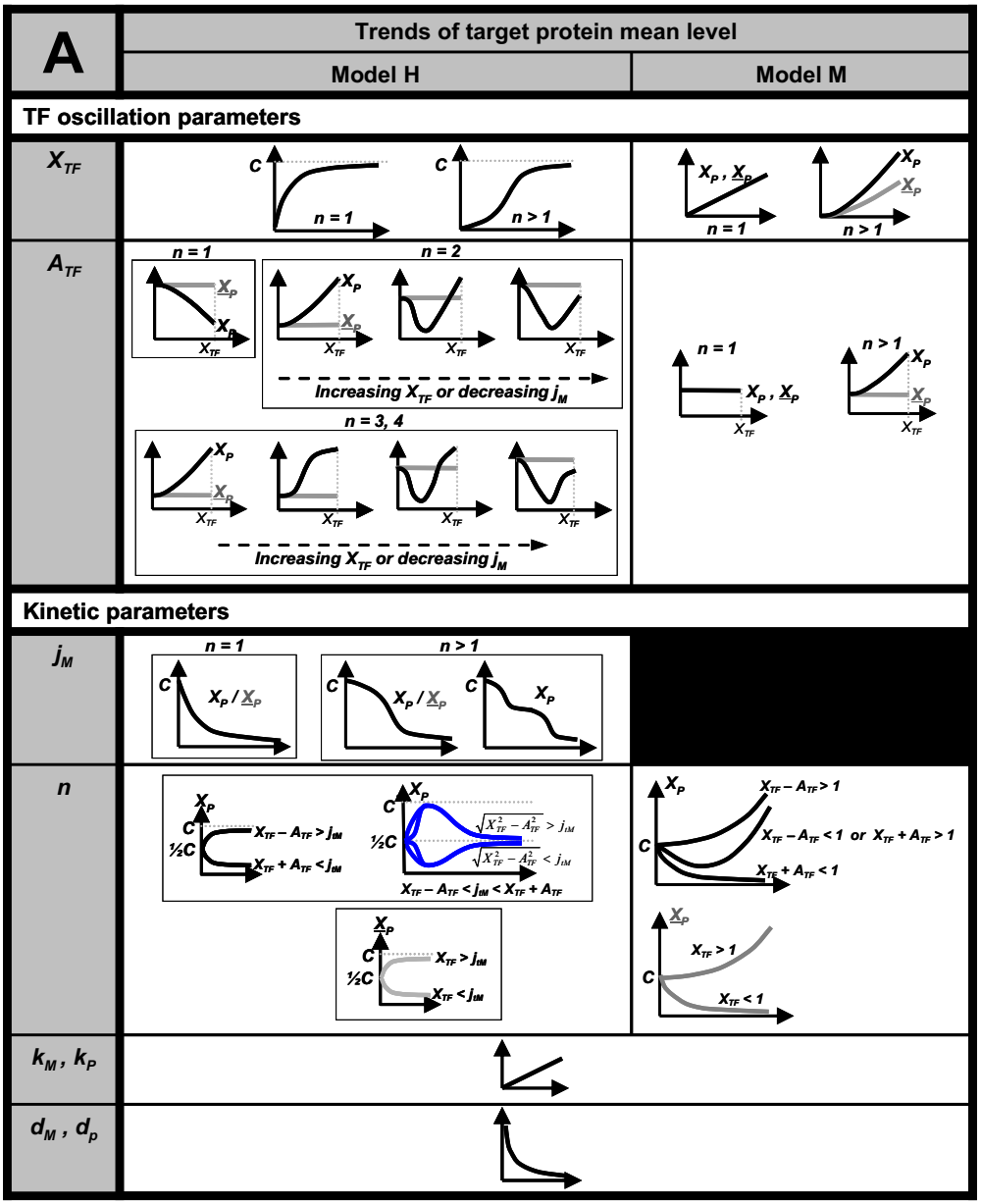

Figure S1A. Trends of target protein mean level as a function of parameters in Models M and H

For each plot, the vertical axis represents the protein mean level that is either induced by an oscillatory TF (denoted as X_P) or a non-oscillatory TF (denoted as $\underline{X}_P$); the level of a non-oscillatory TF is set to be equal to the mean level of the oscillatory TF. Where

applicable, $\underline{X_P}$ trends are shown in gray. The horizontal axis represents the varied parameter as indicated in column 1. Blue curves signify possible trends under the same condition. C is given as $k_M k_P / (d_M d_P)$.

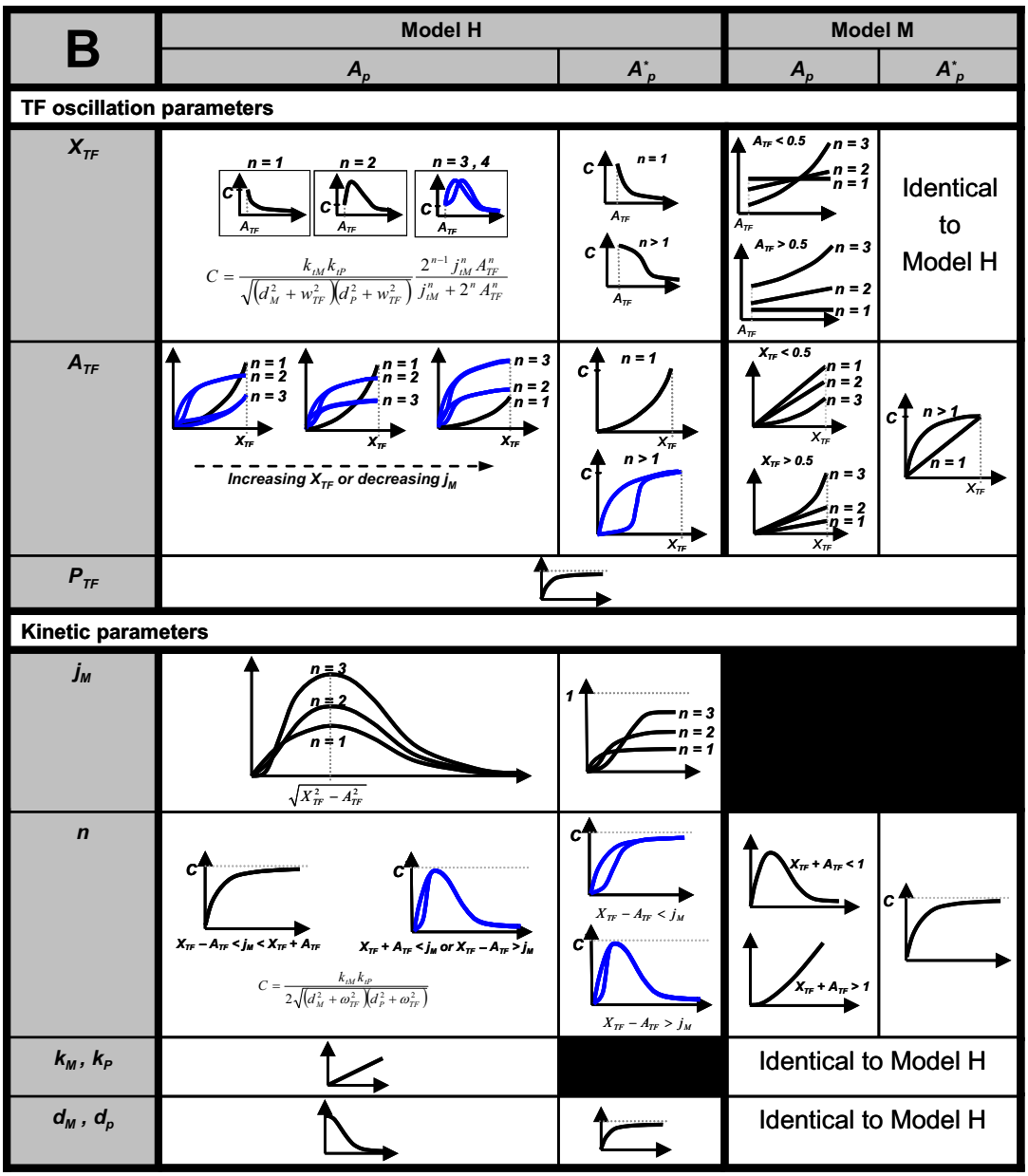

Figure S1B. Trends of target protein amplitude and normalized amplitude as a function of parameters in Models M and H

For each plot, the vertical axis represents the protein oscillation amplitude (A_P) or normalized oscillation amplitude (A^*_P). The horizontal axis represents the varied parameter as indicated in column 1. Blue curves signify possible trends under the same

condition. C is given as $\frac{d_M d_P}{\sqrt{\left(d_M^2+\omega_{TF}^2\right)\left(d_P^2+\omega_{TF}^2\right)}}$ unless otherwise stated where w_{TF} is TF oscillation frequency defined as $2\pi/P_{TF}$.

7.2 Solution of Model M and H

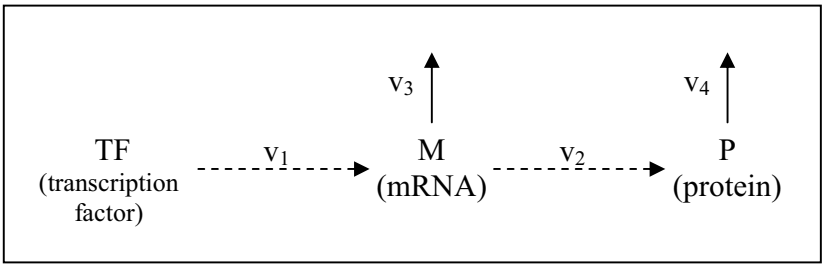

7.2.1 Model H: Transcription is modeled with Hill-type kinetics

$$IC: TF(t<0)=M(t<\theta_M)=P(t<\theta_M+\theta_P)=0$$

Obtain an expression for M(t).

$$\frac{dM}{dt}=\frac{k_M[TF(t-\theta_M)]^n}{j_M^n+[TF(t-\theta_M)]^n}-d_M M$$

$$\frac{dM}{dt}=k_M\left\{\frac{[TF(t-\theta_M)]^n+j_M^n-j_M^n}{j_M^n+[TF(t-\theta_M)]^n}\right\}-d_M M$$

$$\frac{dM}{dt}=k_M\left\{1-\frac{j_M^n}{j_M^n+[TF(t-\theta_M)]^n}\right\}-d_M M$$

$$\frac{dM}{dt}=k_M\left\{1-\frac{j_M^n}{j_M^n+[TF(t-\theta_M)]^n}\right\}-d_M M$$

$$e^{d_M t}\frac{dM}{dt}=\left\{k_M-\frac{k_M j_M^n}{j_M^n+[TF(t-\theta_M)]^n}\right\}e^{d_M t}-d_M M e^{d_M t}$$

$$\frac{d}{dt}\left[Me^{d_M t}\right]=\left\{k_M-\frac{k_M j_M^n}{j_M^n+[TF(t-\theta_M)]^n}\right\}e^{d_M t}$$

$$\Rightarrow Me^{d_M t}=\int\left\{k_M-\frac{k_M j_M^n}{j_M^n+[TF(t-\theta_M)]^n}\right\}e^{d_M t}dt+C_1$$

$$Me^{d_M t}=\left(\frac{k_M}{d_M}\right)e^{d_M t}-k_M j_M^n\int\frac{e^{d_M t}}{j_M^n+[TF(t-\theta_M)]^n}dt+C_1$$

$$\Rightarrow M(t>\tau_1)=\left(\frac{k_M}{d_M}\right)-k_M j_M^n e^{-d_M t}\int\frac{e^{d_M t}}{j_M^n+[TF(t-\theta_M)]^n}dt+C_1 e^{-d_M t}\ldots\ldots\ldots\ldots\ldots\ldots(A)$$

Solve M(t).

Let

$$TF = f(t, \underline{P})$$
$$= X_{TF} + A_{TF} \sin \frac{2\pi}{P_{TF}}(t)$$

Note: $X_{TF} \geq A_{TF}$. X_{TF} signifies the mean of the oscillation; A_{TF} signifies the amplitude of the oscillation; P_{TF} signifies the period of the oscillation.

Thus, from (A):

$$M(t > \tau_1) = \left(\frac{k_M}{d_M}\right) - k_M j_M^n e^{-d_M t} \int \frac{e^{d_M t}}{j_M^n + [TF(t - \theta_M)]^n} dt + C_1 e^{-d_M t}$$

$$M(t > \tau_1) = \left(\frac{k_M}{d_M}\right) - k_M j_M^n e^{-d_M t} \int \frac{e^{d_M t}}{j_M^n + \left[X_{TF} + A_{TF} \sin \frac{2\pi}{P_{TF}}(t - \theta_M)\right]^n} dt + C_1 e^{-d_M t}$$

To solve the integral analytically, we need to approximate the denominator to a tractable form. Since the aim is to study the amplitude of oscillations, the approximated form needs to retain the same amplitude, period and phase as the original form. One possible approximation is:

$$\frac{1}{j_M^n + \left[X_{TF} + A_{TF} \sin \frac{2\pi}{P_{TF}}(t - \theta_M)\right]^n} \approx \overline{X_{TF}} + \overline{A_{TF}} \sin\left[\frac{2\pi}{P_{TF}}(t - \theta_M) + \pi\right]$$

where

$$\overline{A_{TF}} = \frac{(\max - \min)}{2}$$
$$= \frac{1}{2}\left\{\frac{1}{j_M^n + [X_{TF} + A_{TF}(-1)]^n} - \frac{1}{j_M^n + [X_{TF} + A_{TF}(1)]^n}\right\}$$
$$= \frac{1}{2}\left\{\frac{1}{j_M^n + [X_{TF} - A_{TF}]^n} - \frac{1}{j_M^n + [X_{TF} + A_{TF}]^n}\right\}$$
$$= \frac{\left[j_M^n + (X_{TF} + A_{TF})^n\right] - \left[j_M^n + (X_{TF} - A_{TF})^n\right]}{2\left[j_M^n + (X_{TF} - A_{TF})^n\right] \cdot \left[j_M^n + (X_{TF} + A_{TF})^n\right]}$$
$$= \frac{(X_{TF} + A_{TF})^n - (X_{TF} - A_{TF})^n}{2\left[j_M^n + (X_{TF} - A_{TF})^n\right] \cdot \left[j_M^n + (X_{TF} + A_{TF})^n\right]}$$

$$\begin{aligned}\overline{X_{TF}} &= \min + \overline{A_{TF}} \\ &= \frac{1}{j_M^n + \left[X_{TF} + A_{TF}(1)\right]^n} + \frac{\left(X_{TF} + A_{TF}\right)^n - \left(X_{TF} - A_{TF}\right)^n}{2\left[j_M^n + \left(X_{TF} - A_{TF}\right)^n\right]\cdot\left[j_M^n + \left(X_{TF} + A_{TF}\right)^n\right]} \\ &= \frac{2\left[j_M^n + \left(X_{TF} - A_{TF}\right)^n\right] + \left(X_{TF} + A_{TF}\right)^n - \left(X_{TF} - A_{TF}\right)^n}{2\left[j_M^n + \left(X_{TF} - A_{TF}\right)^n\right]\cdot\left[j_M^n + \left(X_{TF} + A_{TF}\right)^n\right]} \\ &= \frac{2j_M^n + \left(X_{TF} + A_{TF}\right)^n + \left(X_{TF} - A_{TF}\right)^n}{2\left[j_M^n + \left(X_{TF} - A_{TF}\right)^n\right]\cdot\left[j_M^n + \left(X_{TF} + A_{TF}\right)^n\right]}\end{aligned}$$

Thus,

$$\begin{aligned}&M(t > \tau_1) \\ &= \left(\frac{k_M}{d_M}\right) - k_M j_M^n e^{-d_M t}\int \frac{e^{d_M t}}{j_M^n + \left[X_{TF} + A_{TF}\sin\frac{2\pi}{P_{TF}}(t-\theta_M)\right]^n}dt + C_1 e^{-d_M t} \\ &\approx \left(\frac{k_M}{d_M}\right) - k_M j_M^n e^{-d_M t}\int\left\{\overline{X_{TF}} + \overline{A_{TF}}\sin\left[\frac{2\pi}{P_{TF}}(t-\theta_M)+\pi\right]\right\}e^{d_M t}dt + C_1 e^{-d_M t} \\ &= \left(\frac{k_M}{d_M}\right) - k_M j_M^n e^{-d_M t}\left\{\overline{X_{TF}}\int e^{d_M t}dt + \overline{A_{TF}}\int e^{d_M t}\sin\left[\frac{2\pi}{P_{TF}}(t-\theta_M)+\pi\right]dt\right\} + C_1 e^{-d_M t} \\ &= \left(\frac{k_M}{d_M}\right) - k_M j_M^n e^{-d_M t}\left\{\frac{\overline{X_{TF}}}{d_M}e^{d_M t} + \frac{\overline{A_{TF}}}{\sqrt{d_M^2 + \left(\frac{2\pi}{P_{TF}}\right)^2}}e^{d_M t}\sin\left[\frac{2\pi}{P_{TF}}(t-\theta_M) - \tan^{-1}\frac{2\pi}{d_M P_{TF}}\right] + C_2\right\} + C_1 e^{-d_M t} \\ &= k_M\left(\frac{1 - j_M^n\overline{X_{TF}}}{d_M}\right) - \frac{k_M j_M^n\overline{A_{TF}}}{\sqrt{d_M^2 + \left(\frac{2\pi}{P_{TF}}\right)^2}}\sin\frac{2\pi}{P_{TF}}\left[t - \theta_M - \frac{P_{TF}}{2\pi}\tan^{-1}\frac{2\pi}{d_M P_{TF}}\right] + C_2 k_M j_M^n e^{-d_M t} + C_1 e^{-d_M t}\end{aligned}$$

$$\begin{aligned}&\int e^{d_M t}\sin\left[\frac{2\pi}{P_{TF}}(t-\theta_M)+\pi\right]dt \\ &= \frac{e^{d_M t}}{d_M}\sin\left[\frac{2\pi}{P_{TF}}(t-\theta_M)+\pi\right] + \int\frac{e^{d_M t}}{d_M}\frac{2\pi}{P_{TF}}\cos\left[\frac{2\pi}{P_{TF}}(t-\theta_M)+\pi\right]dt \\ &= \frac{e^{d_M t}}{d_M}\sin\left[\frac{2\pi}{P_{TF}}(t-\theta_M)+\pi\right] \\ &\quad + \frac{2\pi}{d_M P_{TF}}\left\{\frac{e^{d_M t}}{d_M}\cos\left[\frac{2\pi}{P_{TF}}(t-\theta_M)+\pi\right] - \int\frac{e^{d_M t}}{d_M}\frac{2\pi}{P_{TF}}\sin\left[\frac{2\pi}{P_{TF}}(t-\theta_M)+\pi\right]dt\right\} \\ &= \frac{e^{d_M t}}{d_M}\sin\left[\frac{2\pi}{P_{TF}}(t-\theta_M)+\pi\right] \\ &\quad + \frac{2\pi\cdot e^{d_M t}}{P_{TF}{d_M}^2}\cos\left[\frac{2\pi}{P_{TF}}(t-\theta_M)+\pi\right] - \left(\frac{2\pi}{P_{TF}d_M}\right)^2\int e^{d_M t}\sin\left[\frac{2\pi}{P_{TF}}(t-\theta_M)+\pi\right]dt \\ &\Rightarrow \left[1 + \left(\frac{2\pi}{P_{TF}d_M}\right)^2\right]\int e^{d_M t}\sin\left[\frac{2\pi}{P_{TF}}(t-\theta_M)+\pi\right]dt \\ &\quad = \frac{e^{d_M t}}{{d_M}^2}\left\{d_M\sin\left[\frac{2\pi}{P_{TF}}(t-\theta_M)+\pi\right] + \frac{2\pi}{P_{TF}}\cos\left[\frac{2\pi}{P_{TF}}(t-\theta_M)+\pi\right]\right\}\end{aligned}$$

$$\begin{aligned}&\Rightarrow \int e^{d_M t}\sin\left[\frac{2\pi}{P_{TF}}(t-\theta_M)+\pi\right]dt \\ &\quad = \frac{e^{d_M t}}{(d_M)^2 + \left(\frac{2\pi}{P_{TF}}\right)^2}\left\{d_M\sin\left[\frac{2\pi}{P_{TF}}(t-\theta_M)+\pi\right] + \frac{2\pi}{P_{TF}}\cos\left[\frac{2\pi}{P_{TF}}(t-\theta_M)+\pi\right]\right\}\end{aligned}$$

$$\left\{ d_M \sin\left[\frac{2\pi}{P_{TF}}(t-\theta_M)+\pi\right]+\frac{2\pi}{P_{TF}}\cos\left[\frac{2\pi}{P_{TF}}(t-\theta_M)+\pi\right]\right\}$$

$$=\sqrt{{d_M}^2+\left(\frac{2\pi}{P_{TF}}\right)^2}\left\{\begin{array}{l}\dfrac{d_M}{\sqrt{{d_M}^2+\left(\frac{2\pi}{P_{TF}}\right)^2}}\sin\left[\dfrac{2\pi}{P_{TF}}(t-\theta_M)+\pi\right]\\ +\dfrac{2\pi}{P_{TF}\sqrt{{d_M}^2+\left(\frac{2\pi}{P_{TF}}\right)^2}}\cos\left[\dfrac{2\pi}{P_{TF}}(t-\theta_M)+\pi\right]\end{array}\right\}$$

since, $\tan\alpha=\dfrac{2\pi}{P_{TF}d_M}, \alpha=\tan^{-1}\left(\dfrac{2\pi}{P_{TF}d_M}\right)$

$$=\sqrt{{d_M}^2+\left(\frac{2\pi}{P_{TF}}\right)^2}\left\{\cos\alpha\sin\left[\frac{2\pi}{P_{TF}}(t-\theta_M)+\pi\right]+\sin\alpha\cos\left[\frac{2\pi}{P_{TF}}(t-\theta_M)+\pi\right]\right\}$$

$$=\sqrt{{d_M}^2+\left(\frac{2\pi}{P_{TF}}\right)^2}\sin\left[\frac{2\pi}{P_{TF}}(t-\theta_M)+\pi+\alpha\right]$$

Therefore,

$$\Rightarrow \int e^{d_M t}\sin\left[\frac{2\pi}{P_{TF}}(t-\theta_M)+\pi\right]dt$$

$$=\frac{e^{d_M t}}{(d_M)^2+\left(\frac{2\pi}{P_{TF}}\right)^2}\sqrt{{d_M}^2+\left(\frac{2\pi}{P_{TF}}\right)^2}\sin\left[\frac{2\pi}{P_{TF}}(t-\theta_M)+\pi+\alpha\right]$$

$$=\frac{e^{d_M t}}{\sqrt{{d_M}^2+\left(\frac{2\pi}{P_{TF}}\right)^2}}\sin\left[\frac{2\pi}{P_{TF}}(t-\theta_M)+\pi+\alpha\right]$$

Solve P(t).

$$
\begin{aligned}
&P(t)\\
&= k_P e^{-d_P t}\int[M(t-\theta_P)]e^{d_P t}dt + C_3 e^{-d_P t}\\
&\approx k_P e^{-d_P t}\int_0\left[\begin{array}{l}\dfrac{k_M\left(1-j_M^n\overline{X_{TF}}\right)}{d_M}e^{d_P t}+\dfrac{k_M j_M^n\overline{A_{TF}}}{\sqrt{d_M^2+\left(\dfrac{2\pi}{P_{TF}}\right)^2}}e^{d_P t}\sin\dfrac{2\pi}{P_{TF}}\left(t-\theta_M-\theta_P-\dfrac{P_{TF}}{2\pi}\arctan\dfrac{2\pi}{P_{TF}}\dfrac{1}{d_M}\right)\\ +\left(C_1-C_2k_M j_M^n\right)e^{-d_M(t-\theta_P)}e^{d_P t}\end{array}\right]dt + C_3e^{-d_P t}\\
&= k_P e^{-d_P t}\int\frac{k_M\left(1-j_M^n\overline{X_{TF}}\right)}{d_M}dt+\frac{k_M j_M^n\overline{A_{TF}}}{\sqrt{d_M^2+\left(\dfrac{2\pi}{P_{TF}}\right)^2}}k_P e^{-d_P t}\int e^{d_P t}\sin\frac{2\pi}{P_{TF}}\left(t-\theta_M-\theta_P-\frac{P_{TF}}{2\pi}\arctan\frac{2\pi}{P_{TF}}\frac{1}{d_M}\right)dt\\
&\quad +k_P e^{-d_P t}\left(C_1-C_2k_M j_M^n\right)\int e^{-d_M t}e^{d_M\theta_P}e^{d_P t}dt + C_3e^{-d_P t}
\end{aligned}
$$

since $\int e^{d_P t}\sin\left[\dfrac{2\pi}{P_{TF}}(t-\theta)\right]dt = \dfrac{e^{d_P t}}{\sqrt{{d_P}^2+\left(\dfrac{2\pi}{P_{TF}}\right)^2}}\sin\left[\dfrac{2\pi}{P_{TF}}(t-\theta)+\alpha\right]$,

where $\alpha = \tan^{-1}\left(\dfrac{2\pi}{P_{TF}d_P}\right)$

$$
\begin{aligned}
&= \frac{k_P k_M\left(1-j_M^n\overline{X_{TF}}\right)}{d_P d_M}+\left[\frac{k_M j_M^n\overline{A_{TF}}}{\sqrt{d_M^2+\left(\dfrac{2\pi}{P_{TF}}\right)^2}}k_P e^{-d_P t}\right]\left[\frac{e^{d_P t}}{\sqrt{d_M^2+\left(\dfrac{2\pi}{P_{TF}}\right)^2}}\right]\sin\frac{2\pi}{P_{TF}}\left[\left(t-\theta_M-\theta_P-\frac{P_{TF}}{2\pi}\arctan\frac{2\pi}{P_{TF}d_M}\right)-\arctan\frac{2\pi}{P_{TF}d_P}\right]\\
&\quad +k_P e^{-d_P t}\left(C_1-C_2k_M j_M^n\right)e^{d_M\theta_P}\int e^{-d_M t}e^{d_P t}dt + C_3e^{-d_P t}+C_4k_P e^{-d_P t}\\
&= \frac{k_P k_M\left(1-j_M^n\overline{X_{TF}}\right)}{d_P d_M}+\frac{k_P k_M j_M^n\overline{A_{TF}}}{\sqrt{d_P^2+\left(\dfrac{2\pi}{P_{TF}}\right)^2}\sqrt{d_M^2+\left(\dfrac{2\pi}{P_{TF}}\right)^2}}\sin\frac{2\pi}{P_{TF}}\left(t-\theta_M-\theta_P-\frac{P_{TF}}{2\pi}\arctan\frac{2\pi}{P_{TF}d_M}-\frac{P_{TF}}{2\pi}\arctan\frac{2\pi}{P_{TF}d_P}\right)\\
&\quad +\frac{k_P\left(C_1-C_2k_M j_M^n\right)}{d_P-d_M}e^{-d_M(t-\theta_P)}+\left(C_3+C_4k_P\right)e^{-d_P t}
\end{aligned}
$$

7.2.2 Model M: Transcription is modeled with Mass Action kinetics

Solve M(t)

$$\frac{dM}{dt} = k_M\left[TF(t-\theta_M)\right]^n - d_M M$$

Let

$$TF = f(t, \underline{P})$$
$$= X_{TF} + A_{TF} \sin \frac{2\pi}{P_{TF}}(t)$$

$$M(t) = k_M e^{-d_M t} \int [TF(t-\theta_M)]^n e^{d_M t} dt + C_1 e^{-d_M t}$$
$$= k_M e^{-d_M t} \int \left[X_{TF} + A_{TF} \sin \frac{2\pi}{P_{TF}}(t-\theta_M) \right]^n e^{d_M t} dt + C_1 e^{-d_M t}$$

Approximate $\left[X_{TF} + A_{TF} \sin \frac{2\pi}{P_{TF}}(t-\theta_M) \right]^n \approx \overline{X_{TF}} + \overline{A_{TF}} \sin \frac{2\pi}{P_{TF}}(t-\theta_M)$,

where $\overline{X_{TF}} = \frac{(X_{TF} + A_{TF})^n + (X_{TF} - A_{TF})^n}{2}$, $\overline{A_{TF}} = \frac{(X_{TF} + A_{TF})^n - (X_{TF} - A_{TF})^n}{2}$.

$$\overline{A_{TF}} = \frac{(\max - \min)}{2}$$
$$= \frac{1}{2}\left\{ (X_{TF} + A_{TF})^n - (X_{TF} - A_{TF})^n \right\}$$

$$\overline{X_{TF}} = \min + \overline{A_{TF}}$$
$$= (X_{TF} - A_{TF})^n + \frac{(X_{TF} + A_{TF})^n - (X_{TF} - A_{TF})^n}{2}$$
$$= \frac{(X_{TF} + A_{TF})^n + (X_{TF} - A_{TF})^n}{2}$$

$M(t)$

$$\approx k_M e^{-d_M t} \int \left[\overline{X_{TF}} + \overline{A_{TF}} \sin \frac{2\pi}{P_{TF}}(t-\theta_M) \right] e^{d_M t} dt + C_1 e^{-d_M t}$$

$$= e^{d_M t}$$

$$M(t)$$
$$\approx k_M e^{-d_M t}\int\left[\overline{X_{TF}}+\overline{A_{TF}}\sin\frac{2\pi}{P_{TF}}(t-\theta_M)\right]e^{d_M t}dt+C_1e^{-d_M t}.$$
$$=k_M e^{-d_M t}\left\{\overline{X_{TF}}\int e^{d_M t}dt+\overline{A_{TF}}\int\sin\left[\frac{2\pi}{P_{TF}}(t-\theta_M)\right]e^{d_M t}dt\right\}+C_1e^{-d_M t}$$

proven in earlier section that:

$$\int e^{d_M t}\sin\left[\frac{2\pi}{P_{TF}}(t-\theta_M)\right]dt=\frac{e^{d_M t}}{\sqrt{{d_M}^2+\left(\frac{2\pi}{P_{TF}}\right)^2}}\sin\left[\frac{2\pi}{P_{TF}}(t-\theta_M)+\alpha\right]+C$$

$$\text{where } \alpha=\tan^{-1}\left(\frac{2\pi}{P_{TF}d_M}\right)$$

$$\Rightarrow\frac{k_M\overline{X_{TF}}}{d_M}+k_Me^{-d_M t}\overline{A_{TF}}\left\{\frac{e^{d_M t}}{\sqrt{{d_M}^2+\left(\frac{2\pi}{P_{TF}}\right)^2}}\sin\left[\frac{2\pi}{P_{TF}}(t-\theta_M)+\alpha\right]\right\}+C_2k_Me^{-d_M t}+C_1e^{-d_M t}$$
$$=\frac{k_M\overline{X_{TF}}}{d_M}+\frac{k_M\overline{A_{TF}}}{\sqrt{{d_M}^2+\left(\frac{2\pi}{P_{TF}}\right)^2}}\sin\frac{2\pi}{P_{TF}}\left[(t-\theta_M)+\frac{P_{TF}}{2\pi}\alpha\right]+(C_1+C_2k_M)e^{-d_M t}$$

$$\text{where } \alpha=\tan^{-1}\left(\frac{2\pi}{P_{TF}d_M}\right)$$

Solve P(t).

$$P(t)$$
$$=k_Pe^{-d_P t}\int[M(t-\theta_P)]e^{d_P t}dt+C_3e^{-d_P t}$$
$$\approx k_Pe^{-d_P t}\int\left\{\frac{k_M\overline{X_{TF}}}{d_M}+\frac{k_M\overline{A_{TF}}}{\sqrt{{d_M}^2+\left(\frac{2\pi}{P_{TF}}\right)^2}}\sin\frac{2\pi}{P_{TF}}\left[(t-\theta_M-\theta_P)+\frac{P_{TF}}{2\pi}\alpha\right]+(C_1+C_2k_M)e^{-d_M t}\right\}e^{d_P t}dt+C_3e^{-d_P t}$$

since $\int e^{d_P t}\sin\left[\frac{2\pi}{P_{TF}}(t-\theta)\right]dt = \frac{e^{d_P t}}{\sqrt{{d_P}^2+\left(\frac{2\pi}{P_{TF}}\right)^2}}\sin\left[\frac{2\pi}{P_{TF}}(t-\theta)-\alpha\right]$,

where $\alpha = \tan^{-1}\left(\frac{2\pi}{P_{TF}d_P}\right)$

$$= \frac{k_P k_M \overline{X_{TF}}}{d_P d_M} + \frac{k_M \overline{A_{TF}}}{\sqrt{{d_M}^2+\left(\frac{2\pi}{P_{TF}}\right)^2}} \frac{k_P e^{-d_P t} e^{d_P t}}{\sqrt{{d_P}^2+\left(\frac{2\pi}{P_{TF}}\right)^2}} \sin\frac{2\pi}{P_{TF}}\left[(t-\theta_M-\theta_P)-\frac{P_{TF}}{2\pi}\alpha-\frac{P_{TF}}{2\pi}\alpha_P\right]$$

$$+\frac{k_P(C_1+C_2k_M)}{d_P-d_M}e^{-d_M(t-\theta_P)} + C_4 k_P e^{-d_P t} + C_3 e^{-d_P t}$$

$$= \frac{k_P k_M \overline{X_{TF}}}{d_P d_M} + \frac{k_P k_M \overline{A_{TF}}}{\sqrt{d_P^2+\left(\frac{2\pi}{P_{TF}}\right)^2}\sqrt{d_M^2+\left(\frac{2\pi}{P_{TF}}\right)^2}} \sin\frac{2\pi}{P_{TF}}\left(t-\theta_M-\theta_P-\frac{P_{TF}}{2\pi}\tan^{-1}\frac{2\pi}{d_M P_{TF}}-\frac{P_{TF}}{2\pi}\tan^{-1}\frac{2\pi}{d_P P_{TF}}\right)$$

$$+\frac{k_P(C_1+C_2k_M)}{d_P-d_M}e^{-d_M(t-\theta_P)} + (C_3+C_4k_P)e^{-d_P t}$$

7.3 Model M: Estimation of Trends

A. Oscillation mean of target gene

$$X_M = \frac{k_1}{d_M}\overline{X_{TF}} = \frac{k_1}{2d_M}\left[\left(X_{TF}+A_{TF}\right)^n + \left(X_{TF}-A_{TF}\right)^n\right]$$

$$\underline{X_M} = \frac{k_1}{d_M}X_{TF}^n$$

$$X_P = \frac{k_2}{d_P}X_M = \frac{k_1k_2}{2d_Md_P}\left[\left(X_{TF}+A_{TF}\right)^n + \left(X_{TF}-A_{TF}\right)^n\right]$$

$$\underline{X_P} = \frac{k_2}{d_P}\underline{X_M} = \frac{k_1k_2}{d_Md_P}X_{TF}^n$$

Effect of TF oscillation period, ($P_{TF} = 2\pi/w_{TF}$)
Same trend as Hill-type case.

Effect of stoichiometry of TF, *n*

$$\frac{\partial X_M}{\partial n} = \frac{k_1}{2d_M}\left[\left(X_{TF}+A_{TF}\right)^n \ln\left(X_{TF}+A_{TF}\right) + \left(X_{TF}-A_{TF}\right)^n \ln\left(X_{TF}-A_{TF}\right)\right]$$

$$\frac{\partial^2 X_M}{\partial n^2} = \frac{k_1}{2d_M}\left[\left(X_{TF}+A_{TF}\right)^n \ln^2\left(X_{TF}+A_{TF}\right) + \left(X_{TF}-A_{TF}\right)^n \ln^2\left(X_{TF}-A_{TF}\right)\right] > 0$$

When $n = 0$, $X_M = k_1 / d_M$.

$X_{TF} > 1 + A_{TF}$: $X_M \to \infty$ as $n \to \infty$, $\frac{\partial X_M}{\partial n} > 0$.

$X_{TF} < 1 - A_{TF}$: $X_M \to 0$ as $n \to \infty$, $\frac{\partial X_M}{\partial n} < 0$.

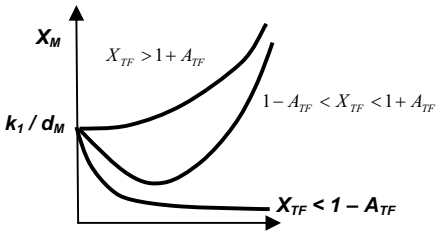

$1 - A_{TF} < X_{TF} < 1 + A_{TF}$:

As $n \to \infty$, $X_M \to \infty$, $\frac{\partial X_M}{\partial n} \to \infty$.

If $X_{TF} < \sqrt{1 + A_{TF}^2}$,

$$\frac{\partial X_M}{\partial n}\Big|_{n=0} < 0.$$

A minimum point exists at $n = \dfrac{\ln\left[-\dfrac{\ln\left(X_{TF}-A_{TF}\right)}{\ln\left(X_{TF}+A_{TF}\right)}\right]}{\ln\left(\dfrac{X_{TF}+A_{TF}}{X_{TF}-A_{TF}}\right)}$.

Note: $1 - A_{TF} < \sqrt{1 + A_{TF}^2} < 1 + A_{TF}$.

If $X_{TF} > \sqrt{1 + A_{TF}^2}$, $\frac{\partial X_M}{\partial n}|_{n=0} > 0$ and no minimum point exists.

$$\frac{\partial \underline{X_M}}{\partial n} = \frac{k_1}{d_M} X_{TF}^n \ln X_{TF}$$

$$\frac{\partial^2 \underline{X_M}}{\partial n^2} = \frac{k_1}{d_M} X_{TF}^n \ln^2 X_{TF} \geq 0$$

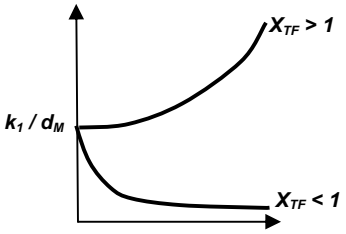

When $n = 0$, $\underline{X_M} = k_1 / d_M$.

If $X_{TF} > 1$, $\frac{\partial \underline{X_M}}{\partial n} > 0$, $\underline{X_M} \rightarrow \infty$ as $n \rightarrow \infty$.

If $X_{TF} < 1$, $\frac{\partial \underline{X_M}}{\partial n} < 0$, $\underline{X_M} \rightarrow 0$ as $n \rightarrow \infty$.

Effect of TF oscillation amplitude, $\underline{A_{TF}}$

$$\frac{\partial X_M}{\partial A_{TF}} = \frac{nk_1}{2d_M}\left[(X_{TF} + A_{TF})^{n-1} - (X_{TF} - A_{TF})^{n-1}\right] \geq 0$$

$$\frac{\partial^2 X_M}{\partial A_{TF}^2} = \frac{n(n-1)k_1}{2d_M}\left[(X_{TF} + A_{TF})^{n-2} + (X_{TF} - A_{TF})^{n-2}\right] \geq 0$$

When $A_{TF} = 0, X_M = \frac{k_1 X_{TF}^n}{d_M}, \frac{\partial X_M}{\partial A_{TF}} = 0$ (minimum point if $n > 1$).

When $A_{TF} \rightarrow X_{TF}, X_M = \frac{2^{n-1} k_1 X_{TF}^n}{d_M}, \frac{\partial X_M}{\partial A_{TF}} > 0$.

$n = 1$:

$$X_M = \frac{k_1 X_{TF}}{d_M}, \frac{\partial X_M}{\partial A_{TF}^*} = \frac{\partial^2 X_M}{\partial A_{TF}^{*\,2}} = 0.$$

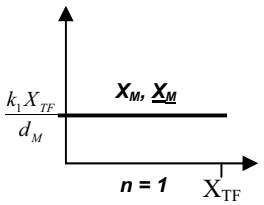

$$\underline{X_M} = \frac{k_1 X_{TF}}{d_M}$$

$Thus, X_M = \underline{X_M}$.

$n = 2$:

$$X_M = \frac{k_1}{d_M}\left(X_{TF}^2 + A_{TF}^2\right).$$

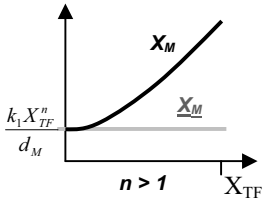

$$\underline{X_M} = \frac{k_1 X_{TF}^2}{d_M}$$

$Thus, X_M > \underline{X_M}$.

$n = 4$:

$$X_M = \frac{k_1}{d_M}\left(1 + 6A_{TF}^2 X_{TF}^2 + X_{TF}^4\right), \frac{\partial X_M}{\partial A_{TF}} > 0.$$

$$\underline{X_M} = \frac{k_1 X_{TF}^4}{d_M}$$

$$Thus, X_M > \underline{X_M}.$$

Effect of TF oscillation mean, $\underline{X_{TF}}$

$$\frac{\partial X_M}{\partial X_{TF}} = \frac{nk_1}{2d_M}\left[\left(X_{TF} + A_{TF}\right)^{n-1} + \left(X_{TF} - A_{TF}\right)^{n-1}\right] > 0$$

$$\frac{\partial^2 X_M}{\partial X_{TF}^2} = \frac{n(n-1)k_1}{2d_M}\left[\left(X_{TF} + A_{TF}\right)^{n-2} + \left(X_{TF} - A_{TF}\right)^{n-2}\right] \geq 0$$

When $X_{TF} \to 0, X_M \to 0.$

When $X_{TF} \to \infty, X_M \to \infty.$.

n = 1:

$$X_M = \underline{X_M} = \frac{k_1}{d_M} X_{TF}.$$

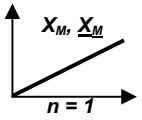

n > 1:

$$X_M = \frac{k_1}{2d_M}\left[\left(X_{TF} + A_{TF}\right)^n + \left(X_{TF} - A_{TF}\right)^n\right]$$

$$\underline{X_M} = \frac{k_1}{d_M} X_{TF}^n$$

$$Thus, X_M > \underline{X_M}.$$

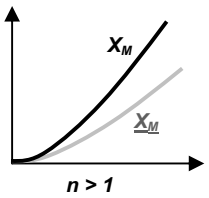

Effect of rates of transcription (k_1) and translation (k_2)
Same trend as Hill-type case.

Effect of degradation rates of mRNA (d_M) and protein (d_P)
Same trend as Hill-type case.

B. Oscillation amplitude of target gene

$$A_M = \frac{k_1}{\sqrt{d_M^2 + w_{TF}^2}} \overline{A_{TF}} = \frac{k_1}{2\sqrt{d_M^2 + w_{TF}^2}}\left[\left(X_{TF} + A_{TF}\right)^n - \left(X_{TF} - A_{TF}\right)^n\right]$$

$$A_P = \frac{k_2}{\sqrt{d_P^2 + w_{TF}^2}} A_M = \frac{k_1 k_2}{2\sqrt{d_M^2 + w_{TF}^2}\sqrt{d_P^2 + w_{TF}^2}}\left[\left(X_{TF} + A_{TF}\right)^n - \left(X_{TF} - A_{TF}\right)^n\right]$$

Effect of TF oscillation period, **($P_{TF} = 2\pi/w_{TF}$)**
Same trend as Hill-type case.

Effect of stoichiometry of TF, *n*

$$\frac{\partial A_M}{\partial n} = \frac{k_1}{2\sqrt{d_M^2 + w_{TF}^2}}\left[(X_{TF} + A_{TF})^n \ln(X_{TF} + A_{TF}) - (X_{TF} - A_{TF})^n \ln(X_{TF} - A_{TF})\right]$$

$$\frac{\partial^2 A_M}{\partial n^2} = \frac{k_1}{2\sqrt{d_M^2 + w_{TF}^2}}\left[(X_{TF} + A_{TF})^n \ln^2(X_{TF} + A_{TF}) - (X_{TF} - A_{TF})^n \ln^2(X_{TF} - A_{TF})\right]$$

When $n = 0$, $A_M = 0$, $\frac{\partial A_M}{\partial n}|_{n=0} > 0$.

$X_{TF} < 1 - A_{TF}$: When $n = 0$, $\frac{\partial^2 A_M}{\partial n^2}|_{n=0} < 0$.

As $n \rightarrow \infty$, $A_M \rightarrow 0$.

A stationary point exists at $n = \frac{\ln\left[\frac{\ln(X_{TF} - A_{TF})}{\ln(X_{TF} + A_{TF})}\right]}{\ln\left(\frac{X_{TF} + A_{TF}}{X_{TF} - A_{TF}}\right)}$.

$X_{TF} > 1 + A_{TF}$: $\frac{\partial A_M}{\partial n} > 0$, $\frac{\partial^2 A_M}{\partial n^2} > 0$.

$1 - A_{TF} < X_{TF} < 1 + A_{TF}$: As $n \rightarrow \infty$, $A_M \rightarrow \infty$.

When $n \rightarrow \infty$, $\frac{\partial A_M}{\partial n}, \frac{\partial^2 A_M}{\partial n^2} \rightarrow \infty$.

$\frac{\partial A_M}{\partial n} > 0$.

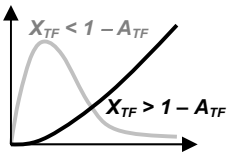

Effect of TF oscillation amplitude, A_{TF}

$$\frac{\partial A_M}{\partial A_{TF}} = \frac{nk_1}{2\sqrt{d_M^2 + w_{TF}^2}}\left[(X_{TF} + A_{TF})^{n-1} + (X_{TF} - A_{TF})^{n-1}\right] > 0$$

$$\frac{\partial^2 A_M}{\partial A_{TF}^2} = \frac{n(n-1)k_1}{2\sqrt{d_M^2 + w_{TF}^2}}\left[(X_{TF} + A_{TF})^{n-2} - (X_{TF} + A_{TF})^{n-2}\right] \geq 0$$

When $A_{TF} = 0$, $A_M = 0$.

When $A_{TF} \rightarrow X_{TF}$, $A_M \rightarrow \frac{2^{n-1} k_1 X_{TF}^n}{\sqrt{d_M^2 + w_{TF}^2}}$.

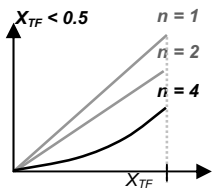

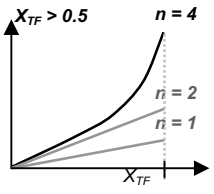

$n = 1, 2$: $\frac{\partial^2 A_M}{\partial A_{TF}^2} = 0$

$n = 4$: $\frac{\partial^2 A_M}{\partial A_{TF}^2} > 0$

Effect of TF oscillation mean, X_{TF}

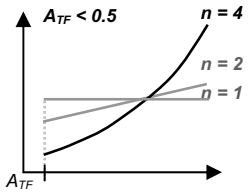

$$\frac{\partial A_M}{\partial X_{TF}} = \frac{nk_1}{2\sqrt{d_M^2 + w_{TF}^2}}\left[(X_{TF} + A_{TF})^{n-1} - (X_{TF} - A_{TF})^{n-1}\right] \geq 0$$

$$\frac{\partial^2 A_M}{\partial X_{TF}^2} = \frac{n(n-1)k_1}{2\sqrt{d_M^2 + w_{TF}^2}}\left[(X_{TF} + A_{TF})^{n-2} - (X_{TF} - A_{TF})^{n-2}\right] \geq 0$$

When $X_{TF} \rightarrow A_{TF}$, $A_M \rightarrow \frac{2^{n-1}k_1}{\sqrt{d_M^2 + w_{TF}^2}} A_{TF}^n$.

When $X_{TF} \rightarrow \infty$, $A_M \rightarrow \infty$.

$n = 1$: $A_M = \frac{k_1 A_{TF}}{\sqrt{d_M^2 + w_{TF}^2}}$. $\frac{\partial A_M}{\partial X_{TF}} = \frac{\partial^2 A_M}{\partial X_{TF}^2} = 0$.

$n = 2$: $A_M = \frac{2k_1 A_{TF}}{\sqrt{d_M^2 + w_{TF}^2}} X_{TF}$. $\frac{\partial A_M}{\partial X_{TF}} > 0, \frac{\partial^2 A_M}{\partial X_{TF}^2} = 0$.

$n > 2$: $\frac{\partial A_M}{\partial X_{TF}}, \frac{\partial^2 A_M}{\partial X_{TF}^2} > 0$.

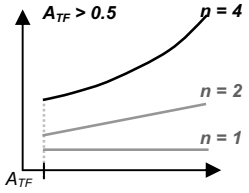

Effect of rates of transcription (k_1) and translation (k_2)
Same trend as Hill-type case.

Effect of degradation rates of mRNA (d_M) and protein (d_P)
Same trend as Hill-type case.

C. Normalized oscillation amplitude of target gene

$$A_M^* = \frac{d_M}{\sqrt{d_M^2 + w_{TF}^2}} \frac{\overline{A_{TF}}}{\overline{X_{TF}}} = \frac{d_M}{\sqrt{d_M^2 + w_{TF}^2}} \left[\frac{(X_{TF} + A_{TF})^n - (X_{TF} - A_{TF})^n}{(X_{TF} + A_{TF})^n + (X_{TF} - A_{TF})^n}\right]$$

$$A_P^* = \frac{d_M d_P}{\sqrt{d_M^2 + w_{TF}^2}\sqrt{d_P^2 + w_{TF}^2}} \left[\frac{(X_{TF} + A_{TF})^n - (X_{TF} - A_{TF})^n}{(X_{TF} + A_{TF})^n + (X_{TF} - A_{TF})^n}\right]$$

Note: as $\frac{(X_{TF}+A_{TF})^n-(X_{TF}-A_{TF})^n}{(X_{TF}+A_{TF})^n+(X_{TF}-A_{TF})^n} > \frac{(X_{TF}+A_{TF})^{n-1}-(X_{TF}-A_{TF})^{n-1}}{(X_{TF}+A_{TF})^{n-1}+(X_{TF}-A_{TF})^{n-1}}$, $A^*_{M,n} > A^*_{M,n-1}$.

Effect of TF oscillation period, ($P_{TF} = 2\pi/w_{TF}$)

Same trend as Hill-type case.

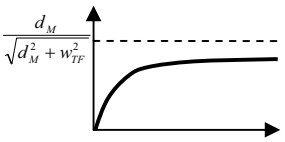

Effect of stoichiometry of TF, n

$$\frac{\partial A^*_M}{\partial n} = \frac{2d_M\left[\ln(1+A^*_{TF})-\ln(1-A^*_{TF})\right]}{\sqrt{d_M^2+w_{TF}^2}} \frac{(1-A^{*2}_{TF})^n}{\left[(1+A^*_{TF})^n+(1-A^*_{TF})^n\right]^2} > 0$$

$$\frac{\partial^2 A^*_M}{\partial n^2} = -\frac{2d_M\left[\ln(1+A^*_{TF})-\ln(1-A^*_{TF})\right]^2}{\sqrt{d_M^2+w_{TF}^2}} \frac{(1-A^{*2}_{TF})^n\left[(1+A^*_{TF})^n-(1-A^*_{TF})^n\right]}{\left[(1+A^*_{TF})^n+(1-A^*_{TF})^n\right]^3} < 0$$

When $n = 0$, $A^*_{AM} = 0$.

When $n \rightarrow \infty$, $A^*_M \rightarrow \frac{d_M}{\sqrt{d_M^2+w_{TF}^2}}$.

Effect of TF oscillation amplitude, A_{TF}

$$\frac{\partial A^*_M}{\partial A_{TF}} = \frac{4d_M n X_{TF}}{\sqrt{d_M^2+w_{TF}^2}} \frac{(X^2_{TF}-A^2_{TF})^{n-1}}{\left[(X_{TF}+A_{TF})^n+(X_{TF}-A_{TF})^n\right]^2} > 0$$

$$\frac{\partial^2 A^*_M}{\partial A^2_{TF}} = \frac{8d_M n X_{TF}(X^2_{TF}-A^2_{TF})^{n-2}}{\sqrt{d_M^2+w_{TF}^2}} \frac{(-nX_{TF}+A_{TF})(X_{TF}+A_{TF})^n+(nX_{TF}+A_{TF})(X_{TF}-A_{TF})^n}{\left[(X_{TF}+A_{TF})^n+(X_{TF}-A_{TF})^n\right]^3}$$

When $A_{TF} = 0$, $A^*_M = 0$, $\frac{\partial^2 A^*_M}{\partial A^{*2}_{TF}} = 0$.

When $A_{TF} \rightarrow X_{TF}$, $A^*_M \rightarrow \frac{d_M}{\sqrt{d_M^2+w_{TF}^2}}$.

$n = 1$: $\frac{\partial^2 A^*_M}{\partial A^{*2}_{TF}} = 0$

$n = 2$: $\frac{\partial^2 A^*_M}{\partial A^{*2}_{TF}} < 0$ as $A_{TF} \rightarrow X_{TF}$. No valid non-trivial point of inflexion exists.

$n > 2$: $\frac{\partial^2 A^*_M}{\partial A^2_{TF}} = 0$ as $A_{TF} \rightarrow X_{TF}$. No other valid non-trivial point of inflexion exists.

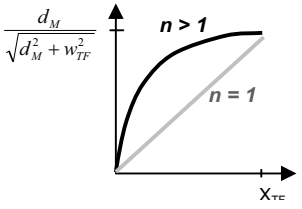

Effect of TF oscillation mean, X_{TF}

$$\frac{\partial A_M^*}{\partial X_{TF}} = -\frac{4d_M nA_{TF}}{\sqrt{d_M^2 + w_{TF}^2}} \frac{\left(X_{TF}^2 - A_{TF}^2\right)^{n-1}}{\left[\left(X_{TF} + A_{TF}\right)^n + \left(X_{TF} - A_{TF}\right)^n\right]^2} < 0$$

$$\frac{\partial^2 A_M^*}{\partial X_{TF}^2} = \frac{8d_M nA_{TF}\left(X_{TF}^2 - A_{TF}^2\right)^{n-2}}{\sqrt{d_M^2 + w_{TF}^2}} \frac{\left(X_{TF} - nA_{TF}\right)\left(X_{TF} + A_{TF}\right)^n + \left(X_{TF} + nA_{TF}\right)\left(X_{TF} - A_{TF}\right)^n}{\left[\left(X_{TF} + A_{TF}\right)^n + \left(X_{TF} - A_{TF}\right)^n\right]^3}$$

When $X_{TF} \rightarrow A_{TF}$, $A_M^* \rightarrow \frac{d_M}{\sqrt{d_M^2 + w_{TF}^2}}$.

When $X_{TF} \rightarrow \infty$, $A^*_M \rightarrow 0$.

$n = 1$: $\frac{\partial^2 A_M^*}{\partial X_{TF}^2} > 0$.

$n = 2$: $\frac{\partial^2 A_M^*}{\partial X_{TF}^2} < 0$ as $X_{TF} \rightarrow A_{TF}$.

$n > 2$: $\frac{\partial^2 A_M^*}{\partial X_{TF}^2} = 0$ as $X_{TF} \rightarrow A_{TF}$.

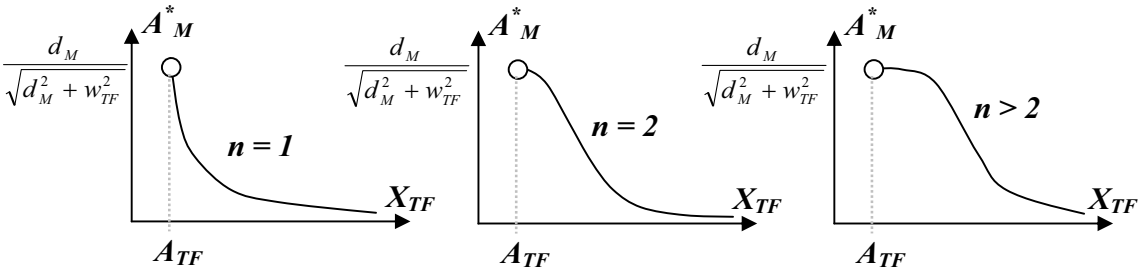

Effect of rates of transcription (k_1) and translation (k_2)
Same trend as Hill-type case.

Effect of degradation rates of mRNA (d_M) and protein (d_P)
Same trend as Hill-type case.

D. Oscillation period of target gene

Same trend as Hill-type case.

E. Time-delay of target gene

$$\theta_M = \theta_1 + \frac{1}{w_{TF}} \arctan \frac{w_{TF}}{d_M}$$

$$\theta_P = \theta_1 + \theta_2 + \frac{1}{w_{TF}} \left(\arctan \frac{w_{TF}}{d_M} + \arctan \frac{w_{TF}}{d_P} \right)$$

Same trend as Hill-type case.

7.4 Model H : Estimation of Trends

A. Oscillation mean of target gene

Oscillating T.A.:

$$X_m = \frac{k_1 - k_1 j_1^n \overline{X_a}}{k_4}$$

$$= \frac{k_1}{k_4} - \frac{k_1}{2k_4} \frac{2 + \left(\frac{X_a + A_a}{j_1}\right)^n + \left(\frac{X_a - A_a}{j_1}\right)^n}{\left[1 + \left(\frac{X_a + A_a}{j_1}\right)^n\right]\left[1 + \left(\frac{X_a - A_a}{j_1}\right)^n\right]}$$

$$= \frac{k_1}{k_4}\left\{1 - \frac{1}{2}\left[\frac{1}{1 + \left(\frac{X_a - A_a}{j_1}\right)^n} + \frac{1}{1 + \left(\frac{X_a + A_a}{j_1}\right)^n}\right]\right\}$$

and

$$X_p = \frac{k_2}{k_5} X_m$$

Non-oscillating T.A.:

$$\underline{X}_m = \frac{k_1}{k_4} \frac{X_a^n}{j_1^n + X_a^n}$$

and

$$\underline{X}_p = \frac{k_2}{k_5} \underline{X}_m$$

Effect of T.A. oscillation period, ($P_a = 2\pi/w_a$)
NA.

Effect of T.A. binding affinity to DNA enhancer site, j_1

$$\frac{\partial X_m}{\partial j_1} = -\frac{n j_1^{n-1} k_1}{2k_4}\left\{\frac{(X_a - A_a)^n}{\left[j_1^n + (X_a - A_a)^n\right]^2} + \frac{(X_a + A_a)^n}{\left[j_1^n + (X_a + A_a)^n\right]^2}\right\} < 0 \text{ for all } j_i.$$

$$\frac{\partial \underline{X}_m}{\partial j_1} = -\frac{n j_1^{n-1} k_1}{k_4}\left\{\frac{X_a^n}{\left(j_1^n + X_a^n\right)^2}\right\}$$

$$\frac{\partial^2 X_m}{\partial j_1^2} = -\frac{n j_1^{n-2} k_1}{2k_4}\left\{\frac{(n-1)(X_a - A_a)^n - (n+1)j_1^n}{\left[j_1^n + (X_a - A_a)^n\right]^3}(X_a - A_a)^n + \frac{(n-1)(X_a + A_a)^n - (n+1)j_1^n}{\left[j_1^n + (X_a + A_a)^n\right]^3}(X_a + A_a)^n\right\}$$

$$\frac{\partial^2 \underline{X}_m}{\partial j_1^2} = -\frac{n j_1^{n-2} k_1}{k_4}\left\{\frac{(n-1)X_a^n - (n+1)j_1^n}{\left(j_1^n + X_a^n\right)^3}X_a^n\right\}$$

Note: when $j_1 = 0$, $X_m = \underline{X}_m = k_1/k_4$, $X_p = \underline{X}_p = (k_2/k_5)X_m$; as $j_1 \rightarrow \infty$, X_m, X_p, $\underline{X}_m$, $\underline{X}_p \rightarrow 0$.

(independent on T.A. oscillations!)

$n = 1$: $\frac{\partial^2 X_m}{\partial j_1^2} > 0$; $\frac{\partial^2 \underline{X}_m}{\partial j_1^2} > 0$.

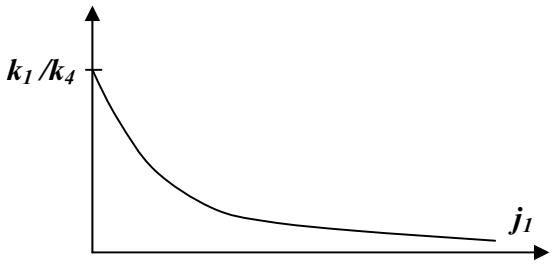

For $n > 1$, $\frac{\partial^2 X_m}{\partial j_1^2} < 0$ if $j_1 \le \left(\frac{n-1}{n+1}\right)^{1/n}(X_a - A_a)$; $\frac{\partial^2 X_m}{\partial j_1^2} > 0$ if $j_1 \ge \left(\frac{n-1}{n+1}\right)^{1/n}(X_a + A_a)$;

$\frac{\partial^2 X_m}{\partial j_1^2}$ can be positive, zero or negative if $\left(\frac{n-1}{n+1}\right)^{1/n}(X_a - A_a) < j_1 < \left(\frac{n-1}{n+1}\right)^{1/n}(X_a + A_a)$.

Matlab: 2 points of inflexion are observed.

For $n > 1$, $\frac{\partial^2 \underline{X}_m}{\partial j_1^2} < 0$ if $j_1 < \left(\frac{n-1}{n+1}\right)^{1/n} X_a$; $\frac{\partial^2 \underline{X}_m}{\partial j_1^2} > 0$ if $j_1 > \left(\frac{n-1}{n+1}\right)^{1/n} X_a$; $\frac{\partial^2 \underline{X}_m}{\partial j_1^2} = 0$

at $j_1 = \left(\frac{n-1}{n+1}\right)^{1/n} X_a$.

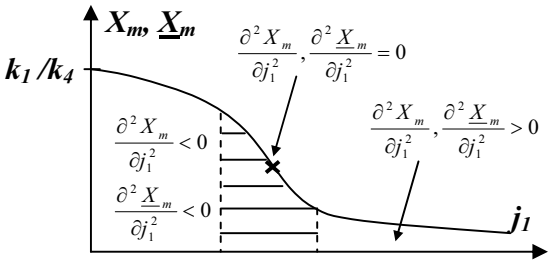

For $\left(\frac{n-1}{n+1}\right)^{1/n}(X_a - A_a) < j_1 < \left(\frac{n-1}{n+1}\right)^{1/n}(X_a + A_a)$ (shaded region), $\frac{\partial^2 X_m}{\partial j_1^2}$ increases from a negative to a positive value. Note: for the purpose of illustration, graphs of X_m and $\underline{X}_m$ are shown as identical curves. While the trends are qualitatively similar, their respective non-stationary points of inflexion do not necessarily occur at the same point.

Effect of binding cooperativity between T.F. and DNA enhancer site, *n*

When $n = 0$, $X_m = \underline{X}_m = 0.5(k_1/k_4)$. $\frac{\partial^2 X_M}{\partial n^2}|_{n=0} = 0$.

Note: $X_m = \frac{k_1}{k_4}\left[\frac{j_1^n\left(X_a + A_a\right)^n + j_1^n\left(X_a - A_a\right)^n + 2\left(X_a^2 - A_a^2\right)^n}{2j_1^{2n} + 2j_1^n\left(X_a + A_a\right)^n + 2j_1^n\left(X_a - A_a\right)^n + 2\left(X_a^2 - A_a^2\right)^n}\right] < \frac{k_1}{k_4}$

$$\frac{\partial X_m}{\partial n} = \frac{k_1}{2k_4}\left\{\frac{\left(\frac{X_a - A_a}{j_1}\right)^n}{\left[1+\left(\frac{X_a - A_a}{j_1}\right)^n\right]^2}\ln\left(\frac{X_a - A_a}{j_1}\right) + \frac{\left(\frac{X_a + A_a}{j_1}\right)^n}{\left[1+\left(\frac{X_a + A_a}{j_1}\right)^n\right]^2}\ln\left(\frac{X_a + A_a}{j_1}\right)\right\}$$

$$\frac{\partial^2 X_m}{\partial n^2} = \frac{k_1}{2k_4}\left\{\frac{\left(\frac{X_a - A_a}{j_1}\right)^n\left[\ln\left(\frac{X_a - A_a}{j_1}\right)\right]^2}{\left[1+\left(\frac{X_a - A_a}{j_1}\right)^n\right]^3}\left[1-\left(\frac{X_a - A_a}{j_1}\right)^n\right] + \frac{\left(\frac{X_a + A_a}{j_1}\right)^n\left[\ln\left(\frac{X_a + A_a}{j_1}\right)\right]^2}{\left[1+\left(\frac{X_a + A_a}{j_1}\right)^n\right]^3}\left[1-\left(\frac{X_a + A_a}{j_1}\right)^n\right]\right\}$$

Hence,

$\frac{\partial X_m}{\partial n}$ is always positive when $\ln\left(\frac{X_a - A_a}{j_1}\right) \geq 0$, i.e., $j_1 \leq X_a - A_a$. $\frac{\partial^2 X_m}{\partial n^2} < 0$.

$\frac{\partial X_m}{\partial n}$ is always negative when $\ln\left(\frac{X_a + A_a}{j_1}\right) \leq 0$, i.e., $j_1 \geq X_a + A_a$. $\frac{\partial^2 X_m}{\partial n^2} > 0$.

$\frac{\partial X_m}{\partial n}$, $\frac{\partial^2 X_m}{\partial n^2}$ can be zero, positive or negative when $\ln\left(\frac{X_a - A_a}{j_1}\right)$ and $\ln\left(\frac{X_a + A_a}{j_1}\right)$ have opposite signs, i.e., $X_a - A_a < j_1 < X_a + A_a$.

$j_1 \leq X_a - A_a$: $\frac{\partial X_m}{\partial n} > 0$, $\frac{\partial^2 X_m}{\partial n^2} < 0$. Note: when $j_1 = X_a - A_a$, as $n \rightarrow \infty$, $X_m \rightarrow 0.75(k_1/k_4)$; when $j_1 < X_a - A_a$, as $n \rightarrow \infty$, $X_m \rightarrow k_1/k_4$.

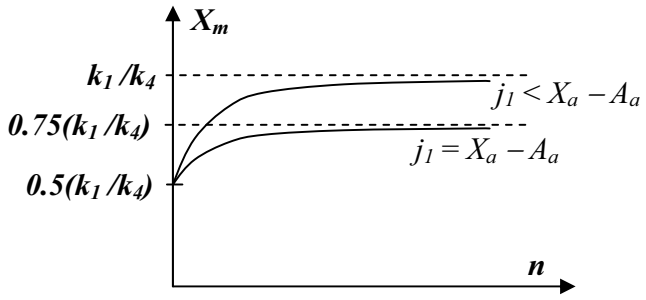

$X_a - A_a < j_1 < X_a + A_a$: as $n \rightarrow \infty$, $X_m \rightarrow 0.5(k_1/k_4)$. $\frac{\partial X_m}{\partial n}$, $\frac{\partial^2 X_m}{\partial n^2}$ can be zero, positive or negative.

$\frac{\partial X_M}{\partial n}|_{n=0} > 0$ if $j_1 < \sqrt{(X_{TF} - A_{TF})(X_{TF} + A_{TF})}$.

$\frac{\partial X_M}{\partial n}|_{n=0} < 0$ if $j_1 > \sqrt{(X_{TF} - A_{TF})(X_{TF} + A_{TF})}$.

Note: $X_{TF} - A_{TF} < \sqrt{(X_{TF} - A_{TF})(X_{TF} + A_{TF})} < X_{TF} + A_{TF}$ is always true.

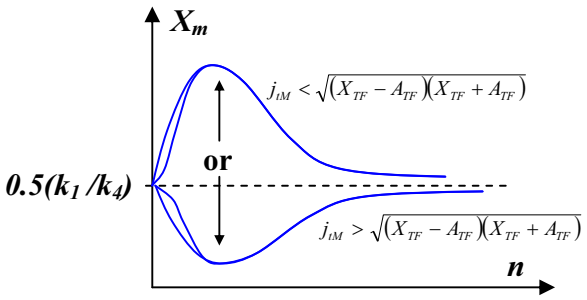

$j_1 \geq X_a + A_a$: $\frac{\partial X_m}{\partial n} < 0$, $\frac{\partial^2 X_m}{\partial n^2} > 0$. Note: when $j_1 = X_a + A_a$, as $n \rightarrow \infty$, $X_m \rightarrow 0.25(k_1/k_4)$; when $j_1 > X_a + A_a$, as $n \rightarrow \infty$, $X_m \rightarrow 0$.

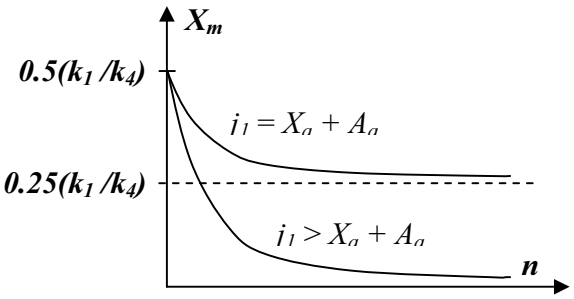

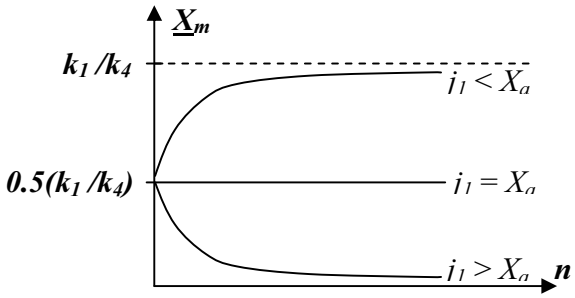

$\underline{X}_m < \frac{k_1}{k_4} \cdot \frac{\partial^2 \underline{X}_M}{\partial n^2}|_{n=0} = 0$.

$$\frac{\partial \underline{X}_m}{\partial n} = \frac{k_1}{k_4}\left\{\frac{\left(\frac{X_a}{j_1}\right)^n}{\left[1+\left(\frac{X_a}{j_1}\right)^n\right]^2}\ln\left(\frac{X_a}{j_1}\right)\right\}$$

$$\frac{\partial^2 \underline{X}_m}{\partial n^2} = \frac{k_1}{k_4}\left\{\frac{\left(\frac{X_a}{j_1}\right)^n\left[\ln\left(\frac{X_a}{j_1}\right)\right]^2}{\left[1+\left(\frac{X_a}{j_1}\right)^n\right]^3}\left[1-\left(\frac{X_a}{j_1}\right)^n\right]\right\}$$

Hence,

$j_1 < X_a$: $\frac{\partial \underline{X}_m}{\partial n} > 0$, $\frac{\partial^2 \underline{X}_m}{\partial n^2} < 0$; as $n \rightarrow \infty$, $X_m \rightarrow k_1/k_4$.

$j_1 = X_a$: $\frac{\partial \underline{X}_m}{\partial n} = \frac{\partial^2 \underline{X}_m}{\partial n^2} = 0$; as $n \rightarrow \infty$, $X_m \rightarrow 0.5(k_1/k_4)$.

$j_1 > X_a$: $\frac{\partial \underline{X}_m}{\partial n} < 0$, $\frac{\partial^2 \underline{X}_m}{\partial n^2} > 0$; as $n \rightarrow \infty$, $X_m \rightarrow 0$.

Effect of T.A. oscillation amplitude, A_a

$$X_m = \frac{k_1}{k_4} - \frac{k_1 j_1^n}{2k_4}\left[\frac{1}{j_1^n + (X_a - A_a)^n} + \frac{1}{j_1^n + (X_a + A_a)^n}\right]$$

$$\frac{\partial X_m}{\partial A_a} = -\frac{nk_1 j_1^n}{2k_4}\left\{\frac{(X_a - A_a)^{n-1}}{\left[j_1^n + (X_a - A_a)^n\right]^2} - \frac{(X_a + A_a)^{n-1}}{\left[j_1^n + (X_a + A_a)^n\right]^2}\right\}$$

$$\frac{\partial^2 X_m}{\partial A_a^2} = -\frac{nk_1 j_1^n}{2k_4}\left\{\frac{(X_a - A_a)^{n-2}\left[(n+1)(X_a - A_a)^n - (n-1)j_1^n\right]}{\left[j_1^n + (X_a - A_a)^n\right]^3} + \frac{(X_a + A_a)^{n-2}\left[(n+1)(X_a + A_a)^n - (n-1)j_1^n\right]}{\left[j_1^n + (X_a + A_a)^n\right]^3}\right\}$$

Note:

$\underline{X}_m = \frac{k_1 X_a^n}{k_4\left(j_1^n + X_a^n\right)}$, i.e., $\frac{\partial \underline{X}_m}{\partial A_a} = \frac{\partial^2 \underline{X}_m}{\partial A_a^2} = 0$.

When $A_a = 0$, $X_m = \frac{k_1 X_a^n}{k_4\left(j_1^n + X_a^n\right)}$; when $A_a \rightarrow X_a$, $X_m \rightarrow \frac{2^{n-1} k_1 X_a^n}{k_4\left(j_1^n + 2^n X_a^n\right)}$.

For turning points of A_a, $\frac{\partial X_m}{\partial A_a} = 0$, i.e.,

$$\left(X_a^2 - A_a^2\right)^{n-1}\left\{\left[(X_a + A_a)^{n+1} - (X_a - A_a)^{n+1}\right] + 4A_a j_1^n\right\} - j_1^{2n}\left[(X_a + A_a)^{n-1} - (X_a - A_a)^{n-1}\right] = 0.$$

By inspection, $A_a = 0$ is a turning point. For $0 < n \le 1$, $A_a = 0$ is a maximum point ($\frac{\partial^2 X_m}{\partial A_a^2} < 0$).

$n = 1$: $\frac{\partial X_m}{\partial A_a} < 0$. When $A_a = 0$, $X_m = \frac{k_1 X_a}{k_4(j_1 + X_a)}$; when $A_a \rightarrow X_a$, $X_m \rightarrow \frac{k_1 X_a}{k_4(j_1 + 2X_a)}$.

$\underline{X}_m = \frac{k_1 X_a}{k_4(j_1 + X_a)}$. X_M never intersect $\underline{X}_M$ at a non-trivial point. $\frac{\partial^2 X_M}{\partial A_a^2} < 0$.

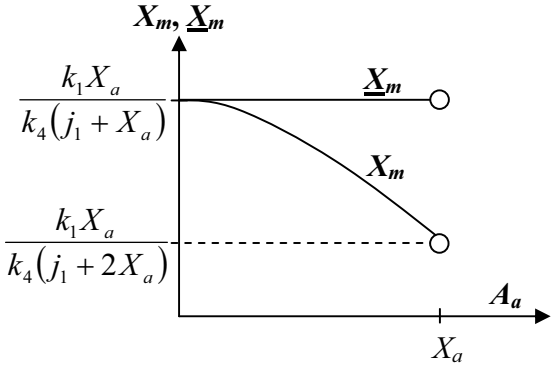

$n = 2$: turning points are $A_a = 0$ and solutions of $A_a^4 + 2(j_1^2 + X_a^2)A_a^2 + (j_1^2 - 3X_a^2)(j_1^2 + X_a^2) = 0$. For a valid solution (i.e., $0 \le A_a < X_a$), $j_1^2 < 3X_a^2$ which gives $A_a = (j_1^2 + X_a^2)^{1/4}\sqrt{2X_1 - \sqrt{j_1^2 + X_a^2}}$ (minimum); $A_a = 0$ is a maximum point. However, if $j_1^2 \ge 3X_a^2$, only one turning point exists at $A_a = 0$ (minimum).

When $A_a = 0$, $X_m = \frac{k_1 X_a^2}{k_4(j_1^2 + X_a^2)}$; when $A_a \rightarrow X_a$, $X_m \rightarrow \frac{2k_1 X_a^2}{k_4(j_1^2 + 4X_a^2)}$ and $\frac{\partial X_m}{\partial A_a} > 0$.

Note: $\frac{2k_1 X_a^2}{k_4(j_1^2 + 4X_a^2)} \ge \frac{k_1 X_a^2}{k_4(j_1^2 + X_a^2)}$ if $j_1^2 \ge 2X_a^2$. $\underline{X}_m = \frac{k_1 X_a^2}{k_4(j_1^2 + X_a^2)}$.

X_M intersects $\underline{X}_M$ at $A_a^2 = 3X_a^2 - j_1^2$. $\frac{\partial^2 X_M}{\partial A_a^2}|_{A_a \rightarrow X_a} > 0$.

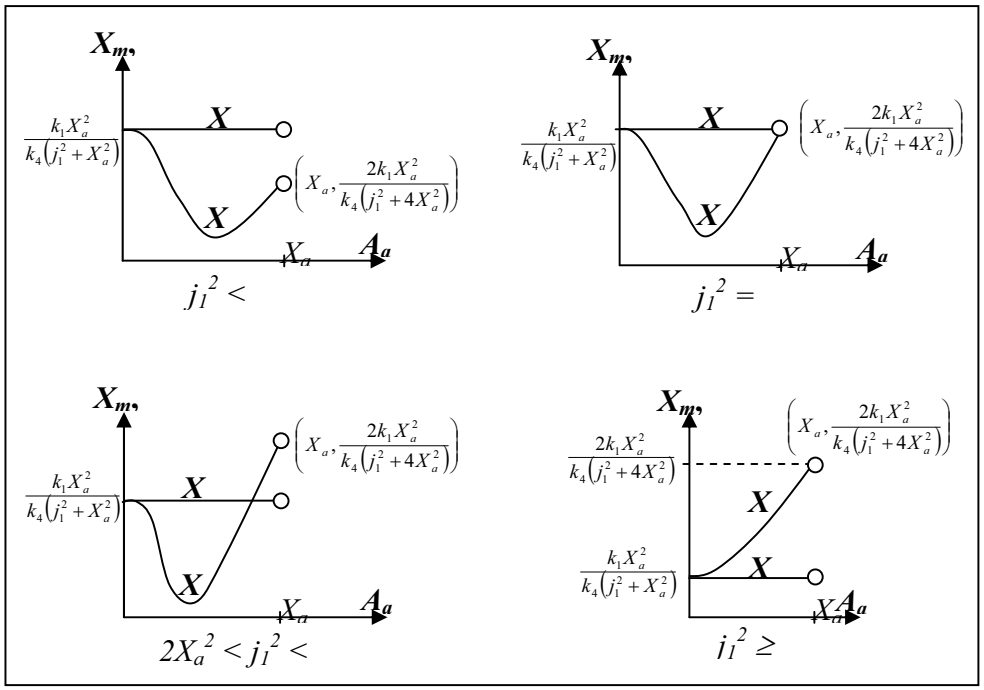

n = 3: When $A_{TF} = 0$, $X_M = \underline{X_M} = \frac{k_{tM}}{d_M}\frac{X_{TF}^3}{j_1^3 + X_{TF}^3}$.

When $A_{TF} \rightarrow X_{TF}$, $X_M \rightarrow \frac{k_{tM}}{d_M}\frac{4X_{TF}^3}{j_1^3 + 8X_{TF}^3}$, $\frac{\partial X_M}{\partial A_{TF}}|_{A_{TF}\rightarrow X_{TF}} > 0$.

Note: $\frac{k_{tM}}{d_M}\frac{4X_{TF}^3}{j_1^3 + 8X_{TF}^3} \geq \frac{k_{tM}}{d_M}\frac{X_{TF}^3}{j_1^3 + X_{TF}^3}$ if $j_1^3 \geq {}^4/_3 X_{TF}^3$.

Turning points:

$A_{TF} = 0$;

$\left(X_{TF}^4 - 2X_{TF}^2A_{TF}^2 + A_{TF}^4\right)\left\{2X_{TF}A_{TF}^2 + 2X_{TF}^3 + j_1^3\right\} - j_1^6X_{TF} = 0$

$2X_{TF}A_{TF}^6 + \left(j_1^3 - 2X_{TF}^3\right)A_{TF}^4 - 2X_{TF}^2\left(j_1^3 + X_{TF}^3\right)A_{TF}^2 - X_{TF}\left(j_1^3 + X_{TF}^3\right)\left(j_1^3 - 2X_{TF}^3\right) = 0$

Hurwitz determinants: $\{1, +(j_1^3 > 2X_{TF}^3) / -(j_1^3 < 2X_{TF}^3), 0\}$ and $\{1, 0\}$.

If $j_1^3 < 2X_{TF}^3$,

$\frac{\partial^2 X_M}{\partial A_{TF}^2}|_{A_{TF}=0} < 0$. Thus, $A_{TF} = 0$ is a maximum point.

If $j_1^3 > 2X_{TF}^3$,

$\frac{\partial^2 X_M}{\partial A_{TF}^2}|_{A_{TF}=0} > 0$. Thus, $A_{TF} = 0$ is a minimum point.

X_M intersects $\underline{X_M}$ at $A_{TF}^2 = \frac{3X_{TF}^2 - \sqrt{12 j_1^3 X_{TF} - 15X_{TF}^4}}{2}$ for $^4/_3 X_{TF}^3 < j_1^3 < 2X_{TF}^3$.

$\frac{\partial X_M}{\partial A_{TF}}|_{A_{TF}\to X_{TF}} > 0$. $\frac{\partial^2 X_M}{\partial A_{TF}^2}|_{A_{TF}\to X_{TF}} > 0$ if $j_1^3 > 16X_{TF}^3$ and $\frac{\partial^2 X_M}{\partial A_{TF}^2}|_{A_{TF}\to X_{TF}} < 0$ if $j_1^3 < 16X_{TF}^3$.

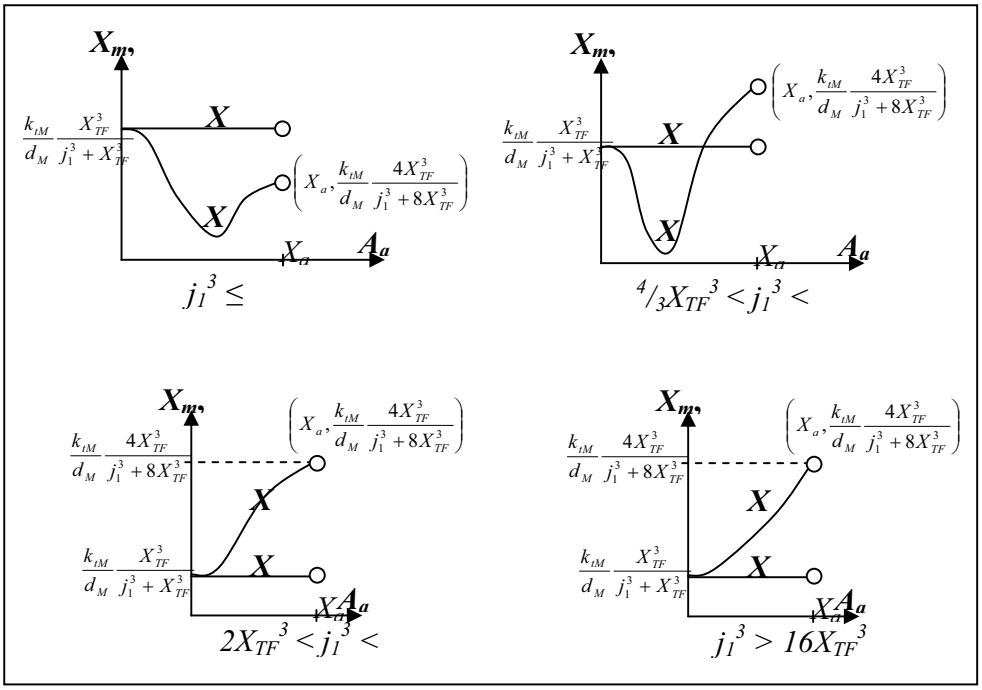

$n = 4$: turning points are $A_a = 0$ and solutions of $A_a^{10} + 7X_a^2 A_a^8 - 2\left(11X_a^4 - j_1^4\right)A_a^6 + 2X_a^2\left(7X_a^4 - 3j_1^4\right)A_a^4 + \left(5X_a^6 + 6X_a^4 j_1^4 + j_1^8\right)A_a^2 + \left(3X_a^2 j_1^8 - 2X_a^6 j_1^4 - 5X_a^{10}\right) = 0$. The maximum possible number of real and positive values of A_a that satisfy the latter expression is determined using Routh-Hurwitz determinants (refer to *Supplemental Data*). The maximum number of positive turning points is bifurcated at $j_1^4 = {}^5/_3 X_a^4$, i.e., four turning points if $j_1^4 < {}^5/_3 X_a^4$ and three turning points if $j_1^4 > {}^5/_3 X_a^4$. However, because of the complexity of the algebraic expression, the condition $A_a < X_a$ can be checked only when numerical values of X_a and j_1 are supplied. Nevertheless, the results show that as n is increased, dynamics of gene transcription exhibits rich behaviors.

When $A_a = 0$, $X_m = \dfrac{k_1 X_a^4}{k_4\left(j_1^4 + X_a^4\right)}$; when $A_a \rightarrow X_a$, $X_m \rightarrow \dfrac{8k_1 X_a^4}{k_4\left(j_1^4 + 16X_a^4\right)}$ and $\dfrac{\partial X_m}{\partial A_a} > 0$.

Note: $\dfrac{8k_1 X_a^4}{k_4\left(j_1^4 + 16X_a^4\right)} \geq \dfrac{k_1 X_a^4}{k_4\left(j_1^4 + X_a^4\right)}$ if $j_1^4 \geq {}^8/_7 X_a^4$. $\underline{X}_m = \dfrac{k_1 X_a^4}{k_4\left(j_1^4 + X_a^4\right)}$.

X_M can intersect $\underline{X}_M$ at 2 to 3 positive non-trivial points given by $A_{TF}^6 - 4X_{TF}^2 A_{TF}^4 + \left(j_1^4 + 5X_{TF}^4\right)A_{TF}^2 + 6j_1^4 X_{TF}^2 - 10X_{TF}^6 = 0$; **2 positive roots if $j_1^4 > {}^1/_3 X_{TF}^4$ whereas 3 positive roots if $j_1^4 < {}^1/_3 X_{TF}^4$**. However, the validity of these points can only be checked when numerical values are supplied.

$\dfrac{\partial^2 X_M}{\partial A_{TR}^2}\Big|_{A_{TR}\rightarrow X_{TR}} > 0$ if $j_1^4 > {}^{80}/_3 X_a^4$ and $\dfrac{\partial^2 X_M}{\partial A_{TR}^2}\Big|_{A_{TR}\rightarrow X_{TR}} < 0$ if $j_1^4 < {}^{80}/_3 X_a^4$.

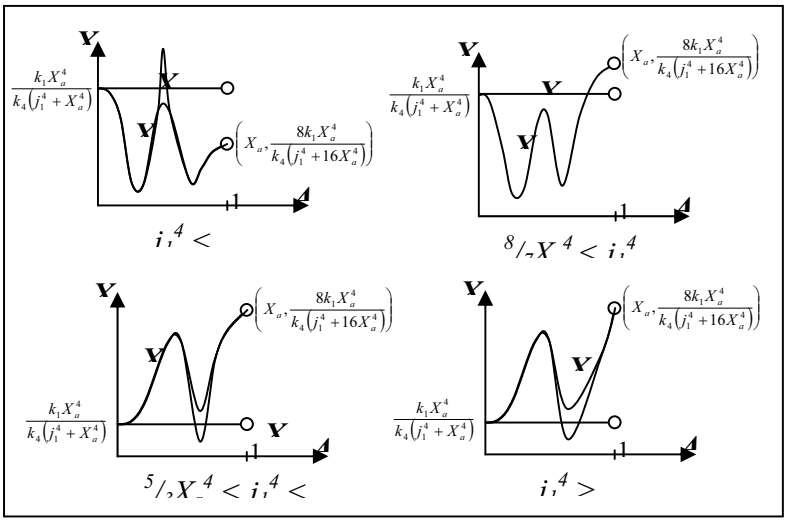

Maple: did not obtain > 1 valid turning points; at most 1 valid turning point is obtained.

Matlab: at most 1 valid turning point is observed.

Effect of T.A. oscillation mean, $\underline{X_a}$

$$\frac{\partial X_m}{\partial X_a} = \frac{nk_1 j_1^n}{2k_4}\left\{\frac{\left(X_a - A_a\right)^{n-1}}{\left[j_1^n + \left(X_a - A_a\right)^n\right]^2} + \frac{\left(X_a + A_a\right)^{n-1}}{\left[j_1^n + \left(X_a + A_a\right)^n\right]^2}\right\} > 0$$

$$\frac{\partial^2 X_m}{\partial X_a^2} = \frac{nk_1 j_1^n}{2k_4}\left\{\frac{\left(X_a - A_a\right)^{n-2}\left[(n-1)j_1^n - (n+1)\left(X_a - A_a\right)^n\right]}{\left[j_1^n + \left(X_a - A_a\right)^n\right]^3} + \frac{\left(X_a + A_a\right)^{n-2}\left[(n-1)j_1^n - (n+1)\left(X_a + A_a\right)^n\right]}{\left[j_1^n + \left(X_a + A_a\right)^n\right]^3}\right\}$$

As $X_a \rightarrow A_a$, $X_m \rightarrow \frac{k_1}{k_4}\frac{2^{n-1}A_a^n}{j_1^n + 2^n A_a^n}$; as $X_a \rightarrow \infty$, $X_m \rightarrow k_1/k_4$ (note: independent on T.A. oscillation!)

$$\frac{\partial \underline{X}_m}{\partial X_a} = \frac{nk_1 j_1^n X_a^{n-1}}{k_4}\left\{\frac{1}{\left(j_1^n + X_a^n\right)^2}\right\} > 0$$

$$\frac{\partial^2 \underline{X}_m}{\partial X_a^2} = \frac{nk_1 j_1^n X_a^{n-2}}{k_4}\left\{\frac{\left[(n-1)j_1^n - (n+1)X_a^n\right]}{\left(j_1^n + X_a^n\right)^3}\right\}$$

As $X_a \rightarrow 0$, $\underline{X}_m \rightarrow 0$; as $X_a \rightarrow \infty$, $\underline{X}_m \rightarrow k_1/k_4$.

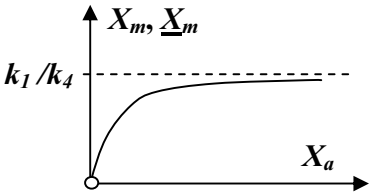

$n = 1$: $\frac{\partial^2 X_m}{\partial X_a^2} < 0$ and $\frac{\partial^2 \underline{X}_m}{\partial X_a^2} < 0$ for n ≤ 1.

For $n > 1$:

$$\frac{\partial^2 X_m}{\partial X_a^2} > 0 \text{ if } X_{TF} \le \left(\frac{n-1}{n+1}\right)^{1/n} j_1 - A_{TF};$$

$$\frac{\partial^2 X_m}{\partial X_a^2} < 0 \text{ if } X_{TF} \ge \left(\frac{n-1}{n+1}\right)^{1/n} j_1 + A_{TF};$$

$\frac{\partial^2 X_m}{\partial X_a^2}$ can be positive, zero or negative for $\left(\frac{n-1}{n+1}\right)^{1/n} j_1 - A_{TF} < X_{TF} < \left(\frac{n-1}{n+1}\right)^{1/n} j_1 + A_{TF}$.

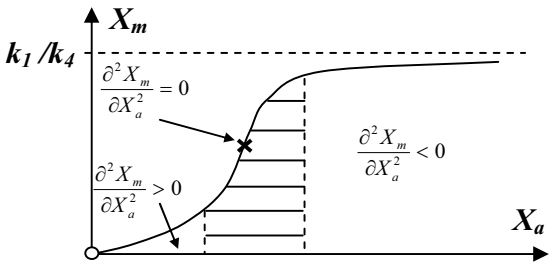

For $\left(\frac{n-1}{n+1}\right)^{1/n} j_1 - A_{TF} < X_{TF} < \left(\frac{n-1}{n+1}\right)^{1/n} j_1 + A_{TF}$ (shaded region), $\frac{\partial^2 X_m}{\partial X_a^2}$ decreases from a positive to a negative value. Note: for the purpose of illustration, graphs of X_m and $\underline{X}_m$ are shown as identical curves. While the trends are qualitatively similar, their respective non-stationary points of inflexion do not necessarily occur at the same point.

$X_{TF} = 0$ is a minimum point;

$$\frac{\partial^2 \underline{X}_m}{\partial X_a^2} > 0 \text{ if } X_a < \left(\frac{n-1}{n+1}\right)^{1/n} j_1;$$

$$\frac{\partial^2 \underline{X}_m}{\partial X_a^2} < 0 \text{ if } X_a > \left(\frac{n-1}{n+1}\right)^{1/n} j_1;$$

$$\frac{\partial^2 \underline{X}_m}{\partial X_a^2} = 0 \text{ if } X_a = \left(\frac{n-1}{n+1}\right)^{1/n} j_1.$$

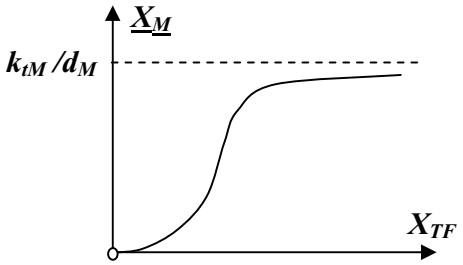

Effect of rates of transcription (k_1) and translation (k_2)

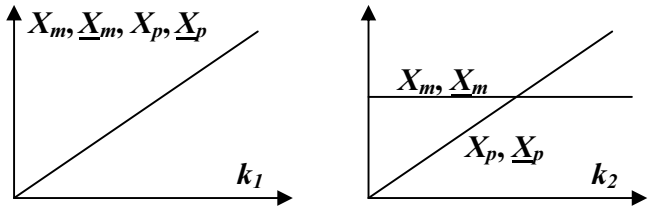

Effect of degradation rates of mRNA (k_4) and protein (k_5)

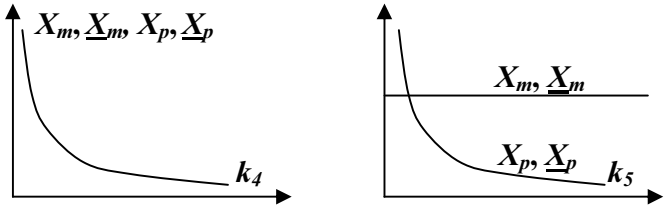

B. Oscillation amplitude of target gene

$$A_m = \frac{k_1 j_1^n \overline{A_a}}{\sqrt{k_4^2 + w_a^2}}$$

$$= \frac{k_1}{2\sqrt{k_4^2 + w_a^2}} \frac{\left(\frac{X_a + A_a}{j_1}\right)^n - \left(\frac{X_a - A_a}{j_1}\right)^n}{\left[1 + \left(\frac{X_a + A_a}{j_1}\right)^n\right]\left[1 + \left(\frac{X_a - A_a}{j_1}\right)^n\right]}$$

$$= \frac{k_1}{2\sqrt{k_4^2 + w_a^2}} \left[\frac{1}{\left[1 + \left(\frac{X_a - A_a}{j_1}\right)^n\right]} - \frac{1}{\left[1 + \left(\frac{X_a + A_a}{j_1}\right)^n\right]}\right]$$

and

$$A_p = \frac{k_2}{\sqrt{k_5^2 + w_a^2}} A_m$$

Effect of T.A. oscillation period, ($P_a = 2\pi/w_a$)

$$A_m = \frac{k_1 j_1^n \overline{A_a}}{\sqrt{k_4^2 + \frac{4\pi^2}{P_a^2}}}$$

$$\frac{\partial A_m}{\partial P_a} = \frac{4\pi^2 k_1 j_1^n \overline{A_a}}{\left(4\pi^2 + k_4^2 P_a^2\right)^{3/2}} > 0$$

$$\frac{\partial^2 A_m}{\partial P_a^2} = -\frac{12\pi^2 k_1 k_4^2 j_1^n P_a \overline{A_a}}{\left(4\pi^2 + k_4^2 P_a^2\right)^{5/2}} < 0$$

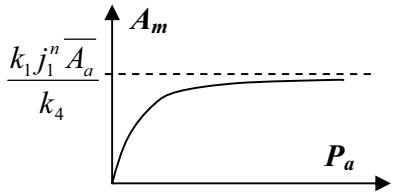

When $P_a \rightarrow 0$, $A_m \rightarrow 0$; when $P_a \rightarrow \infty$, $A_m \rightarrow \frac{k_1 j_1^n \overline{A_a}}{k_4}$.

$$A_p = \frac{k_1 k_2 j_1^n \overline{A_a}}{\sqrt{\left(k_4^2 + \frac{4\pi^2}{P_a^2}\right)\left(k_5^2 + \frac{4\pi^2}{P_a^2}\right)}}$$

$$\frac{\partial A_p}{\partial P_a} = \frac{4\pi^2 k_1 k_2 j_1^n \overline{A_a}\left(k_4^2 + k_5^2 + \frac{8\pi^2}{P_a^2}\right)}{P_a^3\left(k_4^2 + \frac{4\pi^2}{P_a^2}\right)^{3/2}\left(k_5^2 + \frac{4\pi^2}{P_a^2}\right)^{3/2}} > 0$$

$$\frac{\partial^2 A_p}{\partial P_a^2} = -\frac{8\pi^3 k_1 k_2 j_1^n \overline{A_a}\left[\frac{32\pi^2}{P_a^2}\left(k_4^2 + k_5^2 + \frac{4\pi^2}{P_a^2}\right) + \left(3k_4^4 + 3k_5^4 + 2k_4^2 k_5^2\right)\right]}{P_a^4\left(k_4^2 + \frac{4\pi^2}{P_a^2}\right)^{5/2}\left(k_5^2 + \frac{4\pi^2}{P_a^2}\right)^{5/2}} < 0$$

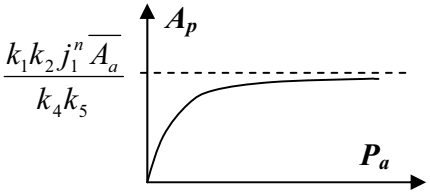

When $P_a \rightarrow 0$, $A_p \rightarrow 0$; when $P_a \rightarrow \infty$, $A_p \rightarrow \frac{k_1 k_2 j_1^n \overline{A_a}}{k_4 k_5}$.

Effect of T.A. binding affinity to DNA enhancer site, j_1

$$\frac{\partial A_m}{\partial j_1} = \frac{n j_1^{n-1} k_1}{2\sqrt{k_4^2 + w_a^2}} \left\{ \frac{(X_a - A_a)^n}{\left[j_1^n + (X_a - A_a)^n \right]^2} - \frac{(X_a + A_a)^n}{\left[j_1^n + (X_a + A_a)^n \right]^2} \right\}$$

$$\frac{\partial^2 A_m}{\partial j_1^2} = \frac{n j_1^{n-2} k_1}{2\sqrt{k_4^2 + w_a^2}} \left\{ \frac{(n-1)(X_a - A_a)^n - (n+1) j_1^n}{\left[j_1^n + (X_a - A_a)^n \right]^3} (X_a - A_a)^n - \frac{(n-1)(X_a + A_a)^n - (n+1) j_1^n}{\left[j_1^n + (X_a + A_a)^n \right]^3} (X_a + A_a)^n \right\}$$ When n

$$j_1^{\max imum} = \sqrt{(X_a + A_a)(X_a - A_a)}$$

$$A_m^{\max imum} = \frac{k_1}{2\sqrt{k_4^2 + w_a^2}} \left[\frac{(X_a + A_a)^{n/2} - (X_a - A_a)^{n/2}}{(X_a + A_a)^{n/2} + (X_a - A_a)^{n/2}} \right]$$

$= 1$: $\frac{\partial A_M}{\partial j_1}|_{j_r=0} > 0;\ \frac{\partial^2 A_M}{\partial j_1^2}|_{j_r=0} < 0.$

When $n = 2$: $\frac{\partial A_M}{\partial j_1}|_{j_r=0} = 0;\ \frac{\partial^2 A_M}{\partial j_1^2}|_{j_r=0} > 0$ (minimum point).

When $n > 2$: $\frac{\partial A_M}{\partial j_1}|_{j_r=0} = 0;\ \frac{\partial^2 A_M}{\partial j_1^2}|_{j_r=0} = 0$ (stationary point of inflexion).

The expressions of mRNA maximum amplitudes for n = 1, 2, 4 and 8 are obtained:

$$A_{m,n=1}^{\max imum} = \frac{k_1}{\sqrt{k_4^2 + w_a^2}} \left[\frac{X_a - \sqrt{X_a^2 - A_a^2}}{2A_a} \right]$$

$$A_{m,n=2}^{\max imum} = \frac{k_1}{\sqrt{k_4^2 + w_a^2}} \left[\frac{A_a}{2X_a} \right]$$

$$A_{m,n=4}^{\max imum} = \frac{k_1}{\sqrt{k_4^2 + w_a^2}} \left[\frac{A_a X_a}{X_a^2 + A_a^2} \right]$$

$$A_{m,n=8}^{\max imum} = \frac{k_1}{\sqrt{k_4^2 + w_a^2}} \left[\frac{2A_a X_a (X_a^2 + A_a^2)}{(X_a^2 + A_a^2)^2 + 4A_a^2 X_a^2} \right]$$

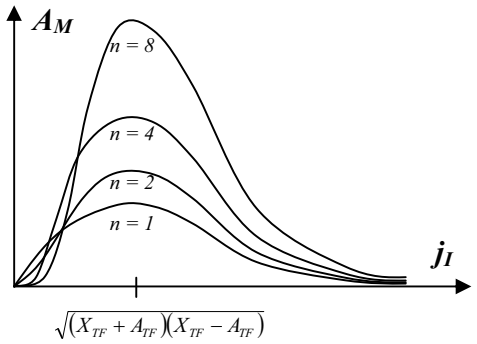

mRNA maximum amplitudes increase as n increases.
Proof:

$$A_{m,n=2}^{\max imum} - A_{m,n=1}^{\max imum} = \frac{\sqrt{X_a^2 - A_a^2}\left(\sqrt{X_a^2} - \sqrt{X_a^2 - A_a^2}\right)}{2A_a X_a} > 0$$

$$A_{m,n=4}^{\max imum} - A_{m,n=2}^{\max imum} = \frac{k_1 A_a (X_a^2 - A_a^2)}{2\sqrt{k_4^2 + w_a^2} X_a (X_a^2 + A_a^2)} > 0$$

$$A_{m,n=8}^{\max imum} - A_{m,n=4}^{\max imum} = \frac{k_1 A_a X_a (X_a^2 - A_a^2)^2}{\sqrt{k_4^2 + w_a^2}(X_a^2 + A_a^2)\left[(X_a^2 + A_a^2)^2 + 4A_a^2 X_a^2\right]} > 0$$

Hence, $A_{m,n=8}^{\max imum} > A_{m,n=4}^{\max imum} > A_{m,n=2}^{\max imum} > A_{m,n=1}^{\max imum}$.

Since X_p is directly proportional to X_m,

$$A_{p,n=8}^{\max imum} > A_{p,n=4}^{\max imum} > A_{p,n=2}^{\max imum} > A_{p,n=1}^{\max imum}.$$

Note: when $j_1 = 0$, A_m, $A_p = 0$; as $j_1 \rightarrow \infty$, A_m, $A_p \rightarrow 0$.

<u>Effect of binding cooperativity between T.F. and DNA enhancer site, *n*</u>

When $n = 0$, $A_m = 0$. $\frac{\partial^2 X_M}{\partial n^2}|_{n=0} = 0$.

Note: $A_m = \frac{k_1}{2\sqrt{k_4^2 + w_a^2}}\left[\frac{j_1^n (X_a + A_a)^n - j_1^n (X_a - A_a)^n}{j_1^{2n} + j_1^n (X_a + A_a)^n + j_1^n (X_a - A_a)^n + (X_a^2 - A_a^2)^n}\right] < \frac{k_1}{2\sqrt{k_4^2 + w_a^2}}$

$$\frac{\partial A_m}{\partial n} = \frac{k_1}{2\sqrt{k_4^2 + w_a^2}}\left\{-\frac{\left(\frac{X_a - A_a}{j_1}\right)^n}{\left[1 + \left(\frac{X_a - A_a}{j_1}\right)^n\right]^2}\ln\left(\frac{X_a - A_a}{j_1}\right) + \frac{\left(\frac{X_a + A_a}{j_1}\right)^n}{\left[1 + \left(\frac{X_a + A_a}{j_1}\right)^n\right]^2}\ln\left(\frac{X_a + A_a}{j_1}\right)\right\}$$

$$\frac{\partial^2 A_m}{\partial n^2} = \frac{k_1}{2\sqrt{k_4^2 + w_a^2}}\left\{-\frac{\left(\frac{X_a - A_a}{j_1}\right)^n\left[\ln\left(\frac{X_a - A_a}{j_1}\right)\right]^2}{\left[1 + \left(\frac{X_a - A_a}{j_1}\right)^n\right]^3}\left[1 - \left(\frac{X_a - A_a}{j_1}\right)^n\right] + \frac{\left(\frac{X_a + A_a}{j_1}\right)^n\left[\ln\left(\frac{X_a + A_a}{j_1}\right)\right]^2}{\left[1 + \left(\frac{X_a + A_a}{j_1}\right)^n\right]^3}\left[1 - \left(\frac{X_a + A_a}{j_1}\right)^n\right]\right\}$$

Hence,

$\frac{\partial A_m}{\partial n}$ is always positive when $\ln\left(\frac{X_a - A_a}{j_1}\right) \le 0$ and $\ln\left(\frac{X_a + A_a}{j_1}\right) \ge 0$, i.e., $X_a - A_a \le j_1 \le X_a + A_a$. $\frac{\partial^2 A_m}{\partial n^2} < 0$.

$\frac{\partial A_m}{\partial n}$ is always negative when $\ln\left(\frac{X_a - A_a}{j_1}\right) > 0$ and $\ln\left(\frac{X_a + A_a}{j_1}\right) < 0$, however, no range of j_1 exists.

$\frac{\partial A_m}{\partial n}$, $\frac{\partial^2 A_m}{\partial n^2}$ can be zero, positive or negative when $\ln\left(\frac{X_a - A_a}{j_1}\right)$ and $\ln\left(\frac{X_a + A_a}{j_1}\right)$ have same signs, i.e., $j_1 < X_a - A_a$ or $j_1 > X_a + A_a$.

$X_a - A_a \le j_1 \le X_a + A_a$: $\frac{\partial A_m}{\partial n} > 0$. Note: when $j_1 = X_a - A_a$, as $n \rightarrow \infty$, $A_m \rightarrow \frac{k_1}{4\sqrt{k_4^2 + w_a^2}}$; when $X_a - A_a < j_1 < X_a + A_a$, as $n \rightarrow \infty$, $A_m \rightarrow \frac{k_1}{2\sqrt{k_4^2 + w_a^2}}$; when $j_1 = X_a + A_a$, as $n \rightarrow \infty$, $A_m \rightarrow \frac{k_1}{4\sqrt{k_4^2 + w_a^2}}$. Discuss the biological implication that Am as n → ∞ depends on wa…

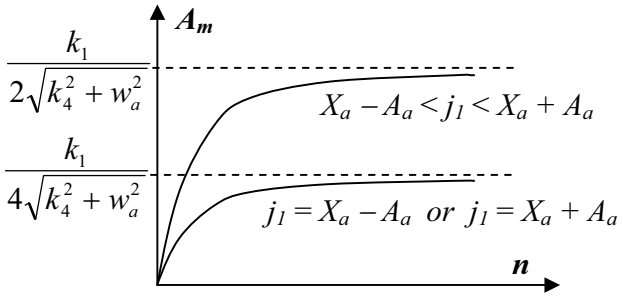

$j_1 < X_a - A_a$ or $j_1 > X_a + A_a$: as $n \rightarrow \infty$, $A_m \rightarrow 0$. $\frac{\partial X_M}{\partial n}|_{n=0} > 0$. Since A_m is also zero at $n = 0$, A_m cannot have a minimum value to satisfy the condition, $A_m \ge 0$.

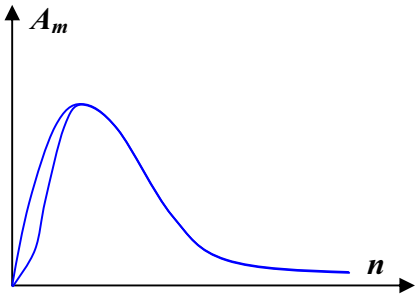

Effect of T.A. oscillation amplitude, A_a

$$\frac{\partial A_m}{\partial A_a} = \frac{nk_1 j_1^n}{2\sqrt{k_4^2 + w_1^2}} \left\{ \frac{(X_a - A_a)^{n-1}}{\left[j_1^n + (X_a - A_a)^n\right]^2} + \frac{(X_a + A_a)^{n-1}}{\left[j_1^n + (X_a + A_a)^n\right]^2} \right\} > 0$$

$$\frac{\partial^2 A_m}{\partial A_a^2} = \frac{nk_1 j_1^n}{2\sqrt{k_4^2 + w_1^2}} \left\{ \frac{(X_a - A_a)^{n-2}\left[(n+1)(X_a - A_a)^n - (n-1)j_1^n\right]}{\left[j_1^n + (X_a - A_a)^n\right]^3} - \frac{(X_a + A_a)^{n-2}\left[(n+1)(X_a + A_a)^n - (n-1)j_1^n\right]}{\left[j_1^n + (X_a + A_a)^n\right]^3} \right\}$$

Hence A_m increase monotonically with A_a, i.e., maximum value of A_m occurs as $A_a \rightarrow X_a$. As $A_a \rightarrow X_a$, $A_m \rightarrow \frac{k_1}{\sqrt{k_4^2 + w_a^2}}\left[\frac{2^{n-1} X_a^n}{j_1^n + 2^n X_a^n}\right]$. Note: when $A_a = 0$, $A_m = 0$ and $\frac{\partial^2 A_m}{\partial A_a^2} = 0$ (trivial non-stationary point of inflexion).

$n = 1$: $\frac{\partial^2 A_m}{\partial A_a^2} > 0$ for $A_a > 0$.

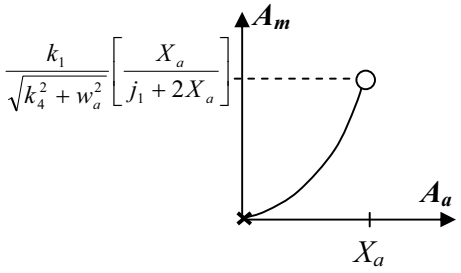

$n = 2$: As $A_a \rightarrow X_a$, $\frac{\partial^2 A_m}{\partial A_a^2} < 0$.

$\frac{\partial^2 A_m}{\partial A_a^2}$ can be negative, positive or zero for $0 < A_a < X_a$. Thus, multiple non-stationary points of inflexion could be present. To obtain the points of inflexion, let $\frac{\partial^2 A_m}{\partial A_a^2} = 0$ gives $3X_a^6 m_a^6 - 3X_a^4 (X_a^2 - j_1^2) m_a^4 - X_a^2 (3X_a^4 + 14 j_1^2 X_a^2 + 3 j_1^4) m_a^2 + 3(X_a^6 + j_1^2 X_a^4 - j_1^4 X_a^2 - j_1^6) = 0$. A maximum number of three non-trivial non-stationary points of inflexion could exist.

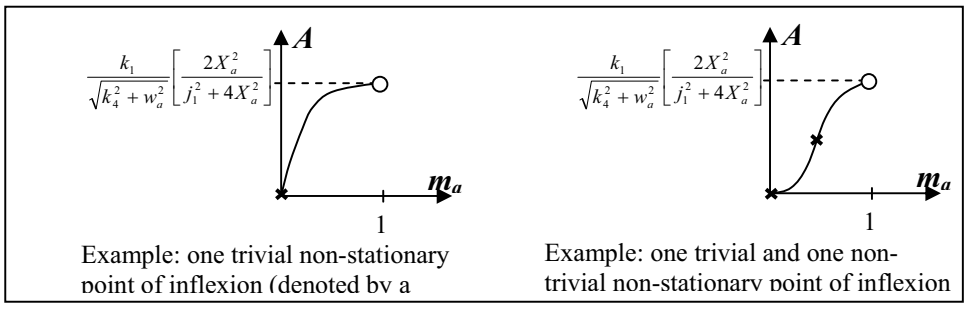

Example: one trivial non-stationary point of inflexion (denoted by a

Example: one trivial and one non-trivial non-stationary point of inflexion

$n = 4$: As $A_a \rightarrow X_a$, $\frac{\partial^2 A_m}{\partial A_a^2} \geq 0$ if $j_1^4 \geq {}^{80}/_3 X_a^4$ or $\frac{\partial^2 A_m}{\partial A_a^2} < 0$ if otherwise.

Similarly, $\frac{\partial^2 A_m}{\partial A_a^2}$ can be negative, positive or zero for $0 < A_a < X_a$. Thus, multiple non-stationary points of inflexion could be present. To obtain the points of inflexion, let $\frac{\partial^2 A_m}{\partial A_a^2} = 0$ gives $c_0 m_a^{16} + c_1 m_a^{14} + c_2 m_a^{12} + \ldots + c_6 m_a^4 + c_7 m_a^2 + c_8 = 0$ where c_1 to c_8 are functions of j_i and X_a. A maximum number of eight non-trivial non-stationary points of inflexion could exist.

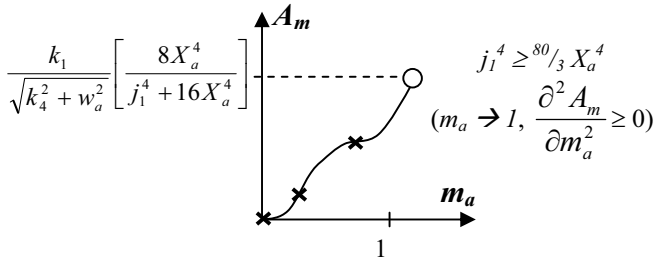

Example: one trivial and two non-stationary points of inflexion (denoted by crosses).

Redo:

$A_{M,n}|_{A_{TF}\to X_{TF}} > A_{M,n-1}|_{A_{TF}\to X_{TF}}$ *if* $j_1 < 2X_{TF}$; $A_{M,n}|_{A_{TF}\to X_{TF}} < A_{M,n-1}|_{A_{TF}\to X_{TF}}$ when otherwise.

$n = 1$: $\dfrac{\partial^2 A_M}{\partial A_{TF}^2} > 0.$

$n = 2$: $\dfrac{\partial^2 A_M}{\partial A_{TF}^2}|_{A_{TF}\to X_{TF}} < 0.$

$n > 2$: $\dfrac{\partial^2 A_M}{\partial A_{TF}^2}|_{A_{TF}\to X_{TF}} > 0$ if $j_1 > 2X_{TF}\left(\dfrac{n+1}{n-1}\right)^{1/n}$;

$\dfrac{\partial^2 A_M}{\partial A_{TF}^2}|_{A_{TF}\to X_{TF}} < 0$ if $j_1 < 2X_{TF}\left(\dfrac{n+1}{n-1}\right)^{1/n}$.

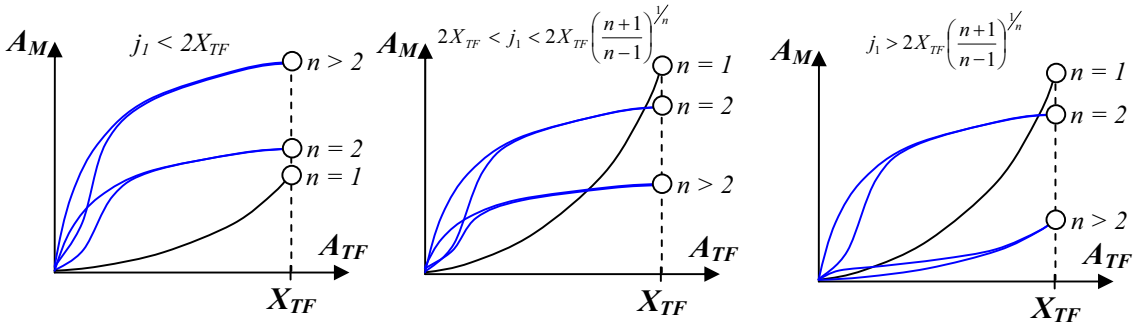

Effect of T.A. oscillation mean, X_a

$$\frac{\partial A_m}{\partial X_a} = \frac{nk_1 j_1^n}{2\sqrt{k_4^2+w_1^2}}\left\{-\frac{(X_a-A_a)^{n-1}}{\left[j_1^n+(X_a-A_a)^n\right]^2}+\frac{(X_a+A_a)^{n-1}}{\left[j_1^n+(X_a+A_a)^n\right]^2}\right\}$$

$$\frac{\partial^2 A_m}{\partial X_a^2} = \frac{nk_1 j_1^n}{2\sqrt{k_4^2+w_1^2}}\left\{\frac{(X_a-A_a)^{n-2}\left[(1+n)(X_a-A_a)^n+(1-n)j_1^n\right]}{\left[j_1^n+(X_a-A_a)^n\right]^3}-\frac{(X_a+A_a)^{n-2}\left[(1+n)(X_a+A_a)^n+(1-n)j_1^n\right]}{\left[j_1^n+(X_a+A_a)^n\right]^3}\right\}$$

As $X_a \to A_a$, $A_m \to \dfrac{k_1 j_1^n}{\sqrt{k_4^2+w_1^2}}\dfrac{2^{n-1}A_a^n}{j_1^n+2^n A_a^n}$; as $X_a \to \infty$, $A_m \to 0$.

$n = 1$: $\frac{\partial A_m}{\partial X_a} < 0$, $\frac{\partial^2 A_m}{\partial X_a^2} > 0$.

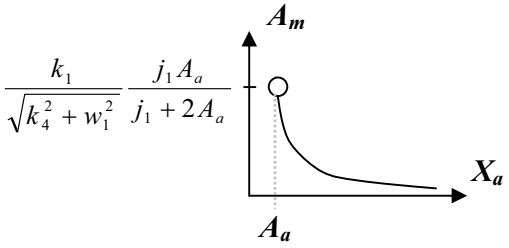

$n = 2$: only one positive turning point at $X_a^2 = \frac{A_a^2 - j_1^2 + 2\sqrt{\left(A_a^2 - j_1^2\right)^2 + 3A_a^2 j_1^2}}{3} > A_a^2$;

since $A_m \rightarrow 0$ as $X_a \rightarrow \infty$, it has to be a maximum point. $\frac{\partial A_M}{\partial X_{TF}}|_{X_{TF} \rightarrow A_{TF}} > 0$; $\frac{\partial^2 A_M}{\partial X_{TF}^2}|_{X_{TF} \rightarrow A_{TF}} < 0$.

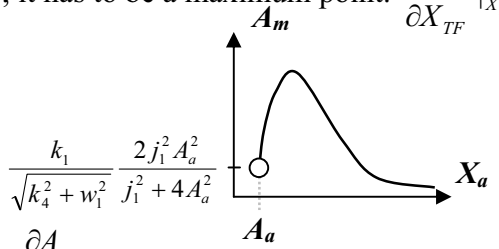

$n = 3, 4$: As $X_a \rightarrow A_a$, $\frac{\partial A_m}{\partial X_a} > 0$. Although 1 to 3 positive turning points, only 1 or 3 plausible turning points since $A_m \rightarrow 0$ as $X_a \rightarrow \infty$. $\frac{\partial A_M}{\partial X_{TF}}|_{X_{TF} \rightarrow A_{TF}} > 0$. $\frac{\partial^2 A_M}{\partial X_{TF}^2}|_{X_{TF} \rightarrow A_{TF}} > 0$ if $j_1 > 2A_{TF}\left(\frac{n+1}{n-1}\right)^{1/n}$; $\frac{\partial^2 A_M}{\partial X_{TF}^2}|_{X_{TF} \rightarrow A_{TF}} < 0$ if $j_1 < 2A_{TF}\left(\frac{n+1}{n-1}\right)^{1/n}$.

Maple: did not obtain > 1 valid turning points; only 1 valid turning point is obtained.

Matlab: 1 valid turning point is observed.

$j_1 < 2A_{TF}\left(\frac{n+1}{n-1}\right)^{1/n}$

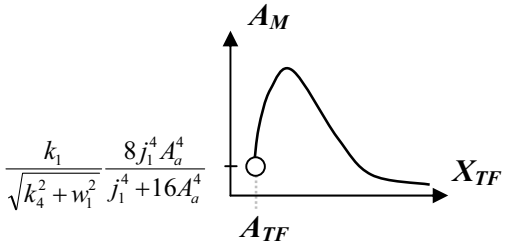

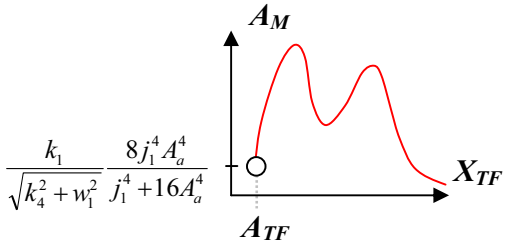

$j_1 > 2A_{TF}\left(\frac{n+1}{n-1}\right)^{1/n}$

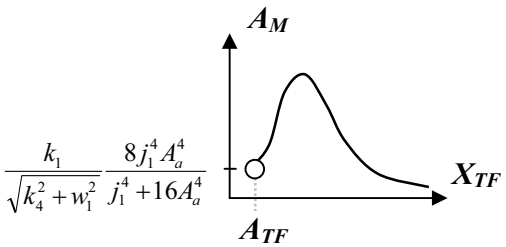

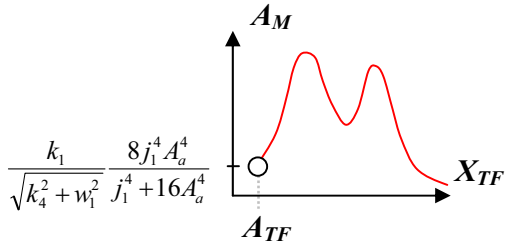

Effect of rates of transcription (k_1) and translation (k_2)

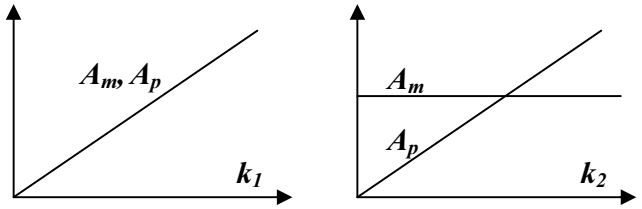

Effect of degradation rates of mRNA (k_4) and protein (k_5)

$$\frac{\partial A_m}{\partial k_4} = -\frac{k_1 j_1^n \overline{A_a} k_4}{\left(k_4^2 + w_a^2\right)^{3/2}} < 0$$

$$\frac{\partial^2 A_m}{\partial k_4^2} = \frac{k_1 j_1^n \overline{A_a}\left(2k_4^2 - w_a^2\right)}{\left(k_4^2 + w_a^2\right)^{5/2}}$$

Thus, A_m ($= \frac{k_1 j_1^n \overline{A_a}}{w_a}$) is maximum at $k_4 = 0$. There is a non-stationary point of inflexion at $k_4 = w_a/\sqrt{2}$. As $k_4 \rightarrow \infty$, $A_m \rightarrow 0$.

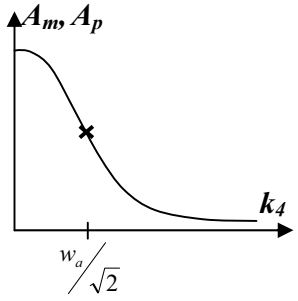

$$\frac{\partial A_p}{\partial k_5} = -\frac{k_2 A_m k_5}{\left(k_5^2 + w_a^2\right)^{3/2}} < 0$$

$$\frac{\partial^2 A_p}{\partial k_5^2} = \frac{k_2 A_m\left(2k_5^2 - w_a^2\right)}{\left(k_5^2 + w_a^2\right)^{5/2}}$$

Thus, A_p ($= \frac{k_2 A_m}{w_a}$) is maximum at $k_5 = 0$. There is a non-stationary point of inflexion at $k_5 = w_a/\sqrt{2}$. As $k_5 \rightarrow \infty$, $A_p \rightarrow 0$.

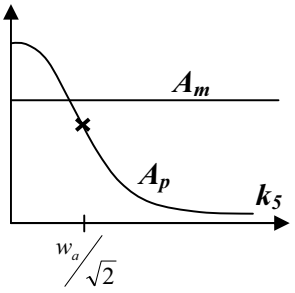

C. Normalized oscillation amplitude of target gene

$$m_m = \frac{A_m}{X_m} = \frac{k_4 j_1^n \overline{A_a}}{\sqrt{k_4^2 + w_a^2}\left(1 - j_1^n \overline{X_a}\right)}$$

$$= \frac{k_4 j_1^n}{\sqrt{k_4^2 + w_a^2}}\left[\frac{\left(X_{TF} + A_{TF}\right)^n - \left(X_{TF} - A_{TF}\right)^n}{j_{tM}^n\left(X_{TF} + A_{TF}\right)^n + j_{tM}^n\left(X_{TF} - A_{TF}\right)^n + 2\left(X_{TF}^2 - A_{TF}^2\right)^n}\right]$$

$$m_p = \frac{A_p}{X_p} = \frac{k_5}{\sqrt{k_5^2 + w_a^2}} m_m$$

Effect of T.A. oscillation period, ($P_a = 2\pi/w_a$)

$$m_m = \frac{k_4 j_1^n \overline{A_a}}{\left(1 - j_1^n \overline{X_a}\right)\sqrt{k_4^2 + \frac{4\pi^2}{P_a^2}}}$$

Since $\frac{\partial X_m}{\partial P_a}$ = 0 (X_m is independent on T.A. oscillation period), $\frac{\partial m_m}{\partial P_a} = \frac{1}{X_m}\frac{\partial A_m}{\partial P_a}$ and $\frac{\partial^2 m_m}{\partial P_a^2} = \frac{1}{X_m}\frac{\partial^2 A_m}{\partial P_a^2}$. Therefore, the effect of P_a on m_m is qualitatively similar to the effect of P_a on A_m, i.e., $\frac{\partial m_m}{\partial P_a} > 0$ and $\frac{\partial^2 m_m}{\partial P_a^2} < 0$.

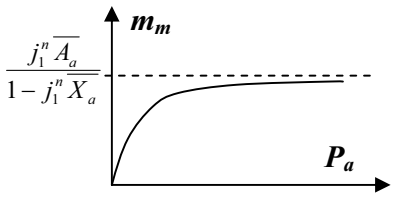

As $P_a \rightarrow 0$, $m_m \rightarrow 0$; as $P_a \rightarrow \infty$, $m_m \rightarrow \frac{j_1^n \overline{A_a}}{1 - j_1^n \overline{X_a}}$.

$$m_p = \frac{k_4 k_5 j_1^n \overline{A_a}}{\left(1 - j_1^n \overline{X_a}\right)\sqrt{\left(k_4^2 + \frac{4\pi^2}{P_a^2}\right)\left(k_5^2 + \frac{4\pi^2}{P_a^2}\right)}}$$

Since $\frac{\partial X_p}{\partial P_a} = 0$ (X_p is independent on T.A. oscillation period), $\frac{\partial m_p}{\partial P_a} = \frac{1}{X_p}\frac{\partial A_p}{\partial P_a}$ and $\frac{\partial^2 m_p}{\partial P_a^2} = \frac{1}{X_p}\frac{\partial^2 A_p}{\partial P_a^2}$. Therefore, the effect of P_a on m_p is qualitatively similar to the effect of P_a on A_p, i.e., $\frac{\partial m_p}{\partial P_a} > 0$ and $\frac{\partial^2 m_p}{\partial P_a^2} < 0$.

When $P_a \rightarrow 0$, $m_p \rightarrow 0$; when $P_a \rightarrow \infty$, $m_p \rightarrow m_m = \frac{j_1^n \overline{A_a}}{1 - j_1^n \overline{X_a}}$.

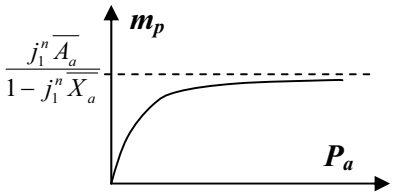

Effect of T.A. binding affinity to DNA enhancer site, j_1

$$\frac{\partial m_m}{\partial j_1} = \frac{2nk_4 X_a^n \left(1 - m_a^2\right)^n \left[\left(1 + m_a\right)^n - \left(1 - m_a\right)^n\right]}{\sqrt{k_4^2 + w_a^2}} \left\{ \frac{j_1^{n-1}}{\left[j_1^n \left(1 + m_a\right)^n + j_1^n \left(1 - m_a\right)^n + 2X_a^n \left(1 - m_a^2\right)^n\right]^2} \right\} > 0$$

$$\frac{\partial^2 m_m}{\partial j_1^2} = \frac{2nk_4 X_a^n \left(1 - m_a^2\right)^n \left[\left(1 + m_a\right)^n - \left(1 - m_a\right)^n\right] j_1^{n-2} \left\{2(n-1)X_a^n \left(1 - m_a^2\right)^n - j_1^n (n+1)\left[\left(1 + m_a\right)^n + \left(1 - m_a\right)^n\right]\right\}}{\sqrt{k_4^2 + w_a^2}\left[j_1^n \left(1 + m_a\right)^n + j_1^n \left(1 - m_a\right)^n + 2X_a^n \left(1 - m_a^2\right)^n\right]^3}$$

When $j_1 = 0$, $m_m = 0$; as $j_1 \rightarrow \infty$, $m_m \rightarrow \frac{k_4}{\sqrt{k_4^2 + w_a^2}}\left[\frac{\left(1 + m_a\right)^n - \left(1 - m_a\right)^n}{\left(1 + m_a\right)^n + \left(1 - m_a\right)^n}\right]$.

$n = 1$: $\frac{\partial^2 m_m}{\partial j_1^2} < 0$. As $j_1 \rightarrow \infty$, $m_m \rightarrow \frac{k_4}{\sqrt{k_4^2 + w_a^2}} m_a$.

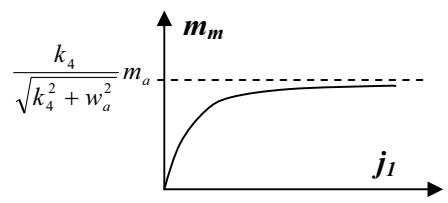

n = 2: When $j_1 = 0$, $\frac{\partial^2 m_m}{\partial j_1^2} > 0$. As $j_1 \rightarrow \infty$, $\frac{\partial^2 m_m}{\partial j_1^2} < 0$, $m_m \rightarrow \frac{k_4}{\sqrt{k_4^2 + w_a^2}} \frac{2m_a}{m_a^2 + 1}$. A non-stationary point of inflexion occurs at $j_1^2 = \frac{2\left(1 - m_a^2\right)^2}{3\left[\left(1 + m_a^2\right)^2 + \left(1 - m_a^2\right)^2\right]} X_n^2$.

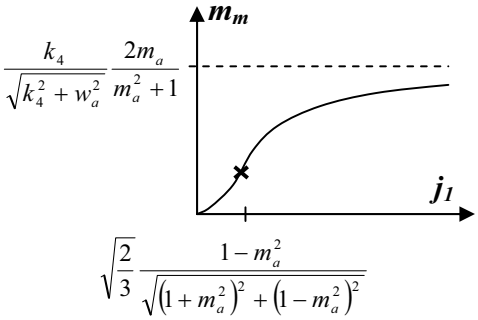

n = 4: When $j_1 = 0$, $\frac{\partial^2 m_m}{\partial j_1^2} > 0$. As $j_1 \rightarrow \infty$, $\frac{\partial^2 m_m}{\partial j_1^2} < 0$, $m_m \rightarrow \frac{k_4}{\sqrt{k_4^2 + w_a^2}} \frac{4m_a\left(m_a^2 + 1\right)}{m_a^4 + 6m_a^2 + 1}$.

Two non-stationary points of inflexion at $j_i = 0$ and $j_1^4 = \frac{6\left(1 - m_a^2\right)^4}{5\left[\left(1 + m_a^2\right)^4 + \left(1 - m_a^2\right)^4\right]} X_n^4$.

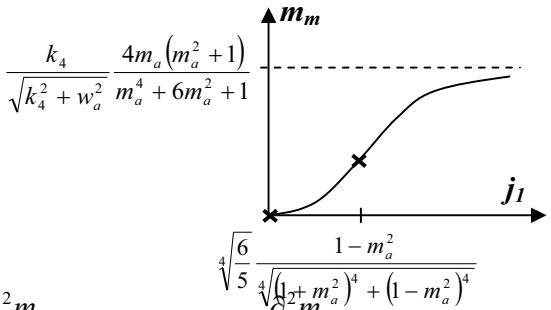

n = 8: When $j_1 = 0$, $\frac{\partial^2 m_m}{\partial j_1^2} > 0$. As $j_1 \rightarrow \infty$, $\frac{\partial^2 m_m}{\partial j_1^2} < 0$, $m_m \rightarrow$ $\frac{k_4}{\sqrt{k_4^2 + w_a^2}} \frac{8m_a\left(m_a^6 + 7m_a^4 + 7m_a^2 + 1\right)}{m_a^8 + 28m_a^6 + 70m_a^4 + 28m_a^2 + 1}$. Two non-stationary points of inflexion at $j_i = 0$ and $j_1^8 = \frac{14\left(1 - m_a^2\right)^8}{9\left[\left(1 + m_a^2\right)^8 + \left(1 - m_a^2\right)^8\right]} X_n^8$. $\frac{k_4}{\sqrt{k_4^2 + w_a^2}} \frac{8m_a\left(m_a^6 + 7m_a^4 + 7m_a^2 + 1\right)}{m_a^8 + 28m_a^6 + 70m_a^4 + 28m_a^2 + 1}$

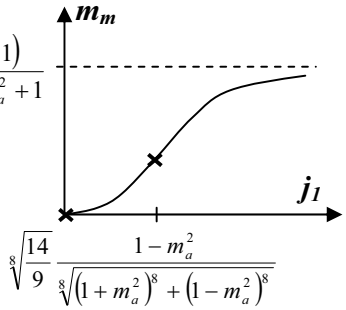

Since $\frac{(1+m_a)^n-(1-m_a)^n}{(1+m_a)^n+(1-m_a)^n} > \frac{(1+m_a)^{n-1}-(1-m_a)^{n-1}}{(1+m_a)^{n-1}+(1-m_a)^{n-1}}$, $m_{m,n} > m_{m,n-1}$ as $j_1 \rightarrow \infty$.

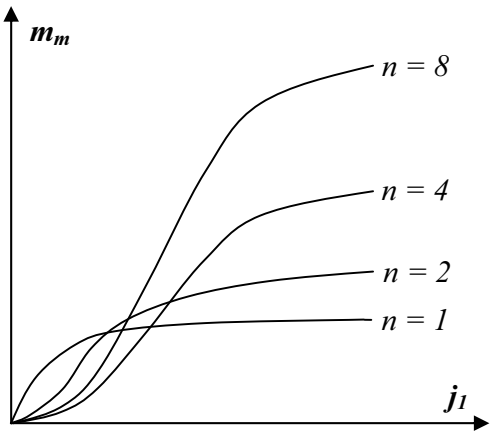

Effect of stoichiometry of T.A. or binding cooperativity between T.F. and DNA enhancer site, *n*

When $n = 0$, $m_m = 0$.

Note: $m_m = \frac{k_4}{\sqrt{k_4^2+w_a^2}}\left[\frac{j_1^n(X_a+A_a)^n - j_1^n(X_a-A_a)^n}{j_1^n(X_a+A_a)^n + j_1^n(X_a-A_a)^n + 2(X_a^2-A_a^2)^n}\right] < \frac{k_4}{\sqrt{k_4^2+w_a^2}}$

$$\frac{\partial m_m}{\partial n} = \frac{2k_4 j_1^n(1-m_a^2)^n\left[j_1^n \ln\frac{1+m_a}{1-m_a} + X_a^n(1-m_a)^n \ln\frac{X_a(1+m_a)}{j_1} - X_a^n(1+m_a)^n \ln\frac{X_a(1-m_a)}{j_1}\right]}{\sqrt{k_4^2+w_a^2}\left[j_1^n(1+m_a)^n + j_1^n(1-m_a)^n + 2X_a^n(1-m_a^2)^n\right]^2}$$

$$\text{or } \frac{\partial m_m}{\partial n} = \frac{2k_4 j_1^n(X_a^2-A_a^2)^n\left[j_1^n \ln\frac{X_a+A_a}{X_a-A_a} + (X_a-A_a)^n \ln\frac{(X_a+A_a)}{j_1} - (X_a+A_a)^n \ln\frac{(X_a-A_a)}{j_1}\right]}{\sqrt{k_4^2+w_a^2}\left[j_1^n(X_a+A_a)^n + j_1^n(X_a-A_a)^n + 2(X_a^2-A_a^2)^n\right]^2}$$

$\frac{\partial m_m}{\partial n}|_{n=0} \alpha \ln\frac{j_1^3}{X_a^2-A_a^2}$. How to use this info?

Hence,

$\frac{\partial m_m}{\partial n}$ is always positive when $\ln\left[\frac{X_a(1-m_a)}{j_1}\right] \le 0$ and $\ln\left[\frac{X_a(1+m_a)}{j_1}\right] \ge 0$, i.e., $X_a(1-m_a) \le j_1 \le X_a(1+m_a)$.

$\frac{\partial m_m}{\partial n}$ can be zero, positive or negative when $j_1 < X_a(1-m_a)$ or $j_1 > X_a(1+m_a)$.

$X_a(1-m_a) \le j_1 \le X_a(1+m_a)$: $\frac{\partial A_m}{\partial n} > 0$. Note: when $j_1 = X_a(1-m_a)$, as $n \rightarrow \infty$, $m_m \rightarrow \frac{k_4}{3\sqrt{k_4^2 + w_a^2}}$; when $X_a(1-m_a) < j_1 \le X_a(1+m_a)$, as $n \rightarrow \infty$, $m_m \rightarrow \frac{k_4}{\sqrt{k_4^2 + w_a^2}}$. Discuss the biological implication that m_m as $n \rightarrow \infty$ depends on w_a…

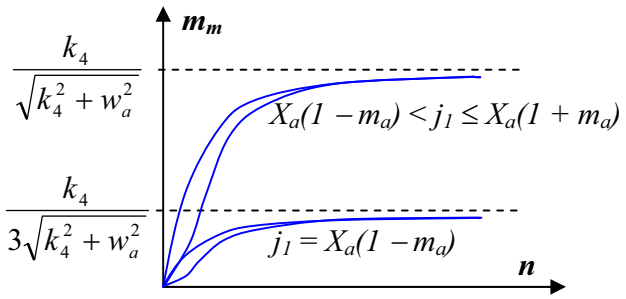

$j_1 < X_a(1-m_a)$: $\frac{\partial X_M}{\partial n}|_{n=0} > 0$. $\frac{\partial m_m}{\partial n}$ can be zero, positive or negative. As $n \rightarrow \infty$, $m_m \rightarrow 0$. Since m_m is also zero at $n = 0$, m_m cannot have a minimum value to satisfy the condition, $m_m \ge 0$.

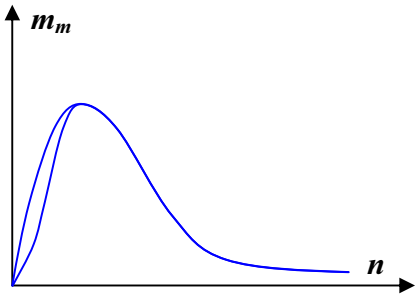

$j_1 > X_a(1+m_a)$: $\frac{\partial m_m}{\partial n}$ can be zero, positive or negative. As $n \rightarrow \infty$, $m_m \rightarrow \frac{k_4}{\sqrt{k_4^2 + w_a^2}}$. $m_m > \frac{k_4}{\sqrt{k_4^2 + w_a^2}}$ for all n. Hence, no maximum point.

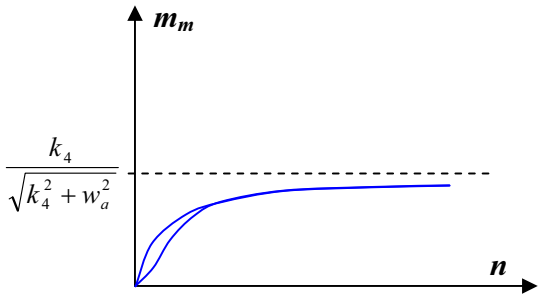

Effect of T.A. oscillation amplitude, A_{TF}

$$\frac{\partial m_m}{\partial A_{TF}}=\frac{2nk_4j_1^n}{\sqrt{k_4^2+w_a^2}}\frac{\left(X_a^2-A_a^2\right)^{n-1}\left[2j_1^nX_a+\left(X_a+A_a\right)^{n+1}+\left(X_a-A_a\right)^{n+1}\right]}{\left[j_1^n\left(X_a+A_a\right)^n+j_1^n\left(X_a-A_a\right)^n+2\left(X_a^2-A_a^2\right)^n\right]^2}>0$$

$$\frac{\partial^2 m_m}{\partial A_{TF}^2}=\frac{2nk_4j_1^n\left(X_a^2-A_a^2\right)^{n-2}}{\sqrt{k_4^2+w_a^2}\left[j_1^n\left(X_a+A_a\right)^n+j_1^n\left(X_a-A_a\right)^n+2\left(X_a^2-A_a^2\right)^n\right]^3}$$

$$\left\{\begin{bmatrix}-4(n-1)j_1^nA_aX_a\left[j_1^n\left(X_a+A_a\right)^n+j_1^n\left(X_a-A_a\right)^n+3\left(X_a^2-A_a^2\right)^n\right]\\+\left(X_a+A_a\right)^{2n+1}\left[(n+1)X_a-(3n-1)A_a\right]\left[j_1^n+2\left(X_a-A_a\right)^n\right]\\-\left(X_a-A_a\right)^{2n+1}\left[(n+1)X_a+(3n-1)A_a\right]\left[j_1^n+2\left(X_a+A_a\right)^n\right]\end{bmatrix}+2n\begin{bmatrix}-2j_1^{2n}X_a\left(X_a^2-A_a^2\right)\left[\left(X_a+A_a\right)^{n-1}-\left(X_a-A_a\right)^{n-1}\right]\\+12j_1^nA_aX_a\left(X_a^2-A_a^2\right)^n\\-j_1^n\left(X_a^2-A_a^2\right)\left[\left(X_a+A_a\right)^{2n}-\left(X_a-A_a\right)^{2n}\right]\\+4A_a\left(X_a^2-A_a^2\right)^n\left[\left(X_a+A_a\right)^{n+1}+\left(X_a-A_a\right)^{n+1}\right]\end{bmatrix}\right\}$$

$$=\frac{2nk_4j_1^n\left(X_a^2-A_a^2\right)^{n-2}}{\sqrt{k_4^2+w_a^2}\left[j_1^n\left(X_a+A_a\right)^n+j_1^n\left(X_a-A_a\right)^n+2\left(X_a^2-A_a^2\right)^n\right]^3}$$

$$\left\{\begin{bmatrix}+2\left(X_a^2-A_a^2\right)^n\left\{(n+1)\left[4j_1^nA_aX_a+\left(X_a+A_a\right)^{n+2}+\left(X_a-A_a\right)^{n+2}\right]+j_1^n\left[(3n+1)X_a^2-(n-1)A_a^2\right]\right\}\\+4j_1^{2n}X_a\left[\left(A_a-nX_a\right)\left(X_a+A_a\right)^n+\left(A_a+nX_a\right)\left(X_a-A_a\right)^n\right]\\-j_1^n(n-1)\left[\left(X_a+A_a\right)^{2n+2}+\left(X_a-A_a\right)^{2n+2}\right]\end{bmatrix}\right\}$$

When $A_a = 0$, $m_m = 0$, $\frac{\partial^2 m_m}{\partial A_{TF}^2}>0$. As $A_a \rightarrow X_a$, $m_m \rightarrow \frac{k_4}{\sqrt{k_4^2+w_a^2}}$.

$n = 1$: $\frac{\partial^2 m_m}{\partial m_a^2}>0$.

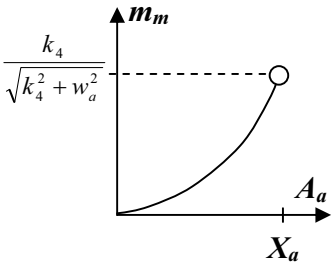

For $n = 2$, $\frac{\partial^2 m_m}{\partial A_{TF}^2}<0$ as $A_a \rightarrow X_a$.

For $n > 2$, $\frac{\partial^2 m_m}{\partial A_{TF}^2} = 0$ as $A_a \rightarrow X_a$.

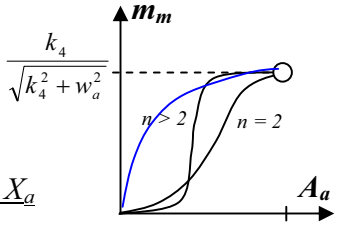

Effect of T.A. oscillation mean, X_a

$$\frac{\partial m_m}{\partial X_a} = -\frac{2nk_4 j_1^n}{\sqrt{k_4^2 + w_a^2}} \frac{\left(X_a^2 - A_a^2\right)^{n-1}\left[2j_1^n A_a + \left(X_a + A_a\right)^{n+1} - \left(X_a - A_a\right)^{n+1}\right]}{\left[j_1^n\left(X_a + A_a\right)^n + j_1^n\left(X_a - A_a\right)^n + 2\left(X_a^2 - A_a^2\right)^n\right]^2} < 0$$

$$\frac{\partial^2 m_m}{\partial X_a^2} = \frac{2nk_4 j_1^n \left(X_a^2 - A_a^2\right)^{n-2}}{\sqrt{k_4^2 + w_a^2}\left[j_1^n\left(X_a + A_a\right)^n + j_1^n\left(X_a - A_a\right)^n + 2\left(X_a^2 - A_a^2\right)^n\right]^3}$$

$$\left\{\begin{array}{l} +2(n+1)\left(X_a^2 - A_a^2\right)^n\left[6j_1^n A_a X_a + \left(X_a + A_a\right)^{n+2} - \left(X_a - A_a\right)^{n+2}\right] \\ +4j_1^{2n} A_a\left[\left(X_a - nA_a\right)\left(X_a + A_a\right)^n + \left(X_a + nA_a\right)\left(X_a - A_a\right)^n\right] \\ -j_1^n(n-1)\left[\left(X_a + A_a\right)^{2n+2} - \left(X_a - A_a\right)^{2n+2}\right] \end{array}\right\}$$

As $X_a \rightarrow A_a$, $m_m \rightarrow \frac{k_4}{\sqrt{k_4^2 + w_a^2}}$; as $X_a \rightarrow \infty$, $m_m \rightarrow 0$, $\frac{\partial^2 m_m}{\partial X_a^2} \rightarrow 0$.

$n = 1$: $\frac{\partial^2 m_m}{\partial X_a^2} > 0$.

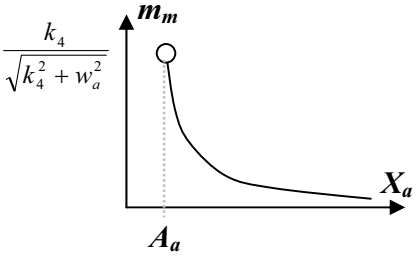

For $n = 2$, $\frac{\partial^2 m_m}{\partial X_a^2} < 0$ as As $X_a \rightarrow A_a$. Thus, a point of inflexion must exist.

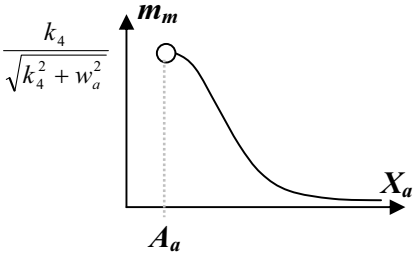

For $n > 2$, $\frac{\partial^2 m_m}{\partial X_a^2} = 0$ as As $X_a \rightarrow A_a$. Thus, a point of inflexion must exist.

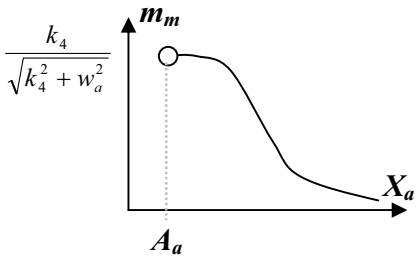

Effect of rates of transcription (k_1) and translation (k_2)

Both m_m and m_p are independent of k_1 and k_2.

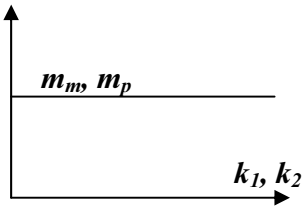

Effect of degradation rates of mRNA (k_4) and protein (k_5)

$$\frac{\partial m_m}{\partial k_4} = \frac{j_1^n \overline{A_a} w_a^2}{\left(1 - j_1^n \overline{X_a}\right)\left(k_4^2 + w_a^2\right)^{3/2}} > 0$$

$$\frac{\partial^2 m_m}{\partial k_4^2} = -\frac{3 j_1^n \overline{A_a} w_a^2 k_4}{\left(1 - j_1^n \overline{X_a}\right)\left(k_4^2 + w_a^2\right)^{5/2}} < 0$$

When $k_4 = 0$, $m_m = 0$; as $k_4 \rightarrow \infty$, $m_m \rightarrow \frac{j_1^n \overline{A_a}}{1 - j_1^n \overline{X_a}}$. (discuss that it is very interesting that a high degradation rate promotes m_m but not vice-versa as anticipated!!!)

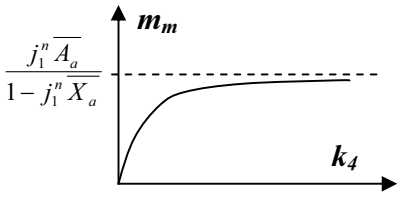

$$\frac{\partial m_m}{\partial k_5} = 0.$$

$$\frac{\partial m_p}{\partial k_5} = \frac{m_m w_a^2}{\left(k_5^2 + w_a^2\right)^{3/2}} > 0$$

$$\frac{\partial^2 m_p}{\partial k_5^2} = -\frac{3 m_m w_a^2 k_5}{\left(k_5^2 + w_a^2\right)^{5/2}} < 0$$

When $k_5 = 0$, $m_p = 0$; as $k_5 \rightarrow \infty$, $m_p \rightarrow m_m$. (discuss that it is very interesting that a high degradation rate promotes m_p but not vice-versa as anticipated!!!)

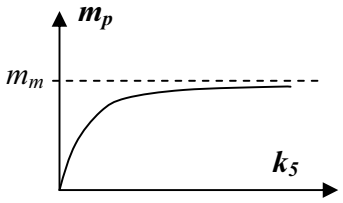

D. Oscillation period of target gene

$$w_m = w_a \Rightarrow P_m = P_a$$
$$w_p = w_a \Rightarrow P_p = P_a$$

The oscillation periods of the target gene mRNA and protein level were compared with the oscillatory T.A. period. In agreement with the analytical solution, the oscillation periods of the target gene mRNA and protein levels are identical to the oscillation period of the T.A. for all simulation runs.

E. Time-delay of target gene

$$\theta_m = \tau_1 + \frac{1}{w_a}\arctan\left(\frac{w_a}{k_4}\right)$$

$$\theta_p = \tau_1 + \tau_2 + \frac{1}{w_a}\left[\arctan\left(\frac{w_a}{k_4}\right) + \arctan\left(\frac{w_a}{k_5}\right)\right] = \theta_m + \tau_2 + \frac{1}{w_a}\arctan\left(\frac{w_a}{k_5}\right)$$

Effect of transcription activator oscillation frequency (w_a)

$$\frac{\partial \theta_m}{\partial w_a} = \frac{1}{w_a^2}\left[\frac{\left(\frac{w_a}{k_4}\right)}{1+\left(\frac{w_a}{k_4}\right)^2} - \arctan\left(\frac{w_a}{k_4}\right)\right] < 0$$

$$\frac{\partial^2 \theta_m}{\partial w_a^2} = \frac{1}{w_a^3}\left[2\arctan\left(\frac{w_a}{k_4}\right) - \frac{\left(\frac{w_a}{k_4}\right)}{1+\left(\frac{w_a}{k_4}\right)^2}\right] - \frac{k_4\left(k_4^2+3w_a^2\right)}{w_a^2\left(k_4^2+w_a^2\right)^2}$$

Note: $\frac{\partial \theta_m}{\partial w_a} < 0$ as $\frac{f(x)}{1+[f(x)]^2} < \arctan[f(x)]$ for $f(x) > 0$. $\frac{\partial^2 \theta_m}{\partial w_a^2}$ can be positive, zero or negative.

As $w_a \rightarrow 0$, $\theta_m \rightarrow \tau_1 + \frac{1}{k_4}$. As $w_a \rightarrow \infty$, $\theta_m \rightarrow \tau_1$. (discuss that the resultant time-delay is always longer than the transcriptional time-delay by $1/k_4$, i.e., the self-degradation rate of mRNA influences its time-delay!!!) Thus,

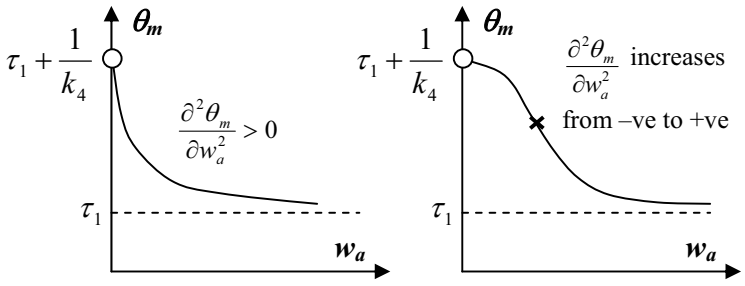

Similarly,

$$\frac{\partial\theta_p}{\partial w_a}=\frac{1}{w_a^2}\left\{\left[\frac{\left(\frac{w_a}{k_5}\right)}{1+\left(\frac{w_a}{k_5}\right)^2}-\arctan\left(\frac{w_a}{k_5}\right)\right]+\left[\frac{\left(\frac{w_a}{k_4}\right)}{1+\left(\frac{w_a}{k_4}\right)^2}-\arctan\left(\frac{w_a}{k_4}\right)\right]\right\}<0$$

Note: $\frac{\partial^2\theta_p}{\partial w_a^2}$ can

$$\frac{\partial^2\theta_p}{\partial w_a^2}=\frac{1}{w_a^3}\left\{\left[2\arctan\left(\frac{w_a}{k_5}\right)-\frac{\left(\frac{w_a}{k_5}\right)}{1+\left(\frac{w_a}{k_5}\right)^2}\right]+\left[2\arctan\left(\frac{w_a}{k_4}\right)-\frac{\left(\frac{w_a}{k_4}\right)}{1+\left(\frac{w_a}{k_4}\right)^2}\right]\right\}-\frac{k_5\left(k_5^2+3w_a^2\right)}{w_a^2\left(k_5^2+w_a^2\right)^2}-\frac{k_4\left(k_4^2+3w_a^2\right)}{w_a^2\left(k_4^2+w_a^2\right)^2}$$

be positive, zero or negative.

As $w_a \rightarrow 0$, $\theta_p \rightarrow (\tau_1+\tau_2)+\left(\frac{1}{k_4}+\frac{1}{k_5}\right)$. As $w_a \rightarrow \infty$, $\theta_p \rightarrow \tau_1 + \tau_2$. (discuss that the resultant time-delay is always longer than the transcriptional and translational time-delay by $1/k_4$ & $1/k_5$, i.e., the self-degradation rate of mRNA & protein influences its time-delay!!!) Thus,

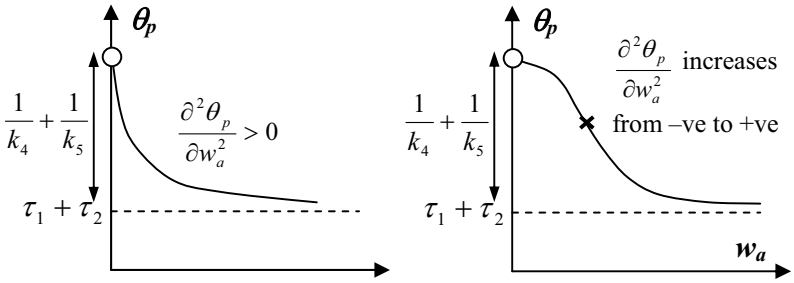

Effect of degradation rates of transcriptional time-delay (τ_1) and translational time-delay (τ_2)

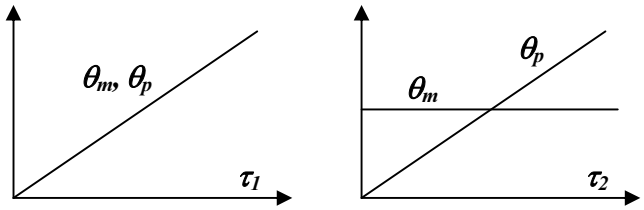

Effect of degradation rates of mRNA (k_4)

$$\frac{\partial \theta_m}{\partial k_4} = -\frac{1}{k_4^2 + w_a^2} < 0$$

$$\frac{\partial^2 \theta_m}{\partial k_4^2} = \frac{2k_4}{\left(k_4^2 + w_a^2\right)^2} > 0$$

As $k_4 \rightarrow 0$, $\theta_m \rightarrow \tau_1 + \frac{\pi}{2}\frac{1}{w_a}$. As $k_4 \rightarrow \infty$, $\theta_m \rightarrow \tau_1$. (similar to the effect of w_a, the resultant time-delay is always longer than the transcriptional and translational time-delay by $1/w_a$)

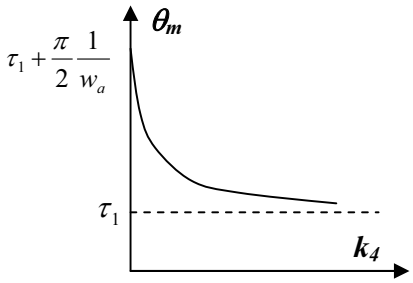

Similarly,

$$\frac{\partial \theta_p}{\partial k_4} = -\frac{1}{k_4^2 + w_a^2} < 0$$

$$\frac{\partial^2 \theta_p}{\partial k_4^2} = \frac{2k_4}{\left(k_4^2 + w_a^2\right)^2} > 0$$

As $k_4 \rightarrow 0$, $\theta_p \rightarrow \tau_1 + \tau_2 + \frac{1}{w_a}\left[\frac{\pi}{2} + \arctan\left(\frac{w_a}{k_5}\right)\right]$. As $k_4 \rightarrow \infty$, $\theta_p \rightarrow$ $\tau_1 + \tau_2 + \frac{1}{w_a}\arctan\left(\frac{w_a}{k_5}\right)$. (similar to the effect of w_a, the resultant time-delay is always longer than the transcriptional and translational time-delay by $1/w_a$)

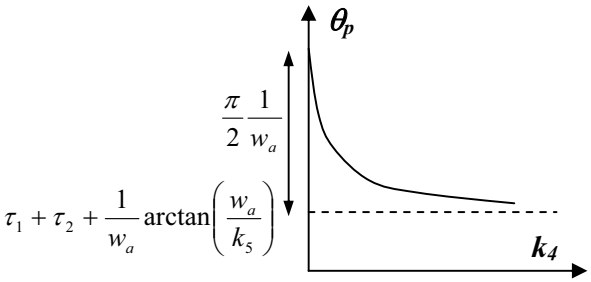

Effect of degradation rate of protein (k_5)

$$\frac{\partial \theta_p}{\partial k_5} = -\frac{1}{k_5^2 + w_a^2} < 0$$

$$\frac{\partial^2 \theta_p}{\partial k_5^2} = \frac{2k_5}{\left(k_5^2 + w_a^2\right)^2} > 0$$

As $k_5 \rightarrow 0$, $\theta_p \rightarrow \tau_1 + \tau_2 + \frac{1}{w_a}\left[\frac{\pi}{2} + \arctan\left(\frac{w_a}{k_4}\right)\right]$. As $k_5 \rightarrow \infty$, $\theta_p \rightarrow$ $\tau_1 + \tau_2 + \frac{1}{w_a}\arctan\left(\frac{w_a}{k_4}\right)$. (similar to the effect of w_a, the resultant time-delay is always longer than the transcriptional and translational time-delay by $1/w_a$)

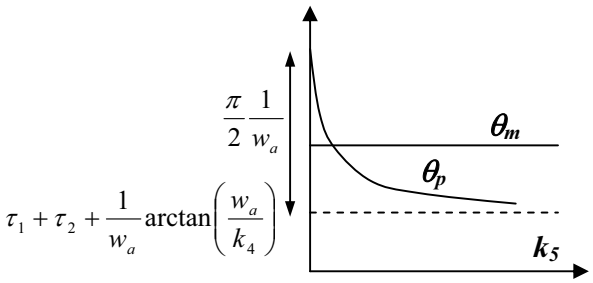

7.5 Simulation source codes

Dynamics_A1_constant_validate.m.txt

```
k1 = 0.1*1000*60;     % [0.001, 1]*1000*60 nM/hr = {0.001, 0.01, 0.1, 1}*1000*60 <insignificant effect>
j1 = 0.53*1000;         % [0.01, 10]*1000 nM = {0.01, 0.1, 1, 10}*1000 -->
k2 = 0.01*60;          % [0.001, 1]*60 /hr = {0.001, 0.01, 0.1, 1}*60
dM = 0.01*60;          % [0.001, 1]*60 /hr = {0.001, 0.01, 0.1, 1}*60 -->; large effect on time to steady state
(large dM => fast; small dM => slow)
dP = 0.01*60;          % [0.001, 1]*60 /hr = {0.001, 0.01, 0.1, 1}*60

n = 4;              % {1, 2, 4, 8} <--
X1 = 0.28*1000;      % [0.0001, 10]*1000 nM = {0.0001, 0.001, 0.01, 0.1, 1, 10}*1000 <--
%%%%%%%%%%%%%%%%%%%%%%%%%%%%%%%%%%%%%%%%%%%%%%%%%%%%%%%%%
%%%%%%%%%%%%%%%%%%%%%%%%%%%%%%%%%%%%%%%%%%%%%%%%%%%%%%%%%
%%%%%%%%%%%%%%%%%%%%%%%%%%%%%%%%%%%%%%%%%%%%%%%%%%%%%%%%%
%%%%%%%%%%
%Setting the Initial Concentrations and Timing Vectors
% y(1) = T.F.
% y(2) = mRNA
% y(3) = Protein
% y(4) = time

y0 = zeros(4, 1);
options = odeset('RelTol', 1e-6, 'AbsTol', [1e-6 1e-6 1e-6 1e-6]);
y0(1) = X1;
t = [0 15];
[T, Y] = ode23s(@Model_A1_constant_validate, t, y0, options);
figure(1);
subplot(2,1,1)
plot(T, Y(:,1), 'b-');
legend('T.F.');
subplot(2,1,2)
plot(T, Y(:,2), 'r-', T, Y(:,3), 'k-');
xlabel('Time');
ylabel('Concentration');
legend('mRNA', 'Protein');
```

Dynamics_A3_constant_validate.m.txt

```
k1 = 0.01*1000*60;      % [0.001, 1]*1000*60 nM/hr = {0.001, 0.01, 0.1, 1}*1000*60 <insignificant
effect>
j1 = 0.01*1000;         % [0.01, 10]*1000 nM = {0.01, 0.1, 1, 10}*1000 -->
k2 = 0.01*60;           % [0.001, 1]*60 /hr = {0.001, 0.01, 0.1, 1}*60
dM = 0.01*60;           % [0.001, 1]*60 /hr = {0.001, 0.01, 0.1, 1}*60 -->; large effect on time to steady state
(large dM => fast; small dM => slow)
dP = 0.01*60;           % [0.001, 1]*60 /hr = {0.001, 0.01, 0.1, 1}*60

n = 1;                  % {1, 2, 4, 8} <--
X1 = 0.0001*1000;       % [0.0001, 10]*1000 nM = {0.0001, 0.001, 0.01, 0.1, 1, 10}*1000 <--
%%%%%%%%%%%%%%%%%%%%%%%%%%%%%%%%%%%%%%%%%%%%%%%%%%%%%%%%%
%%%%%%%%%%%%%%%%%%%%%%%%%%%%%%%%%%%%%%%%%%%%%%%%%%%%%%%%%
%%%%%%%%%%%%%%%%%%%%%%%%%%%%%%%%%%%%%%%%%%%%%%%%%%%%%%%%%
%%%%%%%%%%
%Setting the Initial Concentrations and Timing Vectors
% y(1) = T.F.
% y(2) = mRNA
% y(3) = Protein
% y(4) = time

y0 = zeros(4, 1);
options = odeset('RelTol', 1e-6, 'AbsTol', [1e-6 1e-6 1e-6 1e-6]);
y0(1) = X1;
t = [0 10];
[T, Y] = ode23s(@Model_A3_constant_validate, t, y0, options);
figure(1);
subplot(2,1,1)
plot(T, Y(:,1), 'b-');
legend('T.F.');
subplot(2,1,2)
plot(T, Y(:,2), 'r-', T, Y(:,3), 'k-');
xlabel('Time');
ylabel('Concentration');
legend('mRNA', 'Protein');
```

Model_A1_constant_validate.m.txt

```
function Func = Model_A1_constant_validate(t, y)

%%%%%%%%%%%%%%%%%%%%%%%%%%%%%%%%%%%%%%%%%%%%%%%%%%%%%%%%%%%%%%%%%%%%%%%%%%%%%%%%%%%%%%%%%%%%%%%%%%%%%%%%%%%%%%%%%%%%%%%%%%%%%%
k1 = 0.1*1000*60;     % [0.001, 1]*1000*60 nM/hr = {0.001, 0.01, 0.1, 1}*1000*60 <insignificant effect>
j1 = 0.53*1000;       % [0.01, 10]*1000 nM = {0.01, 0.1, 1, 10}*1000 -->
k2 = 0.01*60;         % [0.001, 1]*60 /hr = {0.001, 0.01, 0.1, 1}*60
dM = 0.01*60;         % [0.001, 1]*60 /hr = {0.001, 0.01, 0.1, 1}*60 -->; large effect on time to steady state
(large dM => fast; small dM => slow)
dP = 0.01*60;         % [0.001, 1]*60 /hr = {0.001, 0.01, 0.1, 1}*60

n = 4;                % {1, 2, 4, 8} <--
X1 = 0.28*1000;       % [0.0001, 10]*1000 nM = {0.0001, 0.001, 0.01, 0.1, 1, 10}*1000 <--
%%%%%%%%%%%%%%%%%%%%%%%%%%%%%%%%%%%%%%%%%%%%%%%%%%%%%%%%%%%%%%%%%%%%%%%%%%%%%%%%%%%%%%%%%%%%%%%%%%%%%%%%%%%%%%%%%%%%%%%%%%%%%%
%ODEs
% y(1) = T.F.
% y(2) = mRNA
% y(3) = Protein
% y(4) = time

% v1    =    k1*(T.F.)^n / (j1^n + (T.F.)^n)
% v2    =    k2*[mRNA]
% v4    =    dM*[mRNA]
% v5    =    dP*[Protein]

% d[T.F.]/dt = A1*w1*cos(w1*t), T.F.(0) = X1, [T.F.] = X1 + A1*sin(w1*t)
% d[mRNA]/dt = v1 - v4
% d[Protein]/dt = v2 - v5

Func = zeros(4, 1);
Func(1) = A1*w1*cos(w1*t);
Func(2) = k1*y(1)^n / (j1^n + y(1)^n) - dM*y(2);
Func(3) = k2*y(2) - dP*y(3);
Func(4) = 1;
```

Model_A3_constant_validate.m.txt

```
function Func = Model_A3_constant_validate(t, y)

%%%%%%%%%%%%%%%%%%%%%%%%%%%%%%%%%%%%%%%%%%%%%%%%%%%%%%%%%%%%%%%%%%%%%%%%%%%%%%%%%%%%%%%%%%%%%%%%%%%%%%%%%%%%%%%%%%%%%%%%%%%%
k1 = 0.01*1000*60;     % [0.001, 1]*1000*60 nM/hr = {0.001, 0.01, 0.1, 1}*1000*60 <insignificant effect>
j1 = 0.01*1000;        % [0.01, 10]*1000 nM = {0.01, 0.1, 1, 10}*1000 -->
k2 = 0.01*60;          % [0.001, 1]*60 /hr = {0.001, 0.01, 0.1, 1}*60
dM = 0.01*60;          % [0.001, 1]*60 /hr = {0.001, 0.01, 0.1, 1}*60 -->; large effect on time to steady state (large dM => fast; small dM => slow)
dP = 0.01*60;          % [0.001, 1]*60 /hr = {0.001, 0.01, 0.1, 1}*60

n = 1;                 % {1, 2, 4, 8} <--
X1 = 0.0001*1000;      % [0.0001, 10]*1000 nM = {0.0001, 0.001, 0.01, 0.1, 1, 10}*1000 <--
%%%%%%%%%%%%%%%%%%%%%%%%%%%%%%%%%%%%%%%%%%%%%%%%%%%%%%%%%%%%%%%%%%%%%%%%%%%%%%%%%%%%%%%%%%%%%%%%%%%%%%%%%%%%%%%%%%%%%%%%%%%%
%ODEs
% y(1) = T.F.
% y(2) = mRNA
% y(3) = Protein
% y(4) = time

% v1    =    k1*(T.F.)^n / (j1^n + (T.F.)^n)
% v2    =    k2*[mRNA]
% v4    =    dM*[mRNA]
% v5    =    dP*[Protein]

% d[T.F.]/dt = A1*w1*cos(w1*t), T.F.(0) = X1, [T.F.] = X1 + A1*sin(w1*t)
% d[mRNA]/dt = v1 - v4
% d[Protein]/dt = v2 - v5

Func = zeros(4, 1);
Func(1) = A1*w1*cos(w1*t);
Func(2) = k1*y(1)^n - dM*y(2);
Func(3) = k2*y(2) - dP*y(3);
Func(4) = 1;
```